

AD-A240 188

WL-TR-91-3010



2

**USAF TESTING IN SUPPORT
OF AIR CUSHION EQUIPMENT
TRANSPORTER (ACET)
TECHNOLOGY**



**GERALD R. WYEN
AIRCRAFT LAUNCH & RECOVERY BRANCH
VEHICLE SUBSYSTEMS DIVISION**

MAY 1987

91-10348

FINAL REPORT FOR PERIOD OCTOBER 1984 - DECEMBER 1986

APPROVED FOR PUBLIC RELEASE; DISTRIBUTION UNLIMITED

**FLIGHT DYNAMICS DIRECTORATE
WRIGHT LABORATORY
AIR FORCE SYSTEMS COMMAND
WRIGHT-PATTERSON AIR FORCE BASE, OHIO 45433-6553**

91-10348

NOTICE

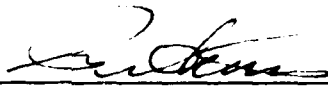
When Government drawings, specifications, or other data are used for any purpose other than in connection with a definitely Government-related procurement, the United States Government incurs no responsibility or any obligation whatsoever. The fact that the Government may have formulated or in any way supplied the said drawings, specifications, or other data, is not to be regarded by implication, or otherwise as in any manner construed, as licensing the holder, or any other person or corporation; or as conveying any rights or permission to manufacture, use, or sell any patented invention that may in any way be related thereto.

This report is releasable to the National Technical Information Service (NTIS). At NTIS it will be available to the general public including foreign nations.

This report has been reviewed and is approved for publication.



GERALD R. WYEN
Project Engineer
Special Projects Group



AIVARS V. PETERSONS
Chief, Aircraft Launch & Recovery Branch
Vehicle Subsystems Division

FOR THE COMMANDER



RICHARD E. COLCLOUGH, JR.
Chief
Vehicle Subsystems Division

If your address has changed, if you wish to be removed from our mailing list, or if the addressee is no longer employed by your organization please notify WL/FIVM, W-PAFB OH 45433-6523 to help us maintain a current mailing list.

Copies of this report should not be returned unless return is required by security considerations, contractual obligations, or notice on a specific document.

Unclassified

SECURITY CLASSIFICATION OF THIS PAGE

REPORT DOCUMENTATION PAGE

Form Approved
OMB No 0704-0188

1a. REPORT SECURITY CLASSIFICATION Unclassified		1b. RESTRICTIVE MARKINGS	
2a. SECURITY CLASSIFICATION AUTHORITY		3. DISTRIBUTION / AVAILABILITY OF REPORT Approved for public release; distribution is unlimited.	
2b. DECLASSIFICATION / DOWNGRADING SCHEDULE		4. PERFORMING ORGANIZATION REPORT NUMBER(S) WL-TR-91-3010	
4. PERFORMING ORGANIZATION REPORT NUMBER(S) WL-TR-91-3010		5. MONITORING ORGANIZATION REPORT NUMBER(S)	
6a. NAME OF PERFORMING ORGANIZATION Wright Laboratory Flight Dynamics Directorate	6b. OFFICE SYMBOL (if applicable) WL/FIVMB	7a. NAME OF MONITORING ORGANIZATION	
6c. ADDRESS (City, State, and ZIP Code) Wright-Patterson AFB OH 45433-6553		7b. ADDRESS (City, State, and ZIP Code)	
8a. NAME OF FUNDING / SPONSORING ORGANIZATION Flight Dynamics Directorate	8b. OFFICE SYMBOL (if applicable) WL/FIVMB	9. PROCUREMENT INSTRUMENT IDENTIFICATION NUMBER	
8c. ADDRESS (City, State, and ZIP Code) Wright-Patterson AFB OH 45433-6553		10. SOURCE OF FUNDING NUMBERS	
		PROGRAM ELEMENT NO 62201F	PROJECT NO 2402
		TASK NO 01	WORK UNIT ACCESSION NO 46
11. TITLE (Include Security Classification) USAF Testing in Support of Air Cushion Equipment Transporter (ACET) Technology			
12. PERSONAL AUTHOR(S) Wyen, Gerald R.			
13a. TYPE OF REPORT Final	13b. TIME COVERED FROM Oct 84 TO Dec 86	14. DATE OF REPORT (Year, Month, Day) 1987 May	15. PAGE COUNT 226
16. SUPPLEMENTARY NOTATION The computer software contained herein are "harmless" - already in the public domain.			
17. COSATI CODES		18. SUBJECT TERMS (Continue on reverse if necessary and identify by block number)	
FIELD 01	GROUP 03	Air Cushion Vehicle, Aircraft Transporter, Equipment Transporter, Survivability	
19. ABSTRACT (Continue on reverse if necessary and identify by block number) The Air Cushion Equipment Transporter (ACET) is designed as an air base survivability item, to transport vital heavy equipment (especially aircraft) across battle damaged terrain. This report presents the results of the first ACET program which consisted of the design, construction, and testing of a prototype vehicle. Based upon the design concept evolved for the AATS program, the ACET is essentially a lower performance derivative of the vehicle proposed for that program. Its construction follows closely the methods used in producing the LACV-30 and its cushion lift air system employs almost exclusively the hardware previously installed on the XC-8A aircraft used in the ACLS program. This report summarizes the evolution of the prototype vehicle and presents the results of the test program with the ACET equipped with a full-fingered skirt carrying on F101B aircraft to simulate realistic payloads.			
20. DISTRIBUTION / AVAILABILITY OF ABSTRACT <input checked="" type="checkbox"/> UNCLASSIFIED UNLIMITED <input type="checkbox"/> SAME AS RPT <input type="checkbox"/> DTIC USERS		21. ABSTRACT SECURITY CLASSIFICATION Unclassified	
22a. NAME OF RESPONSIBLE INDIVIDUAL Gerald R. Wyen		22b. TELEPHONE (Include Area Code) 513-257-7804	22c. OFFICE SYMBOL WL/FIVMB

FOREWORD

This report covers in-house testing of the Air Cushion Equipment Transporter (ACET) by personnel of the Aircraft Launch and Recovery Branch (FIVM), Vehicle Subsystems Division (FIV), Flight Dynamics Laboratory (FI), Wright Research and Development Center (WRDC), Wright-Patterson AFB, OH 45433-6523 under Project 2402, "Vehicle Equipment Technology"; Task 240201, "Vehicle Equipment Mechanical Subsystems"; Work Unit 24020146, "Aircraft Mobility Systems Models."

The work reported herein was conducted between October 1984 and December 1986 under the direction of Mr Gerald R. Wyen (WRDC/FIVMB), Project Engineer for the ACET Program. The testing accomplished during this period included model as well as full-scale testing. All of the model testing was conducted on test equipment located in the Mobility Development Laboratory (MDL), Building 255, Area "C," Wright-Patterson AFB, OH. The test site for the full-scale testing was Airborne Air Park, Wilmington, OH.

Technical support for this effort was supplied by Systems Research Laboratories, Inc. (SRL), 2800 Indian Ripple Road, Dayton, OH 45440 under Air Force Contract Number F33601-84-D-0033.

The author wishes to thank Capt Mark Price, Special Projects Group, for his assistance in the testing of the ACET models, Capt George Reazer, Special Projects Group, for his invaluable assistance during the full-scale tests and demonstrations and Mr Bill Smith for his excellent efforts in providing logistics support for this project. Also, the exceptional efforts of Messers David Pedrick, Tracy Hall, and Lee Riffle, SRL, contributed significantly to the overall success of this project.



Accession Per	
DTIC ONAHL	<input checked="" type="checkbox"/>
DTIC TAB	<input type="checkbox"/>
Unannounced	<input type="checkbox"/>
Justification	
By	
Distribution/	
Availability Codes	
Avail and/or	
Special	
A-1	

TABLE OF CONTENTS

SECTION	PAGE
I INTRODUCTION	1
1. Scope of the Problem	1
II BACKGROUND	3
1. Evolution of the ACET Program	3
III SUMMARY OF CONTRACTOR'S PROGRAM	7
1. Development of the ACET Design	7
2. ACET Structure	11
3. Lift System	14
4. Skirt System Development	23
5. Crosswind and Side Force Control	42
6. Loading and Off-loading of Aircraft	43
7. Test Results	52
IV MODEL TESTING	56
1. Objectives	56
2. Approach	56
3. Design of Models	56
4. Fabrication of Models	62
5. Calibration of Fan	66
6. Testing of Heavy Weight Model	89
7. Results	105
V USAF TESTING OF FULL-SCALE ACET	108
1. Objectives	108
2. Approach	109
3. Heave Stability Tests	110

TABLE OF CONTENTS, CONT'D

SECTION	PAGE
4. Self-Propulsion Tests	120
5. ASP-10 Failure	137
6. Evaluation of Skirt Performance	148
7. Results of Test Program	155
VI DEMONSTRATION OF ACET	161
1. First Demonstration at AMARC	161
2. Second Demonstration at AMARC	194
3. Results of Demonstration	198
VII CONCLUSIONS AND RECOMMENDATIONS	199
VIII REFERENCES	201
APPENDIX A FLOW CALCULATION PROGRAM	203
APPENDIX B AMARC ACET TECHNICAL OBSERVATIONS DEFICIENCY (TOD) REPORT	209
APPENDIX C FDL COMMENTS ON AMARC'S TOD REPORT	213

LIST OF ILLUSTRATIONS

FIGURE		PAGE
1	XC-8A - ACLS Equipped CC-115	4
2	Alternate Aircraft Takeoff System (AATS)	5
3	LACV-30 Operating in Surf	9
4	ACET General Arrangement	12
5	Fabrication of Nose or Power Module	13
6	Installation of Internal Trusses	15
7	Forward Splice Joint	16
8	Final Assembly of ACET	17
9	Schematic for Filtration System	18
10	Typical Damage to First Stage Rotors of F-10 Fan	20
11	First Generation Protective Screen for F-10 Fan	21
12	Typical Off-Runway Foreign Object Environment	22
13	Basic Skirt Systems	24
14	Jupe Skirt System Installed on the ACET	25
15	Details of Jupe Skirt System Design	26
16	Installation of Release Pleat Restraint Straps	27
17	Installation of Cushion Air Deflectors	29
18	Deformation of Jupe Skirt System No. 1	30
19	Stability Vent Door Installations	33
20	Build-up of Snow in Front of Main Cell Jupe Skirt	35
21	Loss of Cushion Because of Debris Inside Main Cell	36
22	Segmented Finger Geometry	37
23	Obstacle Deflector Modification to Finger	40
24	Makeup of Segmented Finger Skirts	41
25	Nose Ramp Trailing Wheel Assembly	44
26	Main Ramp Trailing Wheel Assembly	45
27	Trailing Wheels During Loading/Off-loading	46
28	Main and Nose Wheel Ramp and Track Installation	48
29	Winch Installation	49
30	Aircraft Main Landing Gear Chocks	50
31	Jupe Skirt Installation on Heavy Weight Model	61
32	Basic Structure of Heavy Weight Model	63
33	Fabrication of Air Supply Ducts	64
34	Heavy Weight Model, Forward Fan Installation	65
35	Light Weight Model on Dynamic Test Machine	67
36	Heavy Weight Model Checkout on Static Platform	68
37	1/10 Scale ACET Model Useable CG Range	70
38	Modified Heavy Weight Model	71
39	Cushion Pressure Variation With Fan Input Power	72
40	Frequency Control Console	73
41	Fan Calibration Rig	75
42	"MAXIAX" Installation in Fan Calibration Rig	76
43	Sharp Edge Orifice with Pressure Taps	77
44	Exit Area Control Butterfly Valve	78
45	Inclined Manometer Bank for Calibration Rig	80
46	Verification of Fan Calibration Procedures	82
47	Data Runs for Fan Calibration Tests	84
48	"MAXIAX" 300 Hz Operating Curve	85

LIST OF ILLUSTRATIONS, CONT'D

FIGURE		PAGE
49	Fan Exit And Plenum Pressure Relationship	87
50	Definition of 300 Hz Operating Point	88
51	ACET Full-Scale Cell Loads	91
52	Pitching Moment Effect on Model Attitude	93
53	Comparison of Model Data and Scaled Data	94
54	Pitching Moment Effect on Cushion Pressure	95
55	Effect of Rolling Moment on Model Attitude	97
56	Effect of Rolling Moment on Pressures	98
57	Comparison of Model and Scaled ACET Roll Data	99
58	Drag Test Setup for Heavy Weight Model	100
59	Drag Variation with Mass Flow Rate	103
60	Comparison of Model and Scaled ACET Data	104
61	Effect of Obstacles on Drag	106
62	Heave Stability Boundaries	112
63	Breakaway Drag for Zero Venting	113
64	Breakaway Drag for 185.5 Sq In of Venting	114
65	Definition of Stability Boundaries	117
66	Effect of Operating Time on Stability	118
67	Effect of Operating Time on Performance	119
68	Effect of Surface on Stability	122
69	Effect of Surface on Performance	123
70	Comparison of Drag Data	124
71	Comparison of Cell Pressures	126
72	ACET CG Location	128
73	Variation of Breakaway Drag with CG Position	130
74	Pitch Angle for 185.5 Sq In of Venting	131
75	Pitch Angle Vs CG Location, 0 Sq In Venting	132
76	Effect of ASP-10 Power Setting on Drag	134
77	Impact of Payload Weight on Drag	135
78	Effect of Pitch Oscillation on Drag Forces	136
79	New Damage to Left F-10 Fan Assembly	138
80	Fan Inlet Screen Assembly	140
81	Post Fan Screen Modification Damage	141
82	Data Traces of Left Fan Failure	143
83	External Damage of Left F-10 Fan	144
84	Penetration of Blade Containment Ring	145
85	Upper Exhaust Stub Damage	146
86	Damage to First Stage Rotors of Left F-10 Fan	147
87	Damage to Left F-10 First Stage Rotors	149
88	Damage to Left F-10 First Stage Stators	150
89	Comparison of New and Damaged First Stage Blades	151
90	Sudden Stoppage Damage to Fuel Pump	152
91	Typical Condition of ST6F-70 Fuel Injectors	153
92	Overhauled F-10 Two Stage Rotor Assembly	154
93	Cell Pressure Variations on Grass	156
94	Cell Pressure Variations on Concrete	157
95	New Loading Ramps and Trailing Wheel Assemblies	165
96	Installation of New Load-Bearing Panels	167

LIST OF ILLUSTRATIONS, CONT'D

FIGURE		PAGE
97	Low Bearing Strength Support Mechanism	168
98	FOD Suppression Skirt	169
99	Off-loading of the ACET	171
100	Forward Module Positioned on Maintenance Stands	172
101	Start of ACET Assembly	173
102	Assembled ACET Lowered to Ground	174
103	Repair of Lower ASP-10 Exhaust Stub	175
104	Installation of FOD Suppression Skirts	176
105	Preparing Goodyear Fingers for Installation	177
106	Failure of the Left Trailing Wheel Assembly	179
107	New Trailing Wheel Assembly Attachment Bracket	181
108	Condition of Tow Path in Area 11	182
109	ACET Spotted in Front of F-4J Aircraft	183
110	Field Assembly of Ramps	184
111	Ramps Positioned for F-4 Series Aircraft	186
112	Preparations for Loading F-4J Aircraft	187
113	Winch Bridle Attachment Using Catapult Hooks	188
114	ACET Attitude with F-4J as Payload	189
115	MB-2 Getting Stuck in Area 11 (Scope of Problem)	190
116	ACET Being Towed Out of Area 11	191
117	ACET Being Towed Across Wet Ramp	192
118	Fingers Fabricated From Different Materials	195

LIST OF TABLES

TABLE		PAGE
1	ACET General Specifications	11
2	Aircraft Comparison	28
3	ACET Stability Vent Design Parameters	38
4	Size of Segmented Fingers	39
5	Number of Different Types of Segmented Fingers in Ship's Set	42
6	Typical ACET Tow Forces	53
7	Scaling Factors for ACET	58
8	ACET Model Design Parameters	59
9	Model Weight Breakdown	62
10	Summary of Test Results	159
11	AMARC Demonstration Key Dates	163
12	Design Requirements for Loading Ramps and Area	164

LIST OF SYMBOLS AND ABBREVIATIONS

		DIMENSIONS
AATS	Alternate Aircraft Takeoff System	
ACET	Air Cushion Equipment Transporter	
ACLS	Air Cushion Landing System	
ACV	Air Cushion Vehicle	
AF	Air Force	
AFIT	Air Force Institute of Technology	
AFLC	Air Force Logistics Command	
AFSC	Air Force Systems Command	
AFWAL	Air Force Wright Aeronautical Laboratories	
AMARC	Aerospace Maintenance And Regeneration Center	
ASP-10	Air Supply Package - F-10 Fan	
A&P	Airframe and Propulsion	
BACT	Bell Aerospace Canada Textron	
BAT	Bell Aerospace Textron	
CBR	California Bearing Ratio	
cg	Center of Gravity	
D	Orifice Throat Diameter	Inches
DOD	Department Of Defense	
ECB	Engine Control Box	
EOD	Explosive Ordnance Disposal	
F, f	Force	Pounds, force
F _a	Area Thermal Expansion Factor	Non-dimensional
FDL	Flight Dynamics Laboratory	
FOD	Foreign Object Damage	
Fr	Froude Number	
Fwd	Forward	
g	Gravitational Acceleration	
HP	Horsepower	
HSI	Heave Stability Index	
Hz	Cycles per Second	
in-lbs	Inch-pounds	
K	Flow Coefficient	Non-dimensional
L	Representative Length	
LACV-30	Lighter, Air Cushion Vehicle - 30 Ton Payload	
lbs _m	pounds, mass	
lbs	pounds	
MDL	Mobility Development Laboratory	
Mid	Middle	
MOS	Minimum Operating Strip	
mph	miles per hour	
NDI	Non-Destructive Inspection	
Nf	Rotational Speed of Fan	Revolutions per Minute
P, p	Pressure	Pounds/square inch
psfg	pounds per square foot, gage	
psig	pounds per square inch, gage	
P ₁	Upstream orifice pressure	Inches of water

LIST OF SYMBOLS AND ABBREVIATIONS, CONT'D

		DIMENSIONS
P_2	Downstream orifice pressure	Inches of water
Q	Mass flow rate	Pounds, mass per second
R&D	Research and Development	
rpm	revolutions per minute	
SRL	Systems Research Laboratories	
sq in	square inches	
sq ft	square foot	
TAC	Tactical Air Command	
TOD	Technical Observation Deficiency	
UACL	United Aircraft of Canada, Limited	
US	United States	
USAF	United States Air Force	
V	Reference Velocity	
WRDC	Wright Research and Development Center	
λ	Scale of Model	
ρ	Flow density	Slugs per cubic feet

SECTION I

INTRODUCTION

1. SCOPE OF THE PROBLEM

The United States Air Force (USAF) has been investigating a number of approaches to counter the threat of runway denial to fighter aircraft because of intervening battle damaged terrain between the runway and the aircraft dispersal points. One of the key factors in the recovery of an airfield after an attack is how quickly vital ground equipment, runway repair supplies/materials, and aircraft can be moved from their respective storage areas. Presently, this is accomplished by utilizing vehicles with some type of high pressure tire as the load carrying member. For this reason, these vehicles are dependent upon hard, undamaged surfaces for the movement of aircraft and equipment. Current recovery repair techniques are time consuming and manpower intensive. Therefore, for any proposed system to be effective, it must substantially reduce the workload of the Civil Engineers charged with the responsibility of returning an airbase to an operational status after an attack. Generally, the tasks facing the Civil Engineers can be divided into the following major efforts:

- a. The repair of runways and taxiways damaged either by direct hits or near misses from bombs, missiles, or guns;
- b. The removal of debris on runways and taxiways resulting from ordnance detonating on or near these surfaces;
- c. The location and removal of unexploded ordnance after an enemy air attack, Explosive Ordnance Disposal (EOD).

The runway denial threat has increased significantly with the replacement of General Purpose Iron Bombs by guided munitions such as the AGM-65 Maverick, the GBU-15 and the AGM-130 which is a rocket powered version of the GBU-15 and runway cratering weapons, such as the French-developed Durandal. Trends in the development of runway denial weaponry and runway repair techniques suggest the vulnerability of runways will continue to increase. Aside from the development of repair procedures that require less equipment, manpower, and time to complete, one obvious approach to the problem is to reduce the level of effort required for each of the major efforts. In order to accomplish this goal, the current dependency on hard, undamaged surfaces for the movement of aircraft and equipment must be significantly reduced. Any system which could attain this goal would provide Civil Engineers with means of reducing, to manageable levels, the effort required for returning an airbase to an operational status. If this system would permit the movement of aircraft and equipment over unprepared surfaces adjacent to the runways and taxiways, the repairs, removal of debris, and the locating and disposal of unexploded ordnance could be concentrated on providing a Minimum Operating Strip (MOS) for the launch and recovery of tactical fighter aircraft. General cleanup and repair of the runways, taxiways, and revetment areas

could then be delayed until after the initial emergency has passed. Given the magnitude and complexity of the problem, a radical departure from current design criteria and philosophy was dictated.

SECTION II

BACKGROUND

1. EVOLUTION OF THE ACET PROGRAM

The Air Cushion Equipment Transporter (ACET) evolved from developmental work conducted by the Flight Dynamics Laboratory (FDL) in the area of adapting Air Cushion Vehicle (ACV) technology to aircraft mobility requirements. Work conducted in this area during the late 1960's and the 1970's resulted in the air cushion landing system concept. Prototype systems were designed and tested on two vehicles; an Australian Jindivik, a drone; and a Canadian CC-115 Buffalo, a transport aircraft. The excellent rough field performance of the Air Cushion Landing System (ACLS) equipped CC-115 aircraft, the XC-8A (Figure 1), suggested that the mobility of tactical fighters could be greatly enhanced by alternate means. An Alternate Aircraft Takeoff System (AATS) Feasibility and Preliminary Design Program was initiated to investigate the feasibility of developing an alternate aircraft takeoff system which would permit present and future generation fighter aircraft to be launched from bomb damaged airfields with an absolute minimum amount of repair to the runways and taxiways; to select the optimum approach and to develop a preliminary design based upon the selected approach. During the initial contracted study, in 1977, a total of 70 concepts were considered. From this group, 29 approaches were determined to be, at least, remotely feasible. Further analysis of these potential candidates by an Air Force Institute of Technology (AFIT) Systems Engineering Design Group led to a preliminary design based upon air cushion technology (Figure 2). A comprehensive wind tunnel program was conducted on the air cushion configuration to investigate the separation dynamics of the air cushion platform and the aircraft, for this program an F-4E, during rotation and liftoff.

Even though the results of the preliminary design and the wind tunnel program were very encouraging, the Users did not support the concept of launching fighter aircraft from an air cushion platform. However, a Tactical Air Command (TAC) Statement Of Need, TAC-SON-319-79, did define the requirement for a capability which would permit the movement of aircraft (towed or under its own power) to and from sheltered areas over debris, paved surfaces, or partially damaged taxiways. This requirement was further substantiated by a Logistics Need, LN-80184, authored by the Air Force Acquisition Logistics Center. Finally, in a 1980 message from Air Force Systems Command (AFSC), the Commander suggested that the Flight Dynamics Laboratory (FDL) "Look at a ground effect transporter which would move aircraft from shelters to usable takeoff strips over or around craters and debris." Thus, the ACET Technology Program came into being.

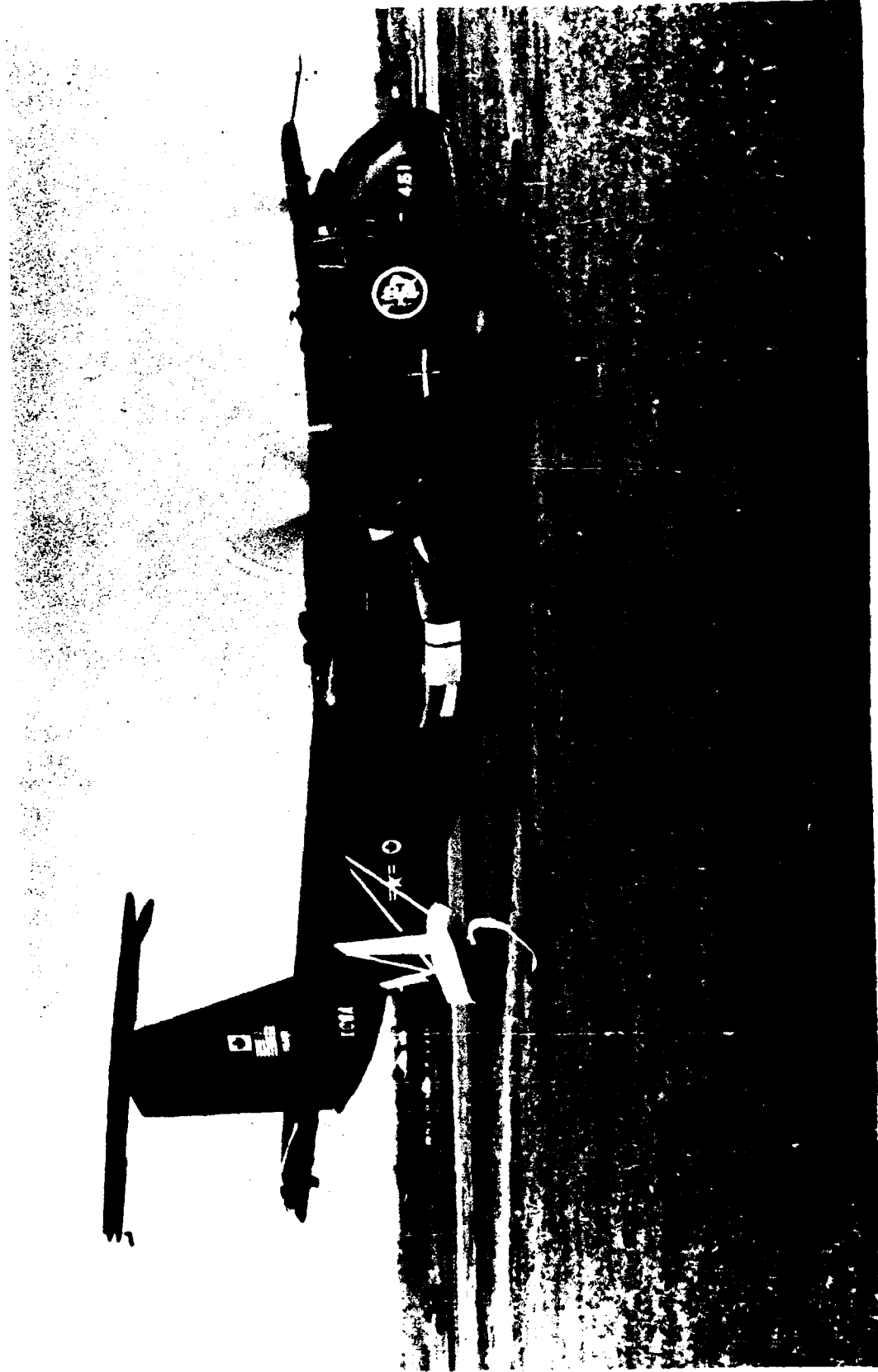


Figure 1. XC-8A - ACLS Equipped CC-115 Aircraft



Figure 2. Alternate Aircraft Takeoff System (AATS)

The key design considerations for this next generation aircraft/equipment transporter were:

a. Totally eliminating any dependency on smooth, hard surfaces for operations,

b. Sufficient payload and space capability to accommodate current tactical fighter aircraft,

c. Substantial increase in towing speeds to allow rapid turn around,

d. System capable of being airlifted in a C-130 transport aircraft.

SECTION III

SUMMARY OF CONTRACTOR'S PROGRAM

1. DEVELOPMENT OF THE ACET DESIGN

A summary of the contractor's program will be presented in this report. The purpose of this summary is to document the evolution of the ACET as operating experience was applied to design deficiencies uncovered during the testing of the transporter and to provide a frame of reference for the discussions covering the In-House testing conducted by the USAF. Excellent sources of detailed information on the BACT ACET Program are References 1, 2, and 3.

In June 1982, the USAF and the Canadian Government signed a contract to jointly investigate the potential of utilizing ACV technology to improve their capability to transport aerospace vehicles and ground equipment over battle damaged taxiways and low strength ground surfaces. The approach employed in the attainment of this objective was to design, fabricate and assemble a full-scale air cushion transporter capable of supporting payloads up to 60,000 pounds; conduct a series of static and dynamic tests using a ballasted non-operational F-101 aircraft as the payload; analyze the experimental test data to evaluate the performance of the transporter and develop recommendations for an optimum ACET design. The prime contractor for the program was Bell Aerospace Canada Textron (BACT). The total cost of the program was shared between the USAF, the Canadian Government, and the contractor, BACT.

The overall design performance requirements for the ACET development were:

- a. The vehicle shall be capable of carrying a payload of 60,000 lbs over rough terrain typical of what can be expected on an airbase after an enemy attack.
- b. The transporter shall operate routinely over surfaces with a California Bearing Ratio (CBR) of 3 (i.e., mud, sand saturated with water or grass saturated with water).
- c. The ACET shall traverse discreet surface irregularities up to plus or minus 12 inches.
- d. The vehicle shall exhibit positive stability characteristics in pitch, roll, and heave, vertical motion, throughout its entire operating envelope.

e. The transporter shall be capable of tow speeds up to at least 25 miles per hour.

f. The ACET shall be modular in construction to allow disassembly and transportation in a C-130 class transport aircraft.

The initial design definition for the ACET was obtained from Reference 2. The AATS, as developed in this design (Figure 2), was a shallow depth air cushion platform supported by three plenum air cushion cells, utilizing jupe skirts. The aircraft main engines supplied the necessary thrust to accelerate the AATS/aircraft combination to the takeoff speed of the aircraft. After separation, the AATS would be stopped with deceleration (drag) chutes. The AATS would then be towed back to the launch area and prepared for another launch.

Dimensionally, the ACET is, in all major aspects, identical to the AATS. The ACET was designed as a tri-cell air cushion vehicle, with the cells having the same geometric orientation as the AATS. Similarly, provisions were incorporated into the transporter for loading, offloading and restraining aircraft; and for supporting the vehicle plus payload when the lift system is turned off. There are, however, two principal differences between the two designs. The first is the criteria employed in the development of the vehicle's structure. The AATS design employed techniques generally applied to aircraft structures. This was necessary since the overall vehicle weight was critical to the performance of the AATS. The ACET, being a towed vehicle with relatively low speed requirements, is much less weight sensitive. Therefore, structural design techniques used in the manufacturing of the US Army's Lighter, Air Cushion Vehicle-30 Ton Payload (LACV-30), Figure 3, were employed. The resulting structure is substantially heavier than a similar design using aircraft structural techniques. A preliminary design weight estimate for the AATS was 6000 pounds (lbs) as compared to 11,000 lbs for the ACET. There are a number of advantages to be gained from the application of this approach to a feasibility demonstration program. A less sophisticated structural analysis can be used to evaluate the overall strength of the structure since the design criteria did not require that the structural weight be optimized. In all cases, if the analysis indicated a marginal Safety Factor, additional structure was added to the design to increase the Margin of Safety. However the structure was optimized to facilitate the fabrication and assembly/disassembly of the transporter.

The second variation is in the lift system. For the AATS design, a single engine-fan unit was proposed to power the air cushion. The gas turbine engine developed for the ACLS Advanced Development Program, Pratt and Whitney's ST6F-70, was selected as the engine to be used in this application. A new fan was to be developed since a flight qualified unit which matched the mass flow and pressure requirements of the AATS application was not available. To eliminate the cost of developing, qualifying and producing a new fan-engine unit for this application, the ACET design incorporated the Air Supply Packages (ASP-10's) from the XC-8A. Each of these units was capable of supplying half of the

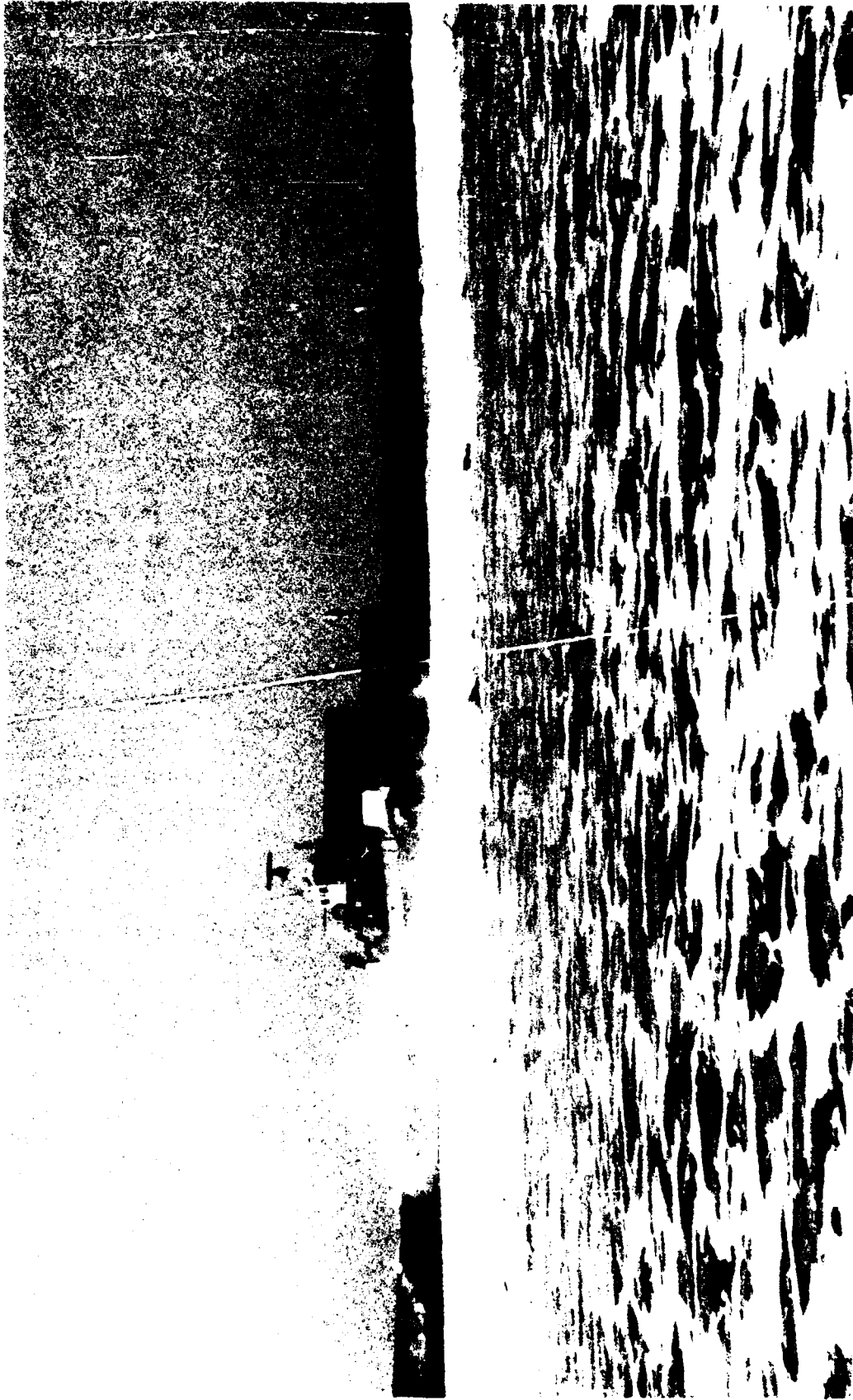


Figure 3. LACV-30 Operating in Surf

calculated mass flow requirements at the design output air pressure. This approach resulted in increased subsystem complexity and weight but reduced the total program cost.

The stability of both the AATS and the ACET were analyzed extensively. From these analyses, it was concluded that both vehicles could be designed to maintain positive pitch, roll and heave stability margins throughout the entire payload range of the transporter without having to resort to centrifugal fans with shallow pressure-to-flow slopes. The analyses were conducted using both simple linear analytical models and complex, nonlinear, coupled pitch and heave simulations. For the heave axis, where the greatest potential for instability was found to exist, excellent agreement was found to exist between the linear and nonlinear analyses used to assess the heave stability of the proposed configuration.

The results of the analyses conducted indicated that the ACET design configuration was stable without any payload and could accept payload weights up to approximately 30,000 lbs before a heave instability boundary was reached. To improve the stability characteristics of the design beyond this point, a supplemental means had to be selected and incorporated into the design of either the skirt system or the vehicle itself. A literature search for any technical investigations into the causes and control of the heave stability problem in ACV's produced data which indicated that the most effective means of controlling heave is to reduce the sensitivity of cushion pressure to changes in mass flow. One method of accomplishing this is to select a fan with a shallow fan curve (i.e., large changes in mass flow produce small changes in pressure ratio). This is one of the advantages of a centrifugal flow fan over an axial flow fan. But, within the context of the ACET Program, this approach was not cost effective. Every effort had already been made to maximize the heave stability characteristics of the transporter. The cushion areas of the ACET were designed as large as practical after giving consideration to the size of the aircraft to be transported (tactical fighters), the empty weight of the vehicle and transportability requirements. The area of the nose cell was frozen at 98 sq ft, while each of the main cells had an area of 235 sq ft. Also, heave stability characteristics, as well as obstacle clearance requirements, were considered while selecting the depth of the jupe skirts. A depth of 24 inches was decided upon for the ACET. Therefore other methods of reducing cushion pressure sensitivity had to be considered.

Having addressed heave stability in every major aspect of the design and ruled out the possibility of using an axial flow fan, the technique with the greatest authority to reduce cushion pressure sensitivity was cushion cell venting. For a nominal main cell pressure of 100 pounds per square foot, gage (psfg), the heave stability analysis, which utilized Boeing's EASY 5 AATS Program, indicated that a vent area of 1.22 square feet would more than double the Heave Stability Index (HSI) of the transporter. With this increase in the HSI, the analysis predicted that the ACET would be stable, in heave, for payload weights up to 87,000 lbs. Further, at the design payload of 60,000 lbs, a heave stability margin of 20 percent was estimated.

Using the previously cited preliminary design for the AATS, changes in design approach, results of the stability analysis, and the performance goals for the ACET Program, BACT developed a general arrangement for the ACET (Figure 4). The specifications for the ACET, as originally designed, are presented in Table 1.

TABLE 1

ACET GENERAL SPECIFICATIONS

Dimensions:

Length, overall	46.8 ft
Width, maximum	36.5 ft
Length of Power Module	28.7 ft
Width of Power Module (Excluding Air Supply Diffuser)	1.7 ft
Depth of Skirt (From Attachment Point)	2.0 ft

Weight Breakdown:

Structure	7,269 lbs	
Power Plant	1,665 lbs	
Skirts	302 lbs	
Systems	764 lbs	
Empty Weight		10,000 lbs
Disposable Payload		58,800 lbs
Maximum Gross Weight		<u>68,800 lbs</u>

2. ACET STRUCTURE

The structure of the ACET was made from aluminum "hollowcore" extruded planking which was machine edge welded to form large panels. The sections required for the fabrication of each module (the nose or power module, the center module, and the aft module) were obtained by cutting these panels to the required shapes using a circular saw with a carbide tipped blade. The individual pieces, starting with the lower deck plate, were placed in a jig and successive sections were then welded to the lower deck (Figure 5). Standard aluminum corner extrusions were welded to the edges of the various sections to form the joints of the structure. Each of the three modules is hollow between the upper and lower deck plates to

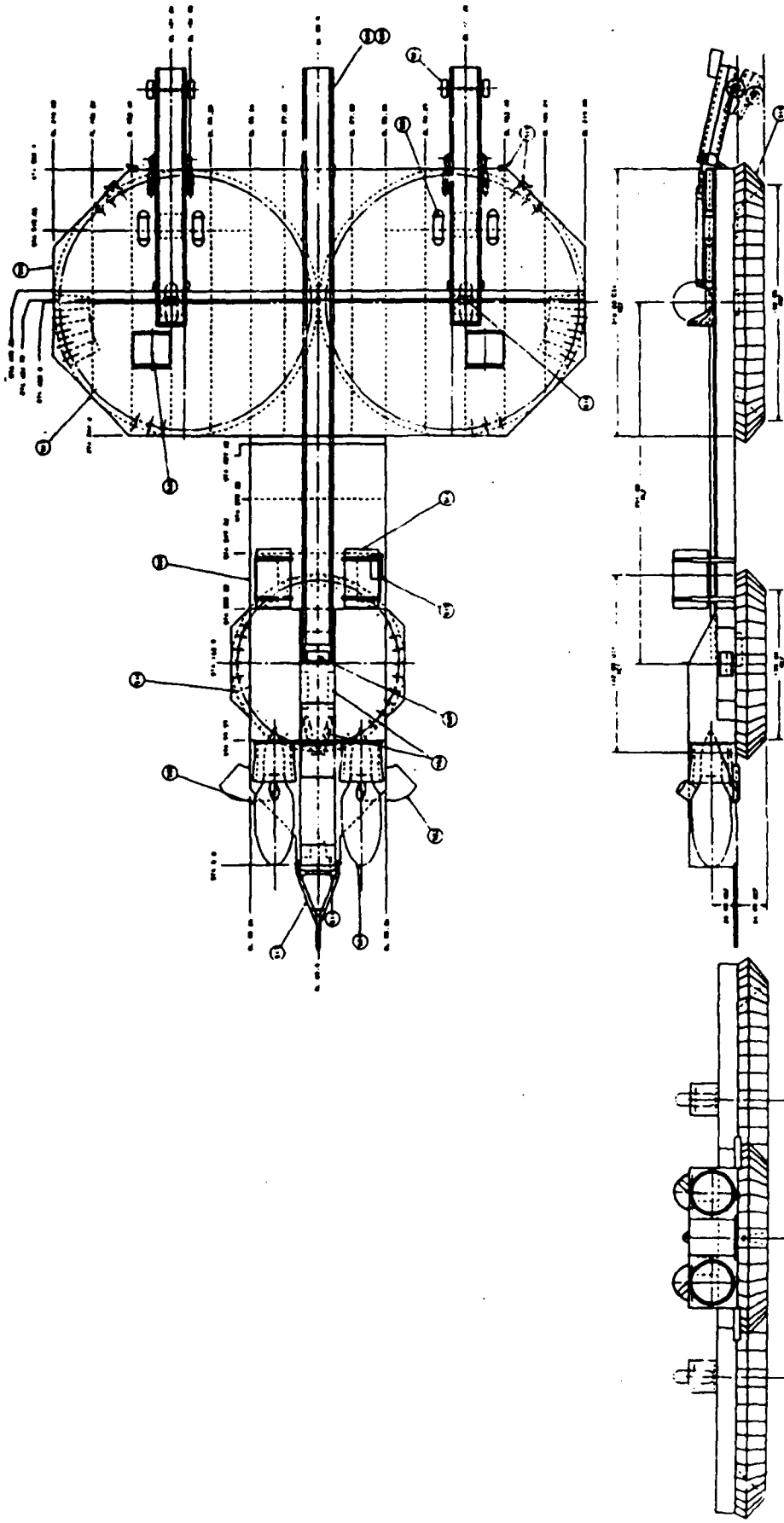


Figure 4. ACET General Arrangement



Figure 5. Fabrication of Nose or Power Module

facilitate the passage of the low pressure, high mass flow air from the ASP-10's to the three air cushion cells. Internal trusses were incorporated in the design (Figure 6) to meet structural stiffness requirements. The three modules were mechanically spliced together (Figure 7) to complete the assembly of the ACET (Figure 8). This also allowed future disassembly for movement of the vehicle to other test sites.

3. LIFT SYSTEM

As previously indicated, the lift system employed on the ACET utilized two ASP-10 air supply packages. Each of these packages consists of a ST6F-70 free turbine engine, an engine reduction gearbox and a F-10 fan. The ST6F-70 is a derivative of the PT-6 family of engines. The "S" denotes a stationary application; the "T6" refers to the parent engine, the PT-6; the "F" specifies the engine as a forward facing application and the "-70" indicates the series nomenclature for a flight qualified version of this engine. The gearbox is a standard 5.33:1 engine reduction gearbox which was modified by extending the output shaft and its housing to accommodate the fan inlet duct. The output shaft is attached directly to the fan shaft. The F-10 fan was specifically designed and flight qualified for the XC-8A. It consists of two axial stages. The design speed is 6,074 revolutions per minute (rpm) which produces a mass flow of 71.4 lbs mass per second at an overall pressure ratio of 1.204:1.

The original nacelle was retained down to the flow diverter section which was not required for the ACET application. Since the installation of the ASP-10's on the ACET was similar to the mounting on the side of the XC-8A fuselage, the original mounting brackets and existing engine pickups were incorporated into the design of the engine/fan installation. The rear of each modified ASP-10 nacelle butts against the "hollowcore" section which forms the front of the cushion diffuser. A mating hole for the fan exhaust was cut into this panel. The pressurized air is then channeled into a common feed duct. From this location, the air flow is distributed to the nose cell and the two main cells with a portion of the air being return to the ASP-10's for combustion.

Approximately 5.0 percent of the combined air flow is required for efficient combustion in the ST6F-70 engines. The engine combustion air intake on the original air supply package was located on the front inboard side of the nacelle. The outside air passed through an inertial separator before entering the annular engine intake. Since the operating environment of the ACET was expected to be considerably dirtier than the XC-8A, an alternate system for protecting the engines from Foreign Object Damage (FOD) was designed. A three stage filtration system (Figure 9) was incorporated into the ACET. Air for the ST6F-70 engines is bled off the fan air being supplied to the nose cell. The fan exit pressure ratio is great enough to overcome pressure losses during filtration. The first stage of the filtration system is a screen across the F-10 fan inlets. The function of this screen is to eliminate any large diameter objects which may be in the air stream. The second stage of the system is located at the point where the air is bled off for the engines. At this point, the air passes through a bank of momentum separators. These separators,



Figure 6. Installation of Internal Trusses

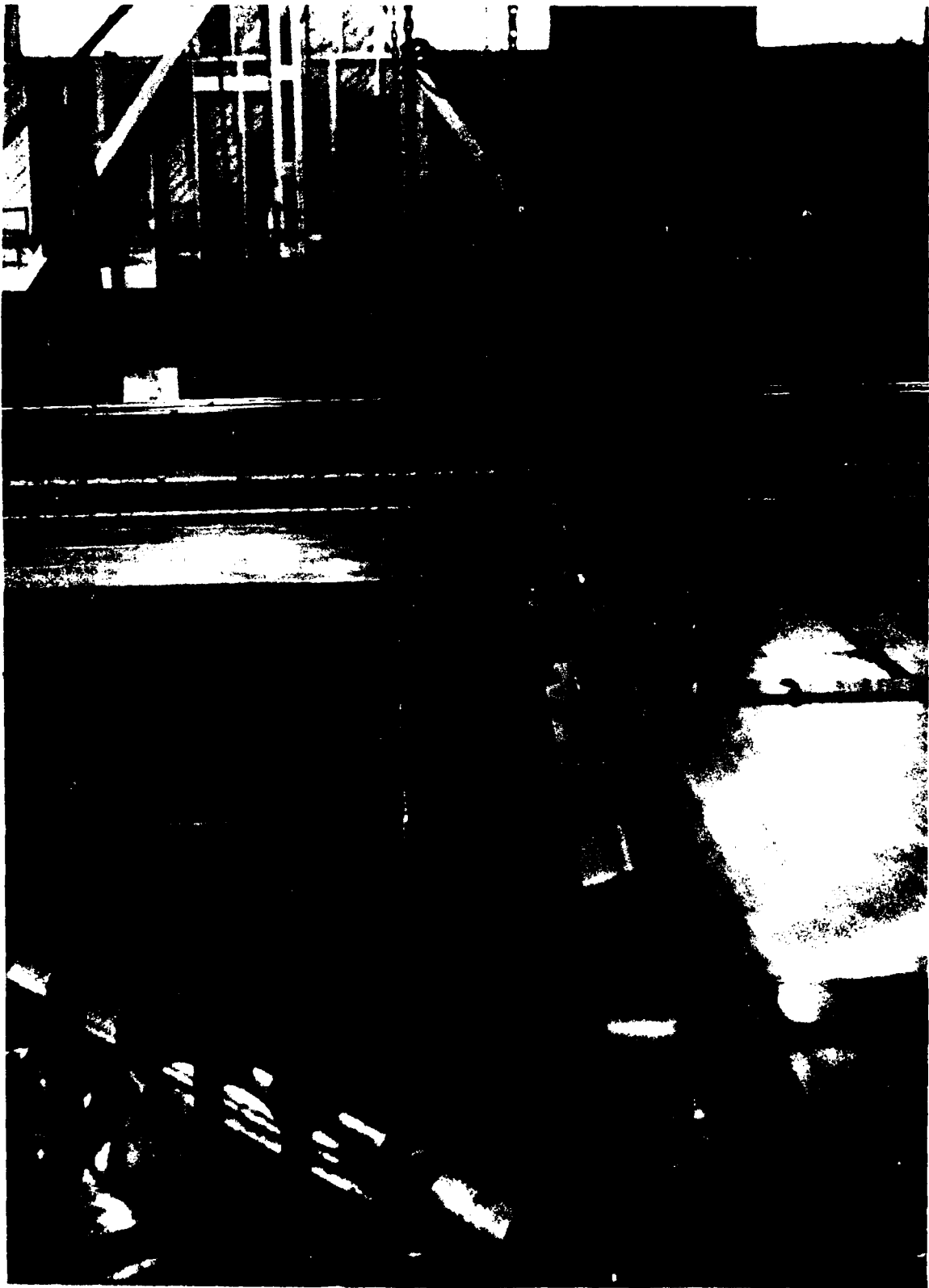


Figure 7. Forward Splice Joint



Figure 8. Final Assembly of ACET

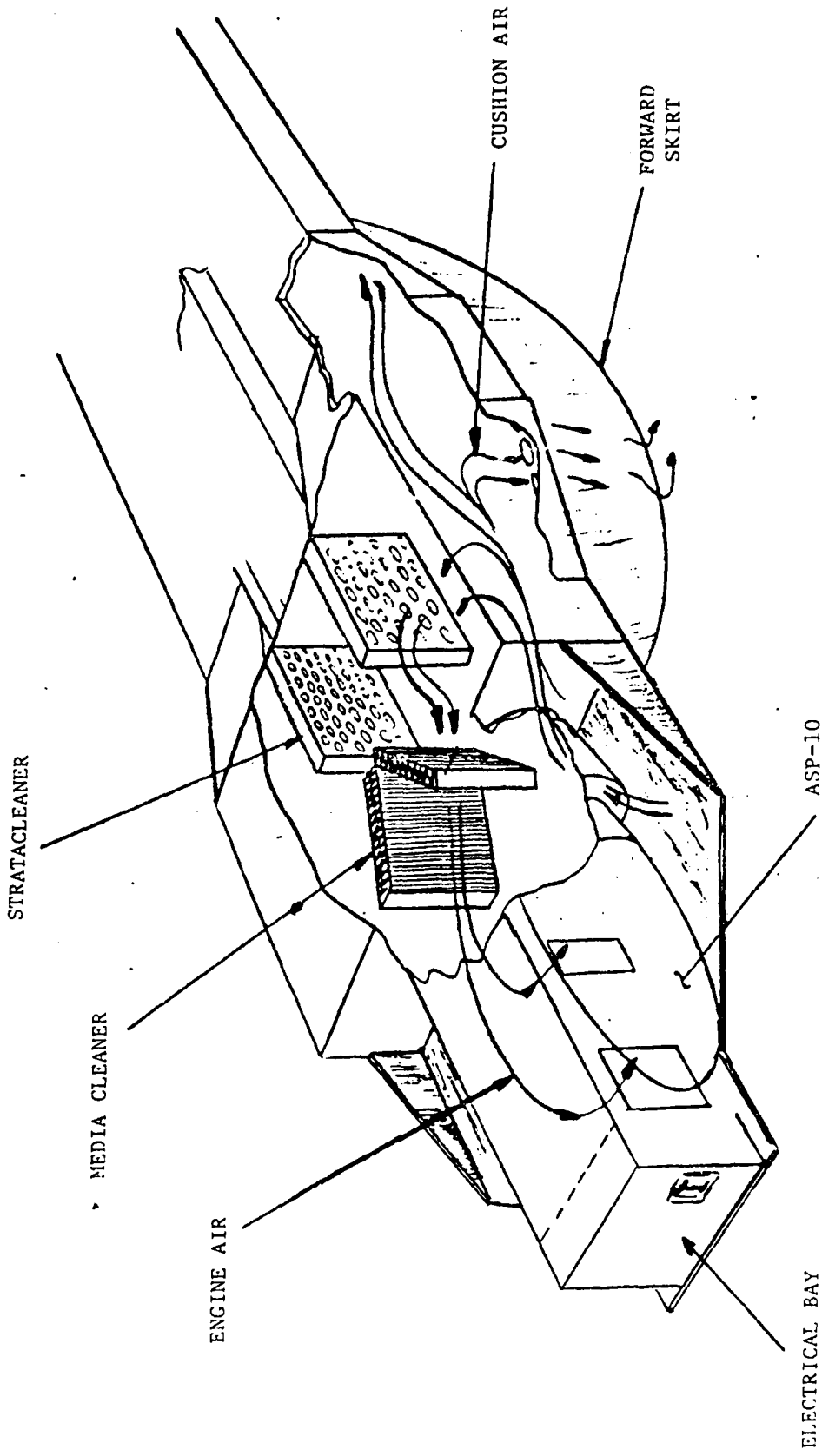


Figure 9. Schematic of Filtration System

with supplemental overboard disposal of foreign objects, were used to eliminate any intermediate sized particles which may have passed through the fan inlet screen and the two stages of the fan. The final stage of the filtration system is a set of pleated barrier screens to remove very fine dust and other small sized objects.

Operating experience has shown this system to be very effective in protecting the combustion section of the ST6F-70 engines. However, other deficiencies were uncovered during the testing of the ACET. The screens over the fan inlet provided adequate protection for the F-10 fan blades as long as the ACET was operating over relatively clean surfaces, such as runways and taxiways. When the contractor's testing progressed to more austere surfaces, damage to the first stage rotor blades was found during subsequent pre-test inspections (Figure 10). After considering a number of alternatives, the decision was made to install a second set of screens over the fan inlets (Figure 11). The original inlet screens were retained. The new screens were displaced outward from the fan inlet. A much finer mesh screen was selected for the new screens to reduce the possibility of large size foreign objects entering the fan inlet and damaging the fan. This supplemental screening did not completely enclose the fan inlet. The screens were placed in the predominate flow patterns as determined by reviewing video recordings of off-runway tests. For the majority of the test conditions, these screens provided the necessary protection. However, during selected maneuvers on austere surfaces, the flow streams are not clearly defined and foreign objects can enter the fan inlet from any direction (Figure 12). This is especially true during turning maneuvers on dry, sandy surfaces with no wind or a tail wind condition.

Additional work on this problem was undertaken during the USAF In-House Test Program when new damage was discovered. This work will be discussed in a later section of this report.

The ASP-10's are controlled in the same manner as they were on the XC-8A. A single control panel houses engine performance monitoring instruments, switches, and the necessary system circuit breakers. The panel is portable and is usually installed in the back of the vehicle towing the ACET. All electric and electronic signals from the control console are carried to the individual Engine Control Boxes (ECB's), located in the forward electrical distribution bay. Not all of the control and engine management functions required for the XC-8A installation were necessary on the ACET. Therefore, modifications were made to the ECB's to eliminate any superfluous functions, such as the thrust or cushion selector switch. The objective of these modifications was to reduce the complexity of the ECB's, if possible, while retaining the critical control authority required for the operation of the ASP-10's (Reference 2). The ECB's were successfully modified to the ACET application. However, very little impact was made in reducing the complexity of these boxes. Fortunately, the reliability of the ECB's has been very high throughout both the contractor's and the USAF's test programs. Continued use of this vehicle will dictate consideration of an



Figure 10. Typical Damage to First Stage Rotors of F-10 Fan



Figure 11. First Generation Protective Screen for F-10 Fan



Figure 12. Typical Off-Runway Foreign Object Environment

alternate lift system for the ACET since only a limited number of spare parts were manufactured for the ASP-10's and the ECB's and these spares cannot be replaced without considerable design analyses.

4. SKIRT SYSTEM DEVELOPMENT

Performance data on a variety of different skirt systems (Figure 13), currently being used in the Air Cushion industry, were reviewed during the design phase of the program to select a skirt system which met the requirements of the ACET Program. The original design selected for the ACET was identical to that recommended in the AATS Preliminary Design except for modifications incorporated to increase heave stability. The ACET air cushion system consisted of three jupe skirted air cushion cells (Figure 14). The smaller cell, 120 inches in diameter, is located on the Power Module to support the load from the aircraft's nose wheel. The two larger cells, 192 inches in diameter, are attached to the Center and Aft Modules to support the loads from the main landing gear of the aircraft. The design of the jupe is illustrated in Figure 15. The skirt material selected was a nylon fabric weave coated with neoprene to a weight of 90 ounces per square yard. This material had been previously qualified for ACV operations. Each basic skirt was fabricated from three segments of this material. When the skirts were assembled, each had an inward taper of 9 degrees to insure stable operation for payload weights below 35,000 lbs. Two release pleats were incorporated into the rear of each cell (Figure 15). These pleats served two functions. The first of these was to permit discreet obstacles to pass out of the air cushion cell without snagging and damaging the skirt. The hoop or circumferential tension was maintained by elastic straps installed over the pleats (Figure 16). Each restraint strap was made from 1/2-inch-diameter "shock" cord. A strap consisted of a continuous piece of cord, looped nine times and fitted into a sleeve of skirt material. Important features of this design were the high initial break-out force required to begin stretching the straps and the non-linear force required to elongate the straps. These characteristics were employed in the second purpose for the release pleats, cushion venting to control heave oscillations.

The calculated venting schedule was zero venting below a payload weight of 35,000 lbs and 0.02 square feet of venting per psfg of cell pressure above 35,000 lbs of payload. A series of holes was cut in each of the release pleats (Figure 15). The total venting area per pleat was 0.57 sq ft or a total venting area of 0.114 sq ft per cell. The cord tension in each the restraint straps was adjusted to meet the required venting schedule, as defined by BACT's stability analysis. Below a cell pressure of 0.585 pounds per square foot gage (psig) which corresponds to a payload of 35,000 lbs there was zero supplemental cushion venting. When the pressure in the cells increases above 0.585 psig, the required 0.02 sq ft of additional venting area per psfg is provided until a cell pressure of 0.76 psig is reached. At this cell pressure and above, the maximum supplemental venting of 0.114 sq ft is applied to each cell.

In a further attempt to improve the heave stability characteristics of the transporter, the air distribution system to the individual cells

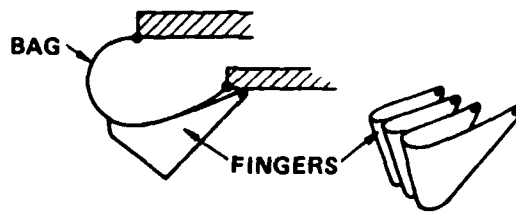


Figure 13a - Bag-Finger Skirt

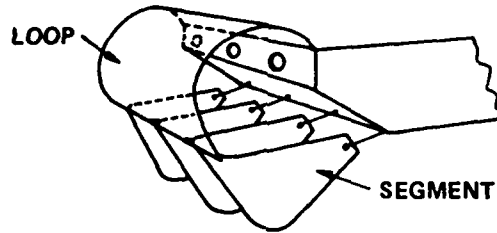


Figure 13b - Loop-Segment Skirt

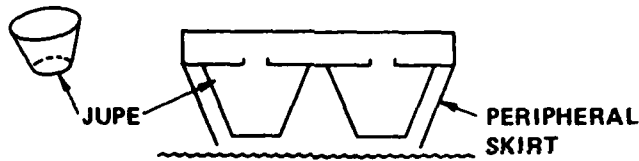


Figure 13c - Jupe Skirt

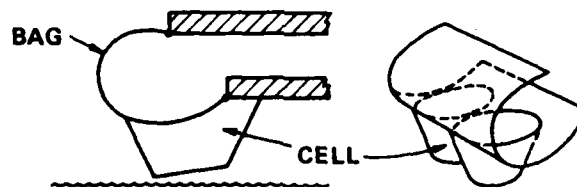


Figure 13d - Pericell Skirts

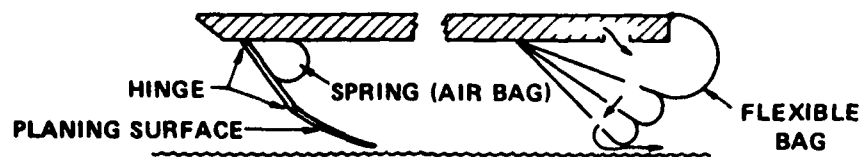


Figure 13e - Hinge Seals

Figure 13. Basic Skirt Systems



Figure 14. Jupe Skirt System Installed on the ACET

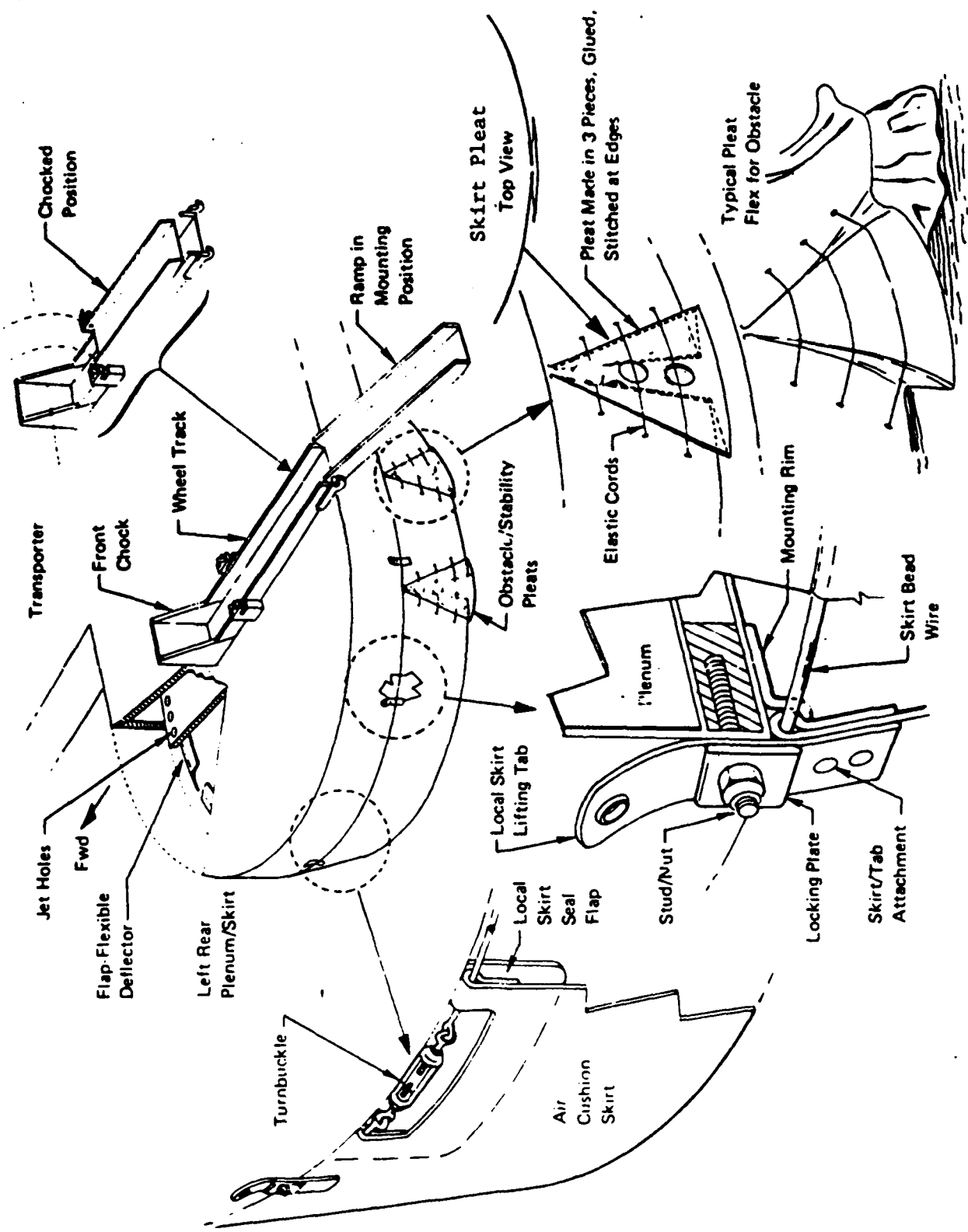


Figure 15. Details of Jupe Skirt System Design

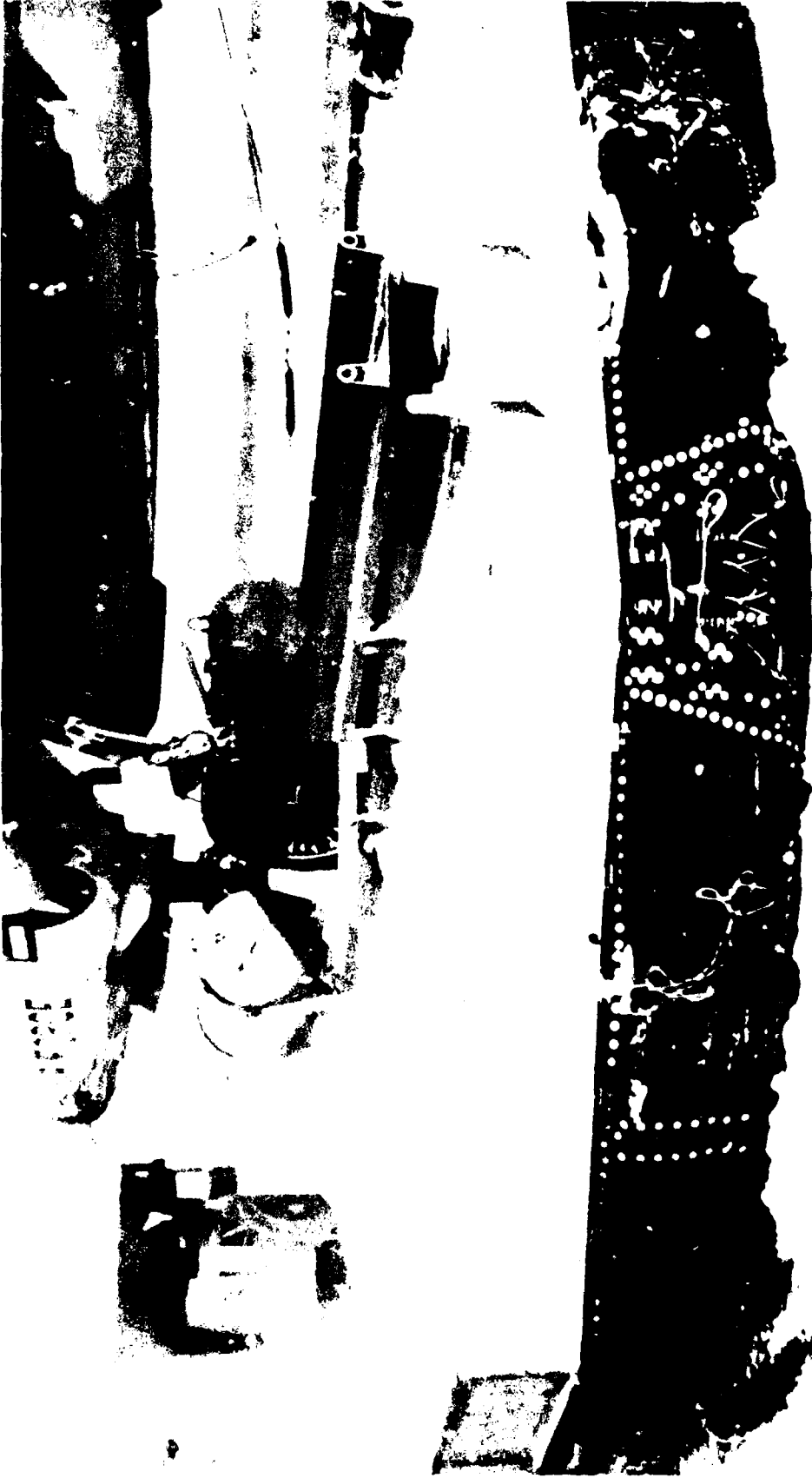


Figure 16. Installation of Release Pleat Restraint Strap

was modified for the ACET. The literature search for potential solutions to heave instabilities also revealed that a single orifice feed from the plenum to the cushion cell can be destabilizing under certain loading conditions when jupe skirts are installed on the vehicle. The approach which produced the most consistent positive results was to employ a series of orifices around the periphery of each cell instead of a single orifice near the center of each cell. In conjunction with the peripheral feed holes, a ring of deflectors was incorporated into the design (Figure 17). The function of these deflectors, installed immediately inboard of the feed holes, is to redirect the flow of the cushion feed air and force this flow to follow the inside contour of the jupe skirts. The purpose of this approach was to reduce skirt oscillation and improve the heave stability of the transporter.

This was the configuration of the skirt system at the start of the ACET Test Program. A de-commissioned F-101b aircraft was used as the payload for the testing of the ACET. This aircraft was selected because of its availability and its close approximation to the F-4 series aircraft (Table 2). For the first series of tests the empty configuration of the aircraft was used as the payload. In this configuration, without ferry tanks, the F-101B weighs 30,475 lbs. The first checkout runs produced encouraging results. The ACET was stable in pitch, roll, and heave. The tow loads were well within the capabilities of a standard two wheel drive truck on a concrete surface and dry grassy terrain. After approximately 5 hours of operations, the jupe skirt began to deteriorate. The original 9 degrees of inward taper had been reduced to 0 degrees of taper overall and certain areas of the skirt exhibited a slight outward taper. This configuration (Figure 18) is unstable for a jupe skirt and heave instabilities were encountered at lower gross weights, 30,475 lbs, and higher frequencies, 6 Cycles per Second (Hz), than were predicted by the stability analysis.

TABLE 2

AIRCRAFT COMPARISON

	F-101B	F-4E
MAXIMUM GROSS WEIGHT (LBS)	51,000	57,000
WHEEL BASE (FT)	23.0	23.8
WHEEL TRACK (FT)	20.0	17.9



Figure 17. Installation of Cushion Air Deflectors

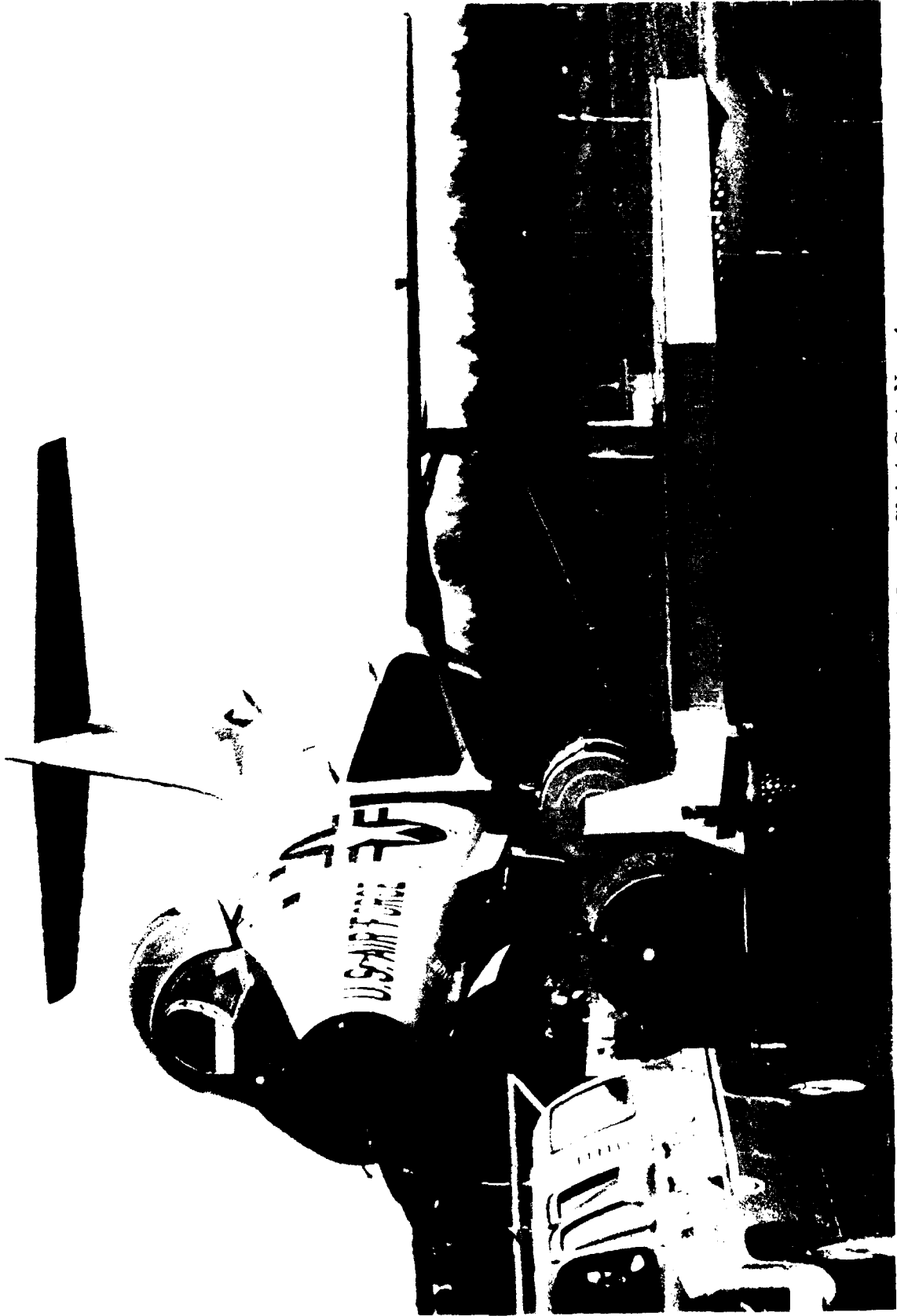


Figure 18. Deformation of Jupe Skirt Set No. 1

A material stretch problem was suspected. A series of modifications were incorporated into Skirt Set No. 1 in an attempt to control the growth of the skirts and recover a stable configuration. These attempts were unsuccessful and the stability of the skirts continued to deteriorate. Thus, the ACET Program was forced into parallel skirt development and stability improvement efforts while in the middle of the testing of the vehicle. A second ship's set of jupe skirts was designed and manufactured for the ACET. This set included a number of design changes based upon a series of coupon tests conducted on various skirt materials. The number of segments was increased from 3 to 15. This was done in an attempt to align the circumferential or hoop stresses of the skirt with the orientation of the nylon fabric of the material wherever possible. The coupon testing provided data which indicated that material stretch could be held to 5.0 percent if the load path was along the axis of the fabric. If, however, the load was applied transverse to the fabric, material growth on the order of 20.0 percent can be expected. A limited number of tests were conducted with the load applied 45 degrees to the nylon fabric. A 20.0 percent growth was recorded for this loading also. Therefore the load path must be aligned with the axis of the fabric wherever possible to minimize skirt growth. The inward taper of the second set was increased to 12 degrees to accommodate the anticipated growth of the skirts and still maintain a 9-degree operating configuration. Two reinforcing belts were also sewn onto each of the skirts in the peripheral direction to further restrict the outward growth of the jupe skirts. The obstacle release pleats were also deleted to increase the hoop strength of the new skirt system. Finally, the skirt material thickness was increased from 0.070 inches to 0.125 inches to improve skirt wear characteristics.

Initially, the design changes incorporated into Skirt Set No. 2 were successful. A stable configuration for the jupe skirt was achieved, and satisfactory performance both on hard surface and off-runway conditions was demonstrated at a payload of 30,475 lbs. However, after approximately 4 hours of operation, a significant (measurable) elongation of the skirts was observed and the heave oscillation problem re-occurred at payloads of 30,475 lbs and above. Depending upon the payload weight, the location of the payload on the deck of the ACET and the power setting of the ASP-10's; heave oscillations of 2 Hz and 6 Hz were observed. The occurrence of these oscillations was limited to hard, smooth surface operations. Localized skirt contact produced sufficient damping to control the heave during off-runway operations. This same effect could be artificially induced on a smooth surface by decreasing the power setting of the ASP-10's. This reduces the mass flow to each of the air cushion cells and causes an increase in skirt contact area. While this served as an interim solution to the problem, it was unacceptable as a long term answer because of the increased skirt wear. An alternate solution had to be incorporated into the system to permit operations on hard, smooth surfaces at high ASP-10 Power Settings, 90.0 to 100.0 percent, to minimize skirt wear.

A review of video tapes of several tests revealed a number of pertinent factors to be considered in the search for a solution to the heave problem:

a. The obstacle release/stability pleats reduce the circumferential (hoop) tension of the jupe skirt and contribute to the de-stabilizing growth of the skirts.

b. The response of the pleats was too slow to control either the 2-Hz or the 6-Hz heave oscillations.

c. The ACET was reacting essentially as the original stability analysis predicted the jupe skirt system would respond to increase in payload if pressure sensitive cushion venting was not incorporated in the design. The only major difference, aside from the unpredicted 6-Hz oscillation, was that heave stability boundary was slightly lower than the analysis indicated.

These observations lead to the decision to conduct a second stability analysis to investigate a different approach to the passive venting of each cell. The new system was a hinged, spring loaded door with damping in each of the cells to provide positive venting of the cell whenever the cushion pressure exceeded the predicted maximum pressure for stable operation. This condition could occur either during hover, zero forward velocity when the payload weight caused the cushion pressure to exceed the limit for stable, unvented operations, or during towing operations when traversing uneven terrain causes the cushion pressure fluctuations exceeded the response limits of the doors.

The heave stability analysis was conducted by the Landing Systems Group of the Boeing Military Aircraft Company. Again, the EASY 5 air cushion models and programs were used to accomplish this analysis. The goal of this analysis was to size the stability vents required to eliminate both the 2-Hz and the 6-Hz heave oscillations. The results of this analysis are presented in Table 3. Of particular interest, is the effective vent slope required for the stability vent doors. Even with the updating of the analysis by inclusion of test results, the analysis indicated that the same venting schedule was required to achieve heave stability throughout the payload range for the ACET.

With this passive venting system installed on the ACET (Figure 19), improvements were noted and it was observed that the doors actively responded to the 2-Hz oscillation. However, the stability vent doors did not totally eliminate the 2-Hz heave. Sufficient flexibility had been designed into the vent doors to permit tuning of the doors to correct any factors not included in the analysis. Preliminary adjustments of the spring and damping constants suggested that a configuration for the main and nose vent doors could be found which would provide the necessary control for the 2-Hz oscillation. However, these tests clearly indicated that vent doors were totally ineffective in controlling the 6-Hz heave oscillation, the more violent and potentially more damaging of the two oscillations. A detailed review of the stability vent door system revealed that the natural frequency of the main cell doors was very near 6 Hz. Thereby necessitating a modification to the doors to change their natural frequency. However, a more disabling problem was discovered during low-speed tow tests over broken asphalt and snow covered terrain.

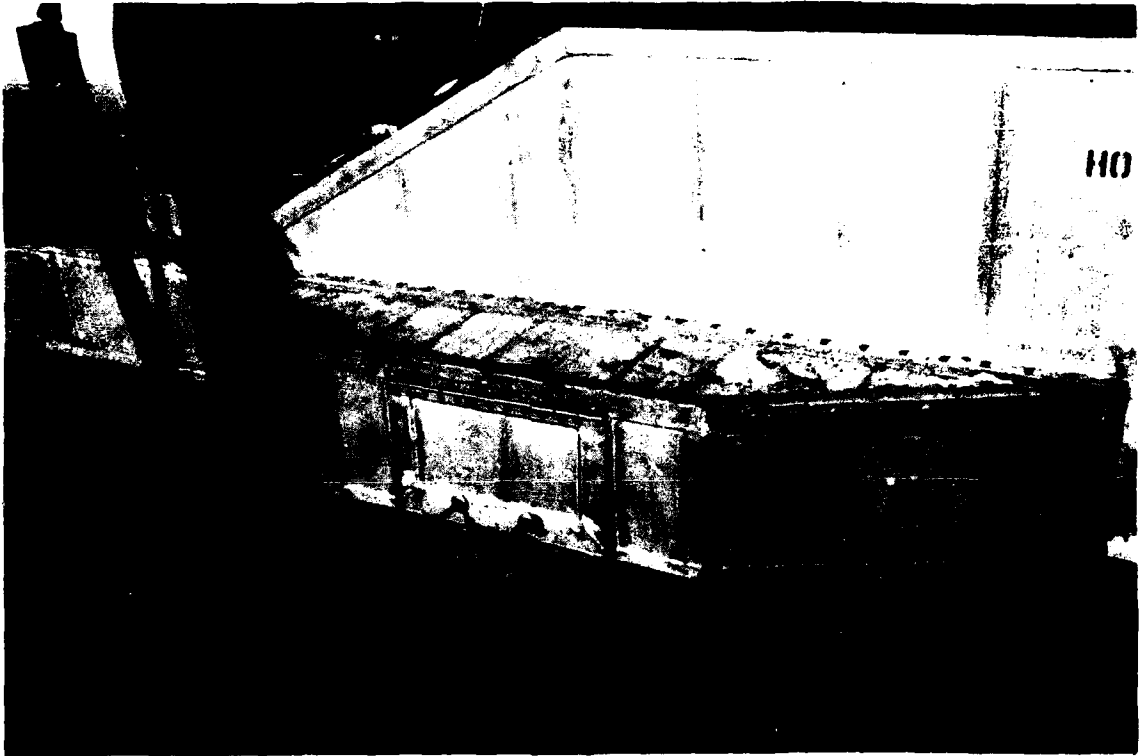


Figure 19a. Nose Cell Door

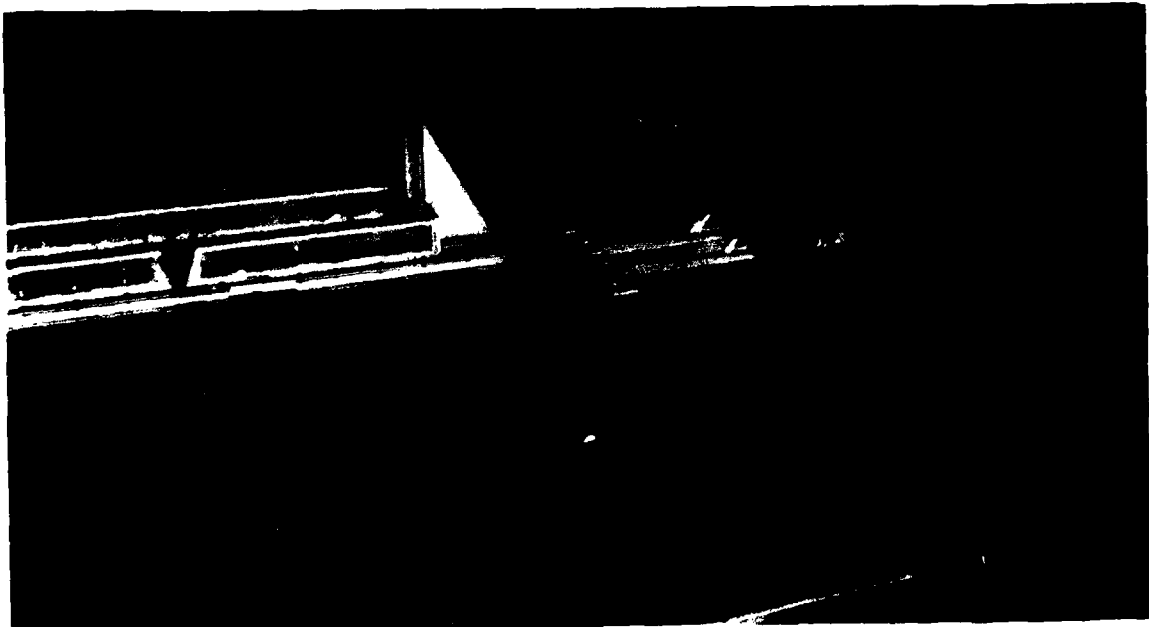


Figure 19b. Main Cell Door, Typical

Figure 19. Stability Vent Door Installations

The problem centered around the sweeping action of the jupe skirts as the ACET traverses a surface. If the surface is relatively free of debris, the performance of the skirts is not severely affected. However, on the more austere surfaces which have a significant amount of loose material, i.e., rocks, chunks of asphalt, snow, ice, frozen ground, etc., the ability of the ACET to perform its mission is severely impaired. This sweeping of the surface impacts the performance of the ACET in two areas. These areas are increased drag or towing forces and loss of cushion pressure. The increase in towing forces is most noticeable on snow covered surfaces. As the ACET is towed over a snowy surface, the snow is broken up and collects in the converging section of the leading edge of the main cells. Since the skirts physically touch at this point, the snow does not have a clear path to escape this area. Prolonged periods of operating on snowy surfaces result in a substantial build-up of snow (Figure 20). Depending upon the condition of the surface underneath the snow, it is possible for the tow vehicle to lose traction and become stuck. This actually happened during one test. The payload weight was 30,475 lbs, the empty weight of the F-101B. The surface was a frozen grassy field with deep ruts, filled with ice and covered with 9 inches of powdery snow. The ACET was being towed by a Unimog, a four wheel drive utility vehicle. A second vehicle had to be attached to the ACET to pull it out of the field. The build-up of snow rapidly increased the tow forces required to move the ACET and exceeded the capabilities of the tow vehicle. Also, under the condition of a large dam of snow or other debris building up in front of the main cells, there is a high potential for damaging the skirts.

The loss of cushion pressure occurs as a result of the build-up of loose material on the inside trailing edge of both the nose and main cells. The critical surface for this problem is broken up asphalt, similar to a damaged runway. The build-up of pieces of asphalt inside the skirts results in excessive loss of cushion pressure since a jupe skirt does not conform to surface irregularities as well as other types of skirt systems. If the loss exceeds the capabilities of the ASP-10's, the cushion cells will collapse (Figure 21). This characteristic of jupe skirts was aggravated by the deletion of the obstacle release pleats from the skirts to improve the heave stability of the ACET. The inability of the jupe skirts to shed debris that has been captured by the main and nose cell skirts reduces the load carrying capability of the transporter, increases skirt wear and increases the tow forces required to move the ACET.

The failure of the jupe skirt system to supply acceptable off-runway performance and the impact of the skirt shape on heave stability led to the decision to change skirt systems. After reviewing the basic skirt systems currently being used on ACV's (Figure 13), a segmented finger skirt was selected for the ACET. The performance goals of the ACET did not warrant the added complexity and weight of a bag-finger skirt system. The first ship's set of segmented fingers were fabricated from 40 ounce, nylon reinforced hovercraft skirt material (Figure 22). The large cutout in the sides of the fingers which butt together were introduced into the design to reduce the total weight of the segmented finger skirt system and

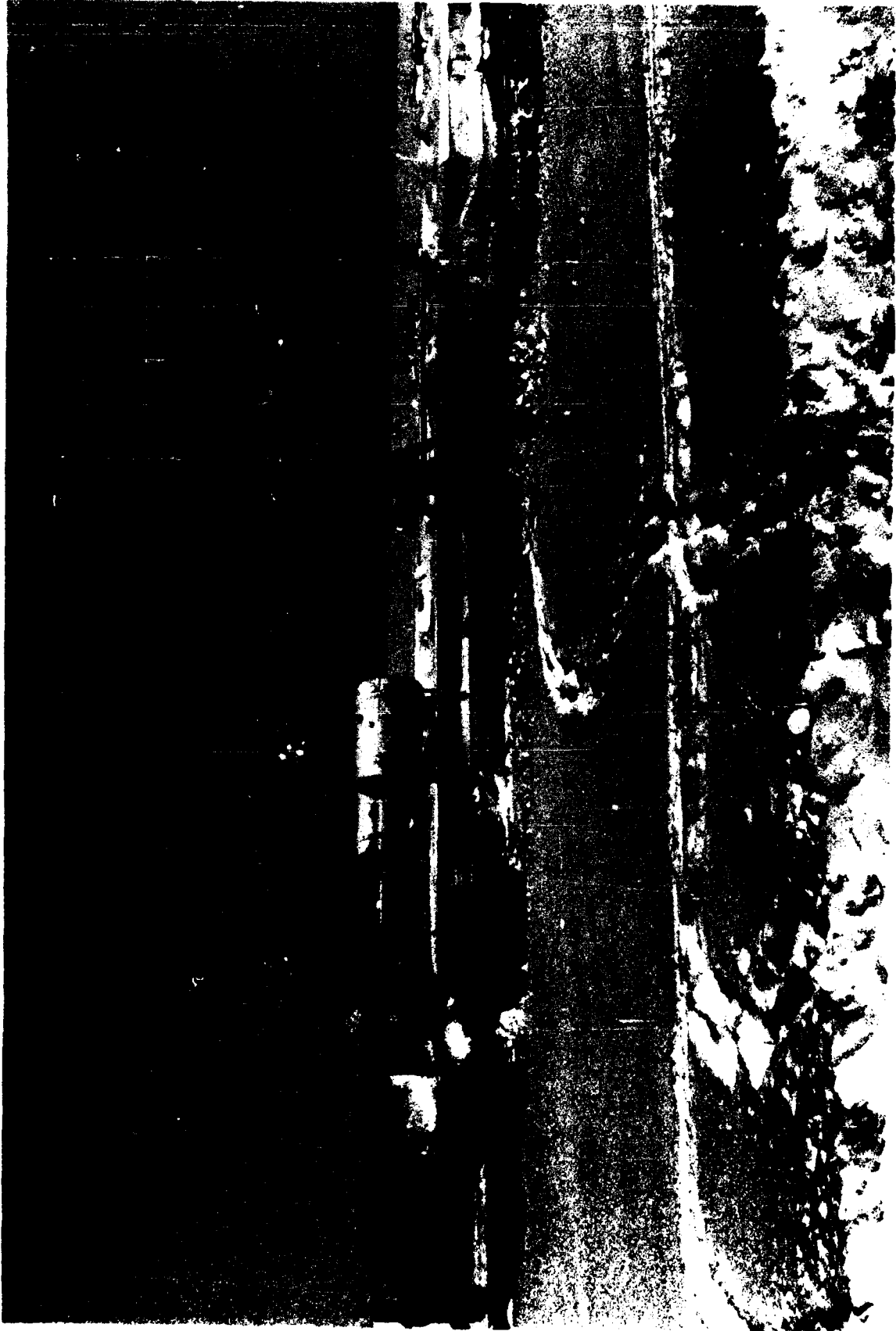


Figure 20. Buildup of Snow in Front of Main Cell Jupe Skirt



Figure 21. Loss of Cushion Because Of Debris Inside Main Cell

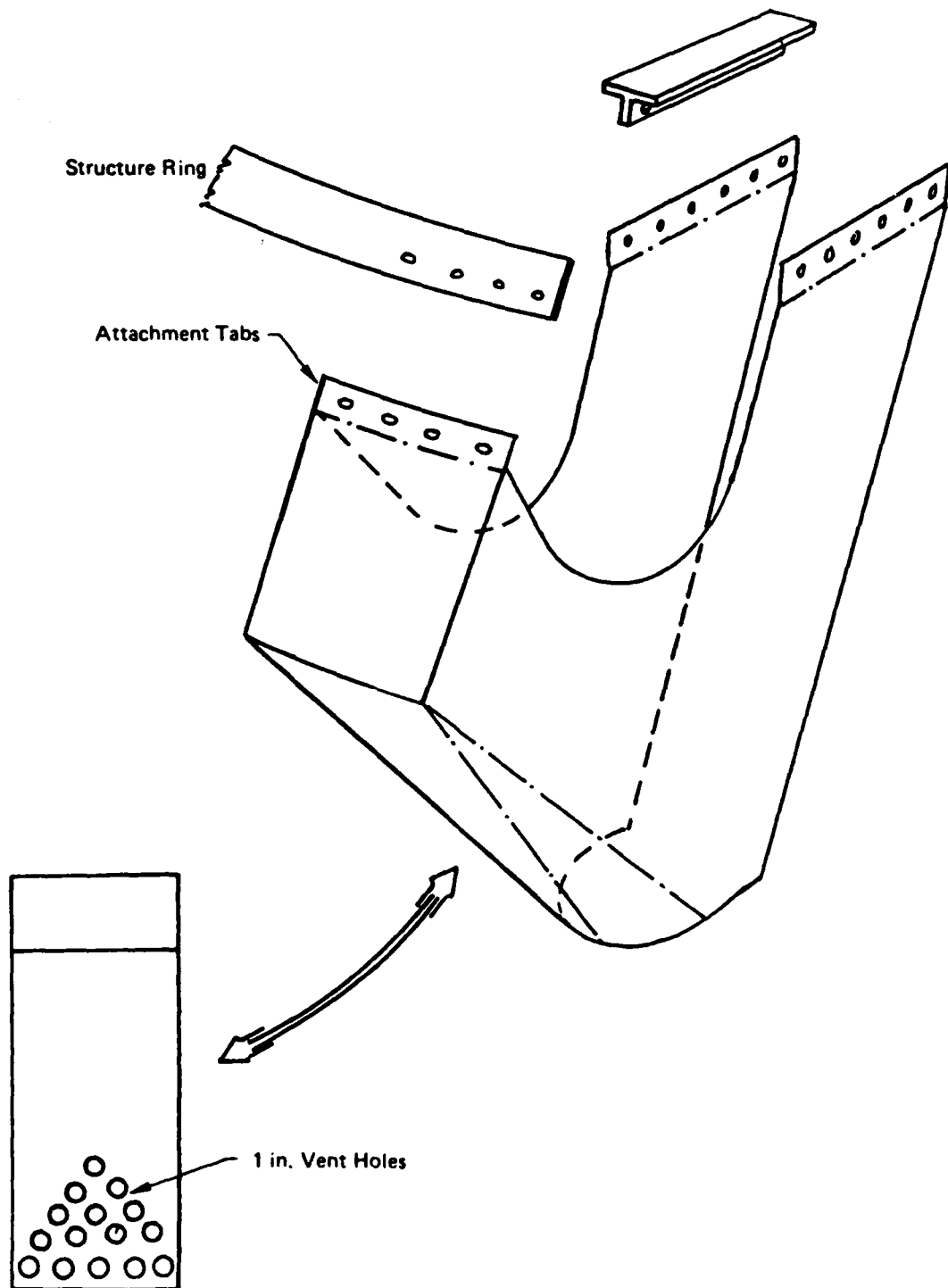


Figure 22. Segmented Finger Geometry

TABLE 3
ACET STABILITY VENT DESIGN PARAMETERS

Parameter	Nose Cell (*)	Main Cell
Natural Frequency (radians/second)	80.0	60.0
Damping Ratio (nondimensional)	0.3	0.3
Discharge Coefficient (nondimensional)	0.85	0.85
Vent Dimension (inches)	14.0	28.0
Nominal Effective Area (square feet)	0.292	1.076
Nominal Pressure (psf)	128.5	117.0
Effective Vent Slope (square feet/psf)	0.004	0.016
Spring Constant (lb/inch)	38.25	75.00
Damping Constant (lb per inch/sec)	0.30	0.75
Spring Preload (lb)	53.0	193.0

(*) Parameters for a single door, two vent doors were installed in the Nose Cell

to allow a small amount of circumferential flow redistribution to eliminate the possibility of pressure gradients within the fingers. The fingers' outward faces are tapered inward for the lower two thirds of the finger depth to enhance heave stability. The individual fingers are attached to the ACET structure at the outer face by means of attachment tabs, an extension of the finger's outer face. These tabs are riveted to a circumferential aluminum ring on the structure. The inner tabs are riveted to 1/8-inch aluminum tee sections attached to the lower deck of the vehicle. Each finger wall shares a tee section with the adjacent

finger. Two finger walls are riveted to each section and washer strips are used to reduce the possibility of ripping out a finger. Rivets were used to facilitate the replacement of damaged or worn out fingers.

A total of 152 fingers are needed to complete a ship's set for the ACET. The nose cell requires 38 fingers while each of the main cells is made up of 57 fingers. Four different size fingers were used on the ACET. The difference was in the width of the finger (Table 4). The number of each size finger

TABLE 4

Size of Segmented Fingers

Finger Type	Width of Finger (Inches)
A	12.00
B	10.50
C	13.37
D	16.00

required for each cell is presented in Table 5. The modified fingers listed in Table 5 refer to those fingers which are installed at the trailing edge of each cell and have an obstacle deflector installed on the inner face of the finger. (Figure 23). The purpose of this deflector is to reduce the amount of debris scooped up by these fingers when the ACET is operating over austere surfaces. The makeup of the cells and the location of the modified fingers is shown in Figure 24. The segmented fingers were oriented to retain the same cushion areas as the jupe skirts. Therefore the operating pressures for the ACET remained the same and the soft surface capability of vehicle was not degraded by the installation of the segmented finger skirt system.

During the checkout of the segmented finger skirt system, the heave stability of the ACET was found to be generally the same, with the two different heave oscillatory modes persisting. An analysis of the data collected revealed the need to desensitize the cushion pressure to height changes. In all probability, this can most effectively be accomplished



Figure 23. Obstacle Deflector Modification to Finger

TABLE 5

NUMBER OF DIFFERENT TYPES OF SEGMENTED FINGERS IN SHIP'S SET

Cell	A	Modified A	B	Modified B	C	Modified C	D
Nose	10	6	14	4			4
Left Main	27	13	9		7	1	
Right Main	27	13	9		7	1	

TOTALS	64	32	32	4	14	2	4

by the use of a centrifugal fan with a flat pressure/flow characteristic curve (Reference 3). However this was not feasible for the ACET Program. Therefore, the pressure/flow curve for the ASP-10's was artificially flattened by cutting a pattern of vent holes in the outward face (skin) of the fingers, Figure 22, near the bottom. The pattern, cut into every fourth finger of both the main and the nose cells, provided an additional 1.0 sq ft of cushion venting area for each main cell and 0.5 sq ft of venting area for the nose cell. This approach, while not the most efficient from an operating viewpoint, was successful in eliminating the 6-Hz oscillation throughout the operating envelope of the ACET.

The installation of the segmented finger skirt system did eliminate the premature cell collapse and the high drag experienced with the jupe skirts when operating over austere surfaces covered with debris. Even though the 2-Hz heave oscillation persisted, adjustments in the ASP-10 power settings could be made which permitted stable operations with acceptable towing forces throughout the payload range of the ACET and the testing of the transporter could continue. In-depth investigations into the cause and control of heave were then deferred until the USAF in-house testing of the ACET. The results of this investigation will be discussed in later sections of this report.

5. CROSSWIND AND SIDE FORCE CONTROL

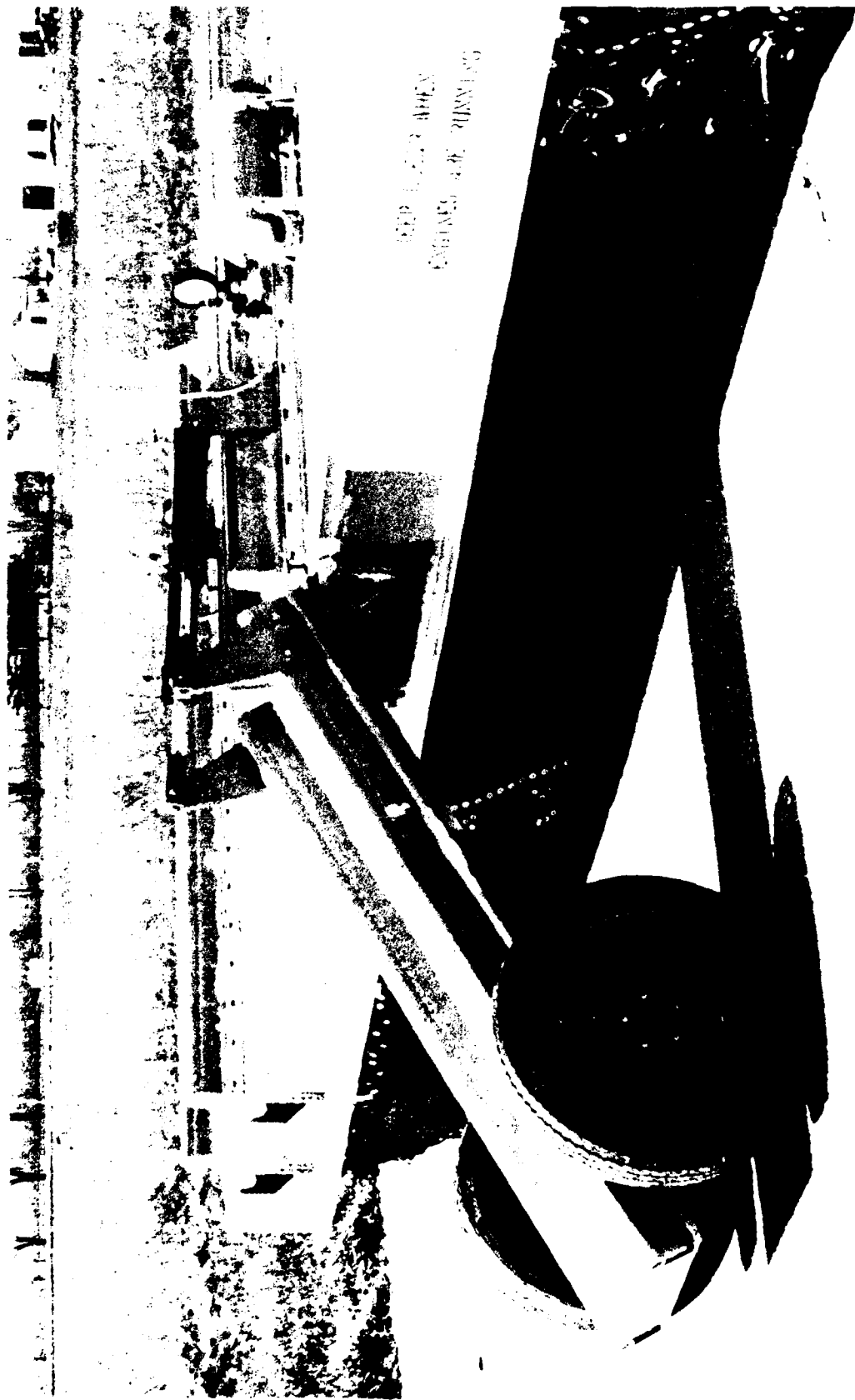
The goal of the ACET design was to keep the tow forces required to move the ACET within the capabilities of government vehicles currently in the inventory. Estimates prepared during the preliminary design efforts

indicated that the maximum force required to move the transporter with maximum payload would be on the order of 10,000 lbs. The tow bar is triangular with a pintle ring at the apex. Provisions were also made for vertical alignment of the tow bar to compensate for any height differences between the tow vehicle and the ACET by attaching the tow bar to the front of the vehicle with a pivot. With the lift system turned on and the cells fully inflated, the air bearing effect of air cushion systems makes controlling the ACET in a wind extremely difficult. The ACET tends to align itself into the wind. A similar control problem must be faced when traversing sloping terrain. There is very little control problems as long as the transporter is being towed straight up or down the slope. However, if the ACET is required to travel along the face of the slope, it will align itself with the direction of the slope. Towing operations can continue under these conditions but precise maneuvering of the vehicle is virtually impossible. To compensate for these characteristics, a quick-disconnect trailing wheel assembly was designed for and installed on the center or nose wheel loading ramp (Figure 25). The wheels were preloaded by pneumatic jacks which placed a nominal vertical of 1750 lbs on the trailing wheels when the vehicle was loaded with 60,000 lbs of payload. Using a friction coefficient of 0.80, a reasonable assumption for the type tire used, the 1750-lb load provides sufficient side force to counter a cross wind of over 30 knots and is sufficient to hold the ACET, at maximum gross weight, on a 3.0 percent side slope.

While the trailing wheel assembly was very effective in controlling the lateral drift of the ACET in direct crosswinds exceeding 25 mile per hour, the requirement to remove the trailing wheel assembly before an aircraft could be loaded or off-loaded was unacceptable from an operational standpoint. Preliminary testing was continued with this configuration to fully evaluate the performance of the trailing wheel assembly and to identify any modifications or improvements. When the ACET was being fitted with the segmented finger skirts, new main landing gear ramps were also installed on the transporter (Figure 26). Trailing wheel assemblies were incorporated into the new design. These assemblies were permanently installed on the main ramps and did not have to be removed to load or off-load an aircraft (Figure 27). The trailing wheel concept has been tested on a wide variety of surfaces, successfully. The only time a loss of control was observed was during a cold weather test. The ACET was being towed over a snow covered taxiway with a 10 mile per hour crosswind. Under the snow were large patches of ice. Whenever the transporter crossed one of these patches the ACET would start to rotate into the wind. This was only a transitory condition since the vehicle corrected its alignment as soon as the trailing wheels were clear of the ice.

6. LOADING AND OFF-LOADING OF AIRCRAFT

Since the primary function of the ACET is to transport aircraft, provisions for accomplishing this task were included in the original design. The components required for the loading and off-loading of aircraft include the following:



DEPT. OF THE ARMY
ENGINEERING DIVISION

Figure 25. Nose Ramp Trailing Wheel Assembly



Figure 26. Main Ramp Trailing Wheel Assemblies



Figure 27. Trailing Wheels During Loading/Off-Loading

- a. Ramps for the main and nose wheels (Figure 28),
- b. Tracks for the main and nose wheels on the deck of the ACET (Figure 28),
- c. Winch for pulling the aircraft during loading and restraining the aircraft during off-loading (Figure 29),
- d. Chocks for holding the aircraft in position (Figure 30).

Details on the design and selection of these components can be obtained from Reference 2.

The static testing of the transporter uncovered a number of deficiencies in the design criteria for the loading and off-loading of aircraft. Some of these were relatively easy to correct while others will require major modifications to the vehicle. The single most difficult problem was the off-loading of aircraft. In the original design approach, the lift system was to be running during the off-loading of the aircraft. The main cells were to be collapsed by artificially increasing the vent area of these two cells. This was accomplished with four ratcheted hand winches. Three cables were run to each winch. These cables were attached to the aftmost section of the main skirts. While the jupe skirts were installed on the ACET, this system worked moderately well. Venting the main cells produced sufficient deck angle to allow the aircraft to roll backwards off the ACET. When the skirt system was changed from the jupe to the segmented finger, the venting system was left unchanged. The cables were attached to twelve consecutive fingers at the rear of each main cell. However, since the segmented finger skirt minimizes the loss of cushion pressure whenever one or a number of fingers are deflected, the venting of the main cells was not as effective with the segmented fingers. A number of alternate approaches were considered during the contractor's testing; however none of the potential solutions were promising enough to warrant incorporation into the vehicle.

The scheme that evolved was to attach a sling to the arresting hook attachment bolt on the aircraft and pull the aircraft backwards until the main landing gear were just starting down their respective ramps. At this point primary control passed to the operator of the winch since the winch was used for controlling the speed of the aircraft going down the ramps. When the F-101B had stopped rolling, the main landing gear were on the hard surface while the nose gear was still on the deck of the ACET. Then the ACET was slowly pulled out from under the aircraft. During this maneuver, the winch cable was slowly played out to avoid overloading the winch motor. While this method was acceptable for a test program, the complexity of this approach combined with the level coordination required between the tow vehicle operators and the winch operator severely limited the applicability of this approach to an operational vehicle. An alternate means of offloading aircraft with minimal risk of damaging the aircraft is required. The best method, found to date, would involve mechanically inclining the ACET by using some type of hydraulic or pneumatic jacks, installed forward of the nose cell. This would involve



Figure 28. Main and Nose Wheel Ramp and Track Installation



Figure 29. Winch Installation

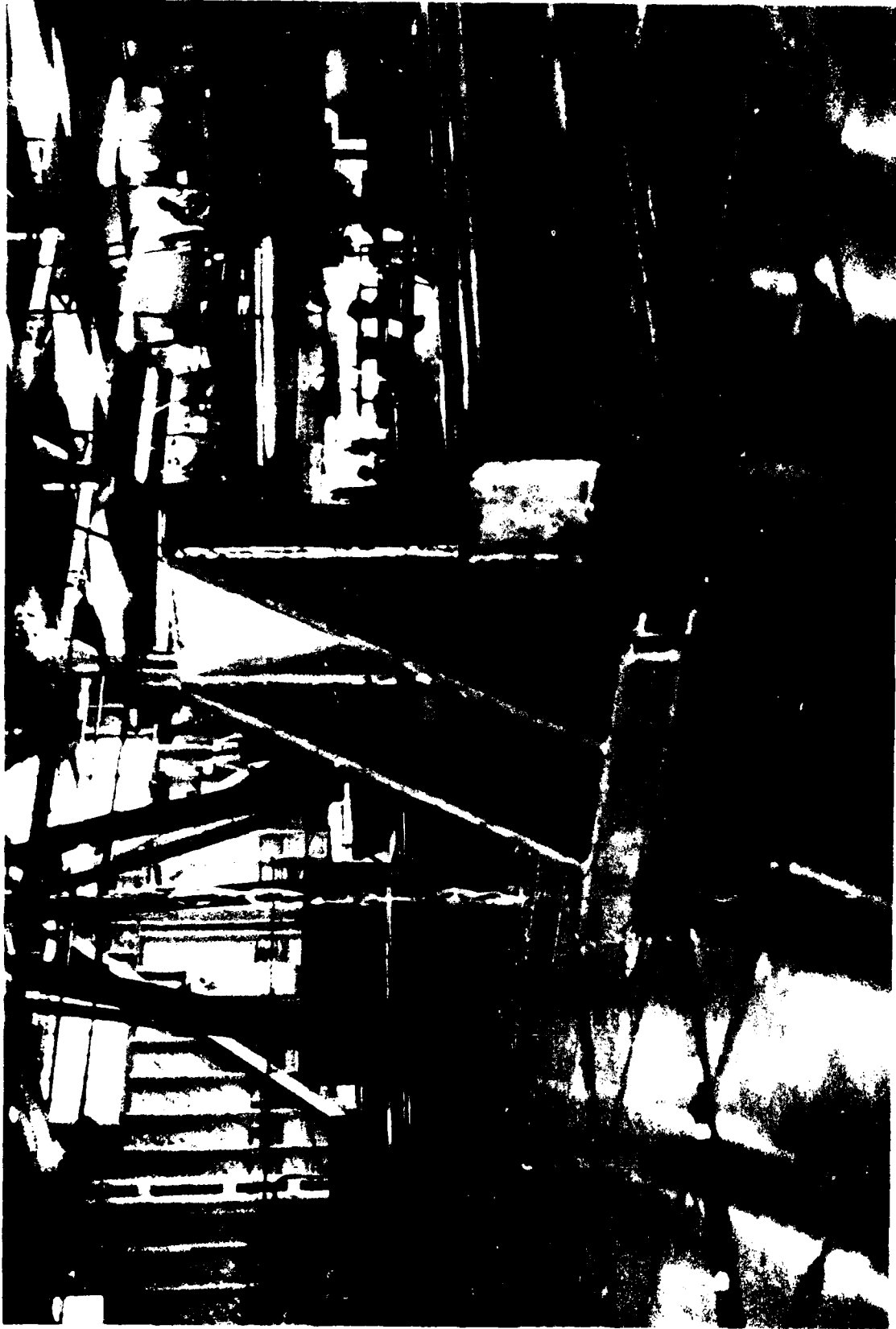


Figure 30. Aircraft Main Landing Gear Chocks

substantial modifications to the vehicle because the ACET was not designed for the bending stresses this approach would introduce into the structure. Additional research on this problem continued during the USAF in-house testing of the transporter.

As previously indicated, the winch was used not only to pull the aircraft onto the deck of the ACET, but also to restrain and control the speed of the aircraft during the off-loading of the aircraft. During the design phase, initial calculations made by BACT indicated that a 60,000-lb aircraft could be pulled up a 16-degree main wheel ramp using a 2-Horsepower(HP) winch, electrically driven from the 24 volt,dc system proposed for the transporter (Reference 1).

The BACT Test Program was plagued by reoccurring failures of the winch. These failures were the result of a number of related factors. The calculated maximum load the winch would have to be capable of generating was determined to be 13,409 lbs. The selection of the winch was based on this figure and the physical space available to install the winch. From the initial selection, the winch was a compromise. The 2-HP unit was marginally acceptable. However, a unit in the 5 to 10 HP range would have provided more margin of safety and faster loading times. BACT attempted to find a winch in this range which would meet the space requirements of the installation but was unsuccessful. In order to use the 2-HP unit a single snatch block had to be used. This reduced the load by half but doubled the time required to load the aircraft. This load, 6,705 lbs, was within the manufacturer's published limits. What was not realized at the time of selection was that winches are rated on the basis of the first wrap of cable on the drum. The rated load capacity drops appreciably with each wrap of cable. The maximum loading on the winch occurred when the cable was on its second and third wrap of the drum. This left very little margin for error.

The acceptability of the winch was further compromised by the dynamics of the loading process. If the loading/off-loading of the aircraft was accomplished in a smooth, continuous operation, the winch completed the task without any problems. If, as was most generally the case, the loading and especially the off-loading had to be interrupted, there was considerable potential for damaging a winch. A number of winch motors and brake assemblies were damaged during the initial testing of the ACET because these components had to absorb excessively high loads caused by the inertia of the aircraft whenever the loading/off-loading was stopped and started again.

Since it had already been determined by BACT that a unit with increased power could not be installed in the available space, other modifications were undertaken to reduce the winch loading and thereby increase the service life of the units. The most notable of these are the reduction of the main gear ramp angle from 16 degrees to 11 degrees. This reduction in ramp angle required a multiple segment main ramp instead of the single segment used for the 16-degree ramps. As previously indicated in the discussion of crosswind and side force control, the primary factors considered whenever the ACET was modified were the correction of the

problem or deficiency and the improvement of the operational capability of the vehicle. Therefore when the main gear ramps were modified, the segments were semi-permanently attached to the transporter, designed to fold into one another and the trailing wheels were made a permanent installation on the main gear ramps, Figure 26. This arrangement, Figure 27, facilitated the loading and off-loading of aircraft and reduced the winch loads by approximately 50 percent. The maximum load recorded during the loading of the F- 101B at maximum gross weight, 55,475 lbs, was 7000 lbs. The new main gear ramps and the stiffening of the winch mounting structure significantly improved the performance of the winch. However, care still had to be exercised during the loading and off-loading of the aircraft. A heavy hand on the winch control switches could still easily cause inertia forces to exceed the capabilities of the winch. The BACT Test Program was completed with the transporter in this configuration. Several attempts were made to refine the off-loading procedures. None of these produced any substantial improvements. Efforts in this area during the USAF in-house testing will be discussed in later sections.

7. TEST RESULTS

Considerable static testing was accomplished during the BACT Test Program. The majority of the this testing was devoted to troubleshooting problems discovered during the initial operation of the ACET and has already been discussed in previous sections of this report. References 2 and 3 are sources of additional information regarding the initial checkout of the ACET.

Once a stable configuration had been achieved, the dynamic testing of the ACET was begun. The payload for these tests was, again, the decommissioned F-101B aircraft. A total of three aircraft weights were used during the dynamic testing of the transporter. These weights were 30,475 lbs, the empty weight of the aircraft; 43,575 lbs, an intermediate aircraft weight; and 55,475 lbs, the maximum gross weight of the aircraft. Water was used to fill the aircraft's fuel tanks instead of JP-4 to reduce potential fire hazards. For a selected number of tests, 3600 pounds of external ballast were added onto the deck of the ACET to conduct tests at the maximum payload capability for the vehicle, 60,000 lbs. Also, the aircraft was spotted at three different positions on the deck of the ACET to evaluate the effect of vehicle center of gravity (cg) on the transporter's performance. During the dynamic testing, the ACET was operated on drv, wet (rain soaked) and snow covered runways, grass, dirt, and gravel.

The ACET met a majority of the original design performance goals. While all of the goals were important, the most critical performance indicator, next to static and dynamic stability in all three axes, throughout the payload range, were the towing forces required to move the ACET across austere surfaces. The ACET was successfully towed across a wide spectrum of surfaces considered to be typical of an airfield after an enemy attack. Tow forces were recorded for selected configurations and maneuvers. The forces for one configuration are presented in Table 6.

TABLE 6

TYPICAL ACET TOW FORCES

Configuration: Payload Wt = 55,475 lbs at Forward Position

<u>Condition</u>	<u>Tow Force (Lbs)</u>
Asphalt	1800
Rough Grass, Level	1350
Rough Grass, Average Uphill Grade of 2 Percent	3000
Sandy Field, 15-Inch-Tall Standing Grass	1500
Simulated Minimum Repair of Crater in Dirt, 12-Inch Lip	6900

Similar values for the tow forces were recorded when the ACET was operated over snow covered surfaces with a segmented finger skirt. The snow did not appear to have a significant impact on the tow force since the skirt system change discussed in previous sections eliminated the plowing problem. Even at the maximum payload condition of 59,075 pounds, the tow forces required to move the ACET were well within the capability of the four wheel drive vehicle being used for these tests. While the tow forces are within the capabilities of current Department Of Defense (DOD) Vehicles, there are other factors which suggest that the full potential of the ACET can only be achieved if it is self-powered. The advantages of a self-powered version of the ACET will be discussed in Section V of this report.

The terrain testing did reveal one of the major design objectives that the ACET could not meet in its present configuration. The design goal in question was that the ACET be towed at ground speeds of 30 knots, 35 miles per hour (mph), over all surfaces. While it is possible and was demonstrated to tow the ACET over a smooth, undamaged runway or taxiway at this maximum ground speed, the maximum attainable tow speed drops off drastically for off-runway conditions. On a relatively level grassy field, representative of the area adjacent to a runway, tow speeds of 15 mph are the maximum that can be achieved. While on a rough, grassy field, the maximum tow speed drops to 8 mph. The reason for this decrease in towing speed is the increasingly hostile environment the tow vehicle operator is forced to endure. Even with lap and shoulder belts, the operator cannot maintain control of the vehicle because he (she) is being thrown around the cab of the vehicle. This is not the case with the ACET.

The segmented finger skirts deflect to conform with surface irregularities and therefore, there is very little loss of cushion pressure which could result in the collapse of one or more of the cells. While the vehicle operator is being exposed to significant vertical accelerations, the vertical accelerations transmitted to the aircraft by the ACET are minimal. If the design tow speed for the transporter is to be achieved over off-runway conditions, an alternate means of propulsion must be incorporated into the ACET.

Controllability of the ACET in crosswind conditions was another major concern during the design of the ACET. In order to evaluate the directional controllability of the transporter, a series of tow tests were accomplished under various crosswind and climatic conditions. These tests started with a dry taxiway and a 5-mph crosswind component and proceeded through a 30-mph direct crosswind on a wet taxiway. Precise control was demonstrated in all cases. The only time the ACET exhibited a tendency to weather-vane, turn into the prevailing wind, is when the vehicle was towed across a short section of ice covered runway, in a 10-mph crosswind. The maximum deviation of the rear of the ACET from the centerline of the track of the tow vehicle was approximately 12 inches before the trailing wheel assemblies recovered and returned the ACET to the desired track. Also, during the directional control tests, the transporter was maneuvered through a 180-degree turn on a snow and ice covered taxiway that was 150 feet wide. The temperature during this test was -10 degrees, Fahrenheit and a 15-mph direct crosswind was blowing across the taxiway being used for the test. The fact that this maneuver was performed within the boundaries of the taxiway clearly demonstrates the controllability and maneuverability of the vehicle under conditions simulating operational deployment of the ACET.

If the ACET is to be used to transport aircraft/equipment across off-runway surfaces, the skirt system must have the capability to traverse discreet obstacles without significant loss of cushion pressure. This required efforts in skirt design which have already been discussed and evaluation of different skirt materials which will be discussed in later sections. As was the case with the jupe skirt, the segmented finger skirt system was designed to traverse discreet obstacles up to plus (bumps) or minus (holes) 12 inches in height or depth. The obstacle tests with the segmented finger skirt showed a marked improvement in the performance of the ACET. The premature or sudden collapsing of the skirt, because of excessive venting of the cushion was eliminated.

With the completion of the Stability and Performance Evaluation Tests, the contractor, BACT, demonstrated that an aircraft of the tactical fighter class can be winched onboard the ACET; secured (chocked) quickly; the ACET with the aircraft as the payload can be towed across terrain typical of what can be expected after an enemy attack; off-load the aircraft on an undamaged or repaired section of runway or taxiway being used to launch aircraft and the transporter can be quickly towed back to the revetment/shelter area to pick up another aircraft. While the results of BACT's Test Program were very positive, a number of technical deficiencies were uncovered and recommendations were made to correct these

problems (Reference 3). The evaluation of three of these recommendations formed the basis for the In-House Testing of the ACET. The details of the USAF Testing are presented in Section V of this report.

SECTION IV

MODEL TESTING

1. OBJECTIVES

The objectives of the model testing effort were to verify air cushion scaling laws, validate testing techniques, and evaluate analytical prediction techniques. The models were to be statically and dynamically tested on test machines located in the Mobility Development Laboratory (MDL). These machines, the Static Test Platform and the Dynamic Test Machine, are uniquely compatible with this type of testing, having been developed for the testing of ACLS models.

2. APPROACH

The model test program was conducted concurrently with the Contractor's Full-Scale Development and Test Program. The full-scale dimensions of the ACET were established during the initial design effort (Table 1) and were used in the development of the ACET models. Two models of the transporter were planned for this effort. The first model of the ACET was a representation of the vehicle at maximum gross weight -- 72,000 lbs (60,000 lbs of payload and 12,000 lbs of vehicle weight). This model was referred to as the Heavy Weight Model. The second model represented the ACET without any payload and was called the Light Weight Model. The Light Weight Model was to be used to investigate the performance of the ACET as a function of payload weight while the Heavy Weight Model was to be used to explore the performance limits of the ACET at maximum gross weight. The data collected during these tests were to be scaled up to predict full-scale values and then compared to actual test data collected during BACT's Test Program.

3. DESIGN OF THE MODELS

The two key limitations or restrictions which must be considered in the development of any model for testing in the MDL are the maximum allowable weight of the test article and the maximum physical dimension of the model. The Static Test Platform can accept model weights up to 7,500 lbs with a maximum dimension of 24 feet without any modifications to the platform. However, the Dynamic Test Machine can accept models which weigh less than 1000 lbs and have a maximum dimension of 12 feet and a ground contact area of 6 feet or less. For this application, the restrictions of the Dynamic Test Machine governed the development of the ACET scale models.

The scale models were designed and built to be dynamically similar to the full scale ACET. However, the models were geometrically similar only in the arrangement of the air cushion cells on the vehicle and their respective orientation with each other. The similarities, both geometric and dynamic, were derived from a dimensional analysis developed from the Buckingham " π " Theorem. This analysis shows that the forces acting on

the model can be described in a finite number of dimensionless groups. One of these groups is the Froude Number (Fr) which is defined by:

$$Fr = V/\sqrt{gL} \quad (1)$$

where V represents a reference velocity, L denotes a representative length and g is the gravitational acceleration. Maintaining a constant Fr insures the proper relationship between gravity and inertia forces. If a constant linear acceleration field is assumed, the dimensional analysis yields the scale factor between the full-scale vehicle and the model value of a particular quantity necessary to maintain the similarity. This relationship will be some function of the scale of the model, λ . A summary of the key scaling factors for the ACET is provided in Table 7.

Having established the scaling factors which will govern the development of the scale models of the ACET, the next step was to select a scale which insures compatibility of the models with both test machines. As previously indicated, the two critical parameters are the weight of the model and the maximum dimension of the test article. The scaling factor for the weight and mass of the model is " λ " to the third power (see Table 7). Using the maximum allowable weight for a test article on the Dynamic Test Machine, 1,000 lbs and the maximum gross weight of the ACET, 72,000 lbs, a " λ " of 0.425 was calculated. However, when this value was used to calculate the dimensions of the model, the maximum width of the model was determined to be 186.15 inches. This value greatly exceeds the maximum allowable of 60 inches. Clearly, the selection of a scaling factor for the ACET models would be controlled by the scaling of the transporter's width. The maximum width of the full-scale ACET is 438 inches. If the width of the models was 60 inches, the scale of the models would be 0.137 and the weight of the model would be 185.1 lbs, well within the weight limitations for the test machines. To insure adequate clearances and to facilitate the fabrication of the models, " λ " was frozen at 0.1. With this scale, the maximum width of the models was 43.8 inches and the model weight corresponding to the full-scale vehicle maximum gross weight was 72.0 lbs. A complete listing of the model design parameters is presented in Table 8.

Once the scale of the model was established, the general layout of the model structure was a straightforward process since the full-scale design was already finalized and the physical dimensions were available (see Table 1). However the weight restrictions for the models did require considerable effort to meet. The target weight for the Heavy Weight Model was 72.0 lbs while the target for the Light Weight Model was 12.0 lbs. Based upon preliminary weight estimates, a design for the Heavy Model was developed using aluminum bar stock and plate. The original target for the basic structure was 50 lbs. An estimate made from the design indicated that the weight would be approximately 45 lbs. The design of the Heavy Model structure was accepted and design efforts were focused on the Light Weight Model. The severe weight restriction precluded the fabrication of this model from aluminum. If extremely thin bar stock and plate were used to meet the weight requirement, the model would not have the necessary structure stiffness. Therefore alternate

TABLE 7

SCALING FACTORS FOR ACET

QUANTITY	FULL-SCALE VALUE	SCALE FACTOR	MODEL VALUE
Length, width, perimeter, height	L	λ^*	λL
Linear acceleration	a	1	a
Force	F	λ^3	$\lambda^3 F$
Moment of inertia	I	λ^5	$\lambda^5 I$
Mass, weight	m	λ^3	$\lambda^3 m$
Time	t	$\lambda^{1/2}$	$\lambda^{1/2} t$
Speed	v	$\lambda^{1/2}$	$\lambda^{1/2} v$
Angular acceleration	α	λ^{-1}	$\lambda^{-1} \alpha$
Pressure	p	λ	λp
Area	A	λ^2	$\lambda^2 A$
Power	HP	$\lambda^{7/2}$	$\lambda^{7/2} HP$
Pressure ratio	P_1/P_2	1	P_1/P_2
Flow	Q	$\lambda^{5/2}$	$\lambda^{5/2} Q$
Reynolds Number	Re	$\lambda^{3/2}$	$\lambda^{3/2} Re$
Volume	V	λ^3	$\lambda^3 V$

* For example, a 1/4 scale model requires that $\lambda = 1/4$.

TABLE 8
ACET MODEL DESIGN PARAMETERS

($\lambda = 1/10$)

PARAMETER	FULL SCALE	SCALE FACTOR	MODEL
Weight, lbs	68,000	$(0.1)^3$	68.8
Length, in	562.0	0.1	56.2
Width (maximum), in	438.0	0.1	43.8
Depth of skirt, in	24.0	0.1	2.4
Total Fan Flow, cfs	2,106.67	$(0.1)^{2.5}$	6.66
Nose cell pressure, psig	0.946	0.1	0.0946
Nose cell diameter, in	142.0	0.1	14.2
Main cell pressure, psig	0.803	0.1	0.0803
Main cell diameter, in	218.0	0.1	21.8

materials were evaluated. One of the first to be considered was fiber glass. While a model constructed from fiber glass would meet the stiffness requirements, a preliminary weight estimate indicated that the resulting structure would exceed the weight allocation for the structure by a significant amount.

After further review of potential materials, a 2-inch-thick sheet of polystyrene plastic was selected for the upper deck and the side walls of the model. The lower deck was fabricated from a thin sheet of aluminum. Aluminum was retained for the lower deck to insure that the peripheral feed holes to the cells were close approximations of a sharp edge orifice. The sharp edge orifice assumption is used in the calculation of flows. The target value for the Light Weight Model structure was 4.0 lbs. A weight estimate of the structure, based on the proposed design indicated a weight of 6.0 lbs. Even though the weight of the structure was considerably heavier than the estimated value required to meet the weight goal, the design was accepted since a lighter material could not be found. However, with the weight of the structure being this high, the designers were forced to consider removing the fan for the Light Model and mounting the unit on an auxiliary structure of some type to remove the fan weight from the total of the model. Different fans for the two models were not considered as a viable alternative because the difference in the fan characteristics would have made a direct comparison of the models' performance invalid.

The air distribution system for the models paralleled the full-scale vehicle. Pressurized air from the fan was directed into a large cavity between the upper and lower deck of the model. The individual air cushion cells were supplied with this pressurized air in the same manner as the full-scale transporter. A series of holes were located in the bottom deck near the outer edge of each cell, thus duplicating the peripheral feed system. Flow deflectors were also incorporated into each of the cells (Figure 31) to enhance the stability of the jupe skirt system. A thin neoprene material was used in the design of the jupe skirts, as well as the segmented finger skirts. No attempt was made to scale the material characteristics of the full-scale skirt.

The selection of the fan unit was critical to meeting the performance goals for the models. The key design parameters for the fan (See Table 8) were the capability to generate a flow rate of 6.66 cubic feet per second and cell pressures of approximately 0.1 psig. Further, we preferred that the fan be powered by a 400-Hz electric motor. A cursory review of off-the-shelf fan units in this performance range indicated that obtaining an exact match to the requirements was practically impossible. A number of engine/fan combinations were very near the performance goals but using any of these units would require that the flow be throttled down to meet the maximum flow condition for the models. During previous test programs, dynamic instabilities necessitated investigating the performance of models at points other than the design operating point. To accomplish this task a variable frequency generator was developed for the MDL. Varying the input power frequency to a 400-Hz electric motor provides an effective means of controlling the output of the fan without damaging the motor by overheating. This equipment was also available for the ACET model tests. The fan which came the closest to matching the 1/10-scale fan performance was the "MAXIAX," produced by Rotron, Inc. The design operating point for this fan is a flow of 7.5 cubic feet per second at a pressure of 0.369 psig. The procedure followed to match the output of the "MAXIAX" fan with the performance requirements for the 1/10-scale models of the ACET will be discussed in detail in Section IV, 5. TESTING OF MODELS.

The weight of the unit was 8.3 lbs. This weight was within the estimates made for the Heavy Weight Model but did verify that the fan could not be mounted on the Light Weight Model if the weight limitation was to be met. Rather, the engine would have to be mounted to an overhead fixture and flexible ducting run from the fan exit to the model. This approach limited the usefulness of the Light Weight Model considerably. Testing of this model was restricted to the Dynamic Test Machine. This installation permitted the support for the fan to be designed into the structure of the test machine without restricting the movement of the model.

During the design of both models, provisions for instrumentation were incorporated. The exact configuration of the instrumentation varied depending on the type of test being conducted. Instrumentation included pressure transducers to measure fan exit, plenum, and cushion cell

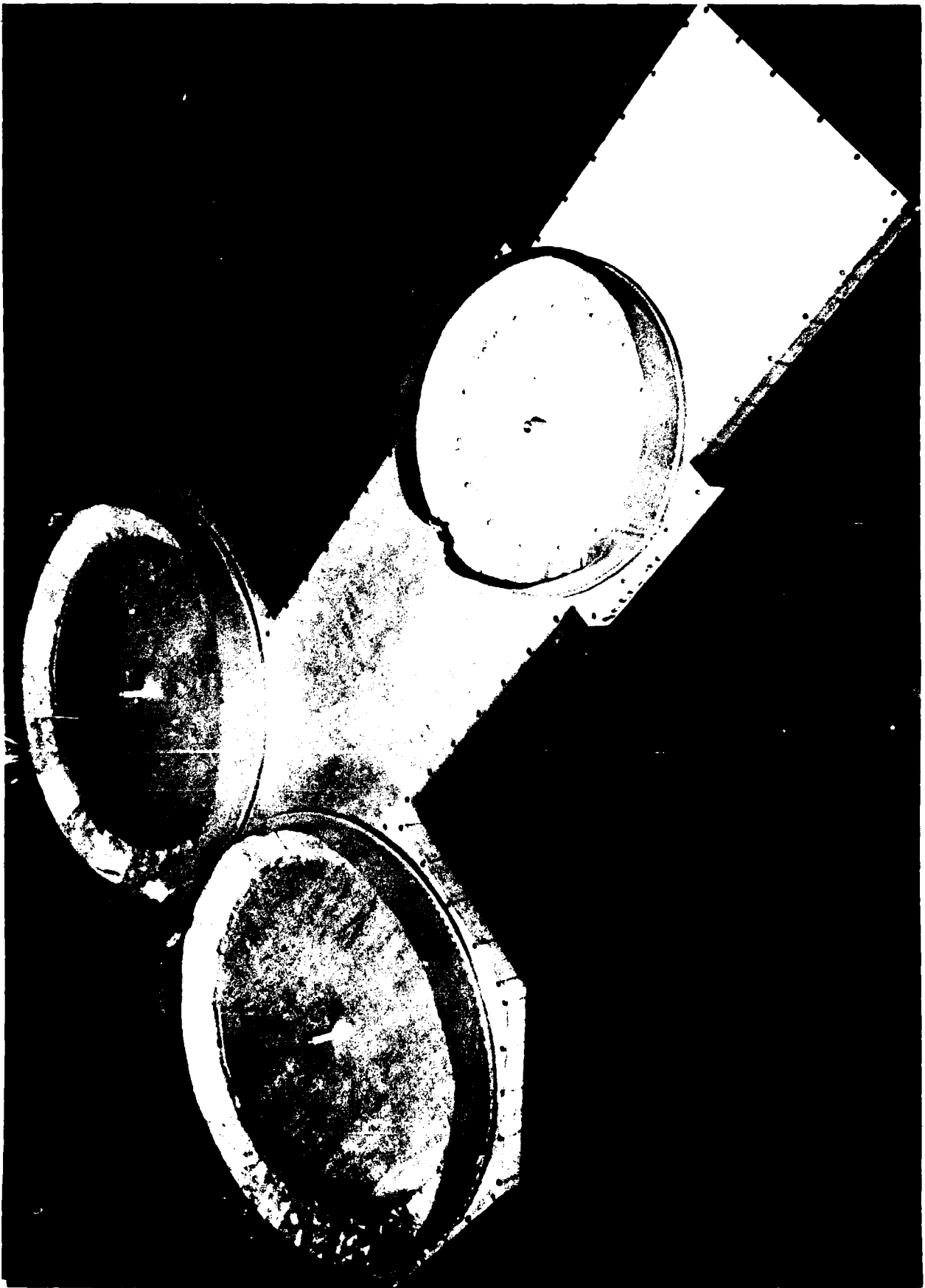


Figure 31. Jupe Skirt Installation on Heavy Weight Model

pressures, an accelerometer for the vertical axis (heave) acceleration, a gimbal to record pitch and roll displacements and a low range load cell to monitor drag loads during simulated low-speed towing.

4. FABRICATION OF THE MODELS

The Heavy Model was constructed from aluminum plate and bar stock. Standard construction techniques and materials were used. Countersunk flat head machine screws were employed in the assembly of the main structure. The junction of the lower deck and the bar stock sides of the model was sealed with a silicon based sealant to reduce air losses. The upper deck was removable (Figure 32) to permit access to the plenum area between the upper and lower deck of the model. This was required to facilitate the periodic calibration, and replacement if necessary, of the pressure sensors. The spacing of the machine screws in the upper deck was kept at 2 inches to minimize air losses between the upper deck and the sides. The weight of the basic structure of the Heavy Model was 46.0 lbs. The ducting from the fan exit to deck cavity was fabricated from fiber glass (Figure 33) to keep the total weight of the model under the limit dictated by the scaling analysis. A constant area was maintained from the fan exit to the plenum area between the decks. Also, the inner surfaces of the ducts were sanded to eliminate as much surface roughness as possible. The goal of these efforts was to keep internal pressure losses to a minimum. After final assembly of the model and installation of instrumentation (Figure 34), the model weight was determined to be 68.25 lbs. A detailed breakdown of the component weights is presented in Table 9. The difference between the assembled weight and the target model weight, 3.75 lbs, was to be used to adjust the cg location.

TABLE 9

MODEL WEIGHT BREAKDOWN

ASSEMBLY	WEIGHT (Pounds)	
	HEAVY WEIGHT MODEL	LIGHT WEIGHT MODEL
Structure	46.00	7.75
Fan Assembly	12.25	
Air Supply Duct		1.19
Skirt System	2.75	2.66
Gimbal	4.75	4.75
CG Adjustment	2.50	0.00
ACTUAL TOTAL	68.25	16.35
DESIGN TOTAL	71.00	11.00

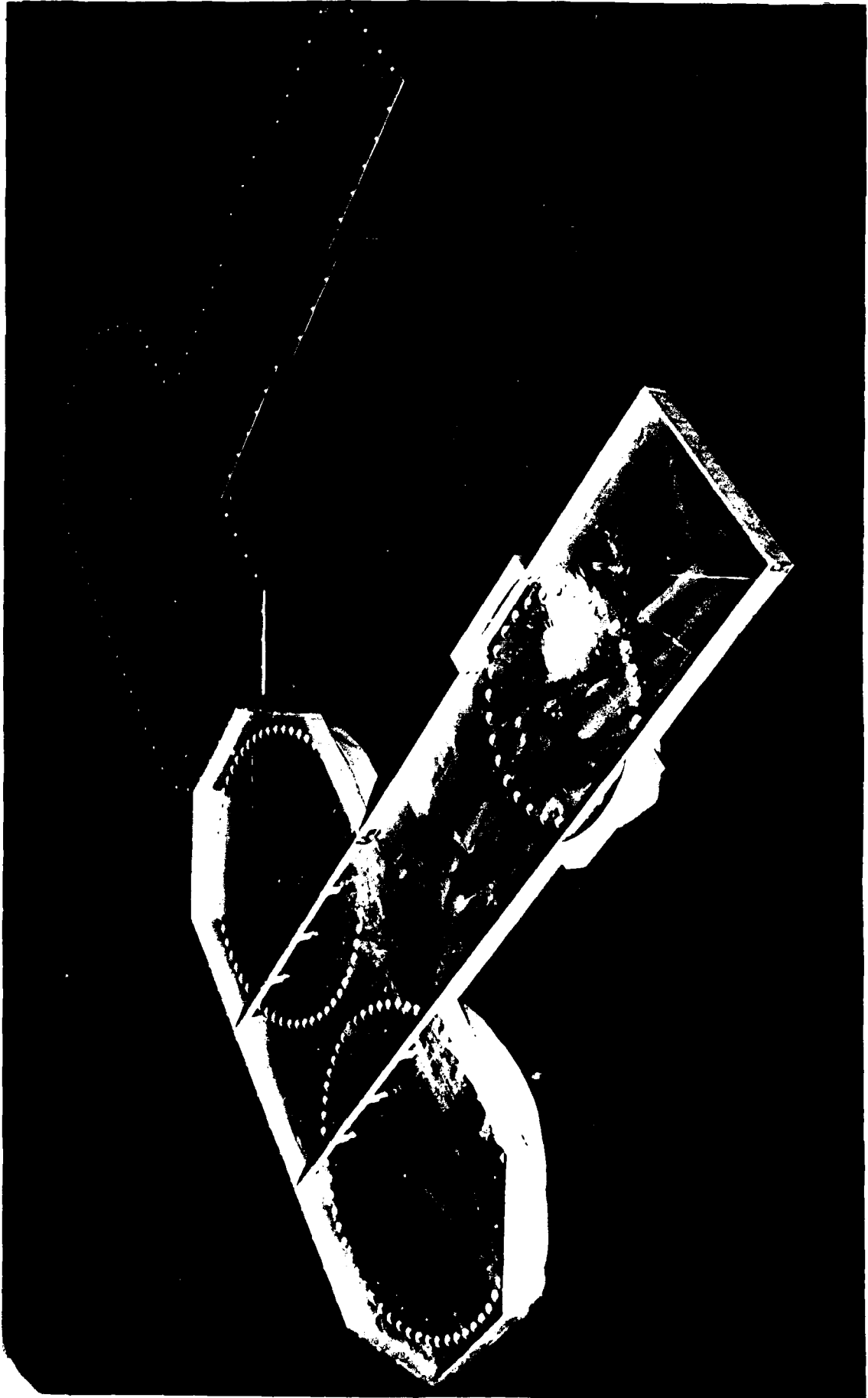


Figure 32. Basic Structure of Heavy Weight Model



Figure 33. Fabrication of Air Supply Ducts



Figure 34. Heavy Weight Model, Forward Fan Installation

As previously indicated, the weight restriction of the Light Weight Model forced a number of novel and unorthodox solutions to problems encountered during the fabrication of the model. Originally, the upper deck and sides of the model were to be fabricated from a single sheet of 2 inch thick polystyrene plastic and the lower deck was to be made from a thin, 1/32 of an inch thick, sheet of aluminum. During the fabrication of the upper deck, it was determined that a 2 inch thick sheet did not have sufficient strength after the material had been removed for the cavity between the two decks. Therefore, it was necessary to increase the thickness of the polystyrene plastic sheet to 4.25 inches to meet the strength and stiffness requirements for the Light Weight Model. While the cavity for the plenum was being cut from the 4.25 inch sheet, a number of deep gouges were accidentally cut into the surface of the plastic sheet, highlighting the need to take the steps necessary to preserve the surface integrity of the model before the start of the testing. After considering a number of possibilities, coating the plastic sheet with fiber glass resin was selected. This was determined as the best method of preserving the integrity of the sheet while keeping weight penalties to a minimum.

While the thin aluminum sheet did provide a means of preserving the sharp edge orifice assumption, it did pose additional problems during the assembly of the Light Weight Model. Since the sheet was very thin, it had a tendency to buckle and warp while the feed and attachment holes were being drilled in the sheet. Some of the warpage was permanent and a thin foam gasket had to be included between the bottom deck plate and the plastic structure. In order to obtain the required seal, additional torque had to be applied to the machine bolts being used to attach the lower deck to the model. This additional torque pulled out the plastic anchor inserts. All of the inserts had to be removed and glued in place with the fiber glass resin used to protect the plastic sheet.

The final assembled weight of the Light Weight Model was 16.35 lbs. This was 5.35 lbs, the weight of the gimbal, over the weight limitation established by the scaling analysis. A review of the weight breakdown of the Light Weight Model (See Table 9) shows that the model structural weight has already been reduced to a minimum value. Further attempts to reduce the model weight would have jeopardized the structural integrity of the model. The Light Weight Model was installed on the Dynamic Test Machine for check-out (Figure 35) without any further attempts at reducing the total weight of the model. As previously stated, this installation was selected because the Dynamic Test Machine provided the necessary support structure for the detached fan unit.

5. CALIBRATION OF FAN

The first model to be tested was the Heavy Weight Model. Prior to starting the tests on Static Test Platform, the cg of the full assembled model was determined by using a balance beam. The cg was 26.54 inches from the trailing edge of the model. During the initial check-out of the Heavy Model (Figure 36), it was found that total inflation of the nose cushion cell could not be achieved. A pressure survey of the internal cavity and the cushion cells revealed excessive flow rates to the main

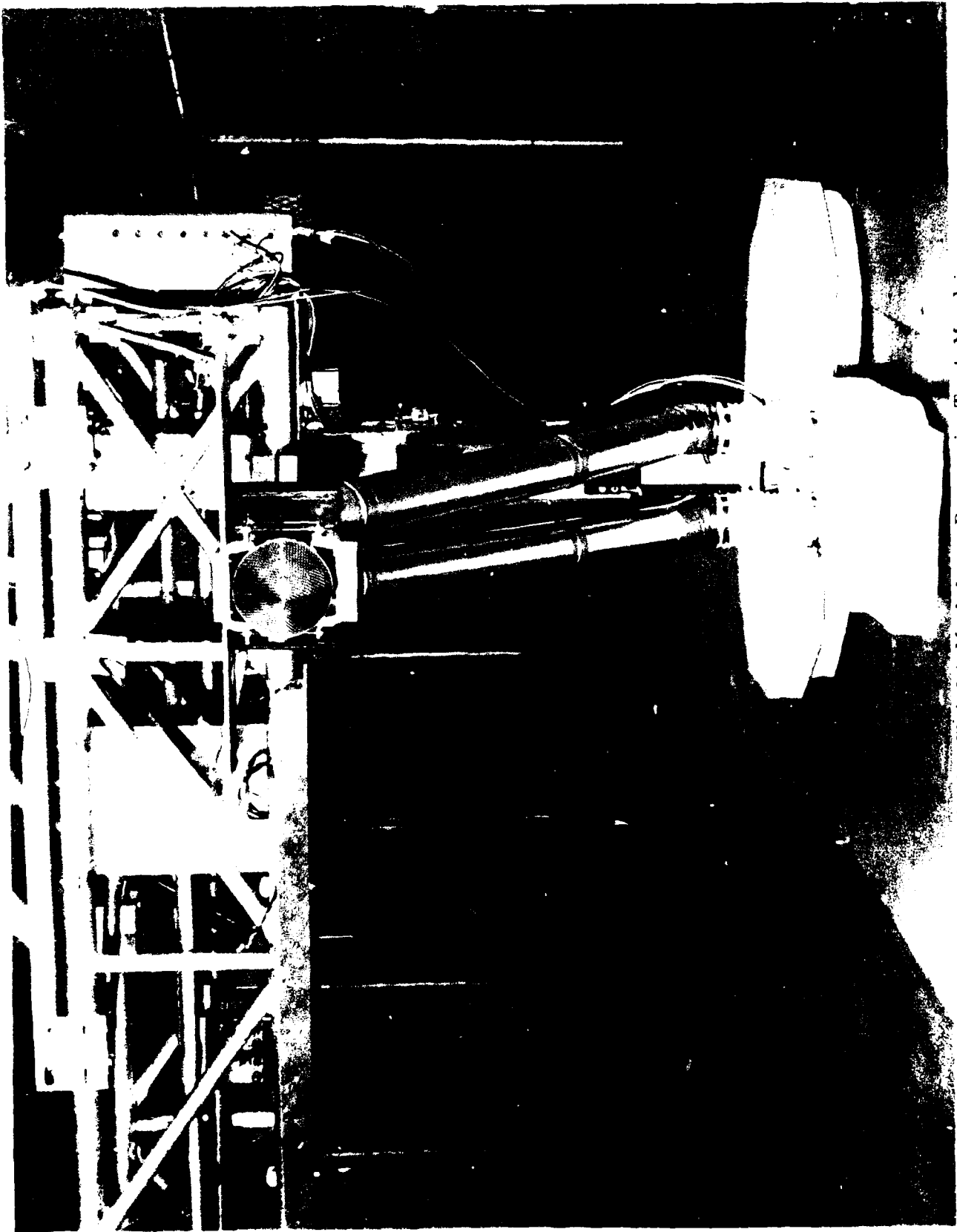


Figure 35. Light Weight Model on Dynamic Test Machine

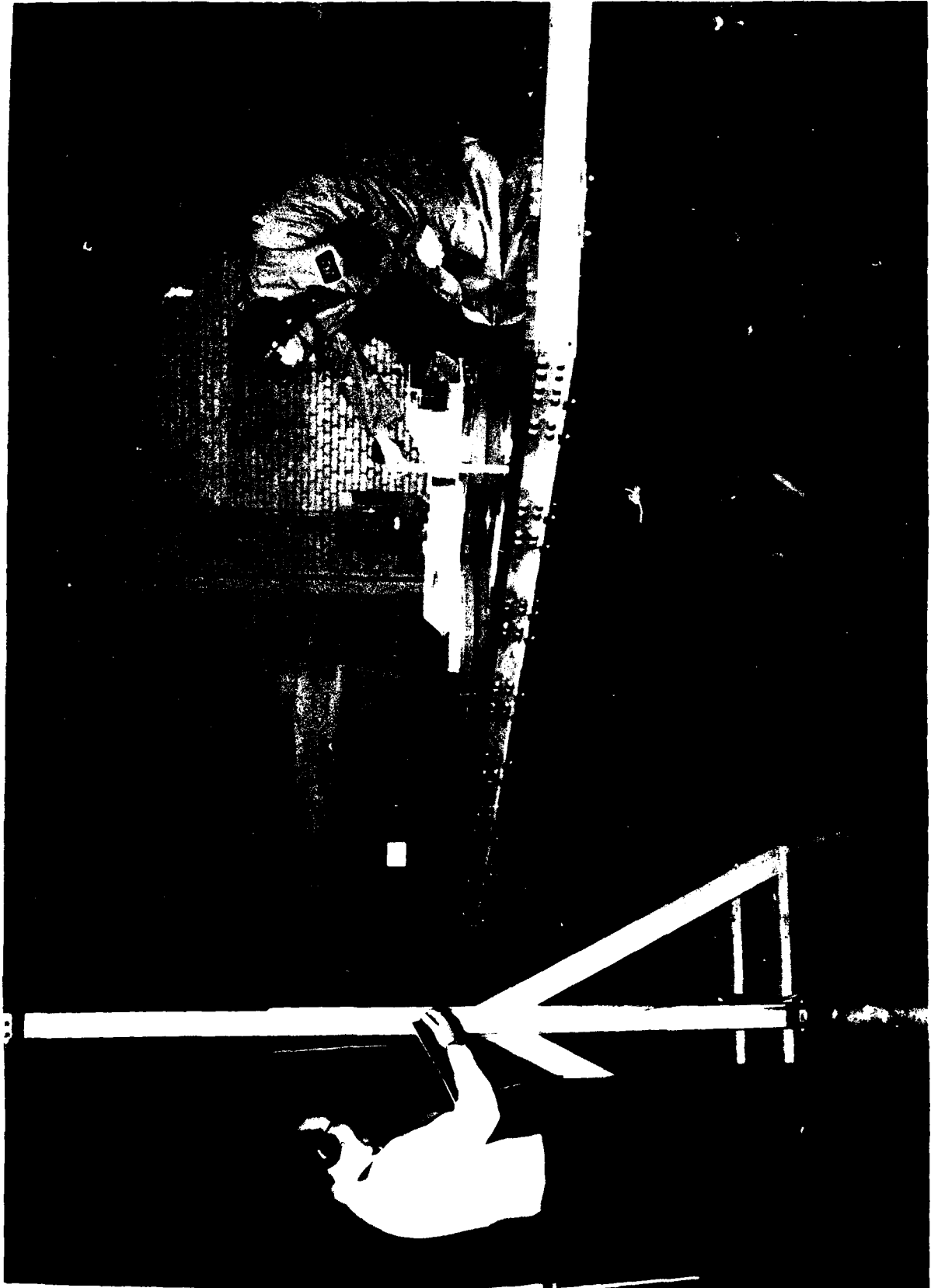


Figure 36. Heavy Weight Model Checkout on Static Platform

cells of the model. We tried a number of adjustments, decreasing the gap of the deflectors, reducing the number of feed holes to the main cell, and installing internal flow guide vanes, to increase the flow to the nose cell. All of these attempts were unsuccessful. The only model configuration change which produced any increase in the inflation of the nose cushion cell was the addition of approximately 3.0 lbs of ballast on the trailing edge of the model.

The sensitivity of the 1/10 scale model to the location of the cg was investigated by increasing the total weight of the model by a fixed amount of ballast, 52.5 lbs. The additional weight was first placed on the trailing edge of the model and then moved progressively forward. With each positioning of the ballast the cg location of the model plus ballast was experimentally evaluated. The model fan was then "turned on" to determine if the nose cushion cell would inflate. If the nose cell did inflate, static pressure readings were taken. In this way, the usable cg range of the 1/10 scale model was evaluated (Figure 37). From these data, a target cg location of 16.54 inches from the trailing edge of the model was established for the Heavy Model. To achieve a 10.00-inch shift in the cg, the fan unit had to be moved from the forward section of the model to a new location at the trailing edge (Figure 38). This move also required a reworking of the air supply ducts and a relocation of the feed holes into the deck cavity. After these modifications were completed, the cg location was again checked. With the addition of a small amount of ballast, a cg position of 16.54 inches was obtained. This cg position was within the scaled cg envelop for the ACET when fully loaded.

With the model in this new or modified configuration, full inflation of the nose cell cushion was achieved at a wide range of fan input power frequencies (Figure 39). Further, it was found that regardless of the input power frequency, the nose cell pressure was below the target value of 0.095 psig while both main cell pressures were above the target value of 0.080 psig. We made several adjustments to the model in an attempt to correct these differences, but they were unsuccessful. The cell pressures were considered to be within acceptable limits and the check-out of the Heavy Model continued.

During the selection of a fan unit to power the 1/10 scale models, we anticipated that if the model was to meet the flow parameters required by the scaling analysis, the fan unit would have to be run at an operating point different than its design point. As previously indicated, a 400-Hz Frequency Control Generator had been developed for the MDL during the initial design of the facility. This generator and the control console (Figure 40) were wired into both the Static Test Platform and the Dynamic Test Machine to meet future test requirements. In addition, a fan calibration rig was developed as part of an in-house test program to investigate the validity of utilizing scale models to evaluate the performance of ACLS's (Reference 4). For this program the Calibration Rig was wired into the 400-Hz Frequency Control Generator to supply the variable frequency power required to evaluate the performance envelope of the fan unit. The "MAXIAX" fan and motor were installed in the Fan Calibration Rig prior to the start of the testing of the Heavy Weight

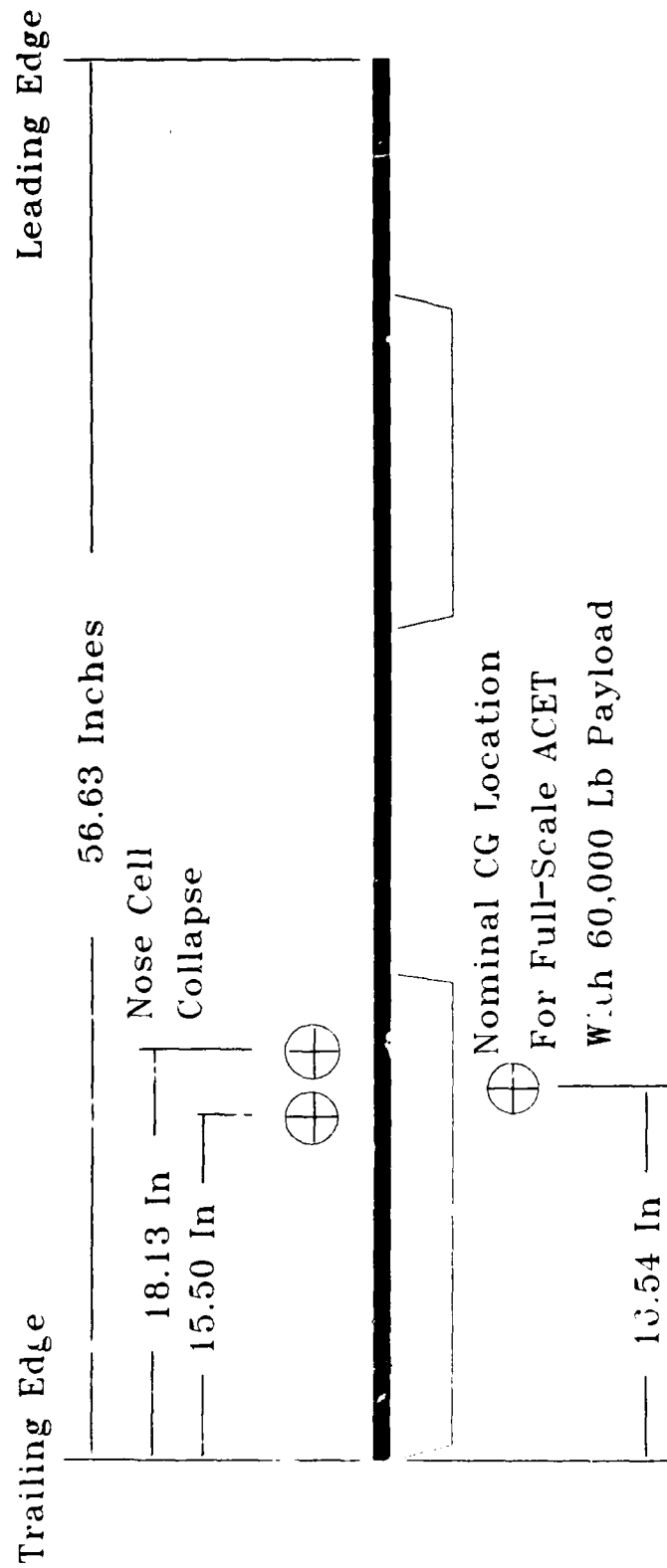


Figure 37. 1/10 Scale ACET Model Useable CG Range

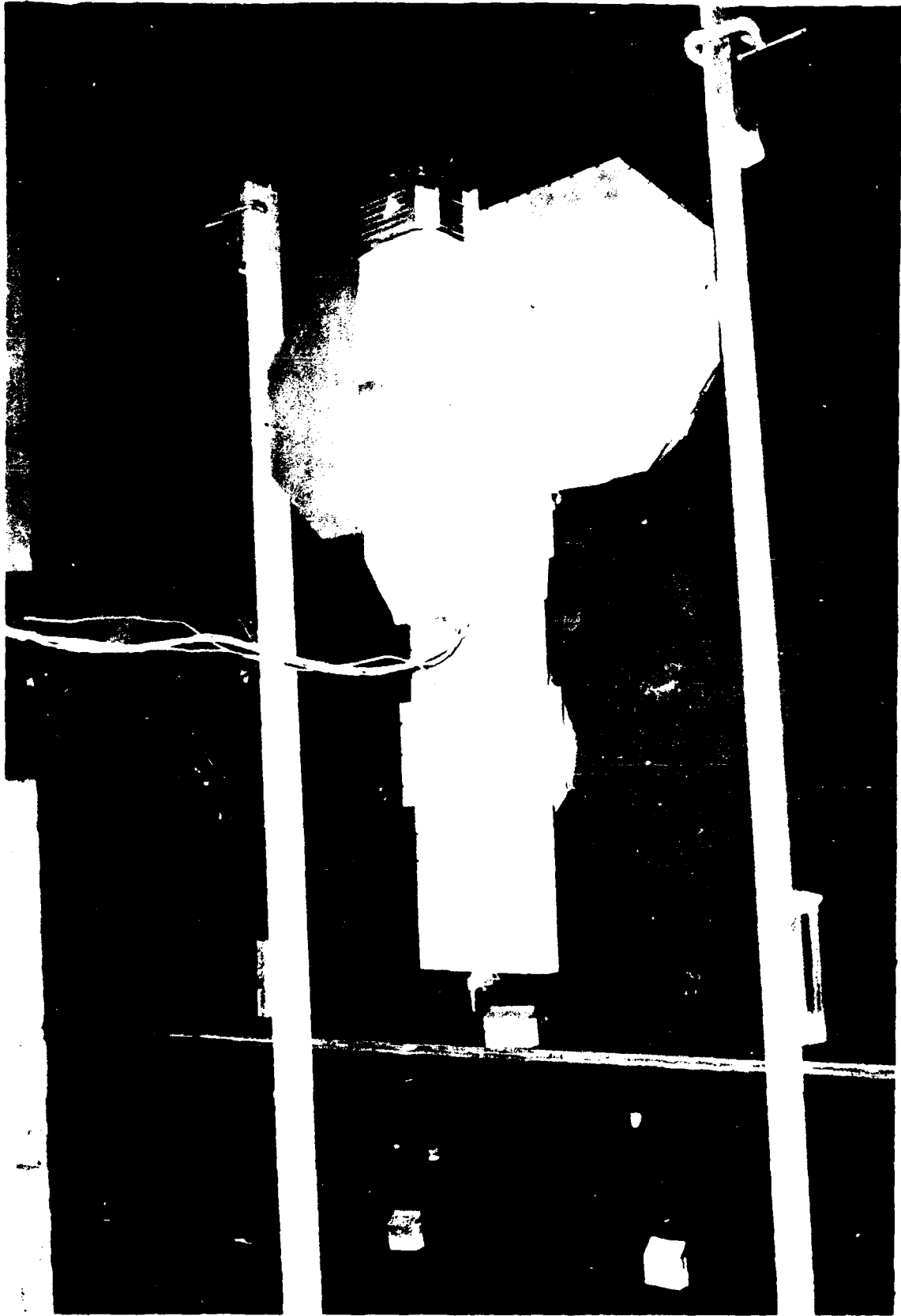


Figure 38. Modified Heavy Weight Model

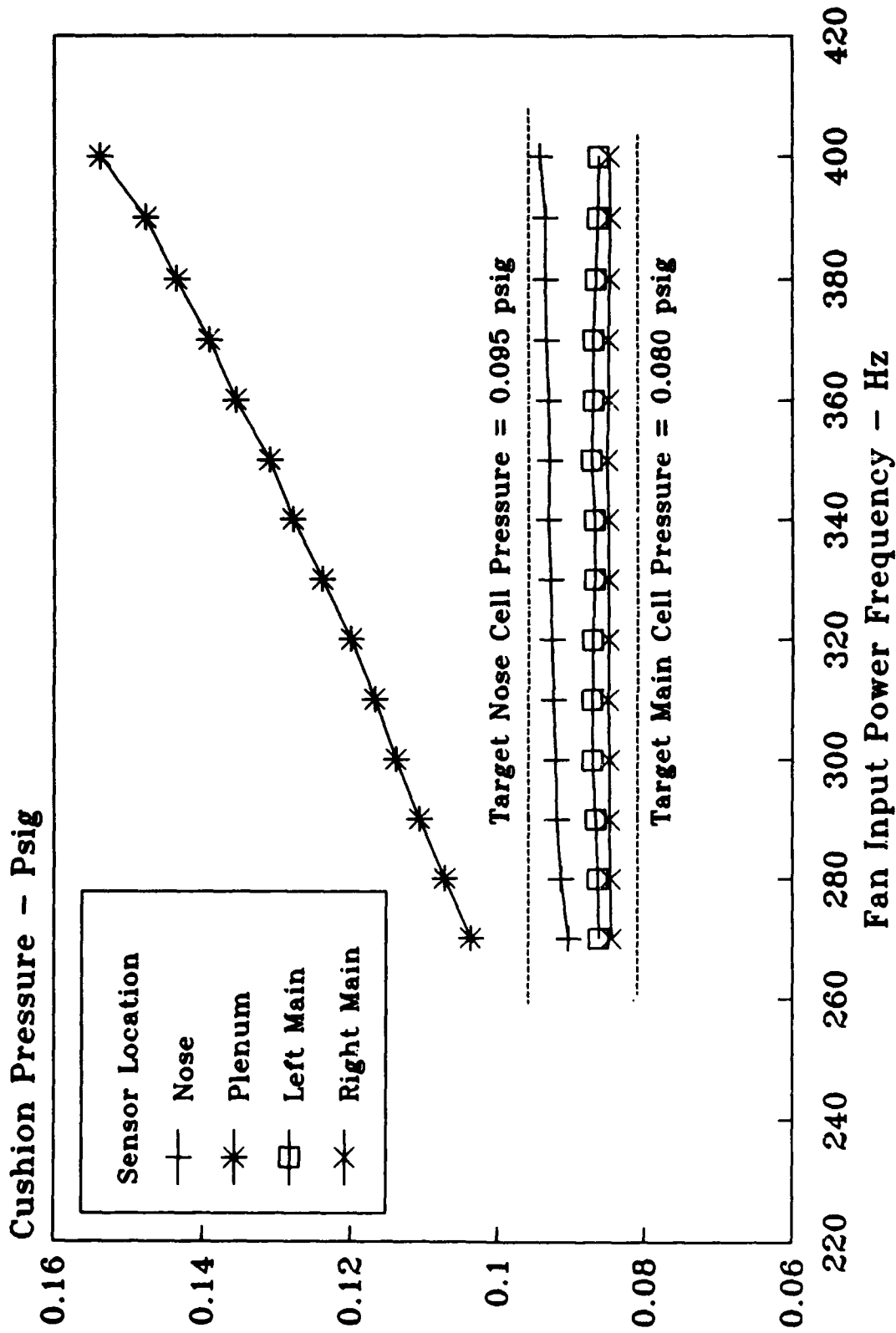


Figure 39. Cushion Pressure Variation with Fan Input Power

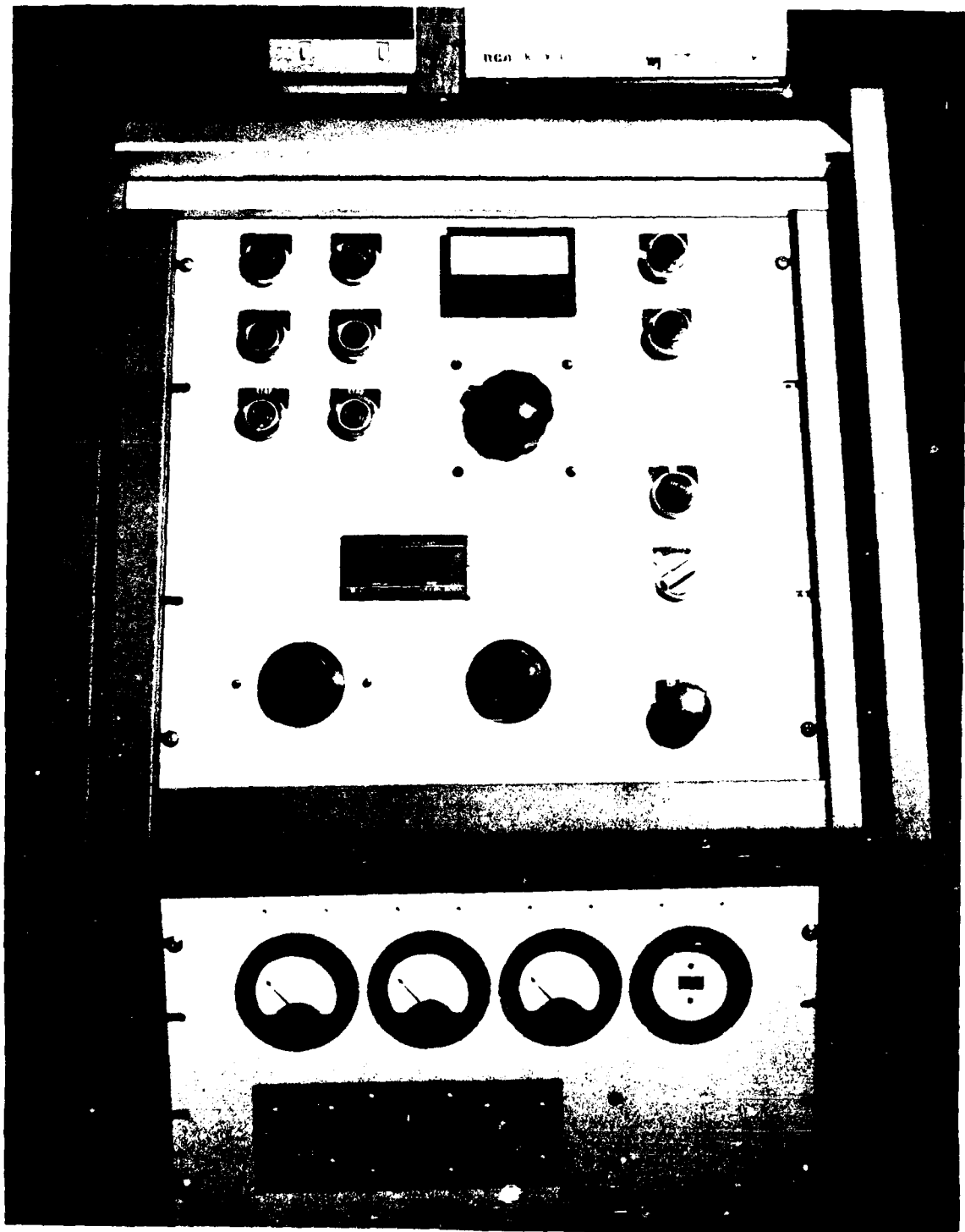


Figure 40. Frequency Control Console

Model. The goal of this task was to establish what fan input power frequency would yield an operating curve for the "MAXIAX" fan which would match the flow and pressure requirements of the scaling analysis.

The Fan Calibration Rig (Figure 41) was fabricated from a number of sections of clear acrylic plastic, seamless tubing with an 8.25-inch inside diameter and a 0.25-inch wall thickness. The tube sections were mated together to provide a smooth, continuous inner surface. Also the junctions were sealed to minimize any airflow losses. The total length of the Rig is 203 inches, without the fan unit installed. The Fan Calibration Rig is composed of four major sections. These sections are:

a. The Fan Adapter Section - This section is 25 inches long without the fan unit. The fan unit mounts to the front of this section. Since the diameter of the "MAXIAX" was smaller than the inside diameter of the Rig, a flexible adapter was fabricated to facilitate the installation (Figure 42). A pressure tap is installed in this section to monitor the fan exit pressure.

b. The Flow Straightener Section - This section mates to the adapter section and is 52 inches long. Housed within this section are the flow straighteners. The straighteners are 35 thin walled tubes approximately 1 inch in diameter and 16.5 inches long (Figure 42). The function of this section is to eliminate as much turbulence from the flow as possible to minimize pressure losses.

c. The Orifice Section - This section attached to the Flow Straightener Section and is 103 inches in length. This is the key section of the Rig. A sharp edge orifice is installed in this section (Figure 43). The orifice was designed to permit the quick replacement of a orifice plate with a plate having a different throat diameter. The plates were fabricated from 0.25-inch-thick clear acrylic plastic. The throat diameters used to calibrate the "MAXIAX" fan were 3.25 and 6.00 inches. The orifice plates were designed to be self-centering to insure that the center of the orifice aligned with the centerline of the Rig. The governing principle for measuring flow of a fluid, in this case air, with this type of test rig is that there is a measurable pressure drop when the fluid passes through an orifice. This measured pressure drop can then be converted into a mass or volume flow rate. To measure this pressure drop, two pressure taps were installed in this section. The upstream pressure tap was located one tube diameter, 8.25 inches, forward of the leading edge of the orifice plate. The downstream pressure tap was located half of a tube diameter, 4.125 inches, past the leading edge of the plate. The location of these pressure taps was in accordance with American Society of Measurement Engineers (ASME) for the measurement of a pressure drop across an orifice plate (Reference 5).

d. The Exit Area Control Section - This last section of the Calibration Rig is 23 inches long. A butterfly valve was installed in this section to regulate the exit area of the rig (Figure 44). The exit area can be varied by fixing the butterfly valve in any one of 10 positions between fully open and fully closed. The valve was constructed

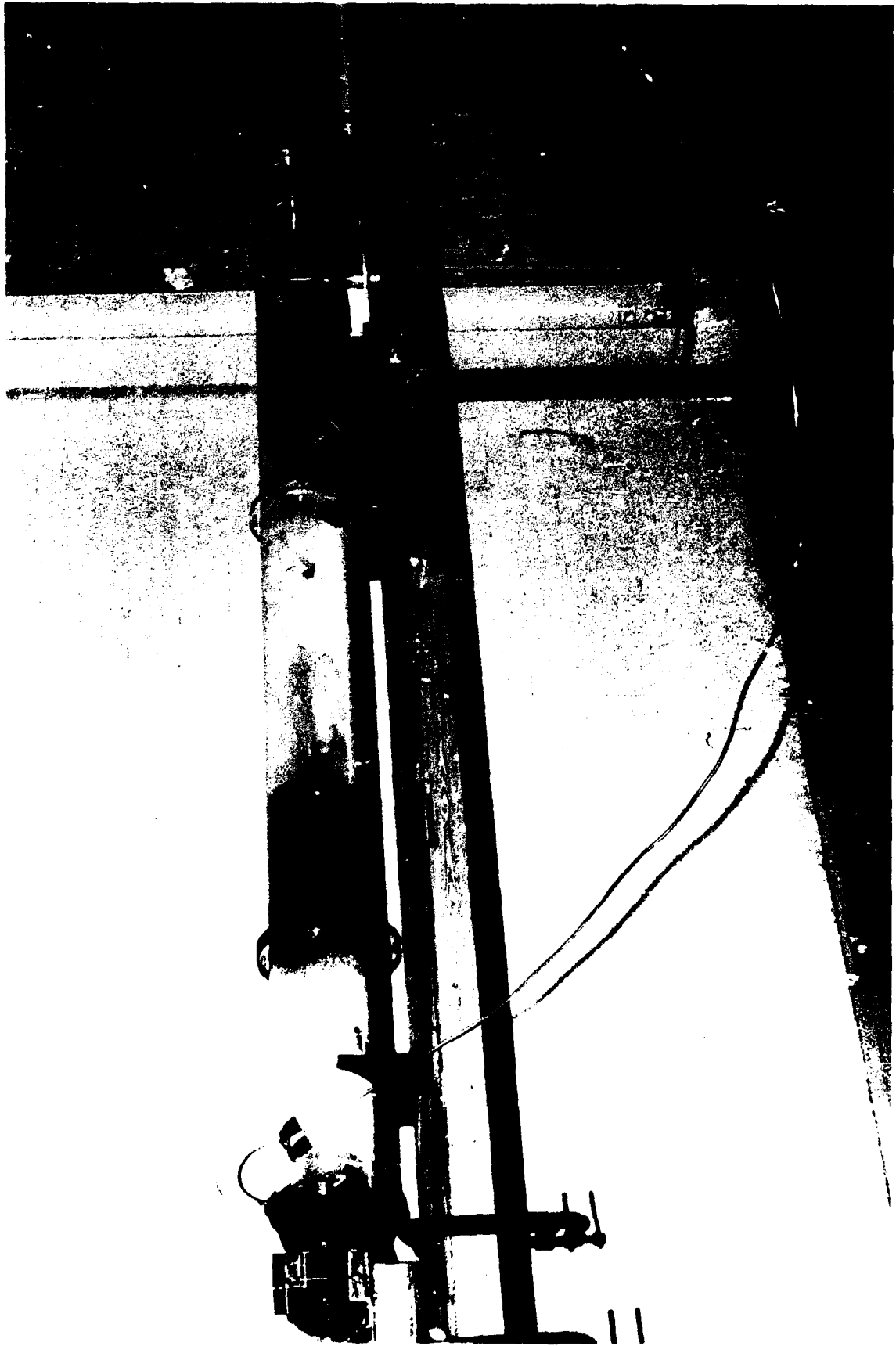


Figure 41. Fan Calibration Rig

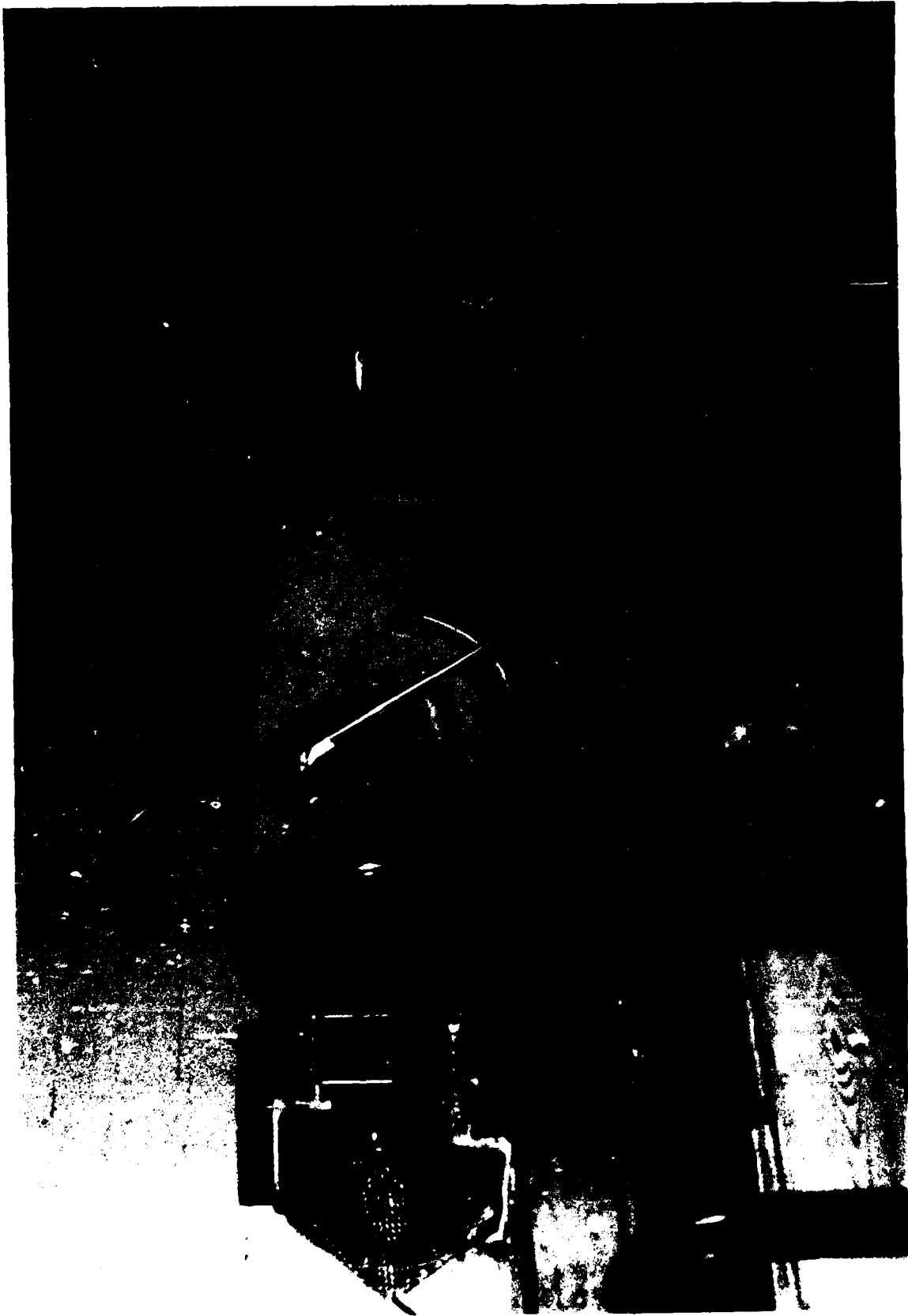


Figure 42. "MAXIAX" Installation in Fan Calibration Rig



Figure 43. Sharp Edge Orifice with Pressure Taps



Figure 44. Exit Area Control Butterfly Valve

from a 1/8-inch aluminum plate. The diameter of the metal disk which was cut from this plate was 1/4 inch smaller than the inside diameter of the tube. This resulted in a small exit area when the valve was closed. This area was provided to reduce the possibility of damage to the rig or the fan unit from excessive back pressures that would result if the exit area were reduced to zero. The valve was bolted to a pivot rod to allow easy positioning of the valve. A pin was used to lock the butterfly valve in the required position to minimize any vibration of the valve and to insure repeatability in the exit area during the data runs. Finally, a position indicator was attached to the end of the rod to facilitate the recording of valve position data.

The three pressure taps described above were mounted perpendicular to the tube surface and flush with the inside wall of the tube. All of the taps were connected to an inclined manometer bank (Figure 45). The bank was inclined at an angle of 60 degrees to achieve a 2-to-1 sensitivity increase. The pressures were recorded in gauge pressure which is the difference between the total pressure and the local atmospheric pressure. Other data recorded during each test were the local weather conditions, pressure and temperature, and the temperature of the air flow downstream of the orifice plate. The Base Weather Service was used to obtain the ambient pressure. Both the ambient and the duct temperature were recorded on an Omega HH-99J Digital Thermocouple. The temperature of the air inside the Rig was measured 45 inches downstream of the leading edge of the orifice plate.

The governing equation for calculating the mass flow rate from the pressure losses across a sharp edge orifice is:

$$Q = KYD^2F_a \sqrt{\frac{(P_1 - P_2)}{\rho}} \quad (2)$$

where:

- Q = Mass Flow Rate -- pounds, mass per second
- K = Flow Coefficient -- non-dimensional
- D = Orifice Throat Diameter -- inches
- Y = Expansion Factor for Gas -- non-dimensional
- F_a = Area Thermal Expansion Factor -- non-dimensional

- ρ = Flow Density -- slugs per cubic feet

- P₁ = Upstream orifice pressure -- inches of water

- P₂ = Downstream orifice pressure -- inches of water

The solution of this equation is an iterative process since K must be determined for each test point. K is a function of Reynolds Number. Therefore, an initial trial value for K was selected and initial volume flow and Reynolds Number were calculated. These initial values were then used to calculate an estimated volume flow and Reynolds Number. This iteration process was continued until the calculated flow, based upon

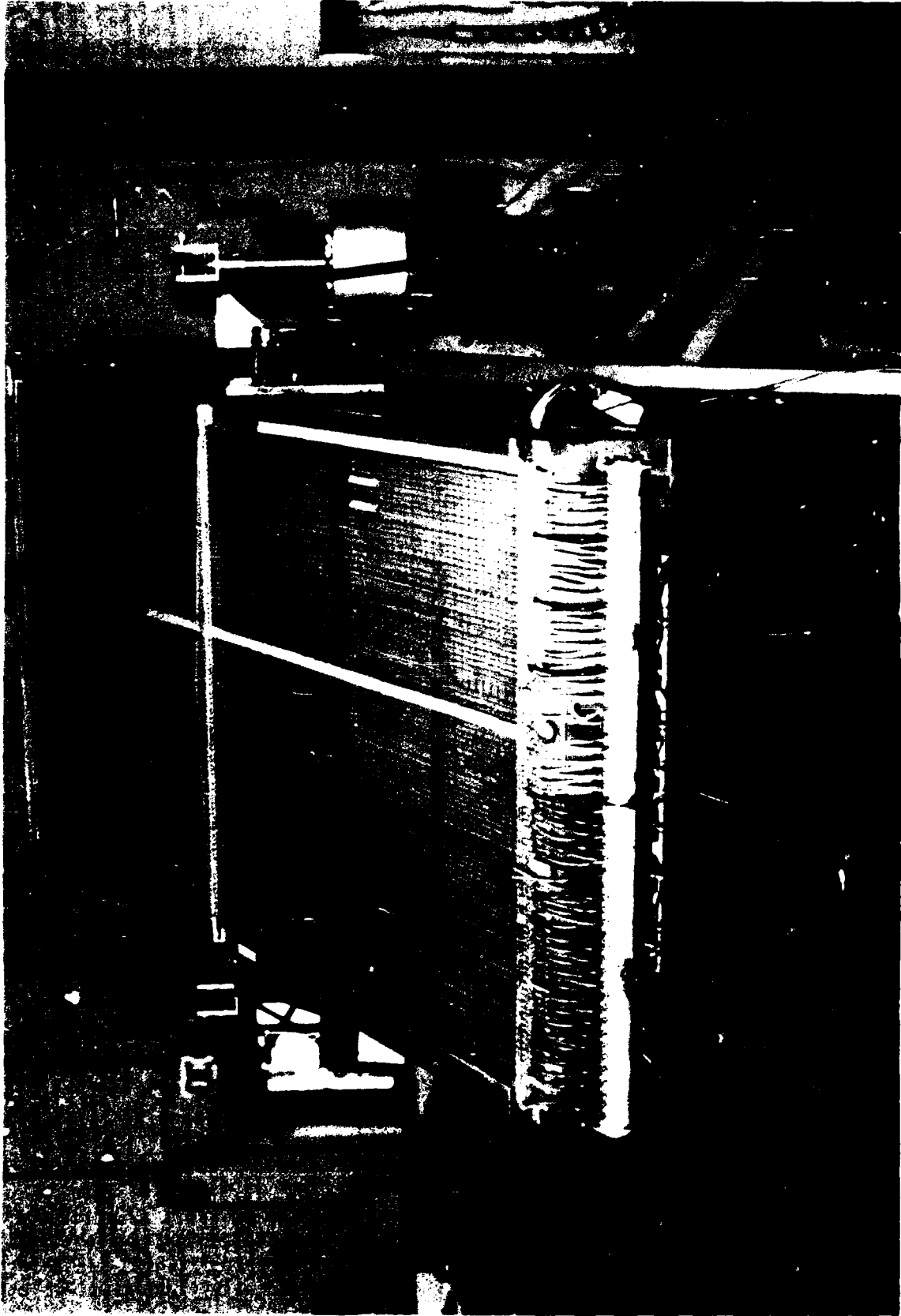


Figure 45. Inclined Manometer Bank for Calibration Rig

tabulated data, agreed with the flow calculated using the Reynolds Number. A computer program (Appendix A) was developed to perform this iteration on the data collected from the Fan Calibration Rig. The Flow Calculation Program was written in FORTRAN 77 language and was designed specifically to be used on a Personal Computer (PC) with dual floppy disk drives. However, the program can be run on a PC with a single floppy disk drive if 116K random access memory is available. A MS-DOS FORTRAN Compiler package is also needed to use this program. In addition, the program has the capability to store the calculated data in files for future analysis. A sample of the program output is also included in Appendix A.

Before the Fan Calibration Rig and the Flow Calculation Program could be used to establish an operating curve for the 1/10 scale model, the accuracy of this combination had to be experimentally verified. Since the manufacturer of the "MAXIAX" fan had supplied an operating curve for 400 Hz, the design operating frequency for this unit, these data were the logical means of verifying the proposed procedure. The "MAXIAX" was installed in the Calibration Rig and a test run was made with the Fan Input Power Frequency set to 400 Hz. A 3.25-inch-diameter orifice was used for these runs. This selection was made, based upon the recommendations in the literature for the measurement of flows using this type of measuring procedure. The data collected during this run were then reduced using the Flow Calibration Program. The resulting mass flow data were then plotted against the fan exit pressure (Figure 46). The manufacturer's fan curve was also plotted on this same graph for comparison. The correlation of the experimentally derived fan curve with the manufacturer's curve was very good overall. The only significant deviation of the two curves occurred as the fan approached stall. At this point the deviation between the two curves was only 4.0 percent.

Having validated the Fan Calibration Rig and the Flow Calculation Program, a series of runs were made to determine what fan input power setting was required to match the scaled operating point of the full-scale ACET. One additional modification was made to the fan unit prior to the start of these runs. A FOD protection screen was fabricated and installed on the "MAXIAX," see Figure 42. This screen served to protect the fan blades from damage as well as protecting personnel from injury while working near the unit. A run was made at the 400-Hz power setting to evaluate the impact of this installation on the performance of the fan. The results of this run are also plotted on Figure 46. The FOD screen installation resulted in a 5 percent degradation in performance. This was well within acceptable limits and did not restrict the use of this unit to power the 1/10 scale model.

The initial series of test runs was again made with the 3.25-inch orifice. Based upon preliminary calculations, the Fan Power Input Frequency was varied from 400 Hz down to 280 Hz in steps of 20 Hz. At each of these frequencies, the position of the butterfly valve in the Exit Area Control Section was varied from 0 degrees (open) to 90 degrees (closed) or that position where fan stall occurred in increments of 10 degrees. Generally, fan stall occurred between the 60- and 80-degree position. Varying the fan exit area allowed pressure data to be collected at

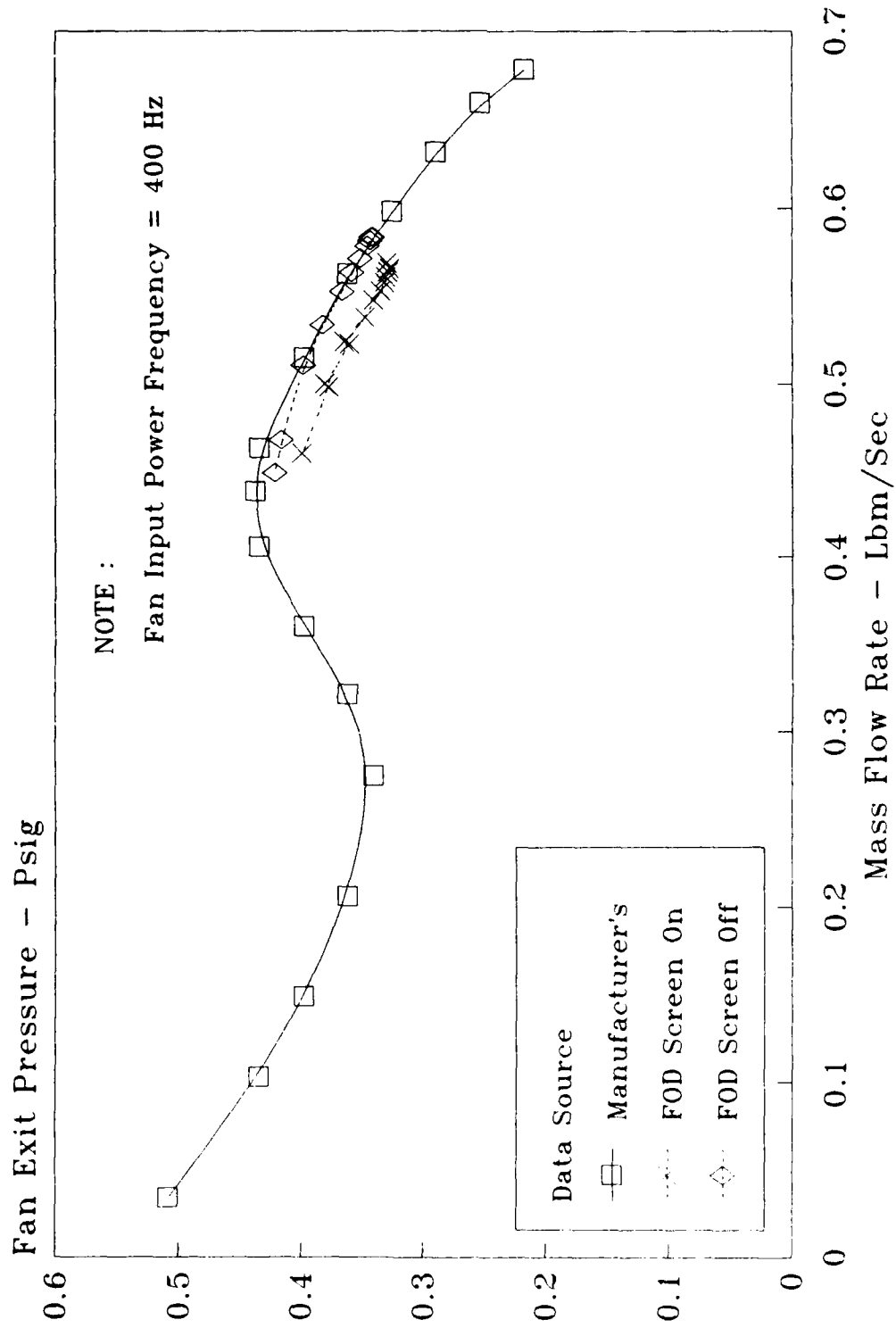


Figure 46. Verification of Fan Calibration Procedures

different mass flow rates. The pressure data collected during these runs were then inputted into the Flow Calculation Program to generate operating curves at various Power Input Frequencies (Figure 47). The data collected during these runs clearly indicated that stable operations with Input Frequencies down to 280 Hz were easily attainable. The next question to be considered was which Input Frequency was to be used for the 1/10 scale model tests.

The ASP-10's used to power the cushion system on the full-scale ACET are capable of generating a total mass flow of 158 lb_m/sec. From this flow 8 lb_m/sec is bled off, filtered and used for combustion in the ASP-10's. Therefore the total flow available to inflate the nose and two main cushion cells is 150 lb_m/sec. Applying the scaling techniques developed in Section IV.3, Design of Models, of this report, results in the requirement for a scaled mass flow of 0.474 lb_m/sec for the 1/10 scale model. This design goal is represented by the vertical dashed line in Figure 47. Nominally, the scaled pressure in the nose and main cells of the model, when considering the maximum payload condition of 60,000 lbs, is 0.1 psig. Preliminary cushion cell pressure surveys conducted on the 1/10 scale model revealed that Fan Exit Pressures in the 0.1 to 0.2 psig range were required to achieve the required cushion pressures. During these preliminary tests, we also noted that if the Fan Power Input Frequency was reduced below 300 Hz, there was a significant loss of clearance between the bottom of the skirt and the operating surface. This contact would bias any drag data collected during the model test program. Therefore, 300 Hz was selected as the Input Frequency to be used for this simulation.

In order to cover the entire Fan Exit Pressure range of 0.1 to 0.2 psig, two separate series of runs had to be accomplished with the Fan Input Frequency set at 300 Hz. The first series of runs was made with the 3.25-inch-diameter orifice installed. During the second series, the 6.00-inch diameter orifice was used. Again, the Flow Calibration Program was used to reduce the data collected. The results from both the 6.00-inch and the 3.25-inch runs are plotted on the same graph and an operating curve for the "MAXIAX" with a Power Input Frequency of 300 Hz was developed (Figure 48). Reviewing the cushion cell pressure data presented in Figure 39 shows that with the fan unit installed in the Heavy Weight Model, operating the "MAXIAX" at a Input Power Frequency of 300 Hz results in acceptable values for the nose and main cell cushion pressures. The Nose Cell Pressure is slightly lower, 6 percent, than the nominal value while the Main Cell Pressures are both slightly higher, 4 percent and 12.5 percent respectively, than the target values for the Heavy Weight 1/10 Scale Model of the ACET.

Finally, a series of static tests were run on the Heavy Weight Model, Figure 38, to develop a correlation between the fan exit pressure and the plenum pressure. The pressure in the plenum, the hollow area between the upper and lower decks of the model, was one of the pressures that was recorded for all of the testing of the Heavy Weight Model. Restrictions on the number of channels available for recording data precluded the recording of the fan exit pressure. The pressure in the fan exit duct of

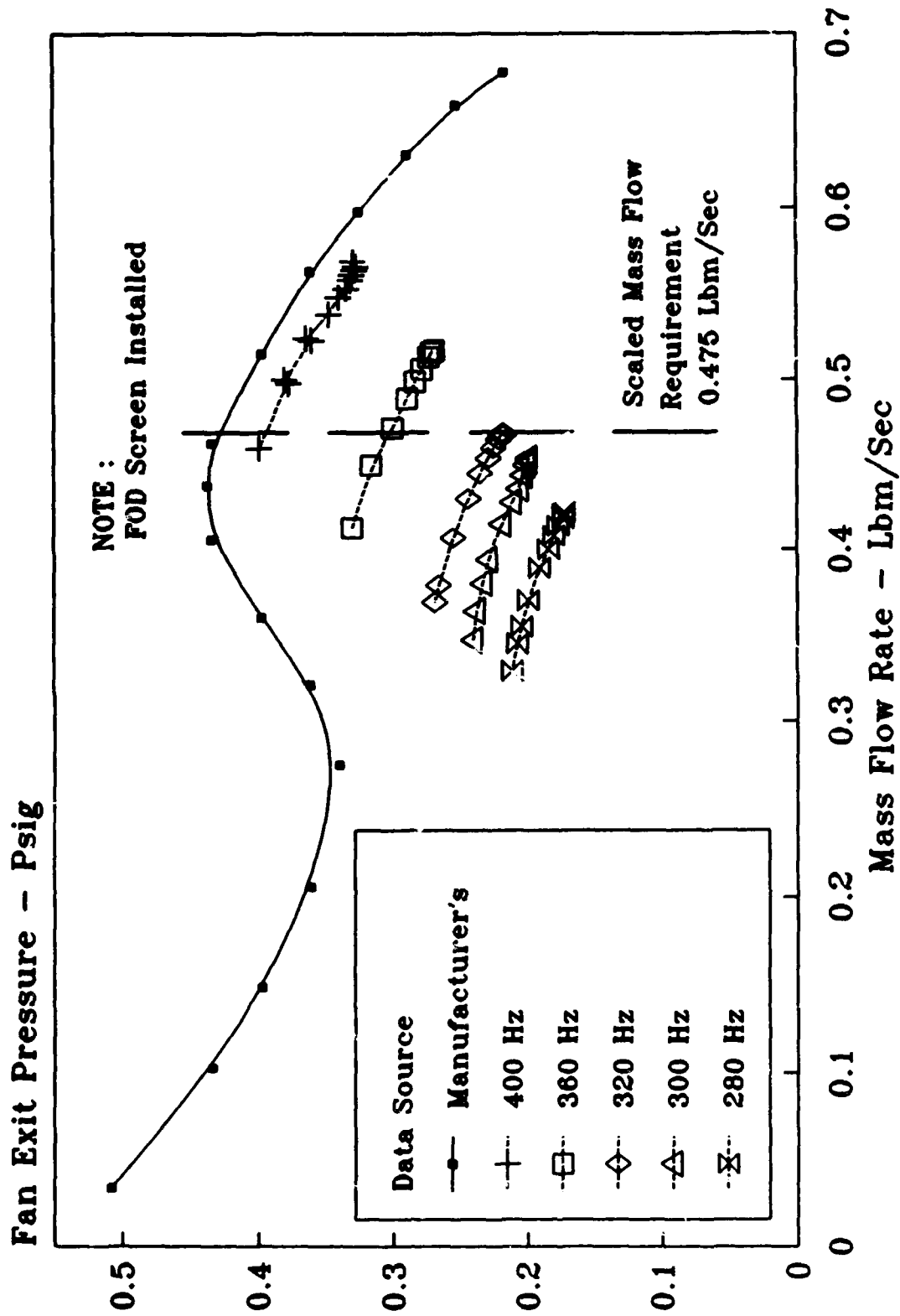


Figure 47. Data Runs for Fan Calibration Tests

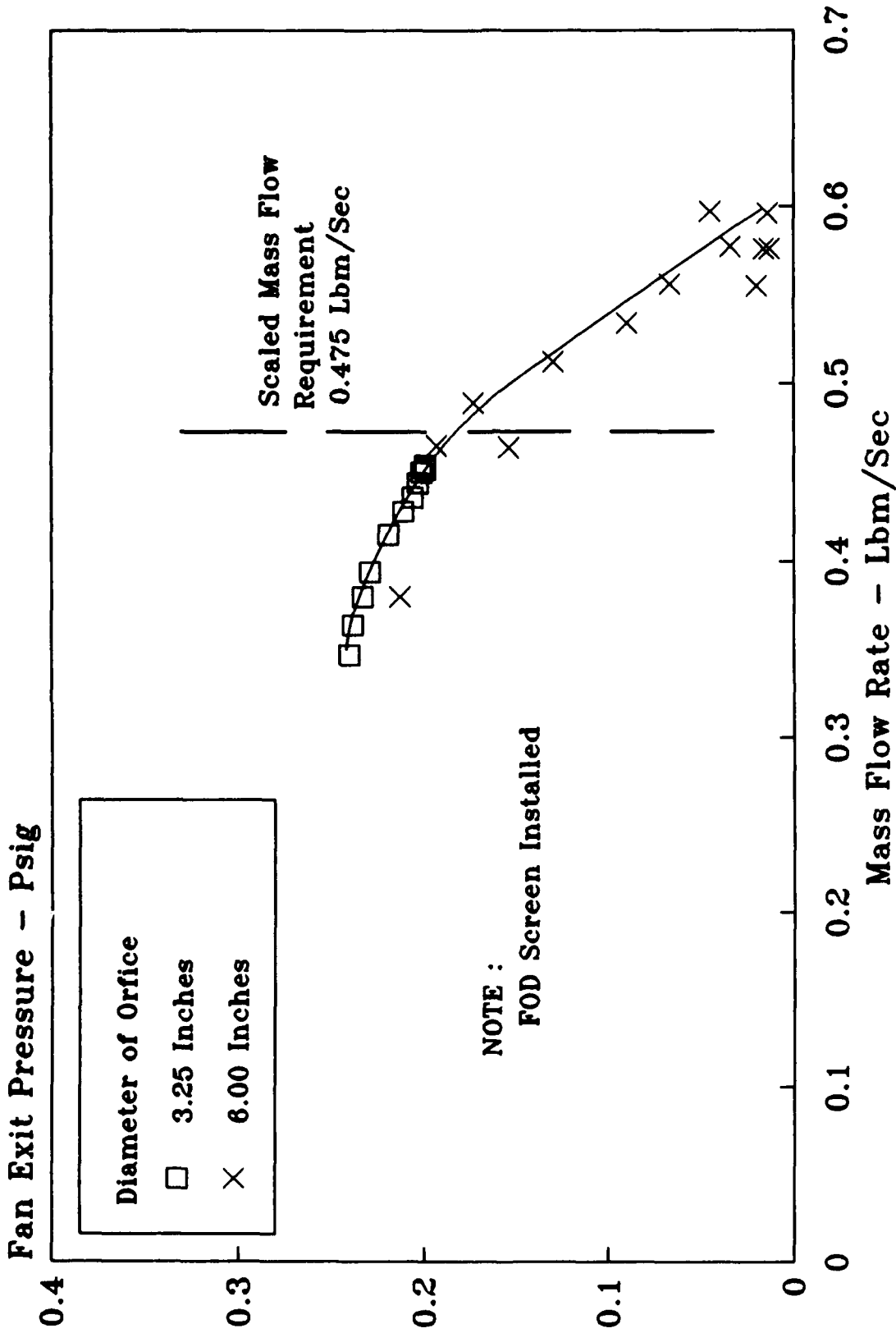


Figure 48. "MAXIAX" 300-Hz Operating Curve

the model was measured in a number of locations. The data collected from these different locations had a great deal of repeatability and were correlatable to fan exit pressure readings recorded during the fan calibration tests. Pressure readings of the plenum also exhibited a high degree of repeatability and were constant throughout the entire plenum. The correlation of the fan exit and the plenum pressures was based on three conditions. These conditions were (1) out of ground effect, (zero cushion pressure in all three cells), (2) the nominal operating condition of the Heavy Weight Model (the ACET supporting its maximum payload of 60,000 lbs), and (3) an overweight condition (52.5 lbs of ballast added to the 1/10 scale model at the cg). This is equivalent to a 52,500-lb overload for the full-scale vehicle. When the pressure data from these conditions were plotted, a linear relationship was found to exist between the Fan Exit Pressure and the Plenum Pressure (Figure 49). With this relationship and a time history of the plenum pressure, it was possible to determine the mass flow rate at any point in a test sequence.

One point that was of immediate interest was the static operating point of the Heavy Weight Model. Using the derived relationship, the nominal value of the fan exit pressure, under static conditions, was determined to be 0.135 psig. When this additional design requirement was added to the 300-Hz operating curve, represented by a horizontal line in Figure 50, the operating point for the Heavy Weight Model with a Fan Input Power Frequency of 300 Hz was uniquely defined. Inspection of this operating point clearly indicates that the exact scaled values of the maximum payload condition could not be met. Instead of the required mass flow rate of 0.475 lbs_m/sec, the "MAXIAX" delivers 0.495 lbs_m/sec when installed in the Heavy Weight Model. This represents a variation of only 4.2 percent. This is the best that can be achieved with this fan unit since reducing the Power Frequency below 300 Hz results in increased contact between the skirt and the operating surface.

While the scaled operating point was closely approximated, there was one characteristic of the ACET full-scale lift system that was not duplicated. This was the slope of the fan curve. A scaled fan curve for the full-scale ACET Lift System has also been plotted on Figure 50 to illustrate the difference between the two curves. The slope of the full-scale system is significantly greater than the lift system for the 1/10 scale model. Of the two fan curves, the 1/10 scale curve has a more stabilizing effect on the dynamics of a vehicle, either full-scale or model. If a fan curve has a slope such that small changes in mass flow result in large changes in fan exit pressure, as is the case with the Lift System installed in the full-scale ACET, small oscillations or variations in the mass flow can induce a destabilizing vertical oscillation referred to as heave in ACV literature. While the matching of the required mass flow rate and the fan exit pressure for a specific scale model is a fairly easy and inexpensive process, matching the fan curve as well would require the fabrication of a custom design fan unit. This assessment was made after an extensive search and review of fan units currently being manufactured for this performance range.

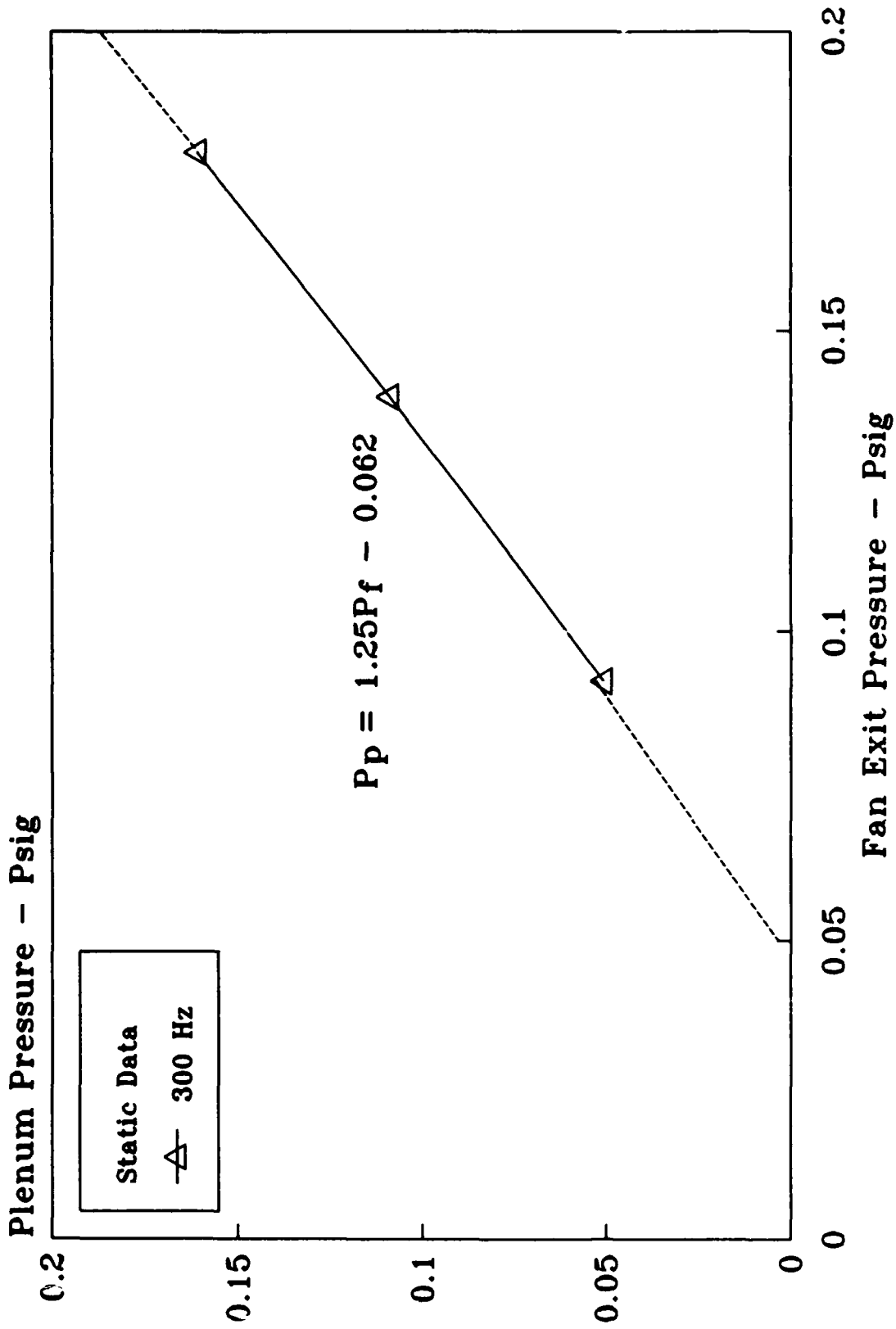


Figure 49. Fan Exit and Plenum Pressure Relationship

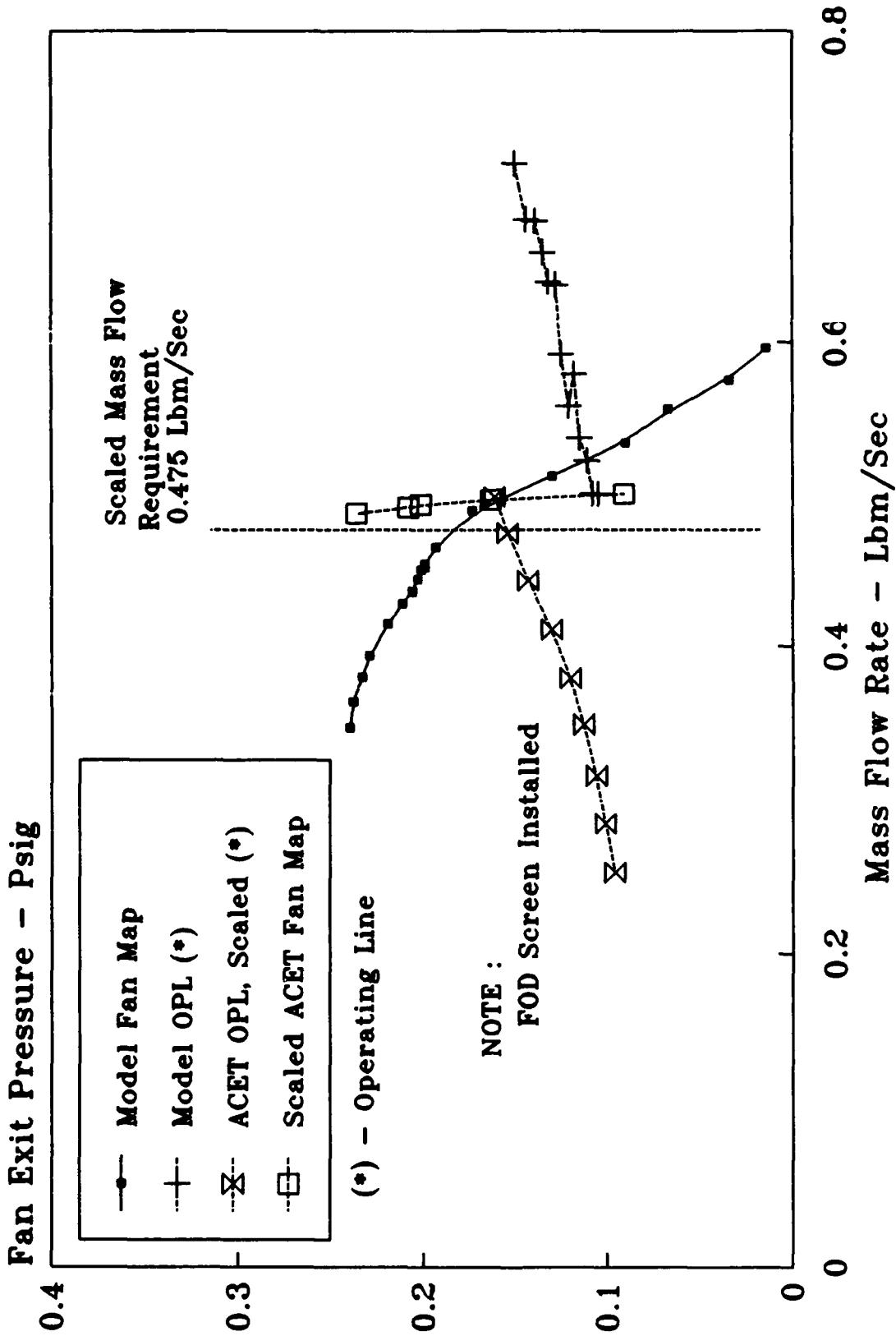


Figure 50. Definition of 300-Hz Operating Point

As indicated by the discussion of the fan calibration for the Heavy Weight Model, the process of defining the operating point for a scale model involves a number of steps with tradeoffs being considered throughout the process. A similar process was planned for the Light Weight Model. During the initial check-out of the Light Weight Model on the Dynamic Test Machine, we determined that the required nose and main cell cushion pressures could be achieved at a number of Fan Input Power Frequencies. However, the Light Weight Model did not exhibit any of the tendencies of the full-scale ACET to become unstable in heave as the payload was increased. For the full-scale ACET, the boundary for heave stability was reached at a payload of 30,000 lbs. Despite repeated attempts with 30, 60, and 112 lb payloads, the Light Weight Model could not be made to oscillate in heave. In addition, the requirement for a remote installation of the fan unit with ducting to the Light Weight Model (See Figure 35) introduced a bias in the pitch and roll data collected during the check-out of the Model. The investigation of the heave, pitch, and roll stability boundaries was the primary objective for the testing of the Light Weight Model. The Heavy Weight Model did not exhibit any instabilities in heave either. This fact clearly indicated that models of this scale could not be used to predict the dynamic responses of the full-scale vehicle, unless the scaling laws are modified. Reviewing the data and the procedures followed during the development of the scaling factors leads to the hypothesis that the scaling factors must be adjusted to account for the fact that the atmosphere can not be scaled. Another alternative approach would have been to use full-scale cushion pressures in the model. Development of these modified scaling laws and fabrication of the resulting new model for either of these approaches was beyond the scope of this effort. However the results of the preliminary check-out of the models did necessitate a redirection of the 1/10 Scale Model Test Program. The decision was made to curtail any further testing of the Light Weight Model and to concentrate the testing of the Heavy Weight Model on the determination of the static characteristics within the rather limited envelope afforded by the model design and of the breakaway and low speed drag forces predicted by the model.

6. TESTING OF HEAVY WEIGHT MODEL

The testing of the Heavy Weight Model was conducted on the Static Test Platform in the MDL. This testing was divided into two types. The first series of tests were conducted with the model stationary, as depicted in Figure 36. The instrumentation varied depending on the nature of the test. The pressures were hand recorded using a water manometer connected to a pressure probe. This arrangement allowed the engineer to conduct pressure surveys without an excessive amount of downtime for re-configuration of the model and/or the instrumentation. The attitude of the model was measured with a machinist's scale. In general, measurements were taken at four different reference points on the model. The reference points were the leading and trailing edge of the model at the longitudinal centerline and the left and right edge of the model at the lateral centerline of the main cushion cells. With these measurements and the known dimensions of the model, it was possible to calculate the pitch and

roll angles for each test point. This approach to data collection provided very accurate data for the static tests.

The primary objectives of the Static Tests of the Heavy Weight Model were to collect data on the performance of the model and compare this performance to the full-scale ACET. The comparison was accomplished via full scale predictions using the scaling laws used in the fabrication of the 1/10 scale models. A limited amount of maximum gross weight full-scale data was available from the contractor's test program. These data were used in the evaluation.

During their initial check-out, BACT conducted a number of static tests to evaluate the static performance of the full-scale ACET as a function of gross weight. One of the relationships developed from this data was the nose and main cell cushion pressures as a function of vertical load supported by the cell (Figure 51). The data plotted in this figure are for 0-degrees pitch and roll. With the model in a 0-degrees pitch and roll attitude, pressure data were collected on all three cells. These pressure readings along with the areas of the nose and main cell were used to calculate the force each cell was generating to support the model. The resulting forces are included on Figure 51. The following relationships, Refer to Table 7, were used to predict full-scale forces:

$$F = \lambda^3 f \quad (3)$$

$$P = \lambda p \quad (4)$$

where the lower case letter represents the model value for pressure and force while the upper case letter is the full scale value of pressure and force. The resulting full-scale predictions were then plotted on this graph. Excellent agreement was noted between full-scale data and predictions based upon model data. Clearly, the 1/10 scale model of the ACET at maximum gross weight accurately represents cg and load distribution of the full-scale vehicle.

Having verified that the Heavy Weight 1/10 scale model did accurately represent the full-scale ACET under ideal static conditions, a number of tests were conducted on the Static Test Platform to investigate the static pitch and roll performance of the model. The goal of these tests was to determine if the performance of the model could be used to predict full-scale pitch and roll stiffness with an acceptable degree of accuracy. As previously indicated, these tests were planned for the Light Weight Model. When the performance of this model proved unacceptable, the roll and pitch stiffness tests were transferred to the Heavy Weight Model. This transfer required considerable modification since a larger percentage of the total weight (See Table 9) was devoted to the structure and the fan assembly. This left very little weight that could be used for CG adjustment, assuming that the maximum weight of the model, 68.25 Lbs, was to be maintained.

Given these restrictions, the range of pitching moments for the Heavy Weight Model was from -172.13 to 61.80 inch-pounds, where a positive

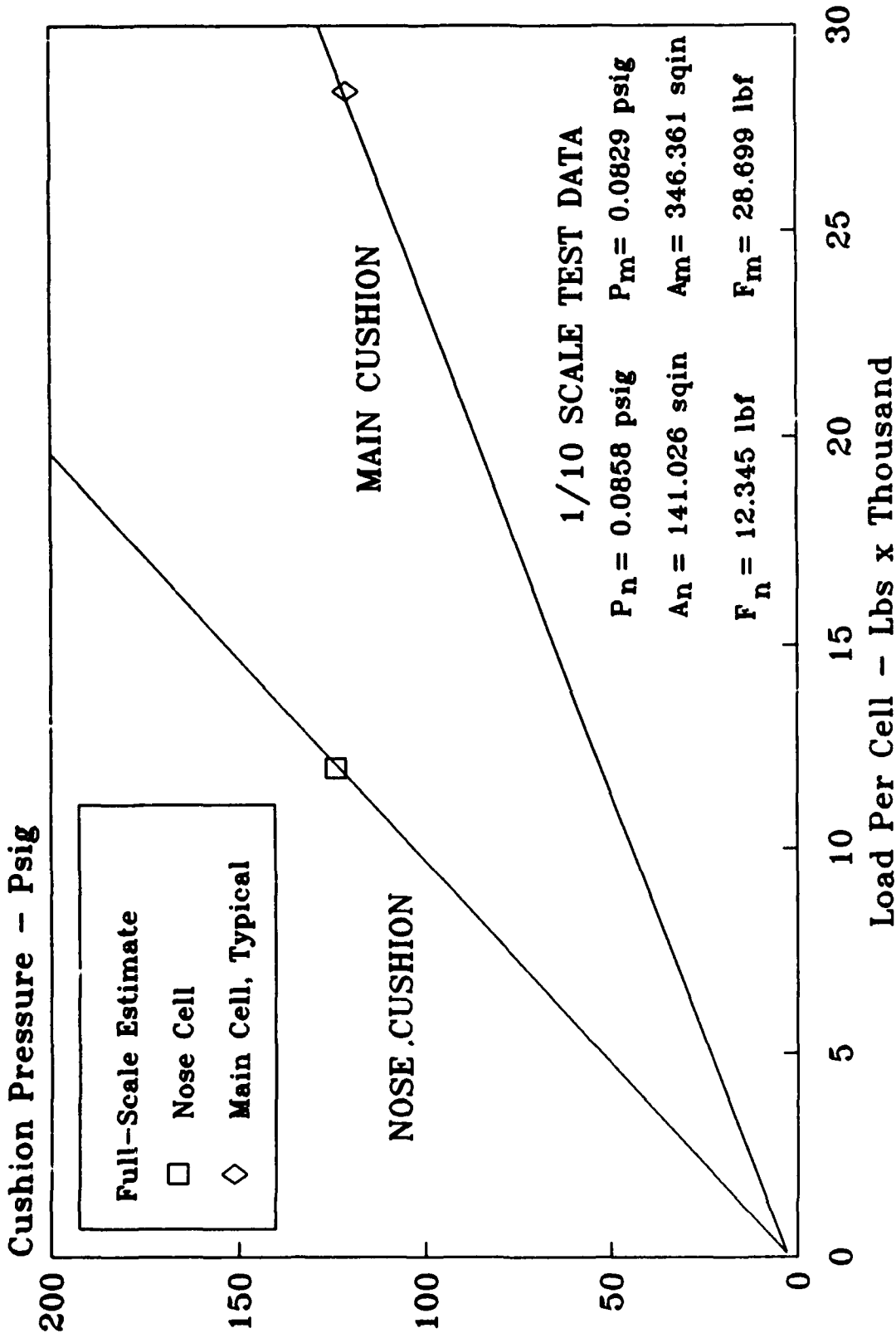


Figure 51. ACET Full-Scale Cell Loads

pitching moment was defined as a pitch up moment imparted to the model. The pitch tests were conducted with the Fan Input Power Frequency set at 300 Hz. A total weight of 4.25 Lbs was moved to various predetermined positions along the longitudinal centerline of the model to create the required pitch moments. At each weight location, hard structure clearance measurements were made at four different locations on the model. These locations were the forward leading edge of the model, the aft trailing edge, the left edge of the model at the lateral centerline of the main cells and the right edge of the model at the lateral centerline of the main cells. The fore and aft measurements were used to calculate the pitch attitude of the model while the left and right measurements were used to determine the roll of the model. Left and right side of the model are determined by looking forward from the rear of the model. The roll angle is considered positive if the left side of the model is higher than the right. From the data taken during these tests, it was determined that negative pitching moments produced a negative or nose down attitude on the model and positive moments yielded a nose up attitude (Figure 52). Also, with zero pitching moment, the model exhibited a positive 0.13-degree pitch attitude. The pitch angles recorded during these tests were consistently lower than those observed on the full-scale ACET. As an example, in a comparable configuration, a pitch angle of 0.68 degrees was recorded on the full-scale vehicle. While the trends provided by the model are the same as the full-scale vehicle (Figure 53), the small angles suggest that the model skirt material characteristics are stiffer than the full-scale article.

A review of the pressure readings in the plenum, nose cell and the two main cells (Figure 54) did not provide any additional explanation of the small variation of pitch angle with pitching moment. It did furnish some insight into what could have caused the reversal in slope as the pitch moment became positive. At this point, the air gap around the nose cell skirt has increased significantly above the nominal operating value and the fan system is having difficulty maintaining sufficient air flow into the nose cell to prevent collapse. While the nose cell did not collapse at a pitching moment of 61.80 in-lbs, the trend in the data suggests that if it would have been possible to increase the pitching moment further, the nose cell would have collapsed.

Testing the Heavy Weight Model to determine its roll characteristics was even more restrictive. While more total weight could be moved for these tests, a 3.6- and 4.25-lb block for a total weight of 7.85 lbs, the distances the weights could be displaced from the longitudinal centerline of the model were limited. The maximum rolling moment that could be created while maintaining a constant model weight of 62.00 lbs was 140.44 in-lbs. Also, we discovered during preliminary roll tests that the torque of the "MAXIAX" fan has a large impact on the roll angle data. For positive rolling moments, the torque reduced the resulting roll angle. While when the model was subjected to negative rolling moments, the torque added to the roll angle. Of the two conditions, we consider the negative rolling moments to be unrealistic.

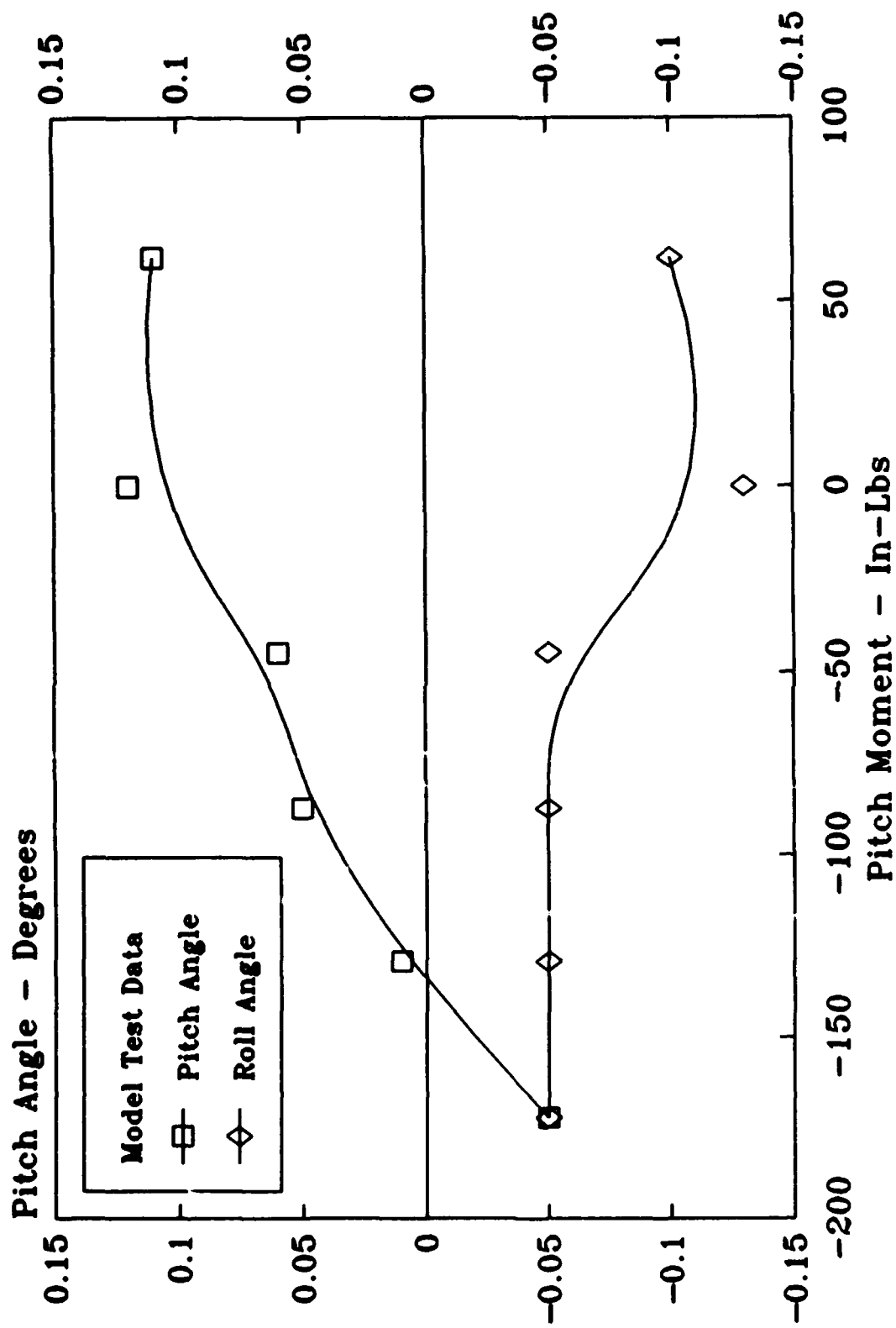


Figure 52. Pitching Moment Effect on Model Attitude

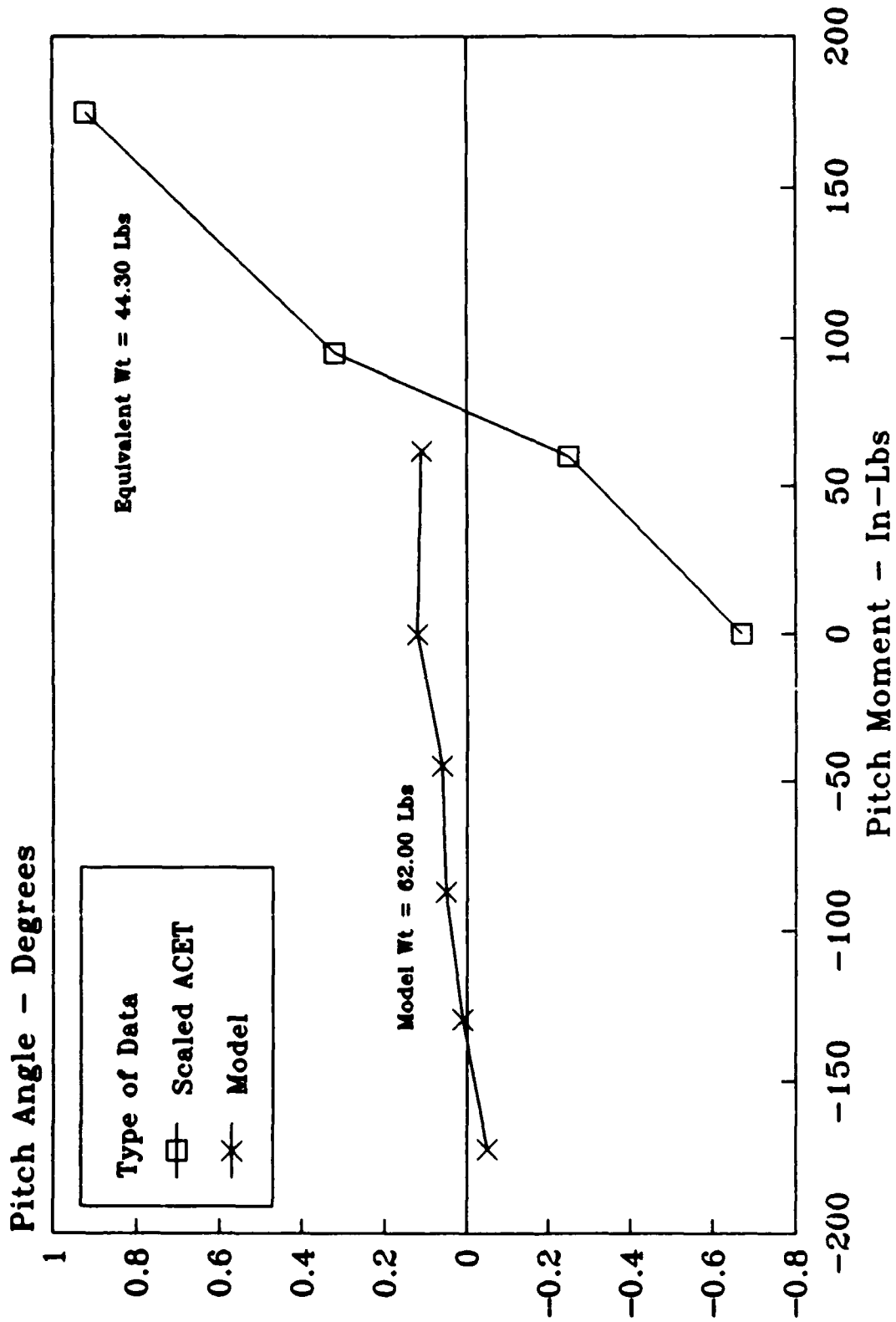


Figure 53. Comparison of Model and Scaled ACET Data

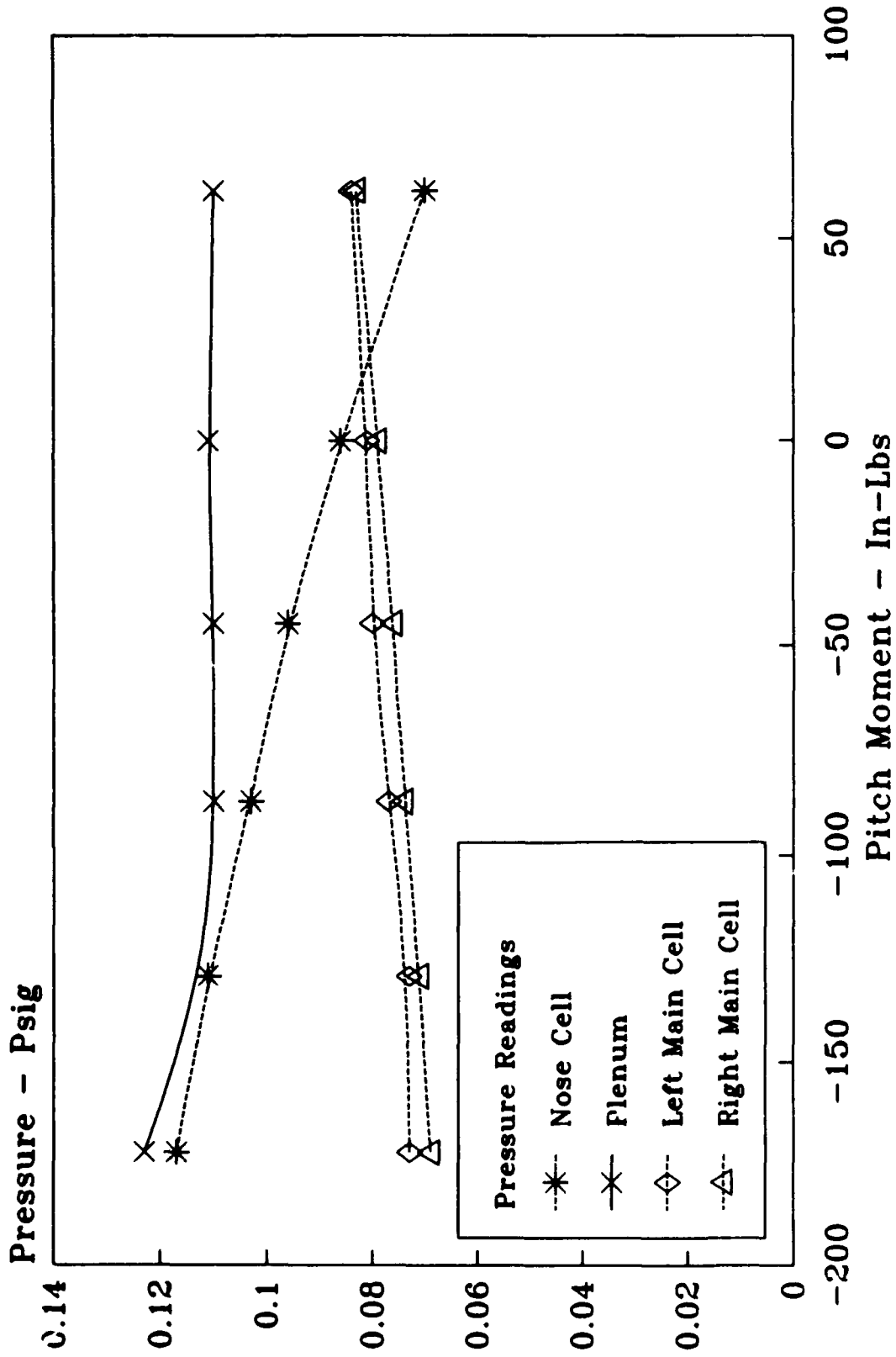


Figure 54. Pitching Moment Effect on Cushion Pressure

The final testing of roll response was restricted to positive rolling moments only (Figure 55). The negative roll attitude of the model is a direct result of the torque. Given the limited range of the rolling moments, excellent roll data were collected. A total of five different rolling moments were used during these tests. The two weights were displaced laterally from the longitudinal centerline of the model in various combinations to achieve the required moments. The maximum lateral displacement of the 3.6-lb weight was 15.4 inches while the 4.25-lb weight could be moved a distance of 20.0 inches. The response of the model in roll is typical of air cushion vehicles which have flat response curves within the limited range of allowable lateral CG shift. Air Cushion vehicles are also extremely sensitive to lateral shifts in CG. Exceeding the lateral limits results in collapse of air cushion cell/cells and sudden changes in vehicle attitude. The pitch attitude remained constant, and nearly zero throughout the entire range of rolling moment inputs. This clearly indicates that neither the nose cell or either of the main cells collapsed during the test runs. Therefore, the lateral limit was not exceeded.

However, the roll angle data and the pressure data (Figure 56) does not give any indication of how close the model was to this limit when the maximum rolling moment was applied. The plenum pressure remained constant throughout the entire range except for the final moment of 140.44 in-lbs. The pressure responses in the left and right main cells were as expected. A positive rolling moment causes the air gap around the periphery of the left main to increase. This results in excessive venting of the cushion and a drop in the cushion pressure. The opposite occurs in the right cell for a positive moment. The gap decreases and the cushion pressure increases. The data indicate an increase in the rate of change of the pressure in all three cells as the rolling moment was increased from 120.89 to 140.44 in-lbs. However, without the application of a larger rolling moment it was impossible to determine if the limit was being approached.

While a comparison of scaled data from the ACET Full-Scale Test Program to model indicated the simulation created by the model was too stiff in pitch, this was not the case when the roll data was reviewed (Figure 57). Allowing for the differences in weight are factored into the evaluation, the slope of the two curves, in the range of available data is very close to being identical. The only difference is the zero moment displacement of the model curve resulting from the torque of the model fan engine.

The second series of tests involved the steady acceleration of the Heavy Weight Model to speeds of approximately 1 foot/second to measure breakaway and steady-state drag. The test setup (Figure 58) and the procedures followed during the these tests evolved from a series of attempts to collect accurate drag data. Prior to starting these tests, a preliminary test had been conducted with a fish scale. The purpose of this tests was to determine what size load cell should be purchased to record the dynamic drag data. These tests yielded breakaway drag forces in the range of 5 pounds, the smallest division on the fish scale. A 0-

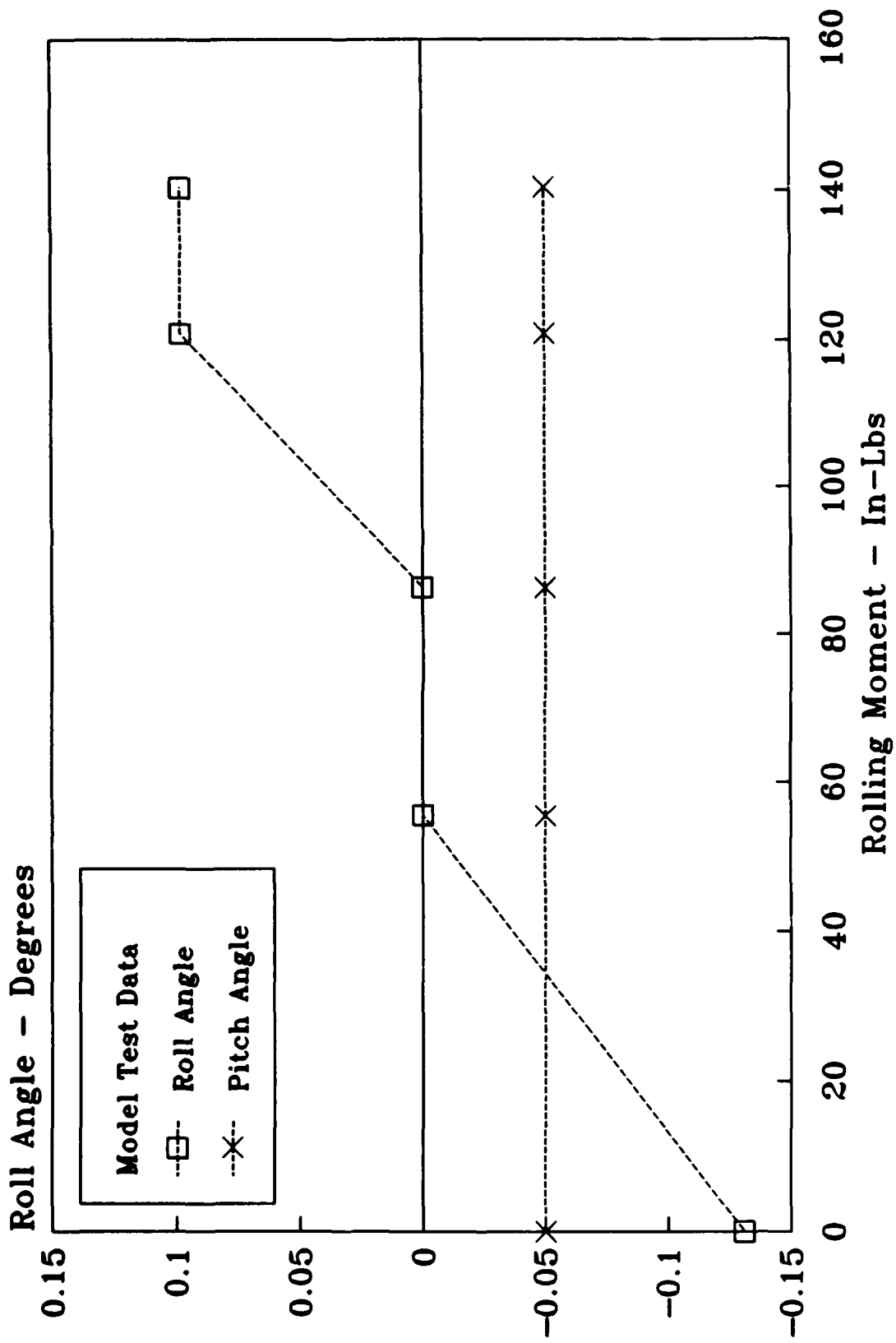


Figure 55. Effect of Rolling Moment on Model Attitude

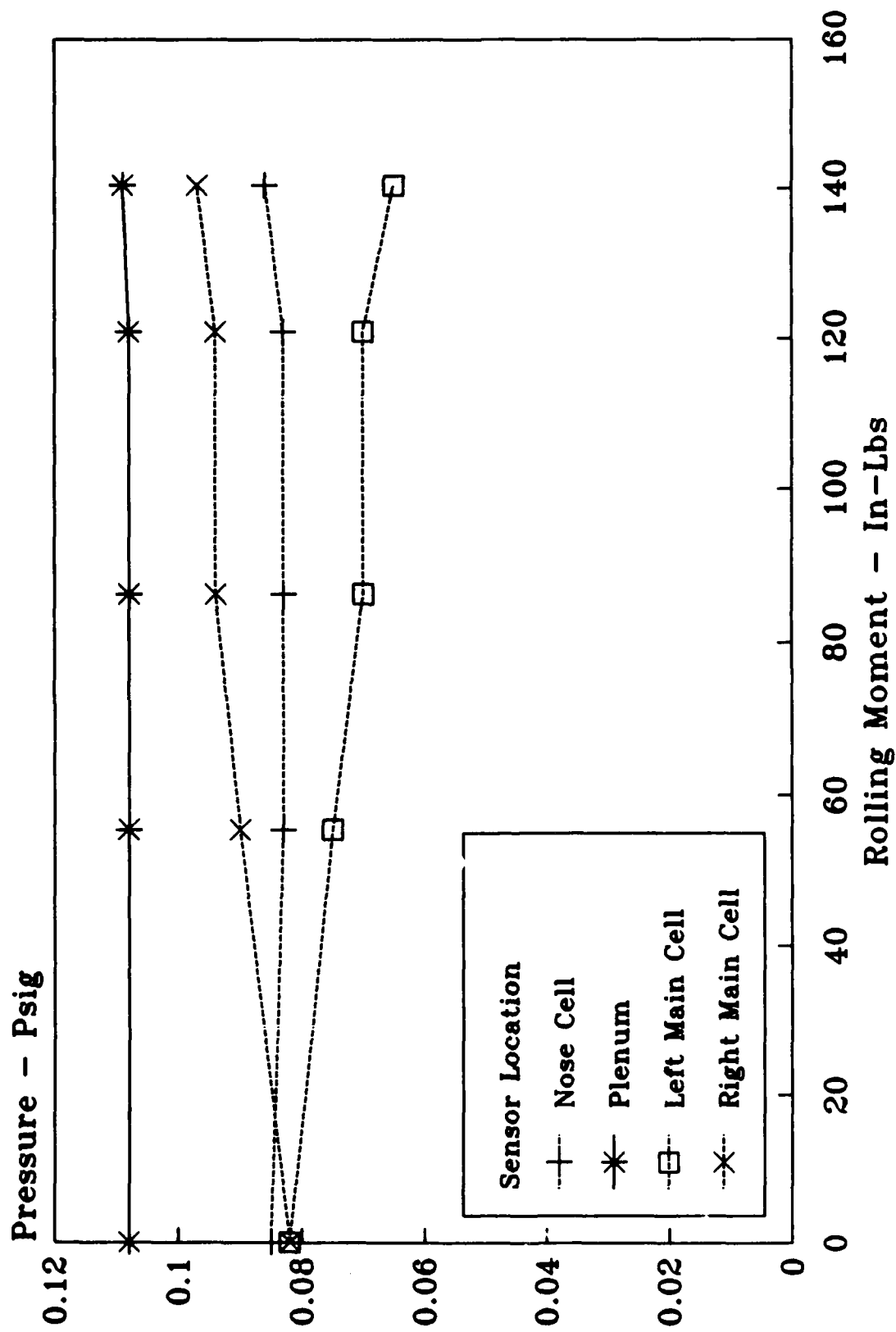


Figure 56. Effect of Rolling Moment on Pressures

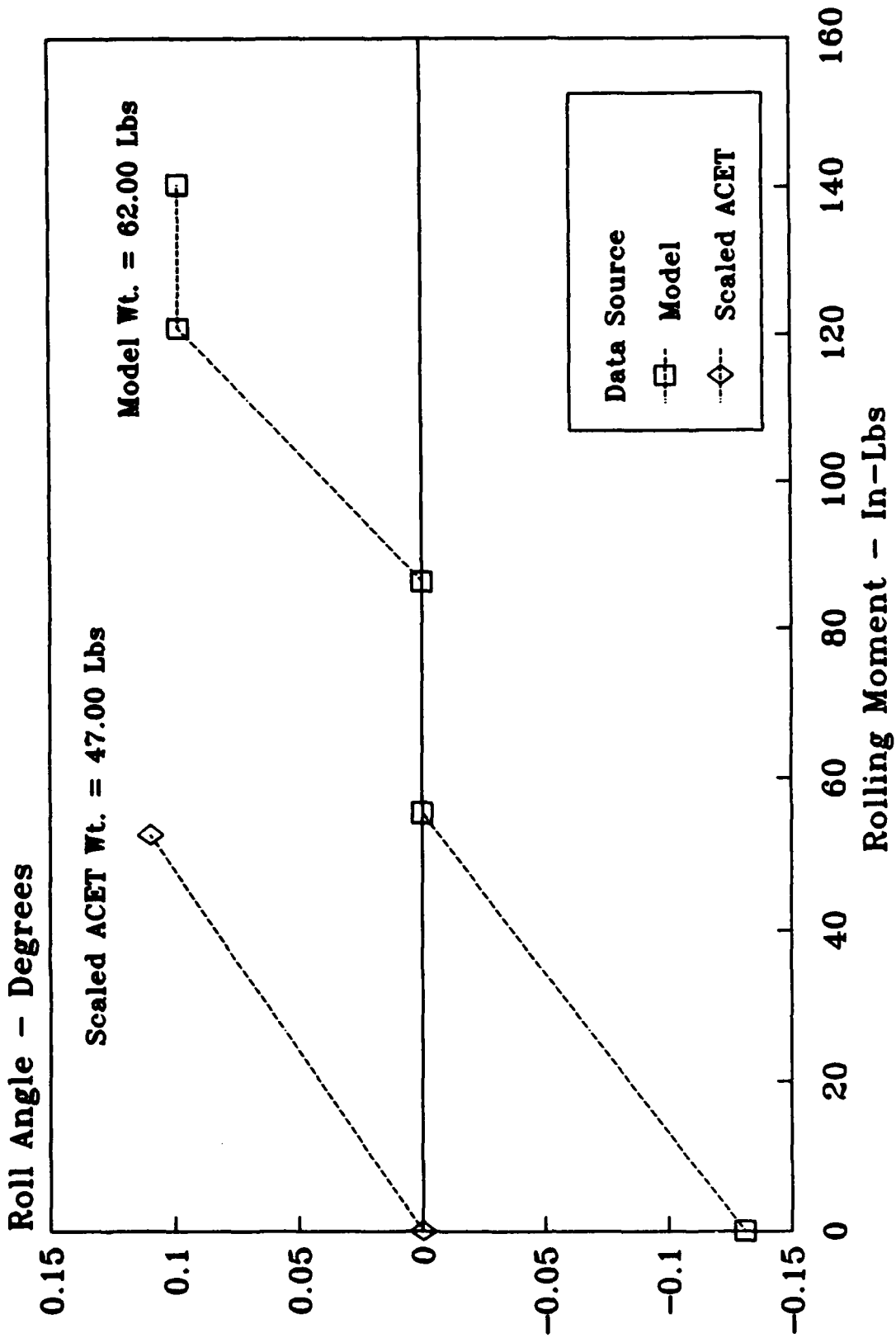


Figure 57. Comparison of Model and Scaled ACET Roll Data



Figure 58. Drag Test Setup for Heavy Weight Model

to 25-pound load cell was purchased for these tests. This range was selected to permit the recording of drag data during obstacle as well as smooth surface tests. The first attempts were made with a nylon coated wire cable and a low speed electrical winch. This approach was totally unacceptable. The initial surge of the winch produced excessively high readings for the breakaway drag force and unacceptable vehicle dynamics. Also, the wire cable biased the steady-state drag data because of the length of cable required to reach from the winch to the model. Even though the first attempt was unsuccessful, the basic approach was considered to be feasible and a series of modifications were made to the test setup. For the second trial run, the electric winch was replaced with a hand operated boat winch and nylon rope was substituted for the wire cable. In addition, two wooden barriers were installed on the Static Test Platform to restrict the lateral movement of the model. This second configuration demonstrated a marked improvement in the dynamics of the model during the initial acceleration. However, random contact with the restraining rails eliminated any possibility of obtaining accurate drag data.

Breakaway drag force readings in the range of 25 pounds were being recorded during tests on a smooth surface. Clearly, additional improvements had to be made to the test setup if any meaningful data were to be collected. After observing a number of trial runs, we determined that the instrumentation cables and the nylon rope being used to tow the vehicle were causing the model to veer into the restraining rails during either the initial acceleration or the constant speed portion of the test run. Of the two problems, the effect of the instrumentation cables was the easiest to eliminate. Since a technician was already stationed on the Static Test Platform to reposition the model after each run, his duties were expanded to include holding the instrumentation cables during the runs. The distance traveled was relatively short, less than 15 feet, and the speed was also low, approximately 1 fps; therefore this approach, while simplistic, was very effective. The problem with the nylon cable was not as easily solved. In order to eliminate or at least to minimize the effects of the cable, the weight of the cable per linear foot had to be reduced significantly. This reduction dictated that nylon string of the type used for fishing be employed as the cable for the drag tests. Therefore the nylon rope was replaced with 50 pound, test, nylon string. Reducing the cable down to this size also required a different winch. After considering and evaluating a number of off-the-shelf hand winches, it was determined that an open faced spinning reel, normally used for fishing, produced the smoothest, constant pulling force. Also, the drag on the reel could be adjusted to compensate for the weight of the cable. This configuration yielded breakaway drag forces in the 1.0 to 4.0 pound range during test runs. However, the problem of contact with the restraining barriers still existed.

The dramatic reduction in the values obtained for breakaway drag clearly indicated that the improvements made to the test setup were effective. The agreement of these readings with preliminary data collected during check-out tests established the validity of the data. The only hurdle remaining was the bothersome problem of maintaining a

straight track during the test run. Once all of the other factors were eliminated, it was easily determined that the primary cause of the model drifting into the barriers was the torque from the electric motor in the "MAXIAX" fan. This was overcome by attaching a second cable and spinning reel to the Heavy Weight Model. The nylon string from this reel was attached to the rear of the model. Since the drag on these reels can be varied, as previously noted, a 0- to 5-pound fish scale was used to set a known pre-load on the model. This pre-load caused the model to maintain a straight track down the middle of the test section. As was the case with any change in the test fixture or procedures, a series of runs were made to determine the smallest amount of pre-load that could be used and still maintain the required directional control. The final pre-load selected for the breakaway drag tests was 2.0 pounds. Since this was a known, constant force, it was simply subtracted out of the readout of the load cell during the data reduction.

Having solved all of the test procedure problems, it was now feasible to proceed with the testing of the Heavy Weight Model. The first area to be investigated was the performance of the model on a smooth, level surface. The goal of these tests was to establish a database for comparison with tests conducted with the full-scale transporter on similar type of surface, a taxiway for example. Using mass flow data collected during the calibration of the "MAXIAX" fan, a number of runs were made at various Fan Input Power Frequencies. The data collected were then used to develop the variation of drag, both breakaway and steady state, as a function of mass flow rate (Figure 59). Each data point was run a minimum of three times to insure accuracy and repeatability. The agreement between individual runs was very good. The trends resulting from the 1/10 scale data were identical to those collected during the full-scale tests.

With a payload of 47,000 lbs, the total weight of the full-scale ACET/Payload combination was 60,822 lbs. This is very close to the design point for the Heavy Weight Model, 62,000 lbs. The 47,000-lb data from the full scale test program was reviewed and the configuration with zero passive venting and the aircraft spotted at the mid position on the deck of the ACET was selected as the most representative of the model. A comparison of the two data sets was made after the appropriate scaling factors have been applied to the full-scale data (Figure 60). While the two data sets did not compare exactly, there was reasonable agreement between the data. The 1/10 scale model predicts a wider spread between the breakaway and steady-state drag readings than actually occurred. Also, the model test data yielded higher values for the breakaway drag while indicating lower steady-state values than actually experienced during the full scale testing. Overall the findings from the low-speed tow test over a smooth surface were encouraging. The general agreement between the two sets of data indicates that with continued refinement of testing procedures and increasing the scale of the model to increase the magnitude of the drag forces, model testing could be used to predict drag forces for future applications and configurations of the ACET.

This finding was upheld during the obstacle traverse testing that followed the level, hard surface tests. For these tests, small, discreet

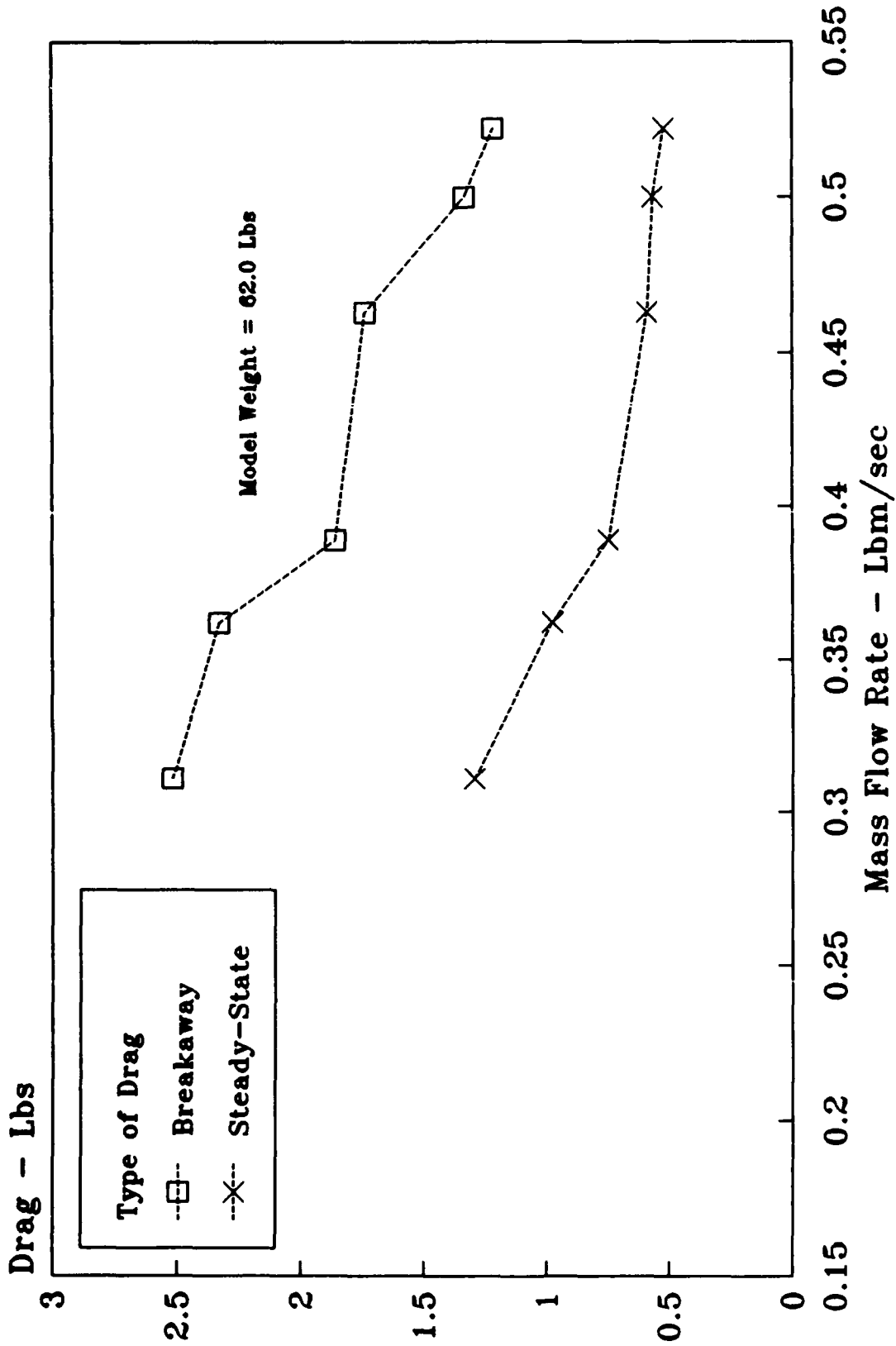


Figure 59. Drag Variation with Mass Flow Rate

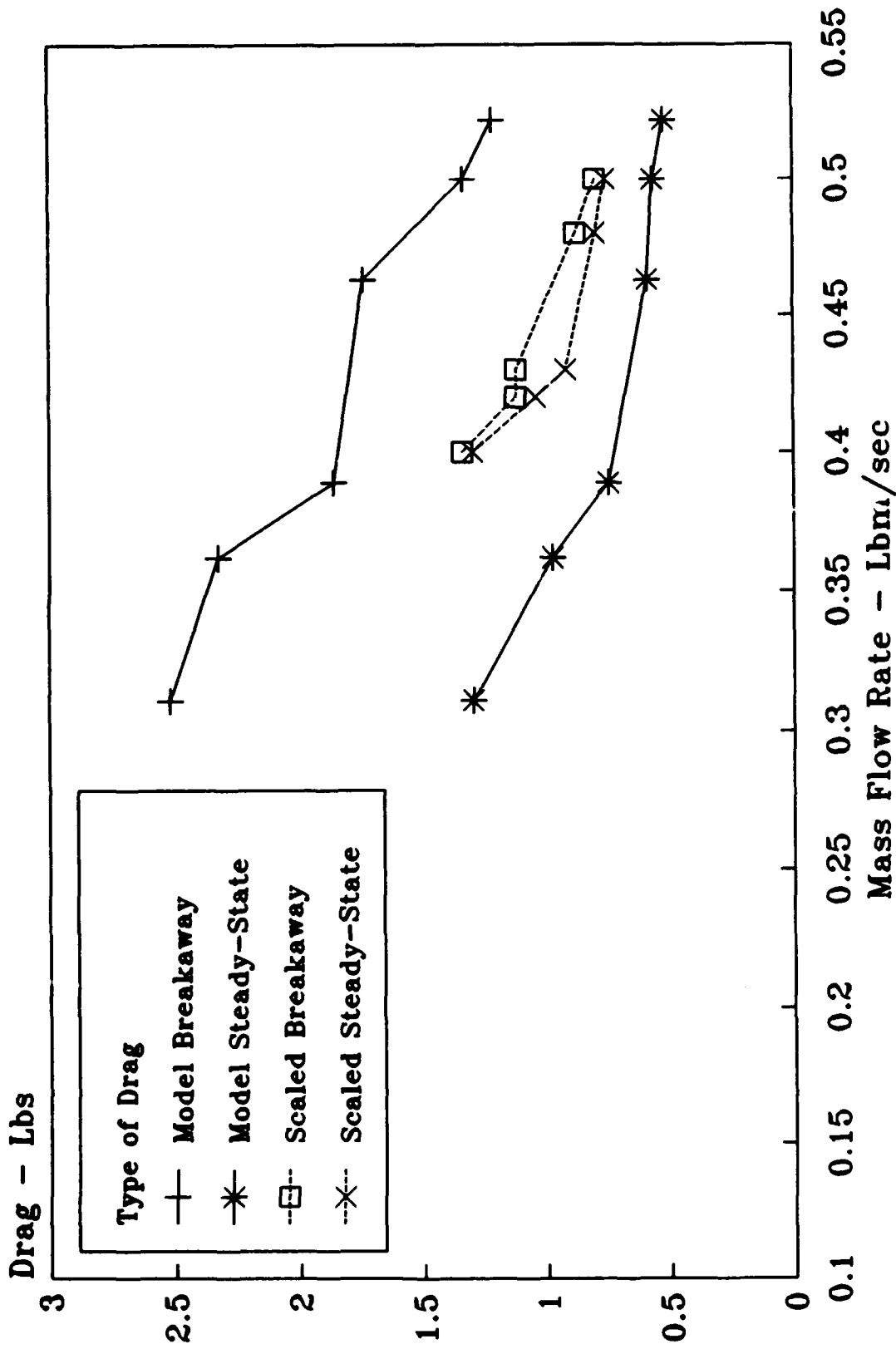


Figure 60. Comparison of Model and Scaled ACET Data

obstacles of known frontal area were placed in the center of the test track. Double backed tape was used to fasten the rectangular obstacles to the smooth, hard surface level. The tape was used to reduce the possibility of damaging the skirt systems. Approach inclines were also added to the obstacles after some initial check-out runs produced minor damage to the trailing edges of the Nose Cell Skirt. The maximum obstacle size used during the testing was 4.32 sq in. This limit was established after several attempts to cross obstacles of greater frontal area were unsuccessful because of snagging on the trailing edge of the Nose Cell Skirt.

The drag readings were recorded for the impact of the obstacle on the leading edge of the nose cell skirt as well as when the obstacle exited the nose cell cavity (Figure 61). The drag recorded as the obstacle exited the cushion cavity was constantly higher than the drag resulting from the initial impact. This is a result of the inward taper of the skirt system. The obstacle deflecting capability of the full-scale system can be simulated at this scale. The consistency of the data is shown by the plots of breakaway and steady-state drag for all of the obstacle tests. Again, indicating that the basic procedures developed for this testing are sound.

Although no pure obstacle tests were conducted with the full-scale vehicle, some comparisons can be made between data collected during the USAF full-scale testing and the 1/10 scale model tests conducted in the MDL. If the established scaling laws are applied to the data collected during drag tests on grass, the resulting scaled values fall in the range of the data collected from the scale model tests. The full-scale tests were conducted with a payload weight of 30,475 lbs, total vehicle weight of 44,297 lbs. Even though there was no way of determining how much frontal area the full-scale vehicle skirt was exposed to during the grass testing, it is evident that the data collected in the lab was again at least representative of the full-scale vehicle.

7. RESULTS

Model testing on this scale cannot provide any data for predicting the full-scale heave stability of an air cushion vehicle, regardless of the application. The "unscaled" atmosphere seems to be the source of the problem in this area. Unless a concentrated effort is made to develop a new set of scaling laws to compensate for this factor or new testing procedures are developed, such as testing in a chamber which can produce and maintain a scaled atmosphere; heave stability investigations will continue to require large model or full-scale vehicle tests to verify existing analytical theories.

Using models to determine the drag and obstacle characteristics of a air cushion system does provide reasonable data. Although model scales larger than 1/10 should be used to facilitate the collection of accurate data. Also considerable attention must be paid to matching the stiffness characteristics of the skirt system and the fan curve of the air supply system used in the full-scale vehicle. These factors indicate that in

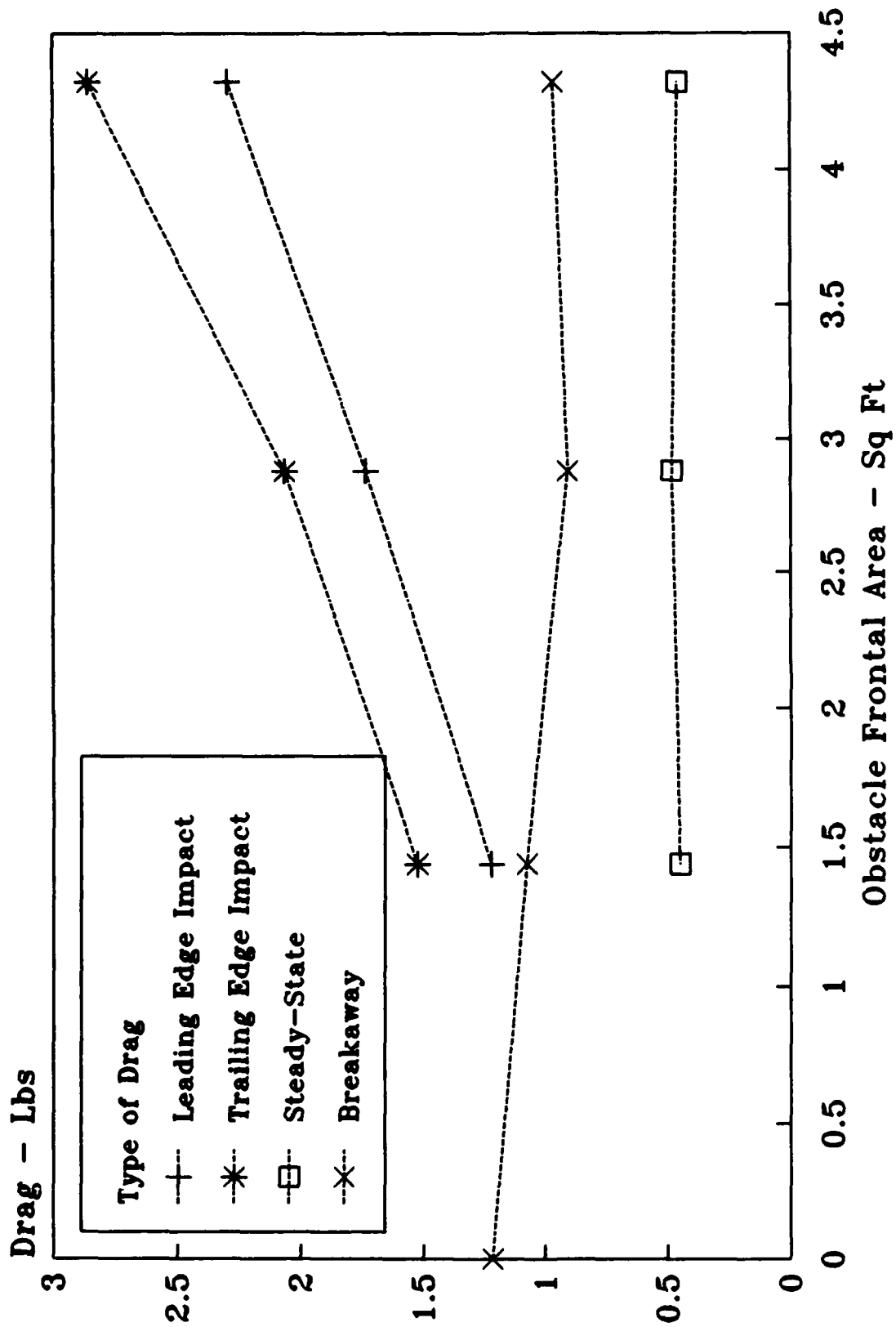


Figure 61. Effect of Obstacles on Drag

order to get an accurate simulation using a model considerable amounts of funding must be devoted to the development of true scaled fans and skirt materials. The model developed for the in-house test was a low cost item, using existing "off the shelf" components and materials whenever possible. The accuracy of the data and capabilities of the model suffered as a result. Future efforts in modeling air cushion systems should allow for investing additional funding for the development of the model.

SECTION V

USAF TESTING OF FULL-SCALE ACET

1. OBJECTIVES

In August 1985, the ACET was turned over to the USAF. The transporter and the decommissioned F-101B, used as a payload during the contractor's, BACT's, Test Program were disassembled at the BACT's facility in Canada by an integrated crew composed of BACT, USAF, and SRL technicians and engineers. The disassembled transporter and aircraft were then moved overland, via semi tractor trailer rigs, to Airborne Air Park, Wilmington, Ohio. This was the test site for all of the USAF testing of the full-scale ACET. An off site location was selected to obtain access to a wider variety of off-runway surfaces without having to deal with the normal restrictions and regulations of an active airfield, such as Wright-Patterson AFB. Both the ACET and the F-101B aircraft were assembled at the test site, using procedures established during the disassembly.

The objectives of the USAF Test Program were to collect data for the definition of a Self-Powering Modification for the ACET, evaluate the need for an active heave control system and formulate a better understanding of the performance of the ACET with the Segmented Finger Skirt installed.

The passive control system installed by BACT did provide a measure of improvement, in that, the 6-Hz heave oscillation was controlled. However, the passive venting of the nose and main cells did not effectively correct the 2-Hz heave problem. Further, it was recognized that this type of venting system is basically wasteful because of the constant bleeding of cushion air regardless of the pressure within the cells. The data collected during the contractor's Test Program suggested the need for the parallel development of an active heave control system. Scale model system development, as reported by Messers J.R. Amyot and H.S. Fowler (Reference 6), attest to the basic feasibility of this approach.

Of equal importance to the future application of the ACET was the identification of the parameters critical to the design of a Self-Powering Modification. This is an extremely difficult task since virtually all of the performance parameters of the transporter would have an impact on the design of this new subsystem. The need for this modification was always one of the first comments made whenever the ACET was demonstrated or briefed to any potential users.

The change from a "jupe" skirt system to a segmented finger skirt (see Section III), was not made until late in the contractor's test program. Therefore, a limited amount of data was collected on this new skirt system. The static and dynamic stability predictions, made during the Design Phase of BACT's Program, were based upon a "jupe" skirt system. A first order analysis was conducted when the skirt system was changed. The material used to fabricate both of the skirt systems was a nylon

fabric with a Neoprene covering. Therefore the material properties of the two skirt systems were the same. However, this material exhibited an excessively high wear rate during extended overland operations. If the operational capabilities of the ACET were to be realized, an alternate material with improved wear characteristics had to be identified and evaluated for this application.

2. APPROACH

A series of static and dynamic tests was formulated to collect the data necessary to meet the objectives of the test program. The static tests were conducted on level concrete and grass with concrete blocks and the F-101B being used as the payload. The dynamic tests consisted of low, 5- to 8-mph, and high, 20- to 25-mph, speed runs on taxiways and grass with the F-101B as the payload. Both the gross weight of the aircraft and the position of the aircraft were varied as part of these tests. The concrete blocks were not used during the dynamic tests. Whenever possible the tests, both static and dynamic, were structured to provide data that could be used in several, if not all, of the analyses being conducted as part of the USAF Test Program on the ACET.

The majority of the data, pressures, accelerations, and drag loads were recorded on a magnetic tape recorder. Certain initial conditions data were hand recorded on data sheets for correlation with the magnetic tape data. Of particular importance was the accuracy and repeatability of the data collected during these tests since the contractor's test program had been plagued by instrumentation problems of all types. After inspecting the instrumentation system supplied with the transporter, the decision was made to scrap the entire system and completely redesign the instrumentation for the ACET. All of the sensors, pressure, acceleration, temperature, and load were bench checked and recalibrated if found to be serviceable. A number of sensors had to be replaced because they failed these critical tests. When the magnetic tape recorder, used by BACT, was bench checked, it was determined that the playback circuit was in need of a major overhaul. Since the entire instrumentation, including the cables was being rebuilt, the decision was made to replace this tape deck with an AMPEX FR1300 Magnetic Tape Recorder. This proved to be an excellent decision. This recorder did not cause any problems throughout the entire test program. The signal conditioning for the various sensors was installed internally within the recorder. Therefore there was no requirement for a separate signal conditioning package. The magnetic tape recorder was installed on the tow vehicle, generally a truck of some type. If room permitted, an instrumentation technician ran the recorder during the tests. However, the system was set up to allow the ASP-10 operator to run the recorder. This feature was used during a number of tests.

3. HEAVE STABILITY TESTS

As part of the heave stability evaluation, the services of Dr. J. R. Amyot, National Research Council, Canada, were enlisted to develop a feedback control circuit for the active control system for the full-scale vehicle, based upon Dr. Amyot's analytical and scale model work in this area. The function of this control circuit would be to sense a build-up in cushion pressure and provide sufficient venting of the air cushion cell to eliminate any significant pressure fluctuations within the three cells of the ACET. The control of pressure fluctuations within the cells is the key to eliminating heave oscillations. Of the two systems, the active heave control system is the more efficient since the normal position of the heave control vent is closed. While in the passive heave control system, the heave control vent is always open once the cell pressure exceeds a predetermined threshold value. Of course, there is a penalty to be paid. The passive system is a simple mechanical system made up of springs and dampers. The active system adds a feedback control system to the passive system. Therefore, all the aspects of the heave oscillations must be fully understood before the control system parameters can be defined.

A series of tests were run at a payload weight of 30,475 lbs, the empty weight of the F-101B aircraft, to collect the data Dr. Amyot needed to begin his analysis of an active control system. After his initial review of the data, Dr. Amyot concluded that the passive control system design had sufficient control authority to eliminate the 2-Hz oscillation. Further, Dr. Amyot stated that performance degradation from the passive system was not sufficiently high to warrant the introduction of the added complexity of an active heave control system. Dr. Amyot was of the opinion that the simulation used to model the full-scale ACET for the stability analysis had not included all of the necessary parameters and, therefore, had not predicted the correct venting schedule for the control vents. If the correct vent schedule could be established, the passive heave control vents could be used to provide an effective means of eliminating the 2-Hz heave oscillation.

The original simulation and analysis predicted a difference in the heave stability of the ACET when moving an aircraft versus a lumped mass. This finding could easily be verified through full-scale tests while serving as a starting point for verifying/evaluating the original results. When the transporter/payload combination was analyzed as a lumped mass, damping not included, a baseline heave stability boundary was defined. When the analysis was repeated with a coupled vehicle model to represent the aircraft shock struts and the damping from the struts and the aircraft tires, substantially greater stability margins were found. This finding was substantiated with full-scale test data. Two different types of payload were used for these tests. The target payload was 30,475 lbs. One payload was the F-101B aircraft. As previously stated, the target weight for these tests corresponds to the empty weight of the aircraft. The second payload consisted of concrete blocks. The blocks were stacked and arranged on the deck of the ACET to simulate the wheel loading of the empty F-101B aircraft at the forward of three storage positions on the

transporter. Since the venting area of the main cell stability vent doors could be controlled more precisely than those installed on the nose cell, Figure 19, supplemental venting was restricted to the main cells. The venting of the nose cell was restricted to the vent holes cut in the outer face of the fingers. For all vent openings investigated, higher ASP-10 settings were attainable when the aircraft was the payload (Figure 62). The higher the ASP-10 setting that can be used for a given configuration the higher the cushion pressure in each of the cells. This translates into improved soft surface performance and reduced tow forces.

The results presented in Figure 62 agree with the findings of the original computer analysis for these two configurations, namely that the dampening introduced by the aircraft landing gear increased the stability of the ACET/Payload combination. However, the heave frequencies predicted by the computer analyses were different from those encountered with the full-scale ACET, 2-Hz versus the predicted 6 Hz. If the original analyses had included a more accurate representation of the vehicle, it should have been impossible to excite these two configurations in heave, even without passive venting of the main cell cushion areas. Clearly, this was not the case. Still, all of the data collected supports the basic validity of the computer simulation but highlights the requirement to refine or tune the simulation. Also, cushion vent areas above 125.0 square inches (sq in) allowed the ACET to be operated at full power. This was a very good indication that passive venting could be used to control the 2-Hz oscillations.

Further tests, both static and tow, were conducted in an attempt to establish a passive cushion venting schedule which provided adequate control throughout the entire payload range of the ACET. The two key questions associated with these tests were: could the 2-Hz heave oscillation be eliminated throughout the entire operating envelope of the ACET and what was the impact of cushion venting on tow forces, principally breakaway drag. To establish the boundaries of the breakaway drag forces, two venting areas were selected. The first was the unvented configuration (Figure 63). Both aircraft gross weight and position on the transporter have a direct effect on the breakaway drag. These tests were conducted on smooth concrete surface. At the beginning of each run, the ASP-10 Power Setting was incrementally increased until heave was encountered. The setting was then decreased until stable operating conditions were achieved. The individual runs were then performed at that setting. Obviously, as payload weight increases, the towing force and the breakaway drag increase as well. However, even in the worst configuration, payload weight of 47,000 lbs in the full aft location, the breakaway drag was still less than 10 percent of the total weight of the vehicle. The second venting area, selected, was 185.5 sq in (Figure 64). This venting area was selected because this area was required to achieve reasonable operating configurations at the higher payload weights. A comparison of the two graphs shows that the trends identified with no venting of the main cells agree with those observed during the runs made with the venting of the main cushion cells.

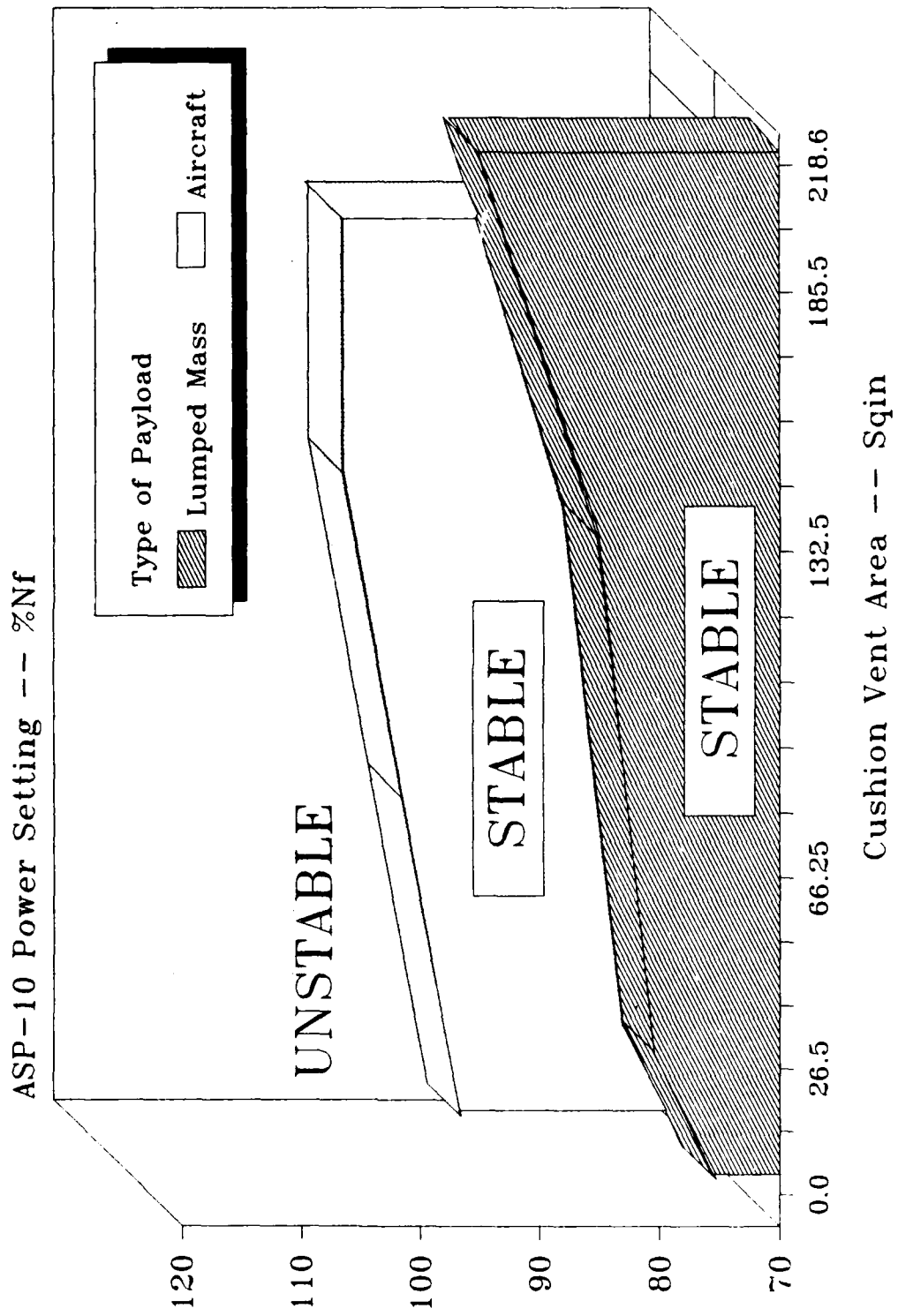


Figure 62. Heave Stability Boundaries

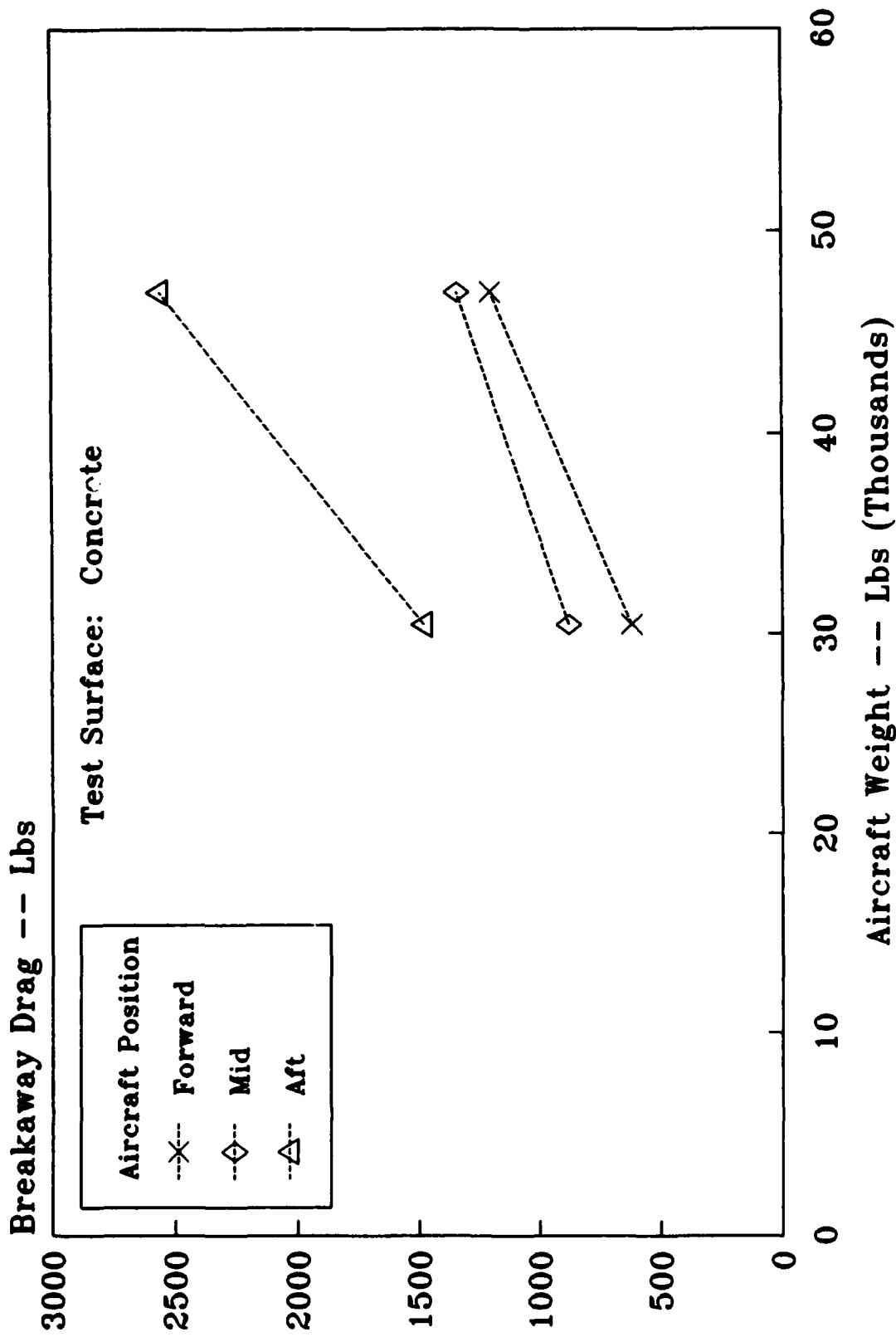


Figure 63. Breakaway Drag For Zero Venting

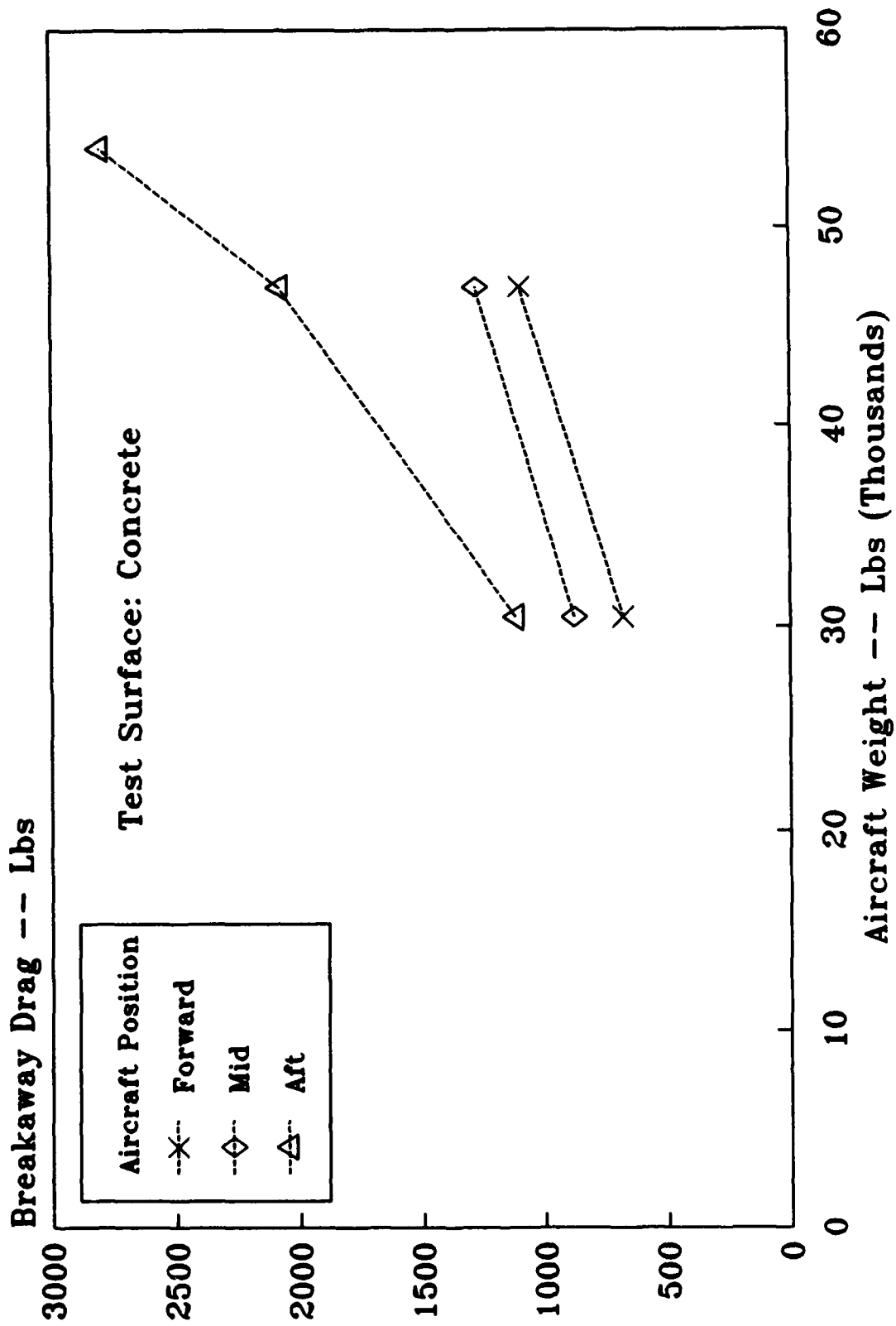


Figure 64. Breakaway Drag For 185.5 SqIn of Venting

Unfortunately, only one run was made with a payload weight of 54,000 lbs before there was an ASP-10 failure. However, the data (collected from the two lower payload weights at various positions) do demonstrate that constant venting of the main cells, to control heave oscillations, does not cause excessive increases in breakaway drag. In fact, because the venting generally allowed the individual runs to be conducted at higher ASP-10 settings, the breakaway drag was lower when identical test conditions were compared.

In support of the evaluation of the effectiveness of the Passive Heave Control System, supplemental pressure data were collected and analyzed to identify potential sources of the heave oscillations. Pressure transducers were installed in three locations in the plenum area to supplement the data being collected in the nose and main air cushion cells. The first plenum transducer was placed near the starboard (right when viewed looking forward) ASP-10 fan exit. The second plenum pressure transducer was installed at the downstream end of the convergent plenum section, again on the starboard side of the transporter. The final transducer was placed at the junction of the Forward or Power Module and the Main Cell Modules.

The goal of this analysis was to identify a parameter which would indicate the onset of heave oscillation regardless of the payload weight, position of the payload on the vehicle or the ASP-10 Power Setting. This parameter proved to be the pressure variation in the convergent plenum section. The importance or significance of this parameter was not immediately discovered because of the relatively small pressure variations, +0.005 psig to -0.05 psig, involved. All of the time histories of the recorded data from these tests were reviewed to determine if there was some type of flag in the data which provided an indication of the oscillations, either pitch or heave, were about to occur. Since these oscillations have been documented as pressure related phenomenon, the analysis centered around possible fluctuations in pressure. One of the first results of this examination was that as the onset of oscillation was approached, pressure fluctuations in the convergent section of the plenum appeared. As the ASP-10 Power Setting was increased beyond this point, the mean pressure and the fluctuations increased until oscillations were noted by observers stationed around the ACET. The presence of these oscillations was confirmed by the data recorded on the vertical axis of the tri-axis accelerometer, installed at the cg of the transporter. Initially, the magnitude of the mean pressure in the convergent plenum section was considered to be the indicator for the onset of oscillation. Attempts to correlate the oscillations of the ACET with the mean pressure of this section of the plenum were unsuccessful. Equally unsuccessful were various attempts to use magnitudes or fluctuations in any of the other pressure readings to the motion of the vehicle.

However, the data from one test with exceptionally strong oscillations suggested a potential correlation between the pressure variation in the convergent section of the plenum and the oscillations. Using the data from this run as a benchmark, a preliminary stability boundary was defined. This boundary required the pressure variation

between the maximum and minimum pressures in the convergent section of the plenum be less than 0.10 psig if the ACET was to be stable. All of the available test data were again reviewed to evaluate the validity of this proposed heave stability boundary (Figure 65). With only a small number of exceptions, this test for oscillation proved to be accurate. Developing an active heave control system to regulate the pressure fluctuations in the convergent plenum section seems to be the most effective means of eliminating the oscillations, based upon the data collected during these test runs. However, since the ACET can be operated effectively throughout its entire operating envelope with a passive control system, the added complexity and cost of an active heave control system was not justified.

Having selected the passive control system as the best means of controlling the ACET's heave oscillations, additional tests were scheduled to further investigate this approach. The goal of this testing was to develop a set of operating curves which would be used as reference charts for an operator. The curves were to mark the boundary between stable and unstable regions of heave oscillation. Variables to be included on these graphs were payload weight, position of the payload on the ACET, the ASP-10 Power Setting and the type of surface the vehicle was traversing. Data were first collected on a concrete surface since operations on a smooth, hard surface produce the worst heave characteristics for the ACET.

Unfortunately, another factor biased the data and prevented a precise definition of the boundary between stable and unstable operations. This factor was finger wear (Figure 66). The effect of finger wear and damage on the operation of the ACET is a shifting of the heave stability boundary. As finger wear increases, the amount of cushion venting area required to achieve stable operating conditions decreases for all ASP-10 power settings. The baseline for the total operating hours presented on the graph is the beginning of the USAF testing. The data collected at 7.7 hours and 15.0 hours are for the same conditions. As indicated, the operating surface was concrete. The payload was the F-101B aircraft at its empty weight, 30,475 lbs, and the aircraft was spotted at the forward position on the vehicle. The only variables between the tests was the additional running time of the ASP-10's with the subsequent finite loss in performance because of operating time and the wear and damage inflicted on the fingers during the 7.3 hours of operating the transporter.

The majority of the finger damage was confined to those fingers having the cushion vent holes cut in the outer face of the finger, Figure 22. The pattern for these holes placed the holes too close together and tears propagated from hole to hole. As a result, the total main cell cushion vent area was increased drastically. This increase in venting area had a stabilizing effect on the ACET. As finger wear and damages increased, stable operations for all configurations were achieved at higher ASP-10 Power Settings. Although the additional venting area did result in an increase in breakaway drag (Figure 67), the ASP-10's still had sufficient reserve capability to supply the airflow required to achieve full inflation of the cells at a Power Setting of 80.0%. This represents an increase of 5.0% in ASP-10 Power Setting after approximately

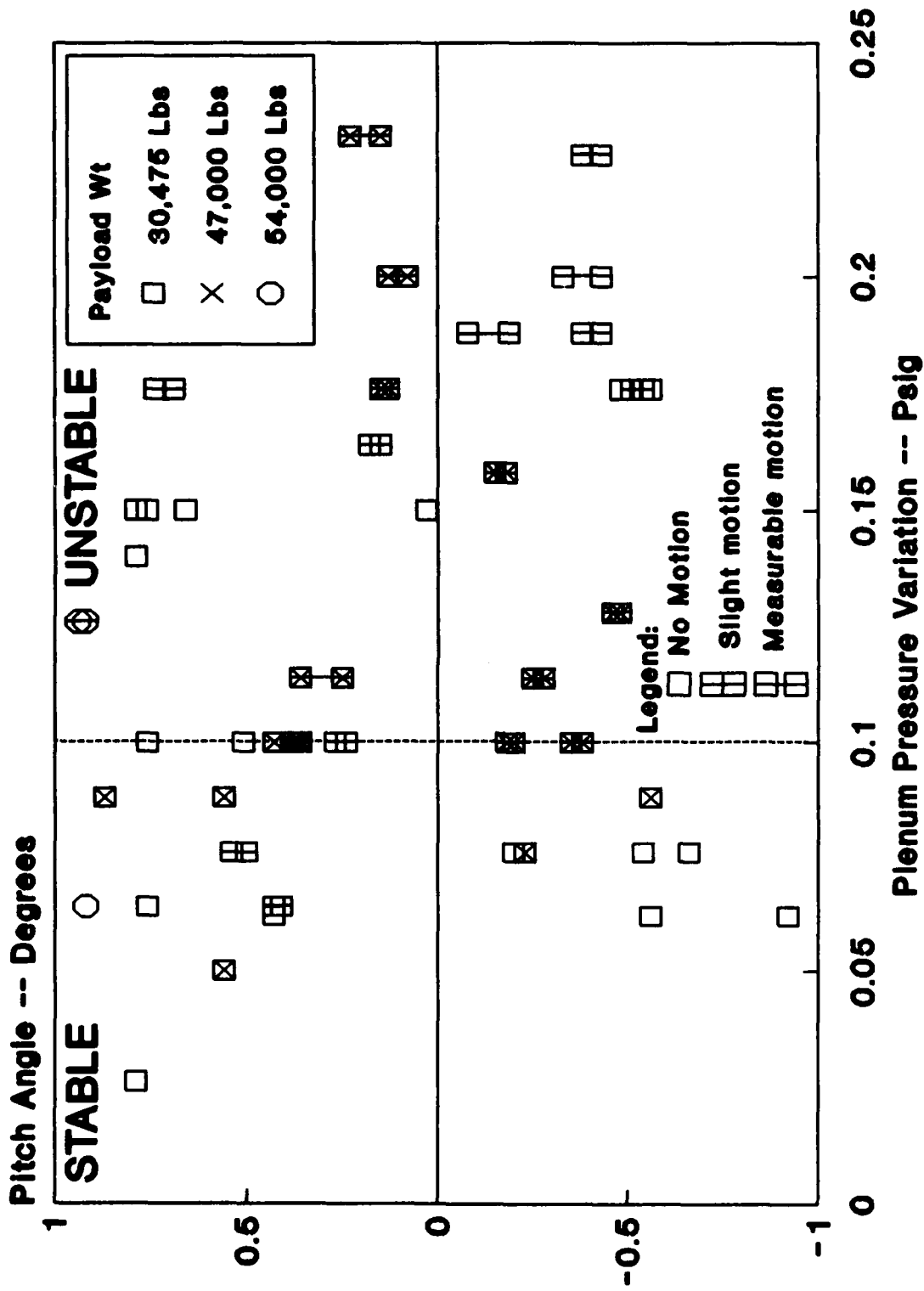


Figure 65. Definition of Stability Boundaries

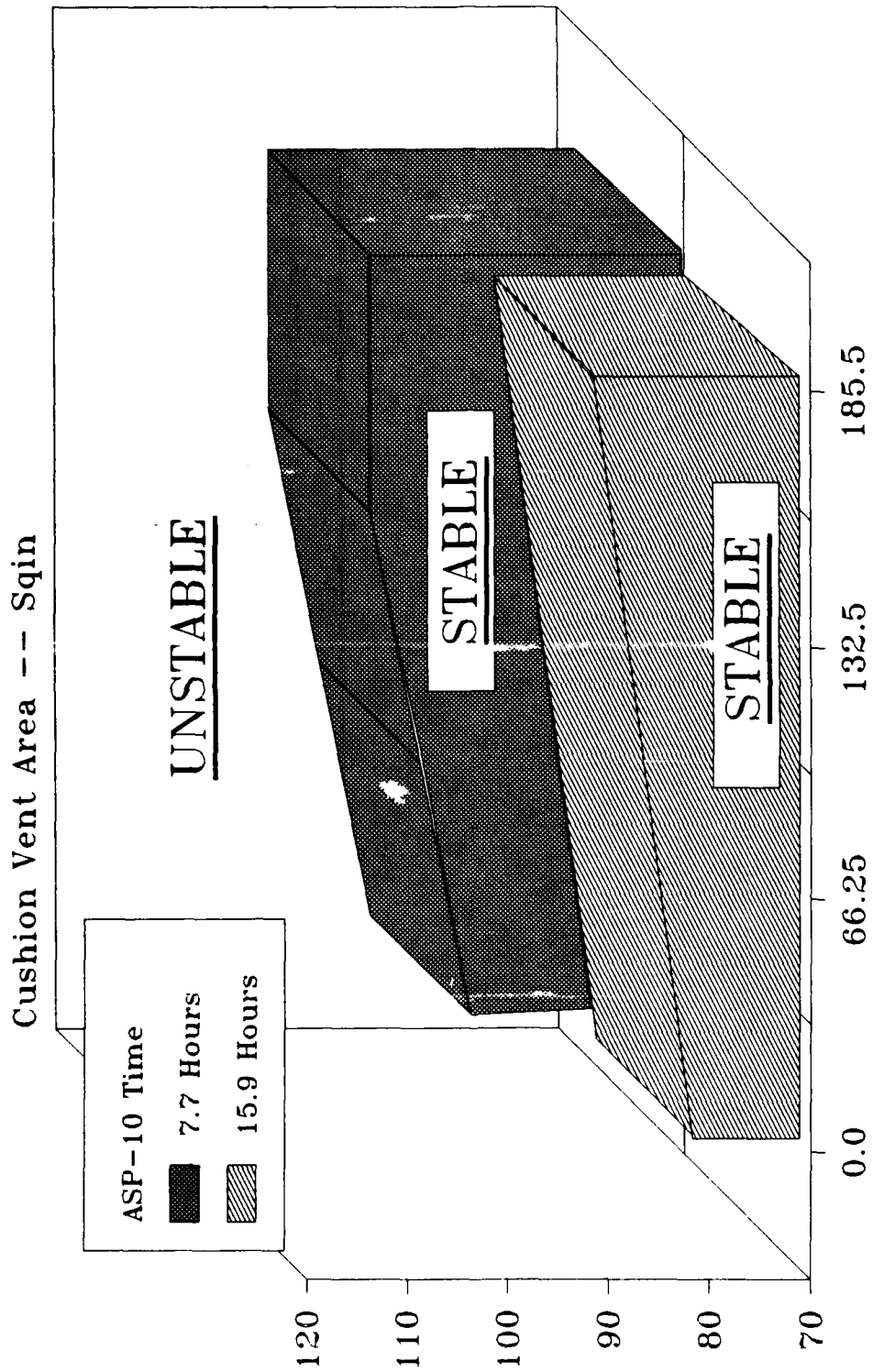
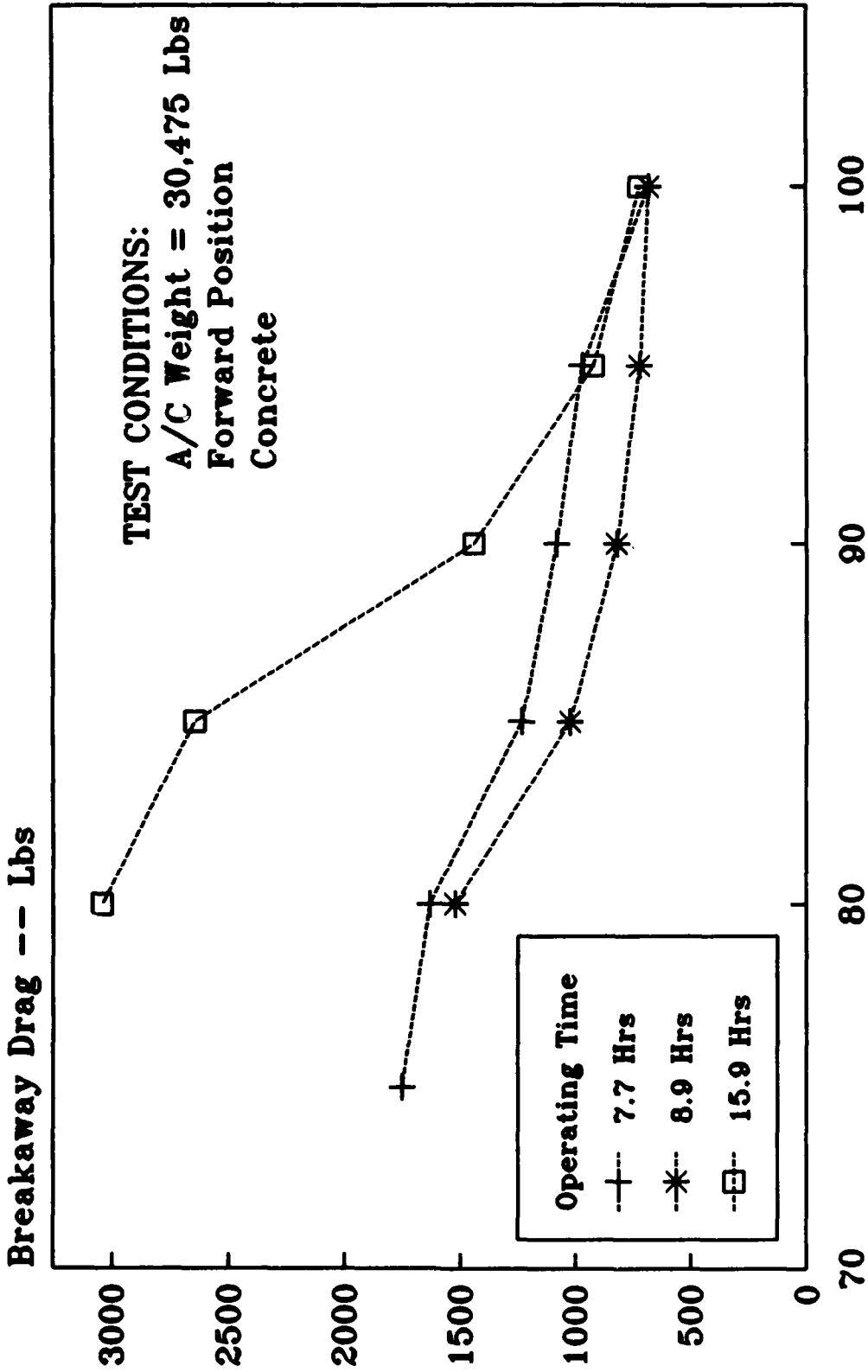


Figure 66. Effect of Operating Time on Stability
 ASP-10 Power Setting -- %Nf



ASP-10 Power Setting --- Nf%
 Figure 67. Effect of Operating Time on Performance

8.0 hours of operations. And, of greater significance, the tow forces required to move the ACET remained well below the values predicted during the design of the vehicle.

In an attempt to eliminate the damage and wear problem, a second set of fingers was fabricated for the ACET. This set had a wider hole pattern and a smaller number of holes per finger. To maintain the same finger venting area, vent holes were cut in each finger instead of every fourth finger as was done with the first set of finger skirts. Also, a number of fingers were fabricated from a heavier weight version of the same type of material, 70 ounces per square yard instead of 41 ounces per square yard to investigate the potentially better wear characteristics. While the increase in the weight of the material and the distribution of the holes did help to retard the damage and wear problem, it did nothing towards eliminating the problem. This problem could only be resolved by initiating an extensive materials qualification program. Such an effort was beyond the scope of this effort. However, a low level effort was undertaken to investigate current "off-the-shelf" materials that could meet the strength and wear requirements of the ACET application. A number of candidate materials were reviewed. Seven fingers were fabricated from a candidate material donated by Goodyear and installed on the ACET for an "on-site" demonstration (Section VI).

Even though the heave stability evaluation did not produce a set of operating curves for the ACET, a number of significant results were obtained from this testing. Passive venting of the cushion cell pressure was determined to be an effective means of controlling oscillations without inducing excessive tow forces. Assuming the finger wear and damage problem with the fingers can be resolved through configuration changes and/or a different material, it should be possible to generate a set of passive venting operating curves that includes all of the major parameters. A candidate method has been identified for determining and predicting when the onset of oscillation, both pitch and heave, will occur. This also suggests that if a requirement for the ACET to have an active heave control system, this system must maintain or limit the pressure fluctuations in the convergent section of the plenum to below 0.10 psig for stable operations throughout the current operating envelope of the transporter.

4. SELF-PROPULSION TESTS

The failure of the left ASP-10 which occurred near the end of the baseline testing on concrete had a severe impact on the in-house test program. At the time of the failure, 2 May 1986, a commitment had already been made to demonstrate the ACET at Davis-Monthan AFB during the next rainy season, February-March 1987 (Section VI). Given this time constraint, the downtime required to repair the ASP-10 and the requirement to incorporate a number of modifications prior to the demonstration, a limited number of off-runway operations were performed before preparations for the demonstration began. While definitive design criteria cannot be developed from the data collected during these tests, trends were established and key parameters identified. Parameters considered during

the Breakaway Drag Tests were type of surface, payload weight, position of the payload on the transporter, and ASP-10 Power Setting. Secondary consideration was also given to passive vent area for the main cells and the stability of the vehicle. In order to maximize the data collected during this limited testing, one payload configuration was selected and all of the tests were completed for that payload weight before starting on the next weight. The order used during these tests was 30,475 lbs., 47,000 lbs., and finally 54,000 lbs. The 30,475 lb configuration, i.e., the F-101B aircraft at the empty weight of 30,475 lbs, was selected first since the largest amount of testing, both contractor and USAF, has been accomplished using this configuration. Therefore, this payload weight has the largest database for making performance comparisons. Also, the lower payload weights reduced ASP-10 fan loading to a minimum.

The initial tests involved determining the breakaway drag forces that would have to be overcome during standing starts on a grass surface. As was the case in all previous drag tests, a calibrated load cell was inserted between the hitch of the tow vehicle and the tow bar of the ACET. The calibration of the load cell was periodically checked to insure the accuracy of the data being collected. The data were displayed on a digital meter and recorded by the ACET operator. Prior to the beginning of each run, a zero load reading was recorded to eliminate errors resulting from cable and connector resistance.

During the first series of tests, the main cell stability doors were closed. The only passive venting used during these tests was from the vent holes in the fingers of each cell. This selection was made based upon past off-runway ACET operating experience. The localized, random skirt contact with the surface as the transporter rests on or moves across the uneven terrain introduces additional damping into the stability equations and alters the stability performance of the vehicle (Figure 68). While operating on grass, the ACET was stable at all ASP-10 Power Settings.

The drag forces recorded during the USAF testing of this configuration were higher than reported during the contractor's program (Figure 69). This difference was first considered to be the result of the gradual increase in finger wear/damage. However, a review of the drag test data did not support this assumption. One possibility did surface during this review. While comparing data collected during tests runs with the aircraft weighing 54,000 lbs, the contractor reported a maximum drag load of 1500 lbs while operating on a hard surface, asphalt. The ASP-10 Power Setting was 70.0 percent Nf. The position of the Stability Vent Doors was not recorded in the contractor's documentation. Prior to the ASP-10 failure, a single drag test was completed at this payload weight. The ASP-10 Power Setting was 95.0 percent Nf and the position of the Vent Doors on the main cells providing 185.5 sq in of vent area. A breakaway drag of 2800 lbs was recorded during this test, a substantially different answer. However, when the drag forces, reported by the contractor as maximum values, were compared to the steady-state drag forces recorded during the USAF's testing, there was considerably better agreement (Figure 70). The difference of these two sets of data can be attributed to such

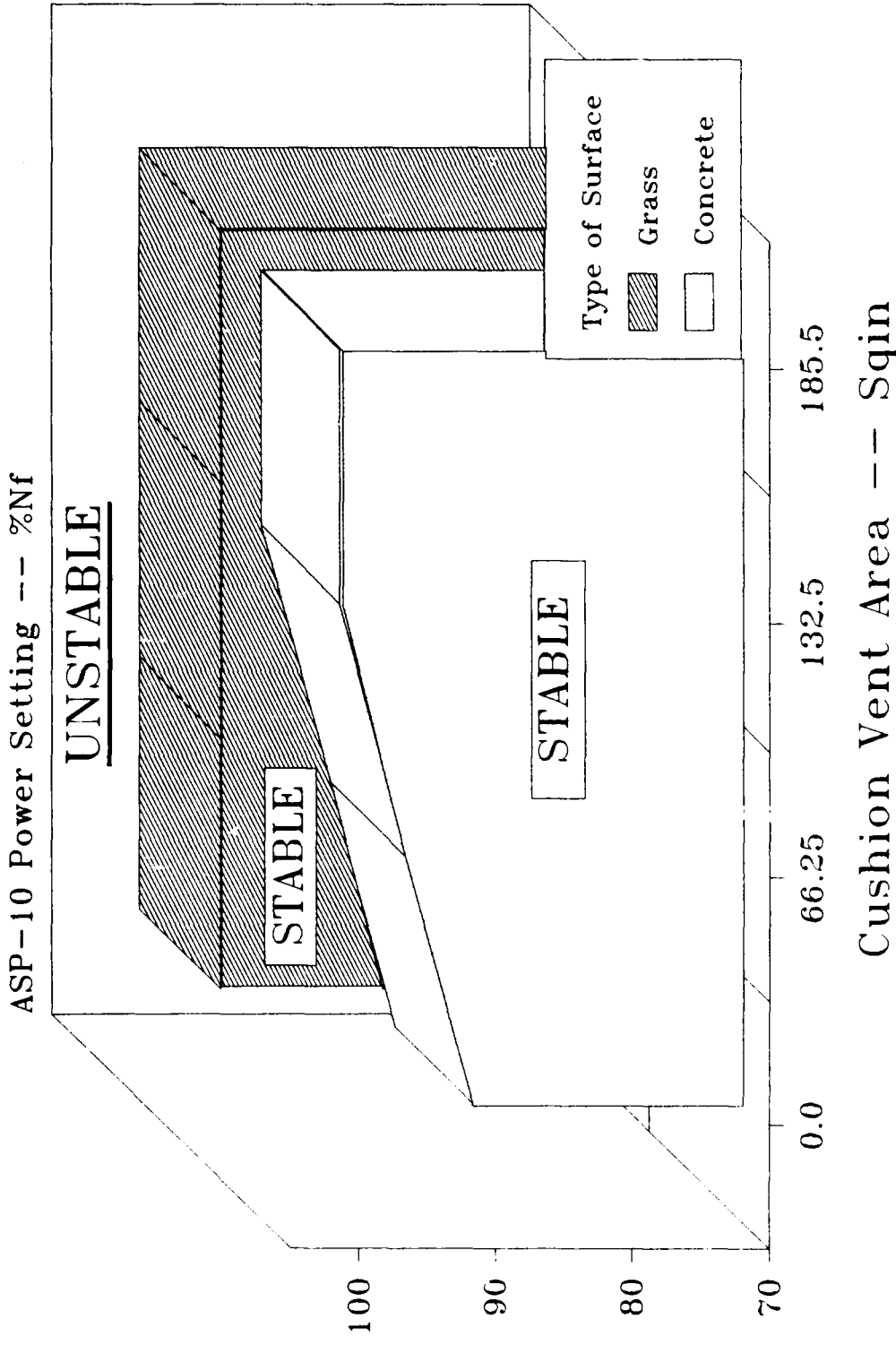
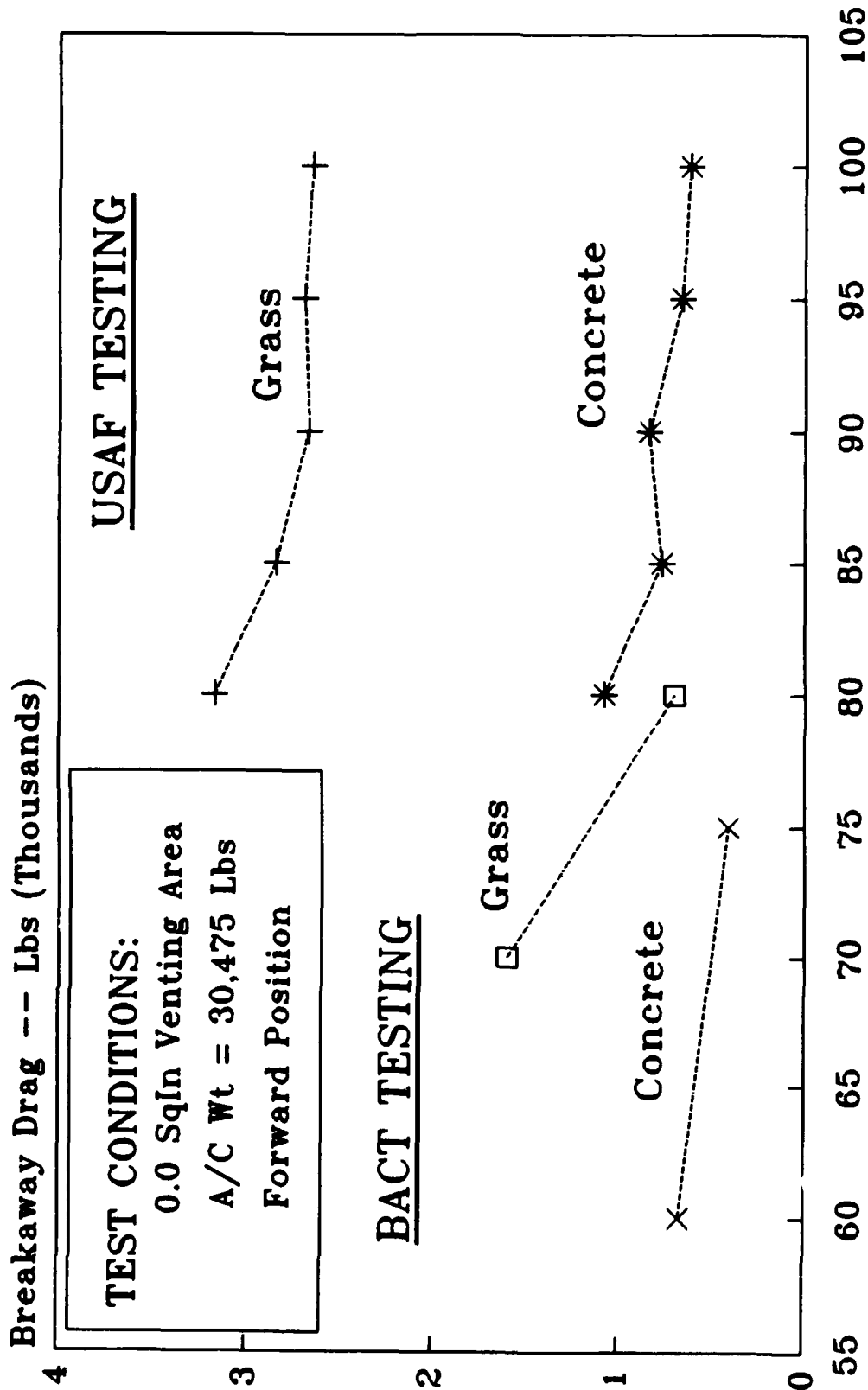


Figure 68. Effect of Surface on Stability



ASP-10 Power Setting -- %Nf

Figure 69. Effect of Surface on Performance

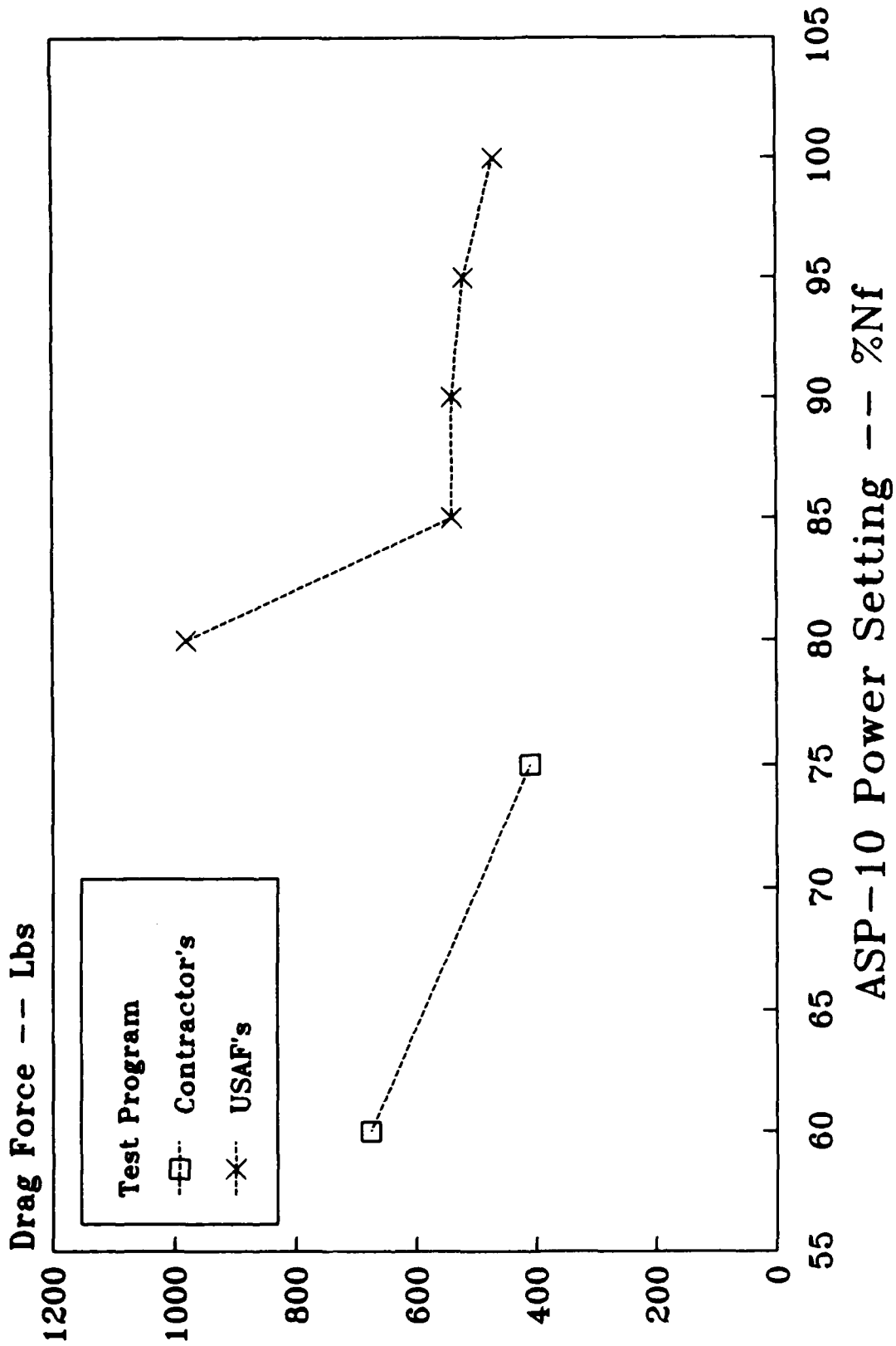


Figure 70. Comparison of Drag Data

factors as load cell calibration, recording errors, difference in surface smoothness, the gradual increase in finger wear/damage, and/or the strength of the underlying soil.

The design criteria for the Self-Propulsion must be based on the maximum forces required to start, traverse, maneuver and stop on all of the surfaces the transporter is expected to operate over. Clearly, the breakaway drag, the force that must be overcome when the transporter is starting from a static position, is a far more important parameter than the steady-state force required to move the vehicle across a surface at a constant forward velocity. This parameter was used to evaluate the effect of changing test conditions on the performance of the ACET.

The breakaway drag forces recorded during USAF tests on a grassy surface were considerably higher than those collected during the concrete surface operations, Figure 69. The maximum Power Setting for stable operations on concrete is 90.0%. At this setting the breakaway drag on concrete is 840 lbs. The ACET was always operated at the highest Power Setting that provided a stable operating condition. This operating procedure was employed to minimize the finger wear/damage and the drag forces required to move the ACET. On a grass covered surface, an ASP-10 Power Setting of 100.0% was attained. The breakaway drag for this setting was 2650 lbs. This represents an increase of 216 percent for a payload weight of 30,475 lbs. The increase in the breakaway drag was the result, primarily, of fingers coming in contact with local irregularities in the surface and the difference in surface strength rather than a loss of cushion pressure in the cells resulting from increased venting area (Figure 71). The relatively small variations in cell pressures between operations on a smooth, hard surface, such as concrete, and uneven surface, such as the grassy area next to a taxiway, is an excellent example of one of the reasons the skirt system was changed from a "jupe" to a segmented finger system, namely ability to maintain cushion pressure. The performance of the skirt system will be discussed in greater detail in a later section of this report.

The average CBR reading for the grass test area used during the USAF Test Program was 7.5. A Cone Penetrometer was used to measure soil strengths. This compares to average CBR readings of 12 to 15 for the tests conducted by BACT on grass. Heavy rains did not have any significant impact on the CBR of this area because of natural drainage and storm tiles installed when the airfield was constructed. Obviously, the strength of the projected operational surfaces will have a direct impact on the design of the proposed modification. The ASP-10 failure, weather conditions during the Test Program and schedule constraints prevented an extensive investigation of the total impact of soil strength on breakaway drag. However, trends were established. Further investigations in this area are considered necessary if the decision is ever made to incorporate this modification on the full-scale ACET. Specific types of surfaces that the ACET will be expected to traverse must be identified prior to the start of this testing to insure the program provides all of the surface data required for the design of the Self-Propulsion Modification.

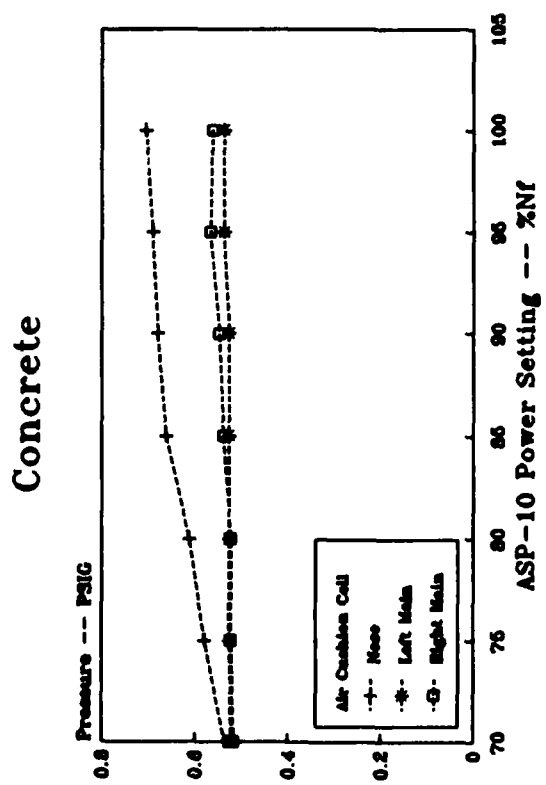
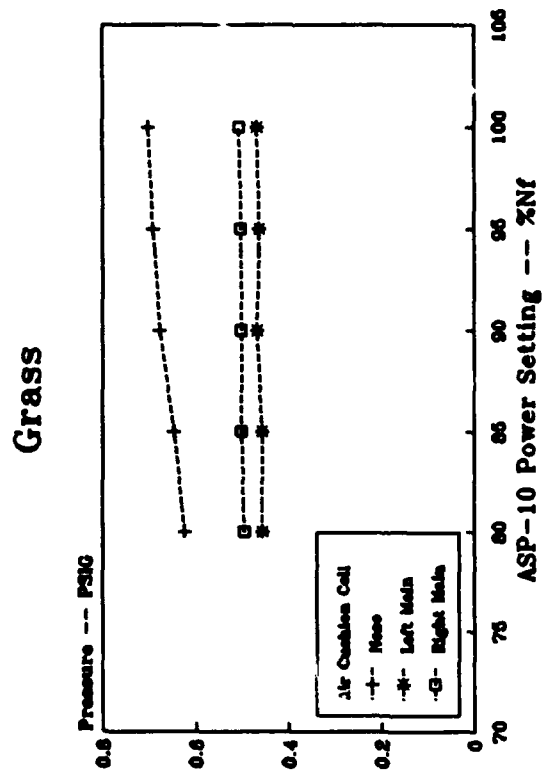


Figure 71. Comparison of Cell Pressures

While only limited data were collected at the maximum gross weight of the aircraft, a complete set of breakaway drag data was collected for the remaining two aircraft weights used in the test program to evaluate the effects of an aircraft as payload on the performance of the ACET. The two parameters considered were aircraft weight and position of the aircraft on the transporter. It is very difficult to isolate the effect of increasing aircraft weight from changing the position of the aircraft on the transporter since changing either of these parameters will cause a shifting of the cg of the ACET/Payload combination (Figure 72). The effects of aircraft weight and location on the CG location of the transporter/payload combination were calculated after the F-101B was weighed in the three test configurations, Figure 72. Shifting the position of the aircraft produced a greater change in CG location than increasing the weight of the aircraft. The increase in weight was accomplished by adding water to the aircraft's fuel system. The intermediate weight was achieved by filling all of the internal tanks while the maximum weight required installing and filling the two 375-gallon drop tanks. The data collected during the Heave Stability Tests, Figures 63 and 64, revealed the general trend that, regardless of the amount of passive venting, breakaway drag readings increased with payload weight. This was expected. However, if any comparisons are to be made, the effect of the CG shift must be removed from the calculations.

The curves in Figures 63 and 64 show that any shift in the CG of the ACET/Payload to the rear, results in an increase in drag. The amount of shift involved in each payload weight change is shown in Figure 72. The shift calculated for the 54,000-lb configuration is consistent with published data on the aircraft. The CG of the drop tanks are forward of the aircraft CG, thus causing this curve to fall between the curves for the other two configurations. Using these curves, it is possible to evaluate the effect of an increase in payload, only. Considering the test condition where there was zero passive venting, Figure 63, the mid aircraft position breakaway drag from the 30,475-lb payload, 720 pounds of drag, must be compared with the forward aircraft position breakaway drag from the 47,000-lb payload, 1960 pounds of drag. These two readings were collected at, approximately, the same ACET/Payload CG position. Turning to the case of 185.5 sq in of passive venting, Figure 64, the breakaway data collected with the aircraft at a weight of 54,000 lbs and spotted at the aft position, 2800 pounds of drag, is compared to the 47,000-lb data with the aircraft at the mid position on the transporter, 1280 pounds of drag. Again, the mid aircraft position for the 30,475-lb payload, 480 pounds of drag, is compared to the forward position 47,000-lb payload data, 1100 pounds of drag. With 185.5 sq in of venting, increasing the payload from 30,475 lbs to 47,000 lbs resulted in an increase in breakaway drag of 620 pounds while increasing the payload weight from 47,000 lbs to 54,000 lbs caused the breakaway drag to increase 1520 lbs. For the case of zero passive venting, increasing the payload weight from 30,475 lbs to 47,000 lbs resulted in a breakaway drag increase of 820 lbs. The payload weight has a strong impact on the breakaway drag and, secondarily, on the steady-state drag. As such, this parameter will have considerable influence over the design of a Self-Propulsion Modification for the ACET.

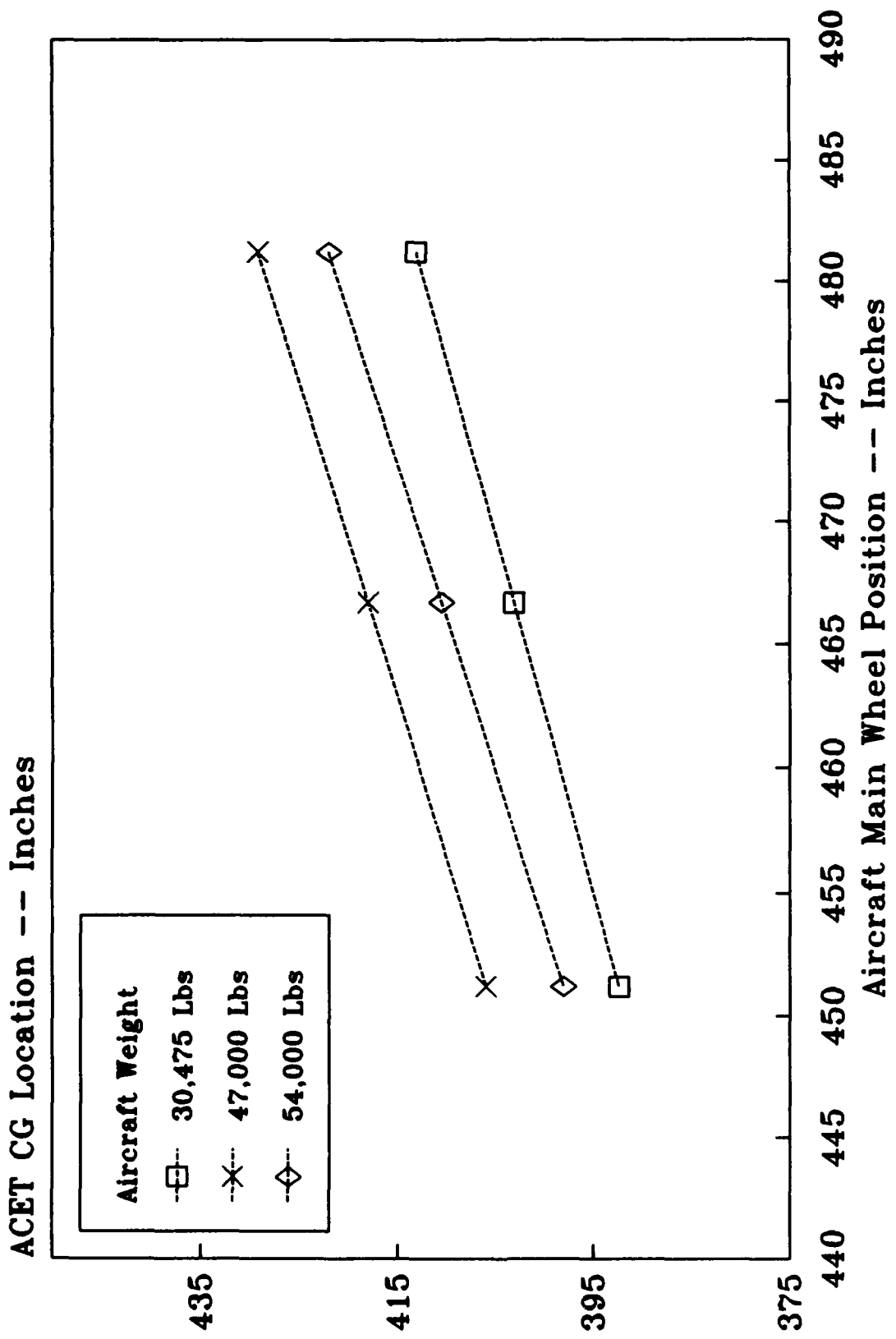


Figure 72. ACET CG Location

Figures 63 and 64 also highlight the sensitivity of breakaway drag forces to the CG of the ACET/Payload combination. The highest drag readings were recorded with the aircraft at the aft position. This was true regardless of payload weight, amount of passive venting area. Insufficient off-runway data were collected to determine if this trend is valid for surfaces other than concrete. Moving the aircraft, and the vehicle CG, forward, generally, reduced the breakaway drag (Figure 73). The nonlinearity of the increases in breakaway drag suggests that a number of factors are contributing to the increases in drag. Also, the tests conducted were not designed or structured to explore the forward or aft limits of the CG envelope.

In fact, the variation in the ACET/Payload combination resulting from the spotting of the aircraft at the three test positions on the deck of the transporter had very little effect on the pitch attitude of the ACET (Figure 74). With 185.5 sq in of passive venting, the ACET is stable at ASP-10 Power Settings of 100 percent Nf. All of the data presented in Figure 74 were collected at this Power Setting. The pitch angle of the unloaded ACET is -0.46 degrees. A negative pitch angle represents a nose-down attitude. Even when the fully loaded F-101B was spotted at the aftmost position on the transporter, a pitch angle of less than 1.0 degrees resulted. Testing of the 1/10 scale model of the ACET indicated that the critical limit is the forward CG limit. Exceeding this limit in the model testing, resulted in immediate collapse of the nose cell cushion. While the maximum payload weight at the full-forward condition was not tested during the USAF Test Program, this configuration was tested by BACT without nose cell collapse.

If the passive venting is reduced to zero, a flattening of the pitch curves results (Figure 75). These data were also collected at 100 percent Nf. Considerable time and patience was required to obtain these data. It was determined that a stable operating condition could be achieved at 100 percent Nf, on concrete if the ASP-10 Power Setting was advanced very slowly and the pressures allowed to stabilize between increases in the Power Setting. However, the slightest local disturbance, such as a gust of wind or a pressure fluctuation in the any of the cell pressures, resulted in an unstable oscillation of the transporter. This is an acceptable procedure for testing a prototype but totally unacceptable for an operational vehicle. For the range investigated, the pitch attitude of the ACET is relatively unaffected by changes in the CG location. As previously indicated, varying the location of the payload on the deck of the transporter was the method used to change the pitching moment of the ACET/Payload combination.

Aside from increasing breakaway drag with an rearward movement of the payload, one other trend was uncovered during the analysis of these data. On concrete, zero passive venting generally yielded higher breakaway drag than 185.5 sq in of venting area for identical test conditions. This was true for both the 30,475- and 47,000-lb payload weights. The 54,000-lb weight could not be evaluated because of insufficient data. The total

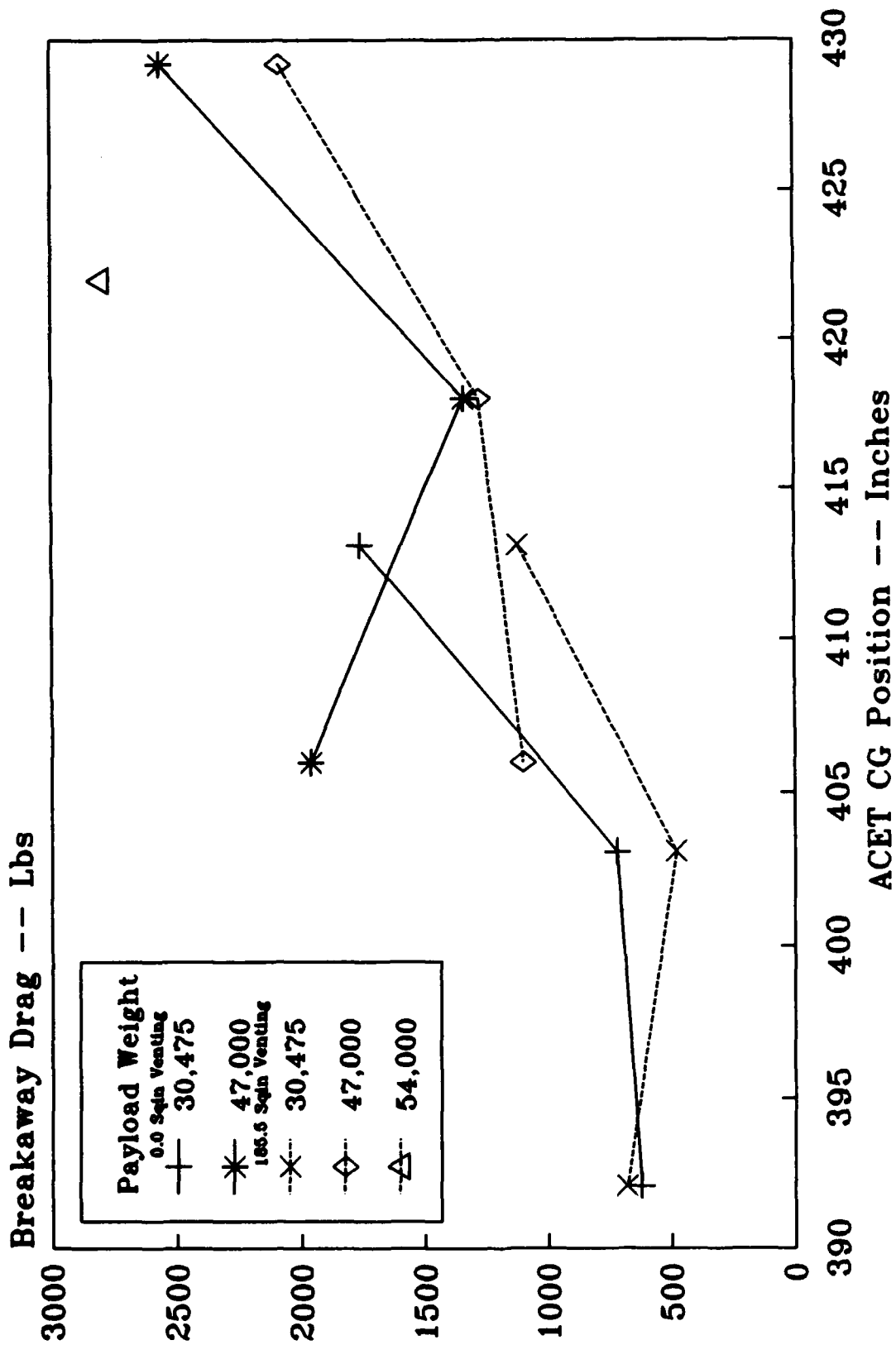


Figure 73. Variation of Breakaway Drag With CG Position

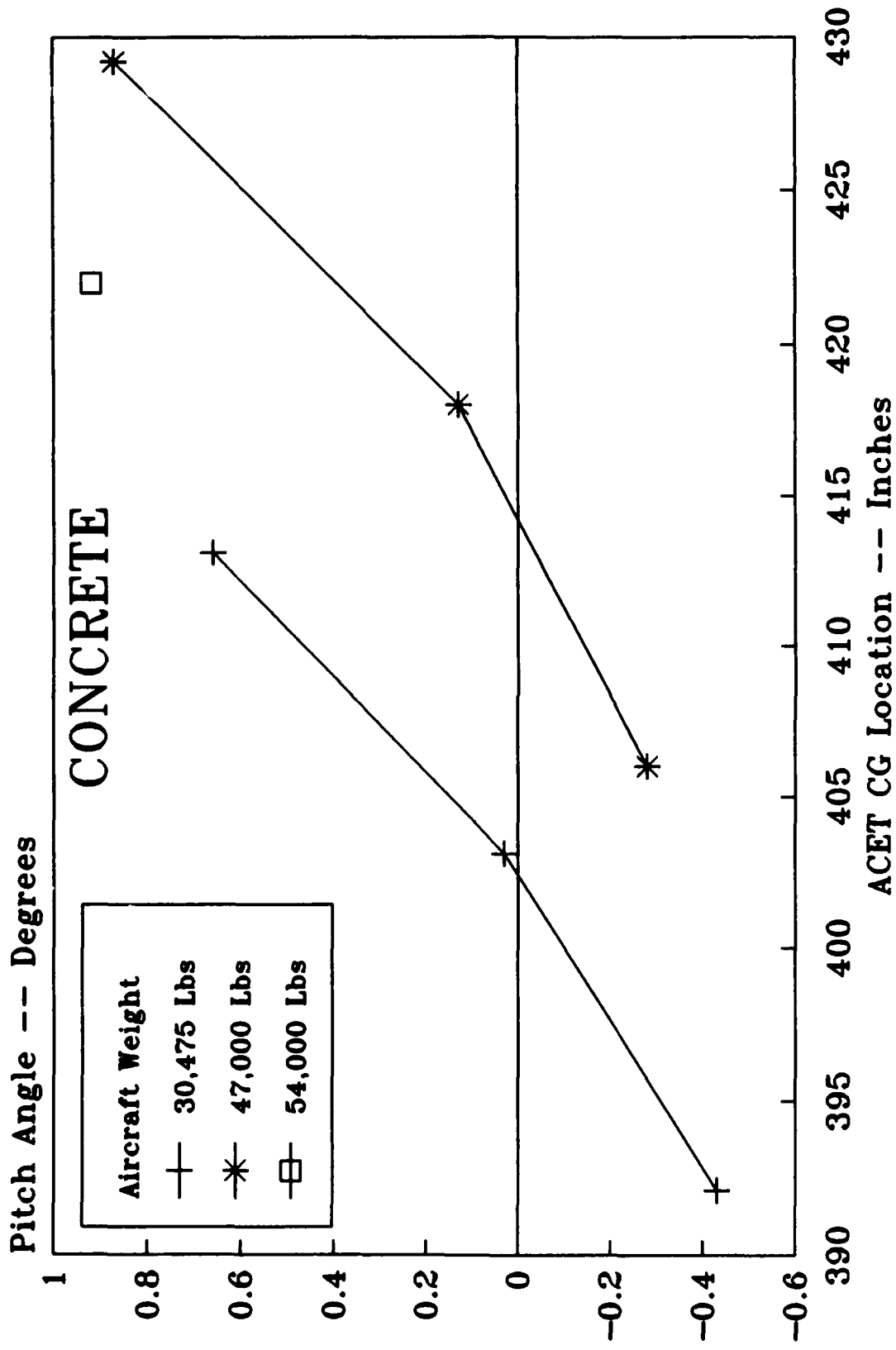


Figure 74. Pitch Angle for 185.5 Sqn of Venting

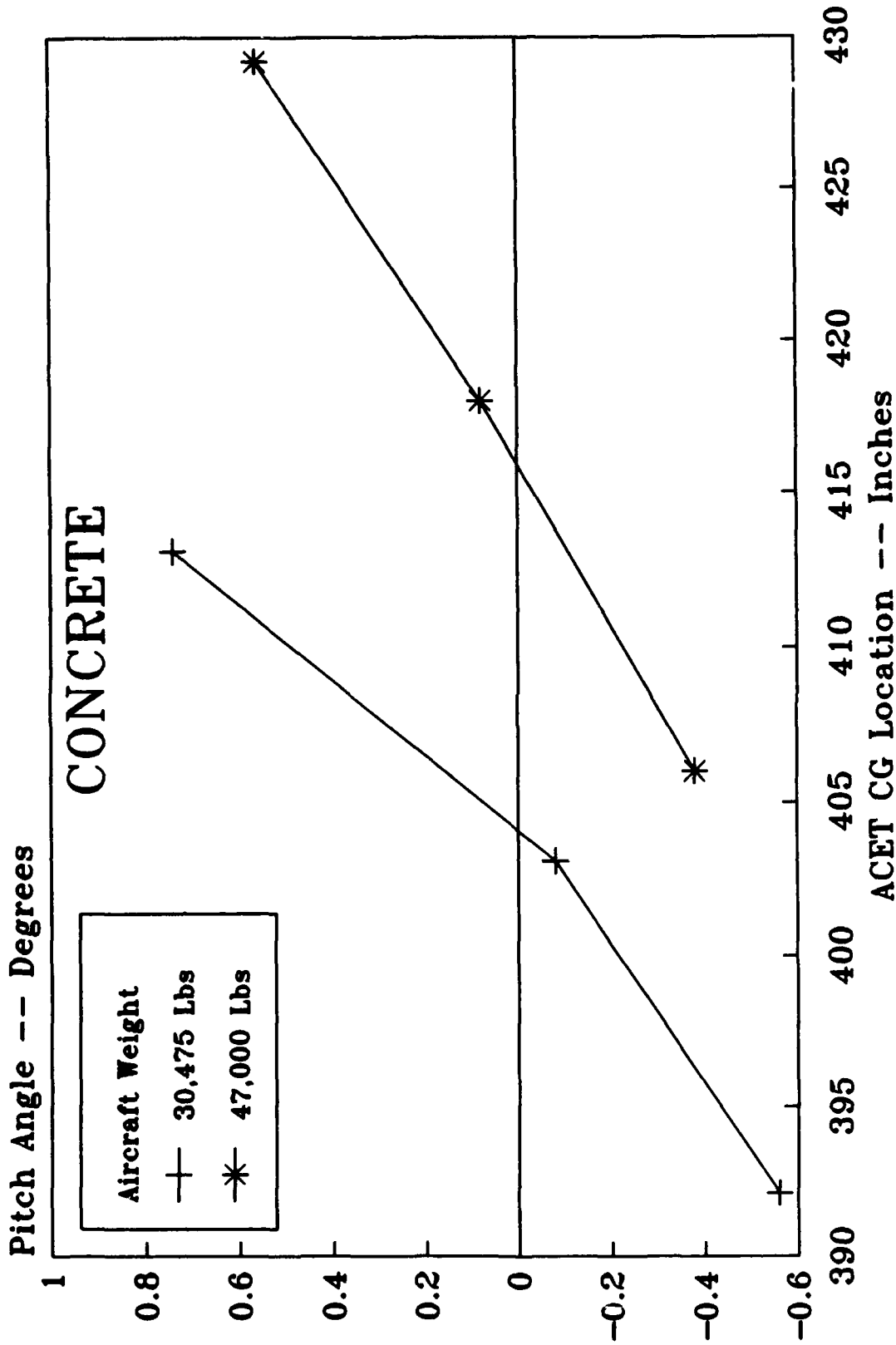


Figure 75. Pitch Angle Vs CG Location, 0 Spin Venting

impact of the payload location on the ACET was not defined during this test program. Additional testing would have to be performed to accurately assess the impact of this parameter on the performance of the ACET.

In general, increasing the ASP-10 Power Setting while testing a given configuration of the ACET and payload reduced the breakaway drag, regardless of the position of the payload on the ACET (Figure 76). Increasing the Power Setting produces an increase in the mass flow of pressurized air to the nose and main air cushion cells. This increased mass flow results in fuller inflation of the individual fingers. With a fuller inflation, the seals between the individual fingers are better, losses are less. This results in reduced contact with the surface. All of these factors serve to reduce the breakaway drag as the ASP-10 Power Setting is increased.

The impact of increasing the Power Setting is a strong function of the location of the payload on the transporter. The further aft the payload is located on the deck of the vehicle, the greater the reduction in breakaway drag in the usable range of the Power Settings, 90.0 to 100.0 percent Nf. Stable configurations are achievable below 90.0 percent Nf; however, skirt drag and therefore finger wear/damage become an important factor. The drag reductions realized decrease significantly as payload increases (Figure 77). The aircraft position was the same for all of three payload weights, the aft position. This configuration was selected because it was the worst condition found during the testing of the ACET. As payload weight increases, it counteracts the positive attributes of increasing the Power Setting and contact of the fingers with the surface increases in spite of the increased mass flow. Whenever finger contact increases, the breakaway and steady-state drag increase substantially.

There is also a limit on decreases in drag, both breakaway and steady state, that can be achieved by increasing the ASP-10 Power Setting. When the ASP-10 Power Setting was increased beyond the range of settings for stable operation of a specific configuration, the breakaway drag forces increased (Figure 78). The increase in drag forces resulted from individual fingers or groups of fingers being forced into local contact with the surface during the oscillation. Therefore, the control of oscillations is an important factor, not only from the standpoint of minimizing the forces and accelerations being transmitted to the payload but also to maintain the tow forces required to move the vehicle to a minimum.

The drag forces required to start, propel, maneuver, and stop an ACET, either by towing or a Self-Propulsion Modification, are dependent upon a number of factors. Clearly, the surfaces the transporter will be traversing will make a major impact on the design of the modification. Another major factor is the weight of the payload to be transported. The location of the payload on the vehicle has a significant effect on the drag forces. To a lesser degree the Power Settings of the ASP-10's and the passive control of oscillations contribute to the total drag required for any configuration. Unfortunately, insufficient data were collected

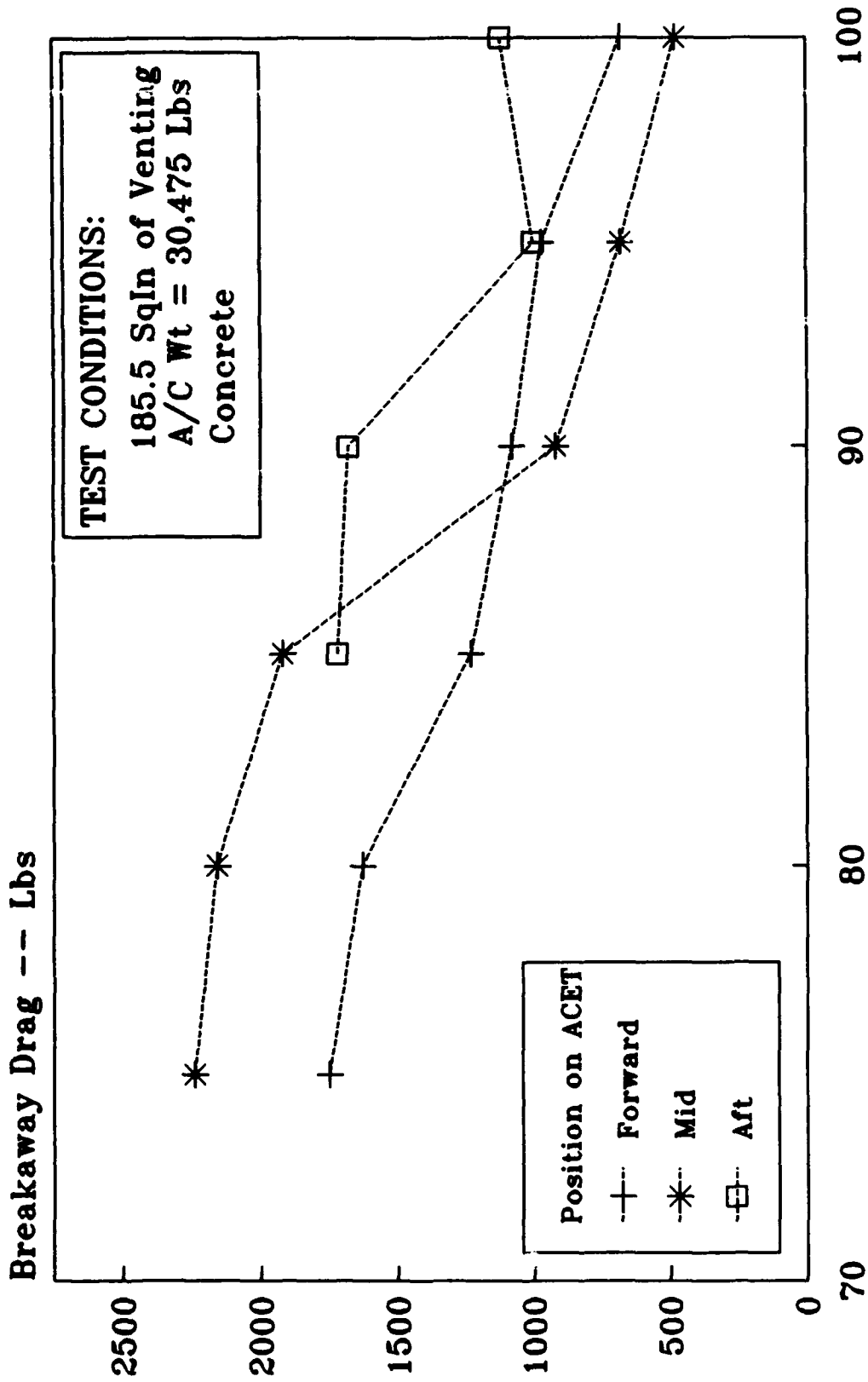


Figure 76. Effect of ASP-10 Power Setting on Drag

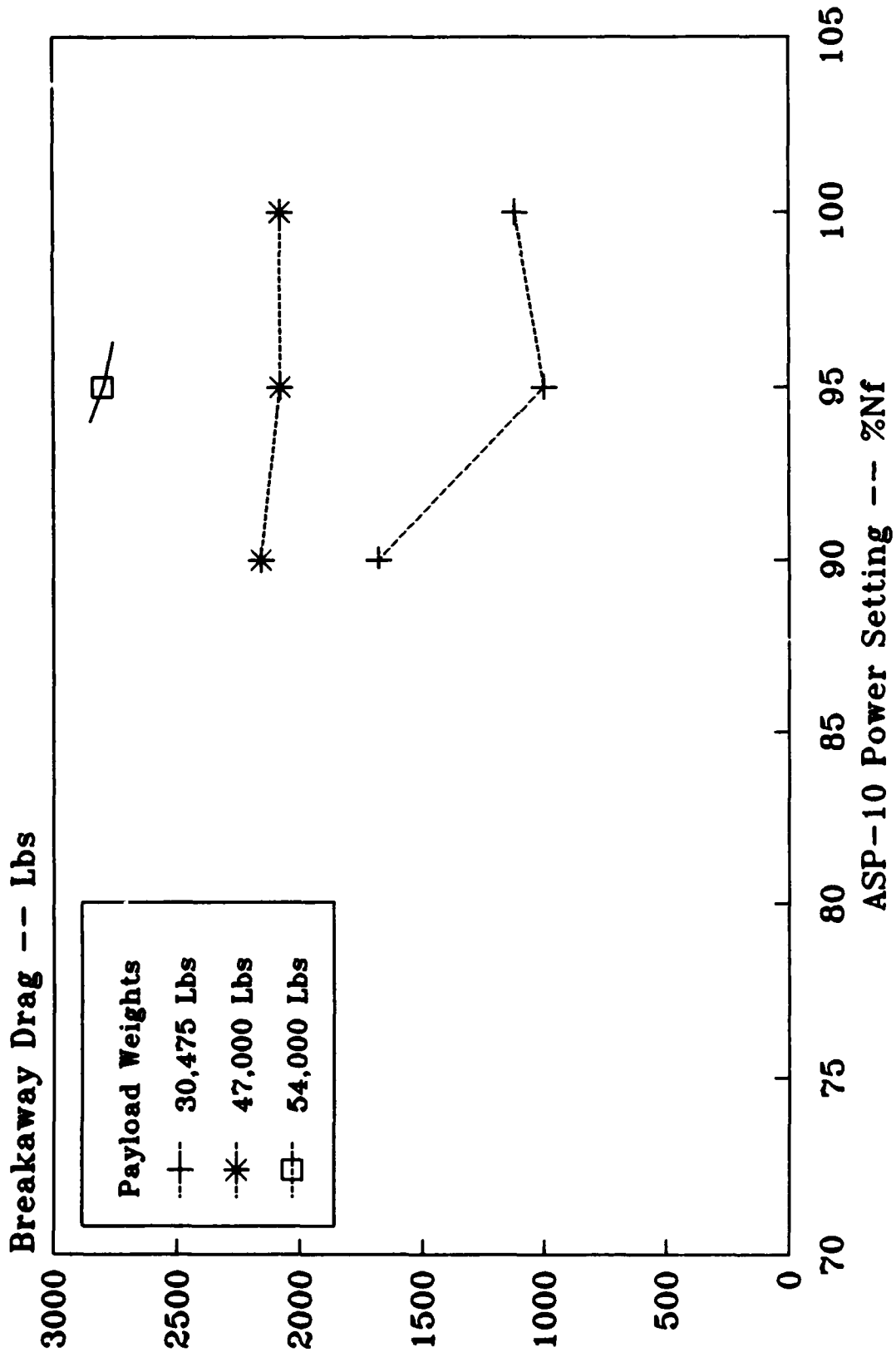


Figure 77. Impact of Payload Weight on Drag

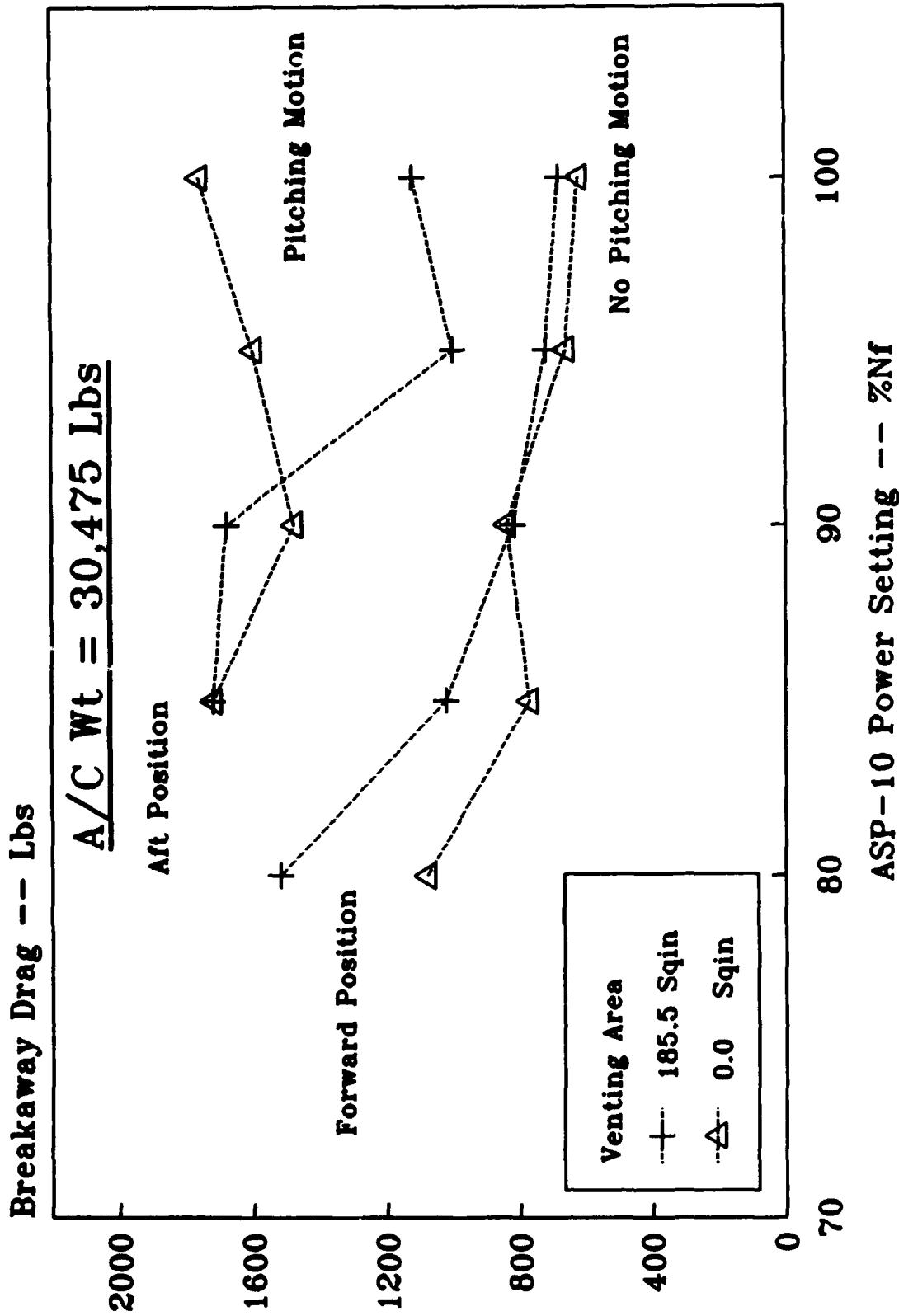


Figure 78. Effect of Pitch Oscillation on Drag Forces

because of system failures, funding, and schedule constraints to provide a clear indication of the interrelation of these factors and their impact on the design of a Self-Propulsion Modification. However, based upon the data that were collected and analyzed, the breakaway drag required to start the vehicle, the most critical factor in the design, is approximately 10 percent of the total vehicle weight. This is a conservative estimate. To obtain a more accurate scope of the drag forces required, a more extensive test program would have to be initiated.

5. ASP-10 FAILURE

The protection of the F-10 fan assembly of the ASP-10's has been a major concern since the initial design of the ACET. The contractor's efforts to provide additional protection are documented in Section III of this document. The condition of the F-10 fan assembly, a two stage fan, is critical to the overall performance of the transporter. The fan inlet screen installations, as they evolved, Figures 8 and 10, provided adequate FOD protection for ACET operations over relatively debris free surfaces, such as active taxiways and runways, but was totally inadequate for operations over austere surfaces, such as the operation shown in Figure 12.

During routine posttest maintenance and inspection of the ACET on 10 Jan 86, significant damage to the leading edges of the first stage rotors was found on the F-10 fan of the left ASP-10 (Figure 79). A closer inspection of the right fan assembly revealed only minimal visible damage to the rotors of that assembly. The total number of operating hours since the ACET was delivered to the USAF was 10.8 hours. Of this total, only 1 hour of operations on off-runway surfaces, primarily grass, were conducted.

A technical field representative from United Aircraft of Canada, Limited (UACL) was called in to inspect the ASP-10's and provide guidance on maintenance actions to be taken during the repair of the fan assemblies. The UACL representative recommended "stoning" the blades. "Stoning" of compressor blades is an accepted maintenance procedure for aircraft jet and turbojet engines. The procedure involves dressing the leading edge of the rotors by hand. The radius of all nicks and dents in the blades are enlarged to reduce stress concentrations and thereby reduce the possibility of a catastrophic failure of a blade. Since this process requires considerable training and experience, the "stoning" of the blades was performed by a qualified Airframe and Propulsion (A&P) technician from Airborne Express, the company operating the airfield where the ACET Tests were conducted. This A&P technician was responsible for inspecting all of the engines on Airborne aircraft and "stoning" compressor blades whenever it was necessary. The Non-Destructive Inspection (NDI) of the first stage rotors on Both ASP-10's cleared the assemblies of any cracks. A visual inspection determined that only the left ASP-10 needed this maintenance. After a short maintenance run on 30 Jan 86, the left ASP-10 was written up as serviceable for testing.



Figure 79. New Damage to Left F-10 Fan Assembly

With the discovery of the damage on 10 Jan 86, investigations were begun to explore potential methods for increasing the level of protection of the F-10 fan assemblies during off-runway operations. These efforts were accelerated when on 25 Feb 86, after only 2.0 hours of operating on concrete, additional damage was discovered during a posttest inspection. The primary deficiency in the second generation fan inlet screen developed by BACT, Figure 11, was that this screen did not cover all possible flow paths to the fans. As can be seen in Figure 12, debris can come from any direction during an off-runway operation, depending upon wind conditions, the surface and the speed and direction the ACET is moving. The approach selected was to totally enclose the fan inlet area of both ASP-10's with screening (Figure 80). The design of this new inlet screen used existing structural lines to create a clean installation which did not significantly alter the profile of the ACET. A smaller mesh stainless steel screen was used to increase the number and size of the foreign objects that could potentially reach the fans. The total screen assembly was fabricated in sections to allow access to various parts of the ASP-10 without having to remove the entire screen assembly. Quick disconnect fasteners were to assemble and secure the assembly to the ACET. These fasteners were selected to facilitate routine ASP-10 maintenance procedures.

The check-out of the new fan inlet screen assembly was very encouraging and testing of the ACET was begun again after the delay to install the new screens. In subsequent tests, everything went smoothly. Posttest inspections of the F-10 fan assemblies did not reveal any new damage. This success continued until 22 Apr 86. After 6.7 hours of operation with the new fan inlet screens, a inspection after a test on concrete revealed significant new damage to the first stage rotors (Figure 81). The cause of this damage and the path it took to get to the fans was never determined.

The field representative for UACL was again called to inspect the blades of the fan assembly. The main concern was that a large percentage of the damage to the blades was located in the critical area of the blade root. Damage in the first inch to inch and one half of the blade must be handled very carefully and inspected frequently. The UACL technical representative authorized a second "stoning" of the blades. However, he placed a limit of 4.0 hours of additional operations on the blades. Also, inspection of the blades after each hour of operation was mandatory. A major overhaul of the left fan assembly would be required after the 4.0 hours were completed. The "stoning" of the blades was accomplished by the same Airborne Express A&P technician. He agreed with the assessment made by the representative from UACL.

Preparations for the next operations were extremely detailed to insure maximum safety of personnel and equipment. The number of personnel involved in the testing of the ACET was reduced to the minimum required to accomplish the objectives of the test. All of the test and emergency shutdown procedures were reviewed by all members of the ACET Test Team. The first test was performed without any problems. It lasted 0.4 hour and was conducted on concrete. Even though it was not required, the fan inlet

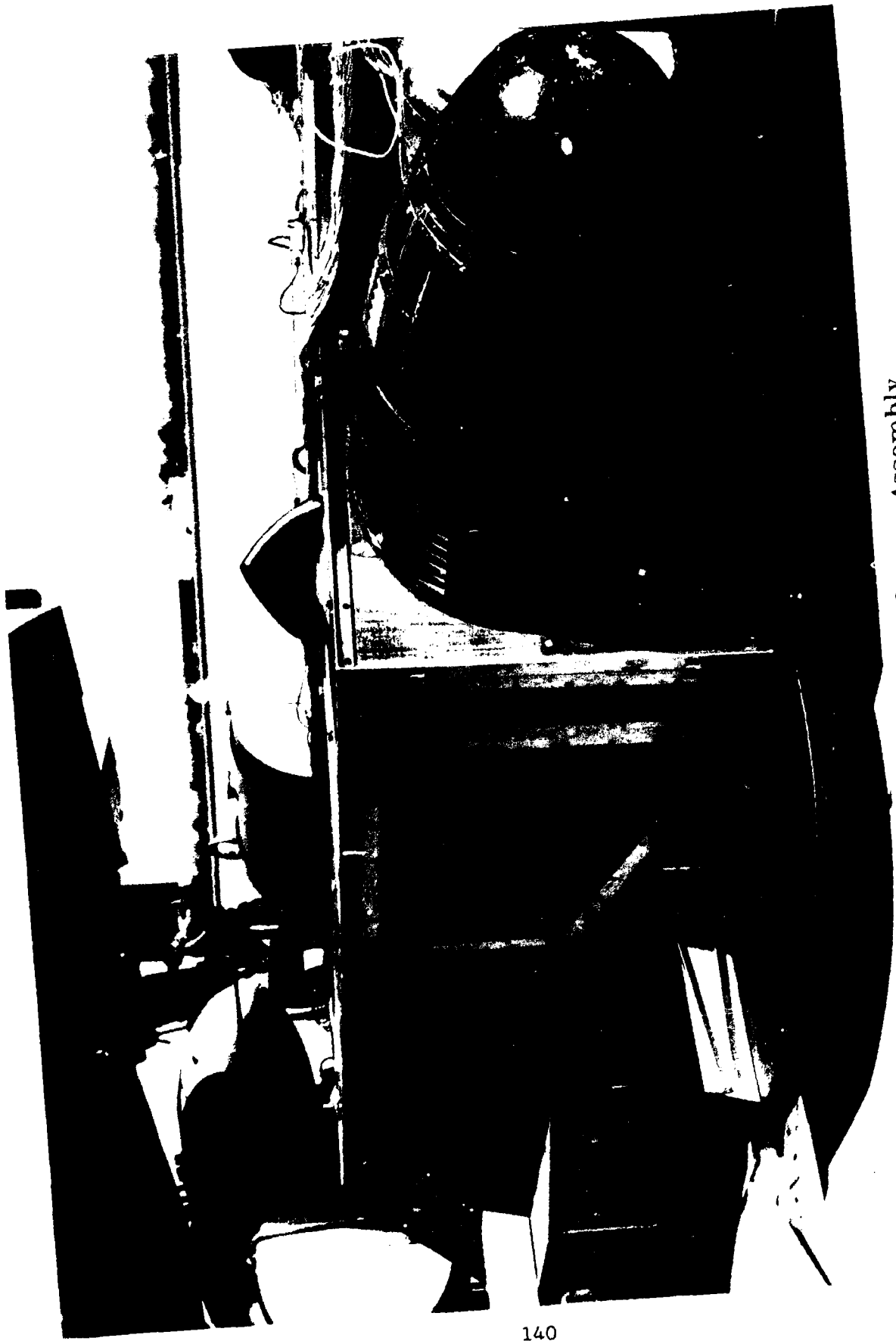


Figure 80. Fan Inlet Screen Assembly



Figure 81. Post Fan Screen Modification Damage

screens were disassembled and the rotors of the first stage of the F-10 fan on both ASP-10 were inspected. Both fan assemblies passed the inspection with no new damage being found.

The next test called for the aircraft to be at its maximum weight, 54,000 lbs, and be spotted in the aftmost position on the deck of the ACET. Again, all procedures were reviewed and the fire department was notified of the test and asked to stand by in case of an emergency. This additional level of preparation was added as a result of comments made during the debriefing after the 30 Apr 88 Test. The initial test point was achieved without any indication of problems, either at the control console or from visual observation of the transporter. While involved in the process of changing ASP-10 Power Settings, there was a failure of the left ASP-10 fan assembly. Within 5 seconds of the initial blade failure (Figure 82). An emergency shutdown was accomplished, the fuel system was isolated and fire extinguishers manned. Although considerable flame was observed during the failure, it disappeared immediately after the ASP-10 stopped rotating. The quick responses of the test team members kept damage to a minimum.

The ASP-10's exhaust stubs were allowed to cool off before the fan inlet screens were removed from both ASP-10's. This delay was necessary to insure that fire did not occur after shutdown. When the screens and nacelle of the left ASP-10 were removed, there was very little visible damage (Figure 83). This lack of visible damage masked the true extent of damage to the fan assembly. One of the first observations made was that the blade containment ring had been penetrated in a number of places just forward of the first stage stators (Figure 84). A closer inspection of these penetrations revealed a first stage rotor blade still in the penetration. Also, the upper exhaust stub had received considerable damage (Figure 85). A visual inspection of the first stage rotors revealed extensive damage to all blades and a number of missing blades (Figure 86).

Even a casual inspection of the left ASP-10 highlighted the need for a major overhaul of the F-10 fan assembly. However, the extent of the damage, if any to the ST6F-70 gas turbine engine could not be ascertained until the entire assembly was removed from the ACET, put on an engine stand, and disassembled for inspection. A similar external inspection of the right ASP-10 did not reveal any damage to the unit. At a minimum the right ASP-10 required a sudden stoppage inspection in order to certify it "flightworthy." The ASP-10's are one of a kind units. Only three units were manufactured. The third unit, stored in the MDL, was used to qualify the ASP-10's for aircraft use. This unit was not modified when the ACET was manufactured. Therefore, it could not be used as a straight substitution for the left ASP-10. Overhaul of the left ASP-10 was the only answer. Although, the units were a unique series development, the ST6F-70 gas turbine engine is a direct adaptation of the PT-6 engine and retains a great deal of commonality with these popular series. A firm, Airworks, was recommended by maintenance personnel at Airborne Express as

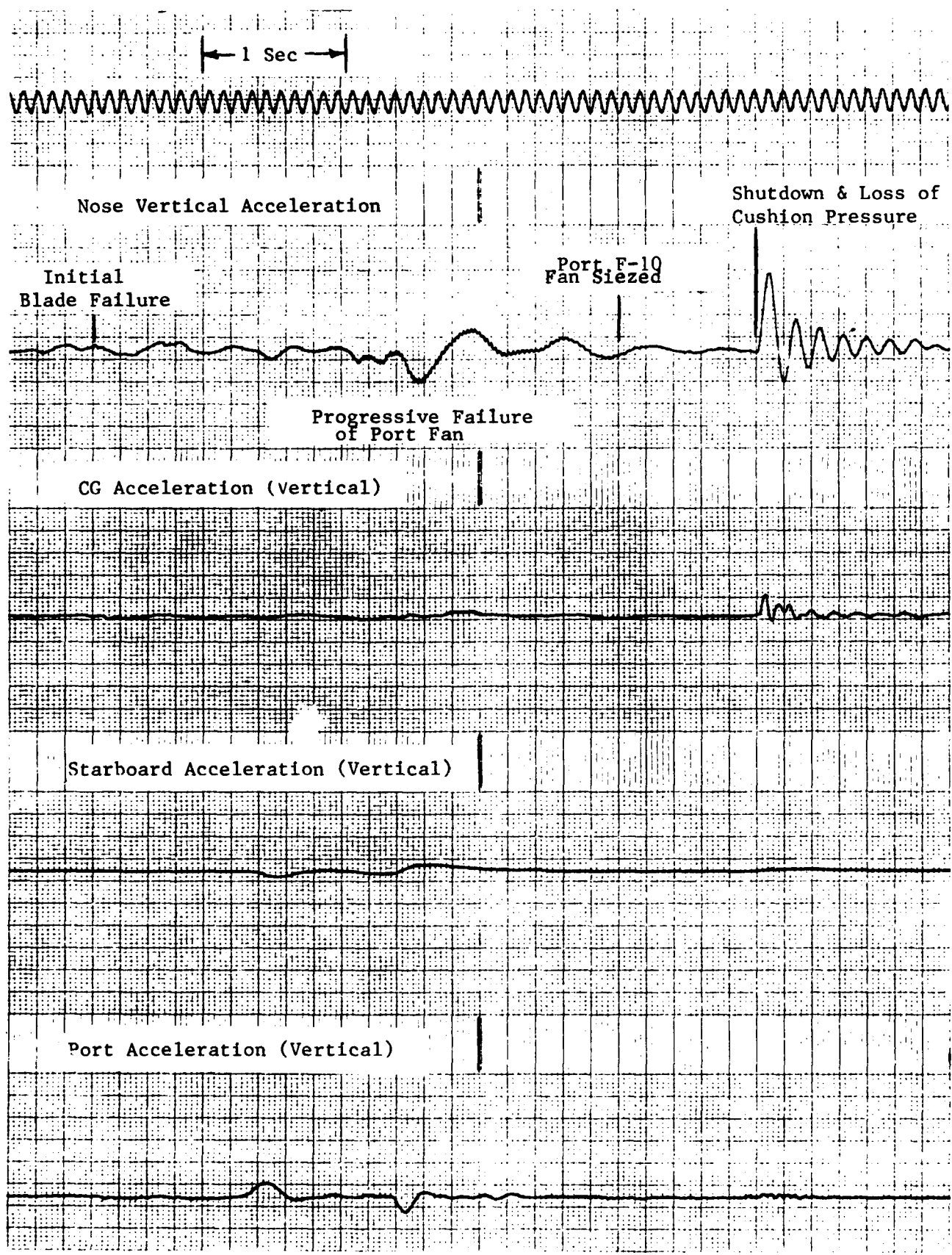


Figure 82. Data Traces of Left Fan Failure

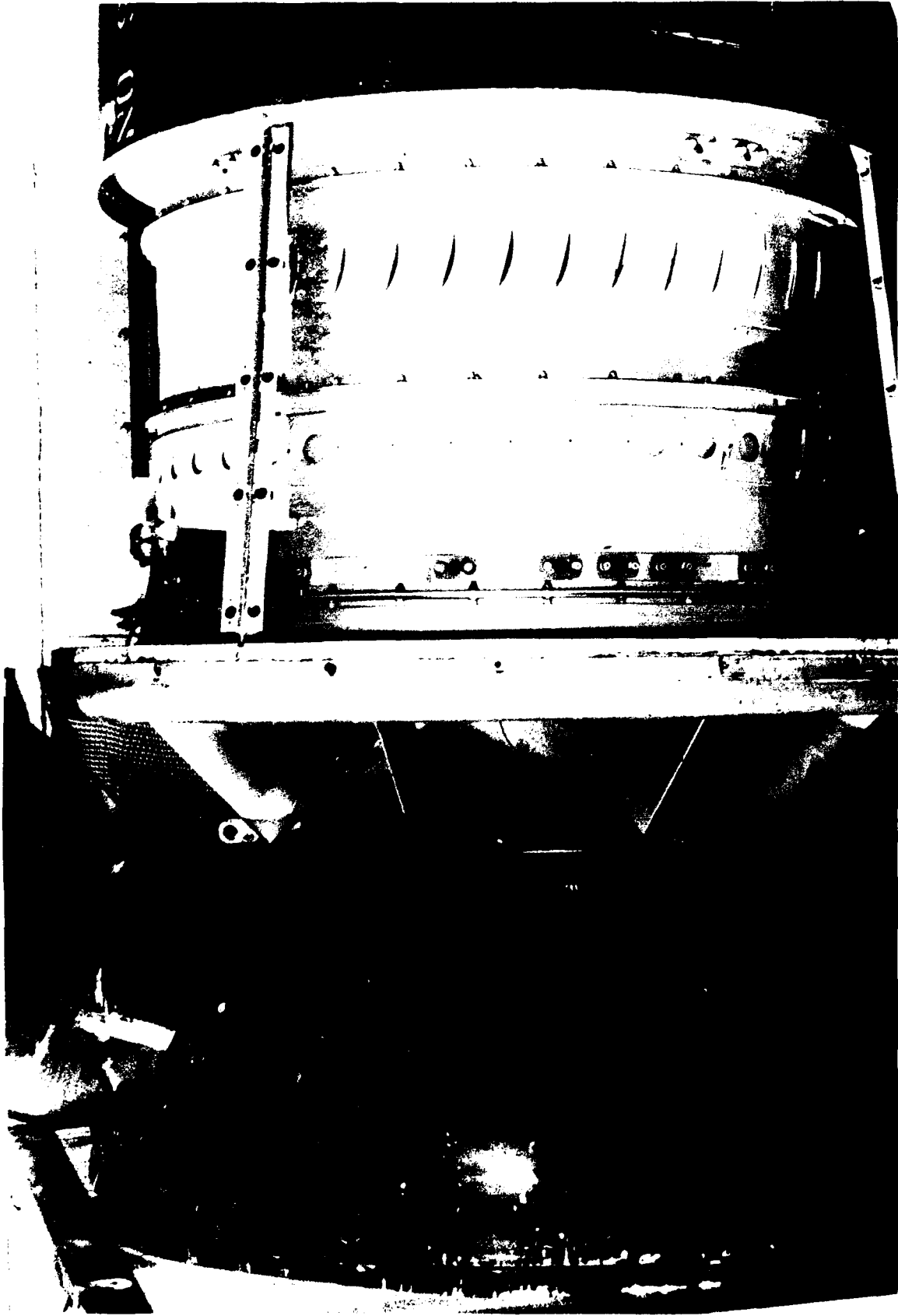


Figure 83. External Damage of Left F-10 Fan

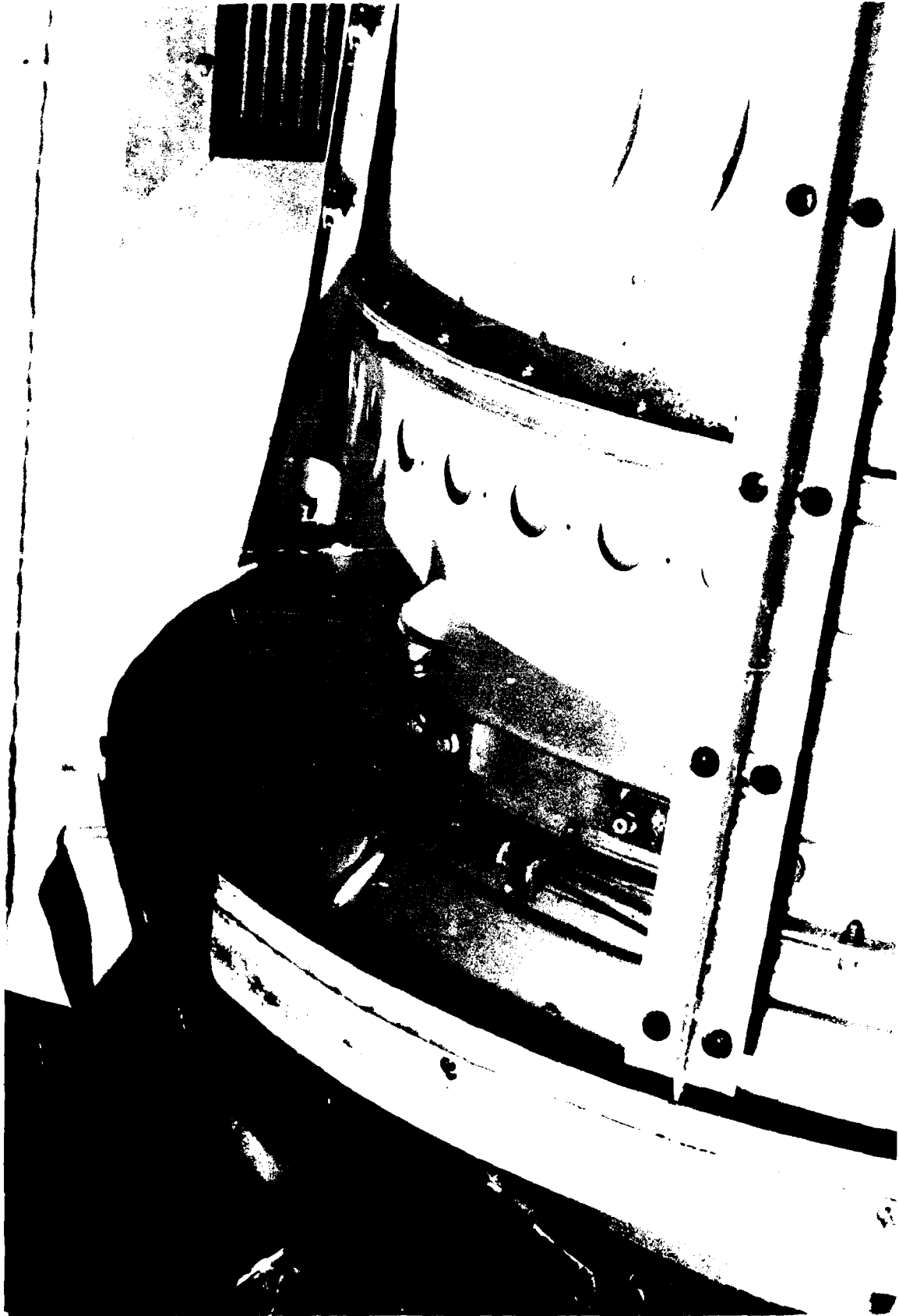


Figure 84. Penetration of Blade Containment Ring



Figure 85. Upper Exhaust Stub Damage

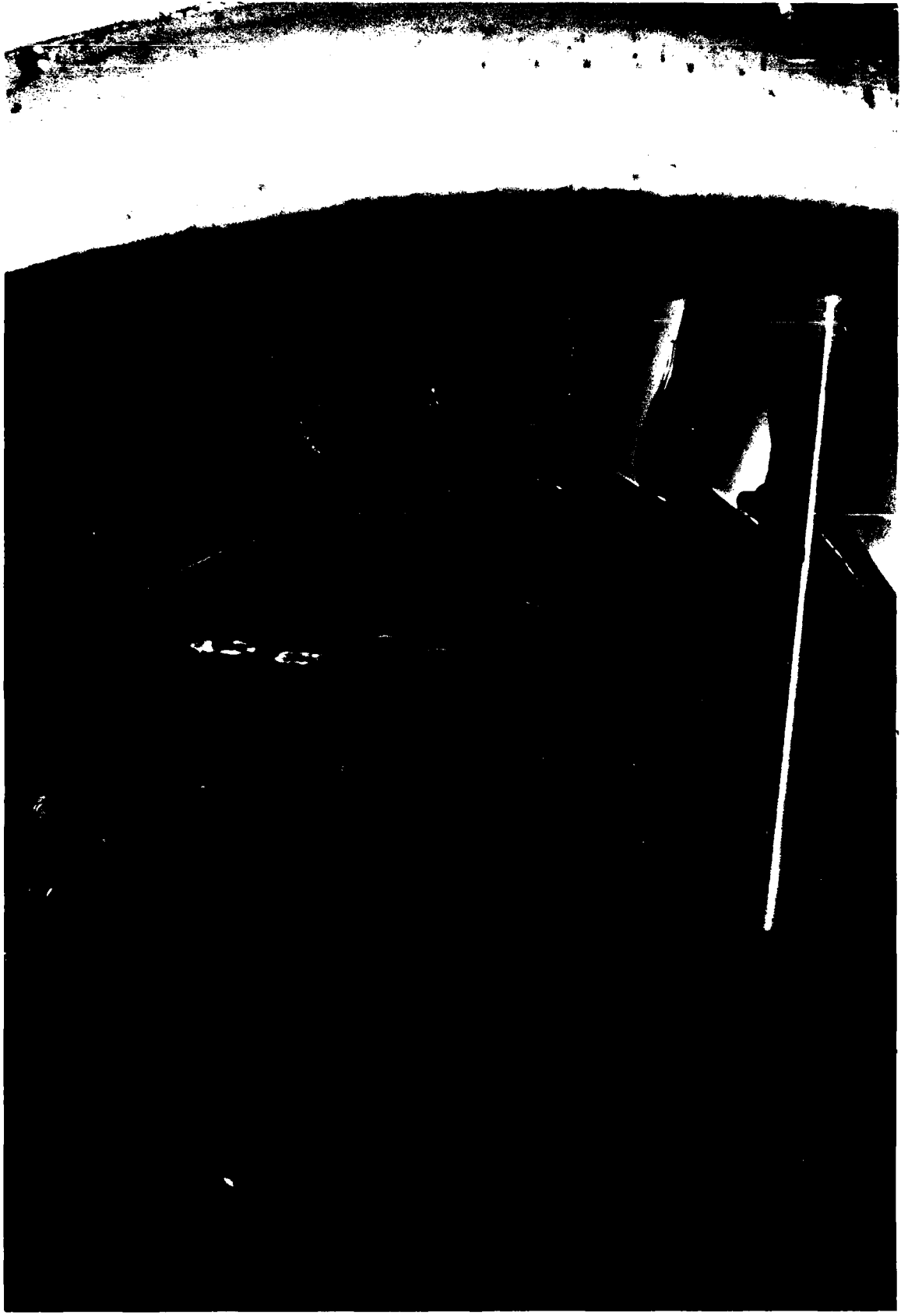


Figure 86. Damage to First Stage Rotors of Left F-10 Fan

having an excellent reputation for their work on PT-6 engines. Both ASP-10's were removed from the ACET and transported to Airworks for the required inspections and repair.

The damage to the left F-10 fan was more extensive than originally realized. The first stage rotors (Figure 87) and stator ring (Figure 88) were complete write-offs, damaged beyond repair. Also a large percentage of the second stage rotors were extensively damaged also (Figure 89). Fortunately, all of the existing spares for these engines were retained with the engines and were, therefore, available for the overhaul of the left F-10 fan. Only a limited number of the blades from the right F-10 fan assembly required replacement. Since the ASP-10's have been subjected to the same operating environment, the difference in damage levels remains an open question.

As part of the sudden stoppage inspection, the hot section of both ST6F-70 engines was inspected. In general, the damage found was considerably less than what is normally found after a stoppage of this type. The torque from this maneuver broke the mounting flange of the fuel pump on the left ST6F-70 engine (Figure 90). Other problems were related to sporadic use of the engines since they were manufactured. All of the fuel injectors required cleaning (Figure 91) and were pressure checked to insure the proper mixture of air and fuel in the combustion chamber. This was necessary to eliminate hot spots such as the one that damaged a burner can in the right ST6F-70 engine.

After the first and second stage rotors were reworked, they were assembled for static and dynamic balancing (Figure 92). This was the final stage of the overhaul and inspection process. During the final assembly of the two units, we found that a number of the spare seals had exceeded their respective shelf lives and replacements had to be ordered. Aside from the seal problem, no additional problems were encountered during the reassembly of the two units.

Generally, the installation of the ASP-10's in the ACET proceeded without any major difficulties. After the initial check-out runs, the ACET was declared ready to resume testing. While the recovery from the fan failure was successful, this failure highlighted the need to find a different engine fan combination to power the ACET. The axial flow F-10 fan does not have the necessary damage tolerance to operate for extended periods of time in the hostile environment that this transporter is required to handle on a routine basis. The demonstration at Davis-Monthan AFB, AZ would confirm this finding.

6. EVALUATION OF SKIRT PERFORMANCE

The segmented finger skirt was an excellent selection for the ACET application. The performance of this system, both on and off runway, allowed the transporter to be maneuvered across a variety of surfaces. For all cases investigated, the tow forces, both breakaway and steady state, were less than 10 percent of the total vehicle weight. A detailed discussion of the findings of the full-scale testing is presented in

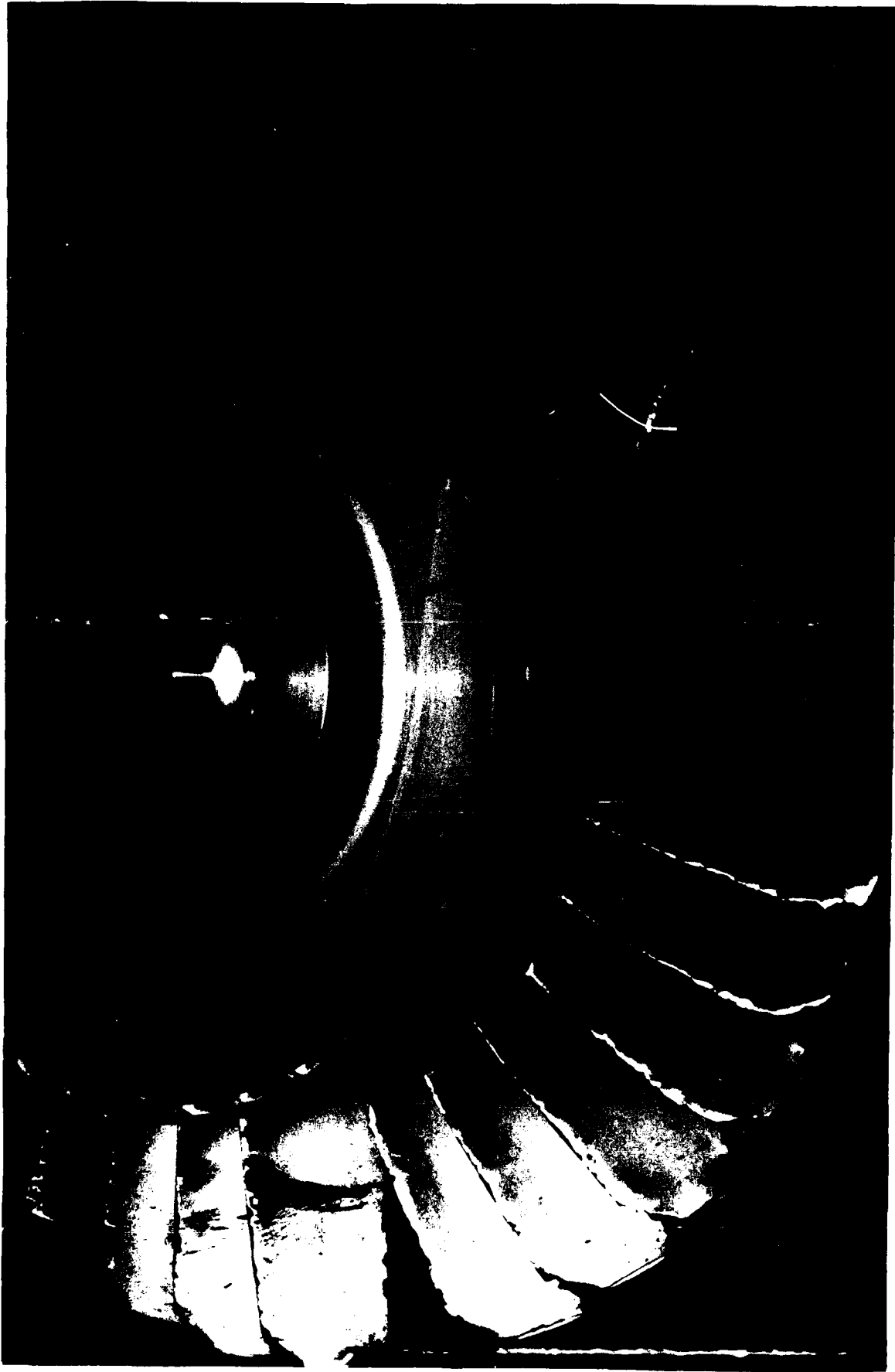


Figure 87. Damage to Left F-10 First Stage Rotors

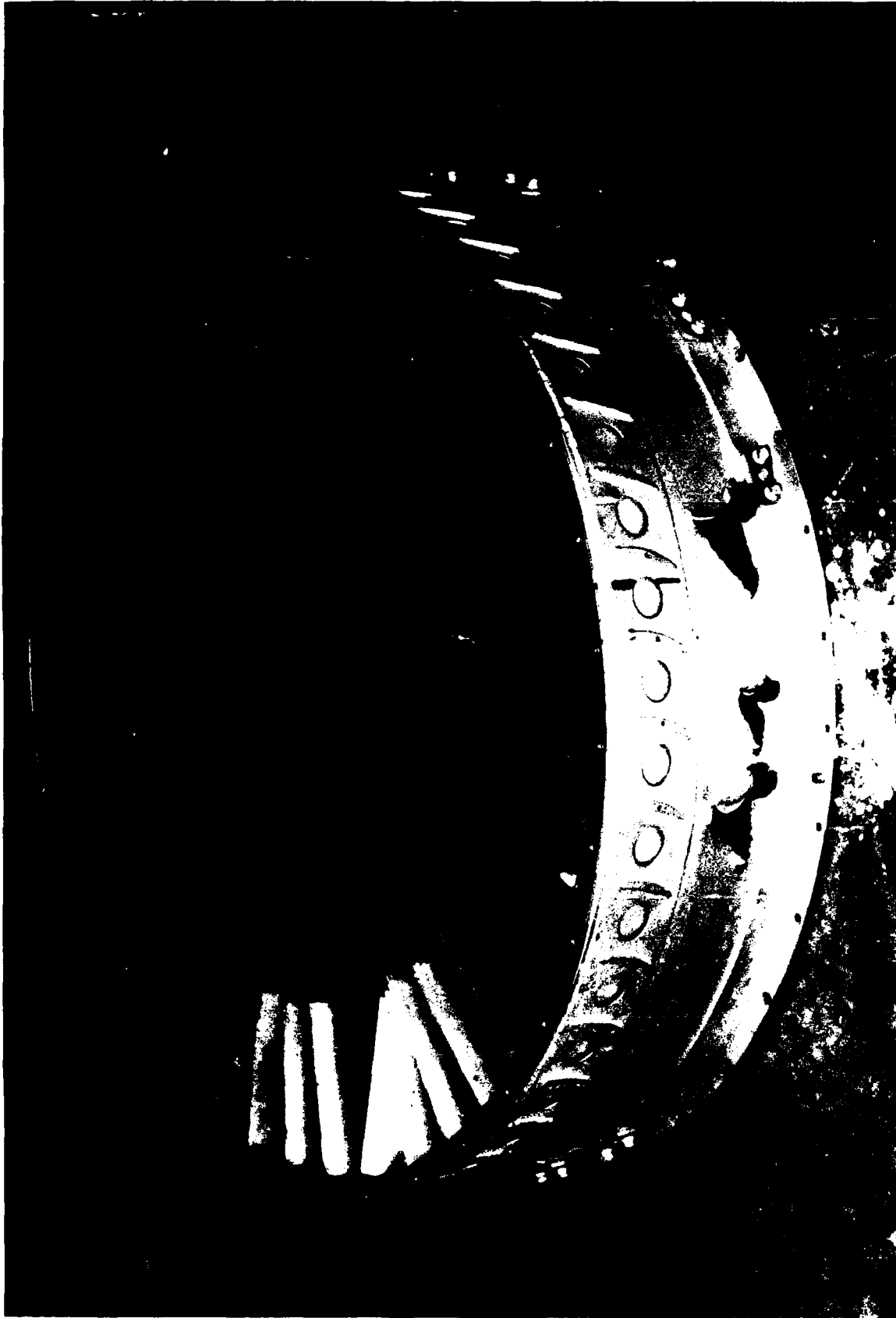


Figure 88. Damage to Left F-10 First Stage Stators



Figure 89. Comparison of New and Damaged First Stage Blades

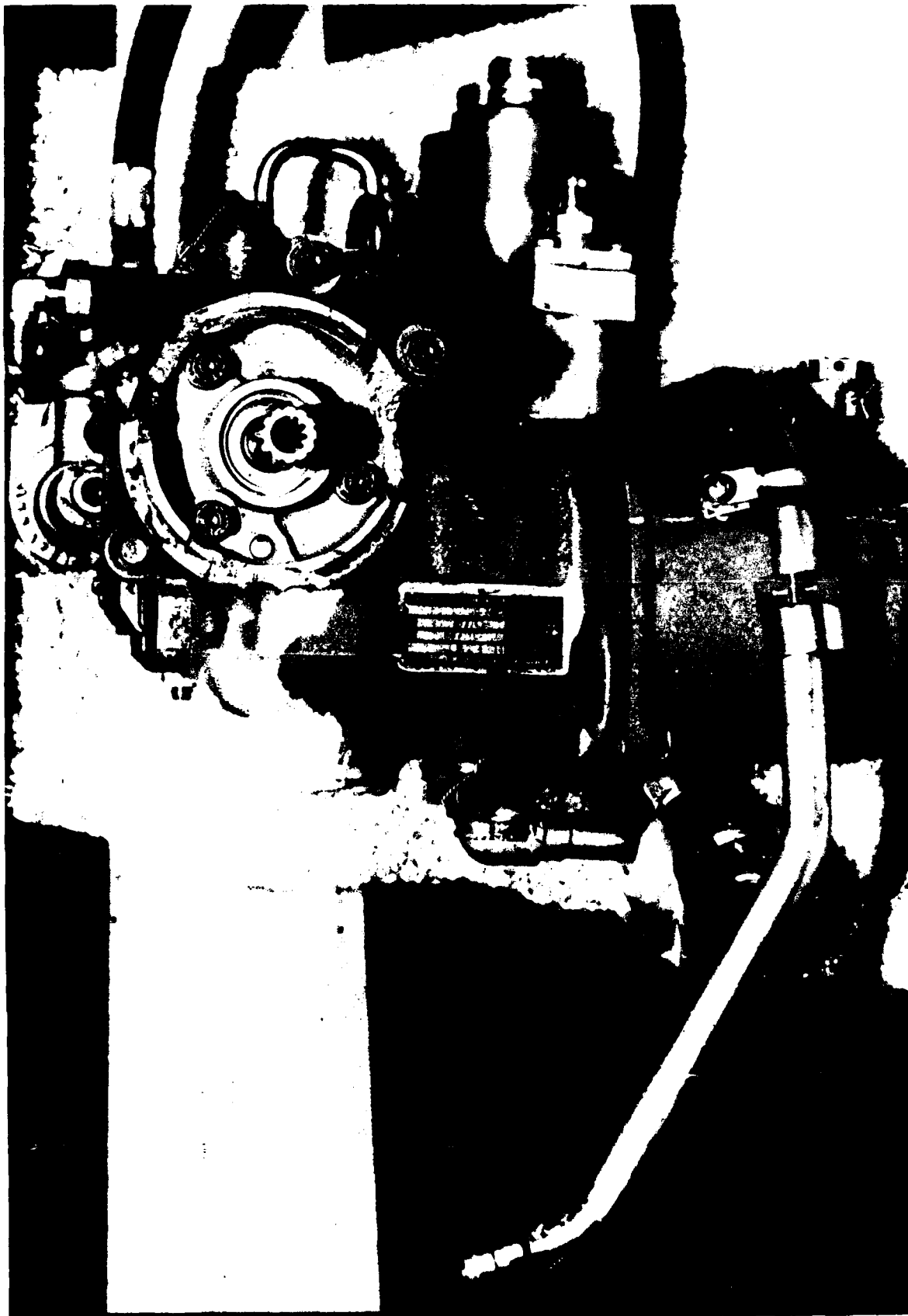


Figure 90. Sudden Stoppage Damage to Fuel Pump



Figure 91. Typical Condition of ST6F-70 Fuel Injectors



Figure 92. Overhauled F-10 Two Stage Rotor Assembly

Paragraph 7 of this section of the report. The key to the performance of the segmented skirt is its excellent seal characteristics. A comparison of the cushion cell pressures on different operating surfaces, grass and concrete, at the same operating conditions shows that this system was able to maintain cell pressures regardless of the condition of the operating surface (Figures 93 and 94). The test conditions were a payload weight of 30,475 lbs located at the forward position on the transporter. There was zero passive venting of the main cells.

The heave stability of the segmented finger skirt was a major concern, initially. However, testing has shown that the heave and pitch oscillations encountered during the contractor's and the USAF's Test Programs can be effectively controlled through passive venting of the system. The performance penalties that must be paid for this type of control are within acceptable limits. In fact, passive venting for operations on concrete at the higher weight payloads resulted in reductions in the tow forces required to move the ACET.

The maintainability of the skirt system is a major concern. The service life of the individual fingers is too low because of the wear characteristics of the material currently being used to manufacture fingers for the ACET are unacceptable. A different material must be identified for the manufacture of these fingers. The second set of segmented fingers manufactured were replaced after approximately 21 hours of operating time. The fingers were not unserviceable; however it was doubtful that there was more than 10 hours of additional life in these fingers. A material must be found that can withstand extended overland operations. Once this material is qualified for ACET operations the maintainability/reliability of the skirt system will increase dramatically. The sectioned design of the system allows the rapid replacement of individual segments damaged during operations. The simple construction, pattern cut from a template and glued and sewn together allows segments to be fabricated in advance. The limited number of different types of fingers, only four, reduces the number that must be stocked.

7. RESULTS OF TEST PROGRAM

Control of the pitch and heave oscillations for payloads above 30,000 lbs is critical to the performance of the ACET. Depending upon the damping of the tires and landing gear of the individual aircraft, damaging loads could be transmitted to the airframe structure. The testing conducted during this test program demonstrated that heave and pitch oscillations can be controlled effectively by a combination of skirt vents and passive cushion vent doors. With this combination the ACET/ Payload can be tuned to achieve maximum performance while operating as a stable platform for transporting aircraft and alternate loads across austere terrains. Analyses conducted during the evaluation of the need to upgrade the passive system to an active one, a system with a feedback control loop, indicated that an alternate approach to the installed passive system could supply the necessary control without having to vent each individual air cushion cell. The data suggest that one of the primary causes of the

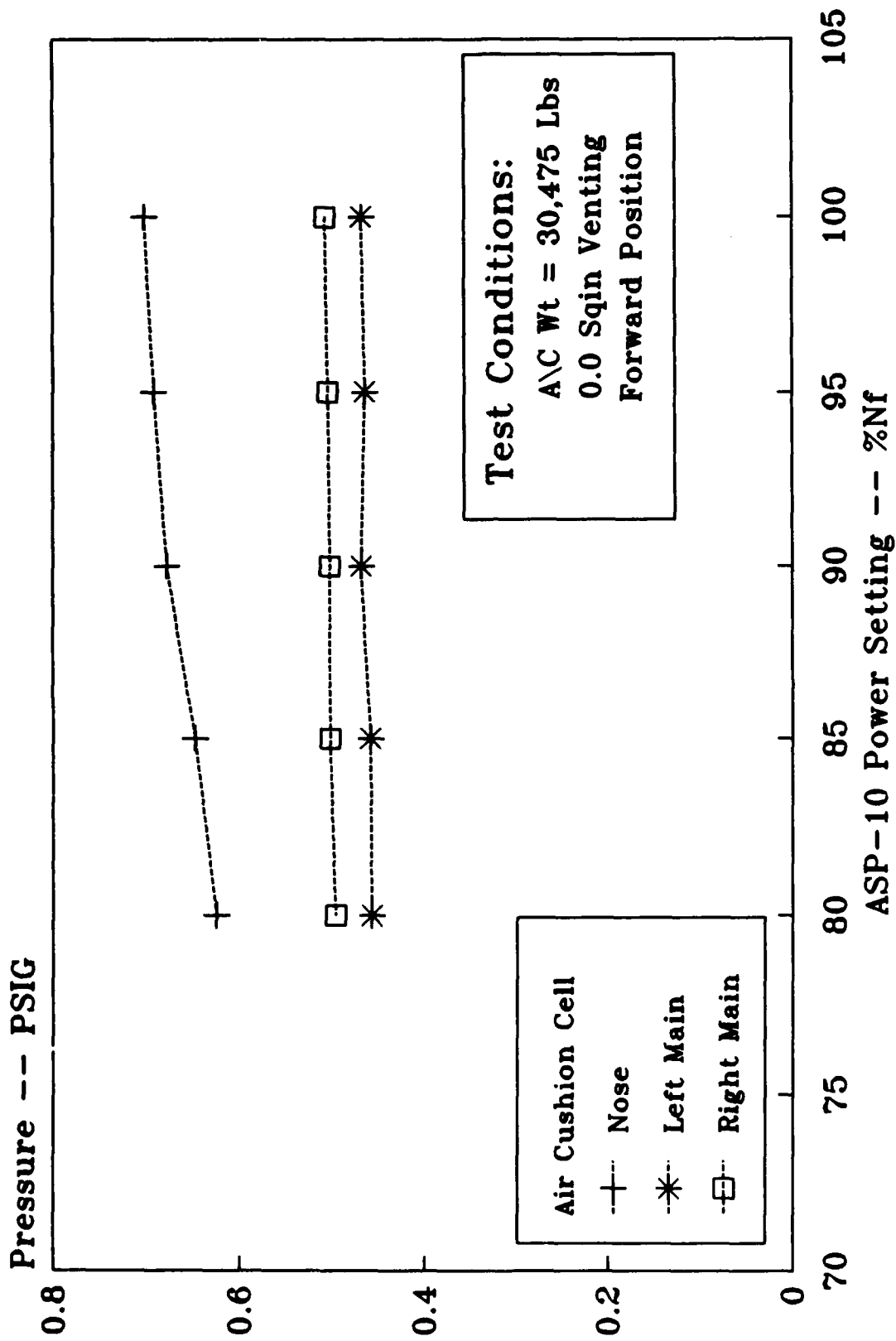


Figure 93. Cell Pressure Variations on Grass

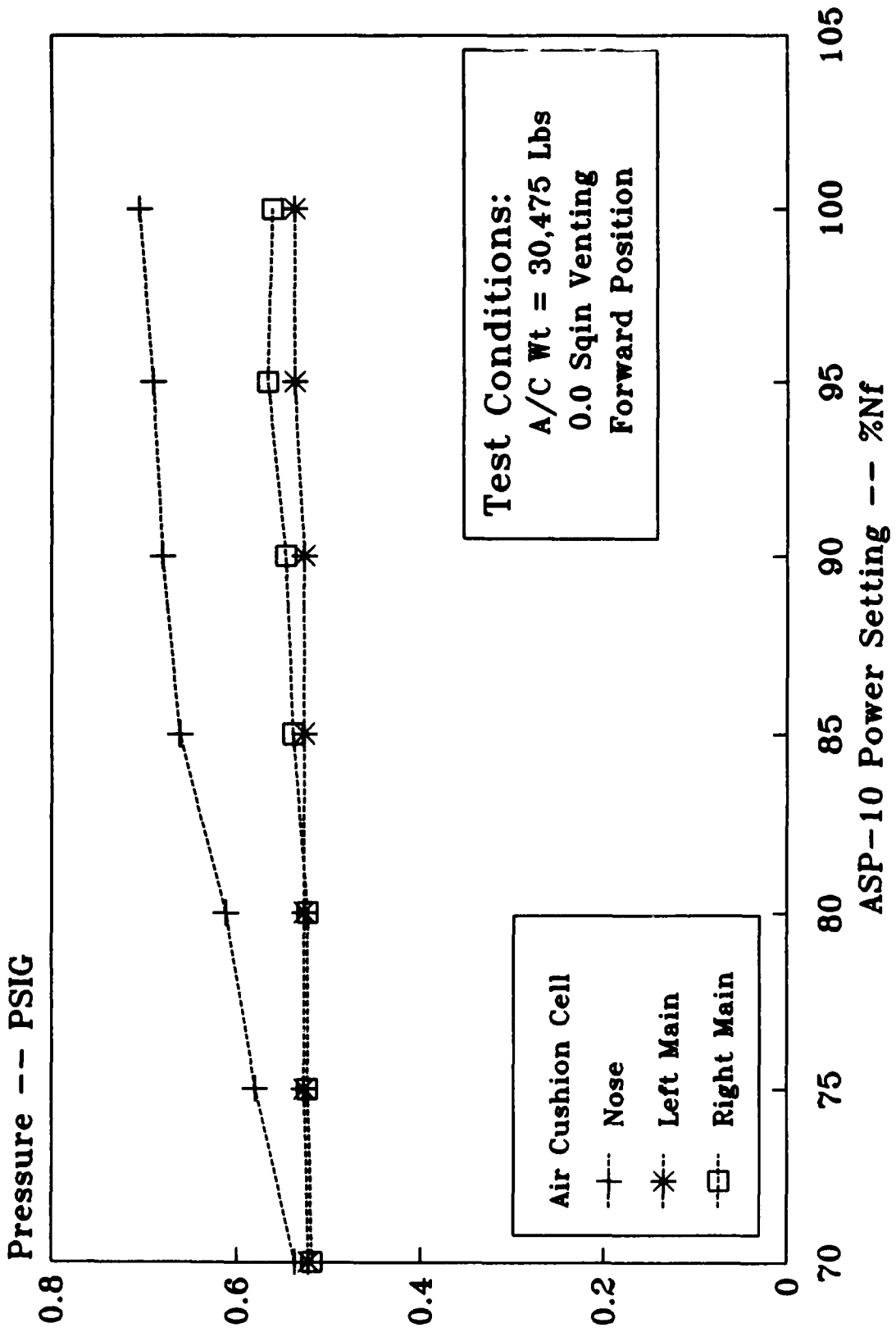


Figure 94. Cell Pressure Variations on Concrete

oscillations is the pressure fluctuations in the convergent section of the plenum aft of the F-10 fan exit. If these pressure fluctuations can be limited to less than 0.10 psig, the oscillations do not occur.

Collecting data to develop design criteria for a Self-Propulsion Modification proved to be a difficult task. The interdependency of the variables tended to mask trends and made it difficult to identify critical parameters. A summary of the breakaway drag data collected during the test program is presented in Table 10. The most influential parameter appears to be the surface the transporter is crossing. Changing this parameter from concrete to grass with an average CBR of 7.5 resulted in the largest change in drag reading, 1810 lbs. The Breakaway drag for this case, 2650 lbs, was still only 6.0 percent of the total vehicle weight, 60,822 lbs. The 47,000-lb payload was located at the aft position on the deck of the ACET.

The total payload weight also has a significant impact on the breakaway drag force. Depending upon the conditions, forces in the range of 1.0 to 4.2 percent of the total vehicle weight were recorded during the testing of the transporter. Difficulties with the protection of the F-10 fans and a compressed schedule prevented any tests to evaluate accumulative effects. Additional testing at higher payload weights and different types of surfaces is required to form a complete picture of the interrelation of these parameters and how they affect the drag required to move the vehicle.

The position of the payload on the ACET also had a sizable impact on the drag. This was expected since increasing the weight of the payload fixed to the deck and moving a fixed weight payload to a different position on the deck have the same effect on the ACET, changing the CG position of the ACET/Payload combination. Both model and full-scale testing has demonstrated that the ACET is extremely sensitive to CG location.

The breakaway drag is strongly influenced by the ASP-10 Power Setting. However, this parameter will not have a strong effect on the design of the modification since the ASP-10's, or any power plant selected, will be run at the highest possible power setting to reduce drag and finger wear while increasing soft surface performance.

The testing conducted to evaluate the feasibility of a Self Propulsion Modification and identify critical design parameters did successfully identify a number of trends. However a much more complex matrix of test conditions must be evaluated to insure the entire scope of the problem is examined. From the testing completed, the proposal of modifying the ACET to be self-powered does appear feasible and will greatly enhance the capabilities of the vehicle.

TABLE 10
SUMMARY OF TEST RESULTS

Parameter/Condition	Variable		
1. Surface	Concrete	Grass	Percent of Total Weight
A/C weight 30,475			
a. Fwd, 0.0 Sq in Venting	840	2650	6.0
b. Aft, 185.5 Sq in Venting	1120	2120	4.8
2. Payload Weight	30,475 lbs	47,000 lbs	
Concrete			
a. Fwd			
0.0 Sq in Venting	840	1960	3.2
185.5 Sq in Venting	720	560	1.5
b. Mid			
0.0 Sq in Venting	1360	1120	3.1
185.5 Sq in Venting	480	600	1.0
c. Aft			
0.0 Sq in Venting	1480	2560	4.2
185.5 Sq in Venting	1120	2080	3.4
3. Position on Transporter	Fwd	Aft	
Concrete			
a. 30,475 lbs			
0.0 Sq in Venting	840	1480	2.4
185.5 Sq in Venting	680	1120	1.8
b. 47,000 lbs			
0.0 Sq in Venting	1960	2560	4.2
185.5 Sq in Venting	560	2080	3.4
4. ASP-10 Power Setting	85.0%	100%	
Concrete			
30,475 lbs Payload			
185.5 Sq in Venting			
a. Fwd	1230	680	2.8
b. Mid	1920	480	4.3
c. Aft	1720	1120	3.9

The failure of the ASP-10 clearly identifies this subsystem as a weak point in the design of the vehicle. Utilizing components designed for other applications is an acceptable approach for demonstrating the feasibility of a concept. However, any serious consideration for the development of the ACET as an operational vehicle must include a matching of the operating environment of the ACET to the damage tolerance of potential fan/engine combinations.

SECTION VI

DEMONSTRATION OF ACET

1. FIRST DEMONSTRATION AT AMARC

As discussed in the previous section of this report, FDL personnel continued to test the transporter after BACT completed their test program and turned the ACET over to the USAF. In addition to this testing, several demonstrations were conducted for interested government personnel. As a result of these demonstrations, inquiries were received from the Aerospace Maintenance And Regeneration Center (AMARC) regarding the ACET as a potential solution to an operational problem they are faced with overcoming twice a year, namely moving "contingency" aircraft during their rainy seasons. A number of aircraft are stored at AMARC in a near flight-ready condition. These aircraft are returned to active duty quickly if a situation develops. If a crisis or situation should arise during a rainy season, AMARC's ability to respond is severely restricted. AMARC personnel have developed techniques for moving aircraft under these conditions. However, these techniques involve high risk and have the potential for damaging the aircraft being towed. AMARC was looking for a low risk, cost effective alternative to their present method of "doing business." The ACET, with a number of minor modifications, offered a solution to this problem.

a. Preparations

(1) Assessment

In September 1985, at the request of the Air Force Logistics Command (AFLC), the FDL performed a preliminary assessment of requirements and applicability of the ACET to resolve the aircraft ground mobility problem at AMARC. The results of the assessment were very positive. The following modifications to the original configuration were identified as being necessary to tailor the operational capabilities of the ACET to the requirements established by AMARC:

(a) Provide for a variable lateral and longitudinal wheel base spacing as regards loading ramps and load bearing area on the deck of the ACET.

(b) Move the lateral location of the trailing stabilizer wheels to allow for the variable width of the main landing gear.

(c) Modify the nose wheel track to accommodate various nose gear widths.

(d) Provide a mechanism for supporting the ACET during aircraft loading and off-loading on soil with a California Bearing Ratio (CBR) of less than 3.

(e) Provide a skirt for prevention of foreign object damage (FOD) and to minimize the dust cloud on dry soil.

A program estimate was prepared for the design, fabrication, and installation of the modifications; the shipping of the ACET to AMARC at Davis-Monthan AFB AZ; and conducting a two week demonstration. In January 1986, AFLC funded the preliminary design of the operational modifications for the ACET. The goals of this design effort were to determine the feasibility of implementing the recommendations reached during the Assessment and completing the design of the required modifications. The critical concerns used in this determination of which modifications to incorporate into or on the ACET were:

The complexity of the proposed modification,

The cost of designing and fabricating the modification,

The time required to install and checkout the modification.

The modifications considered included those previously identified as being critical to the success of the demonstrations and other modifications which would enhance the performance of the ACET at AMARC. Once the modifications were defined, it was agreed that FDL would fund the modification of the ACET, and AFLC would provide the funds to cover the AMARC demonstration and travel budget.

(2) Schedule

After agreement was reached on the scope of the AMARC demonstration and the modifications needed, a 6-month schedule was developed to modify the ACET and prepare for the AMARC demonstration. The first available window for conducting the demonstration was July/August 1986. Delays in identifying a funding source were encountered, and this window was missed. Efforts to obtain the necessary funding continued through late fall and early winter of 1986. Finally, in December 1986, funds were allocated for the demonstration. AMARC requested a demonstration at the earliest possible date. The next rainy season would most likely occur, based upon past meteorological data, sometime in late February to early March 1987. To meet this window required compressing 6 months of contract and in-house work into 3 1/2 weeks. After considerable discussion and review, a definitive schedule was agreed upon by AMARC, FDL, and Systems Research Laboratories, Inc. (SRL), the facility contractor supporting the Mobility Development Laboratory (MDL). The key dates of this schedule are presented in Table 11.

TABLE 11

AMARC DEMONSTRATION KEY DATES

EVENT	DATE
Start Design of Modifications	22 Dec 86
Start Ordering Materials for Modifications	06 Jan 87
Begin Fabrication of Modifications	08 Jan 87
Complete Design of Modifications	14 Jan 87
Start Installation of Modifications	19 Jan 87
Finalize Transportation Requirements	20 Jan 87
Complete Fabrication of Modifications	23 Jan 87
Complete Installation of Modifications	30 Jan 87
Final check-out of ACET	2-4 Feb 87
Disassembly of ACET	5-10 Feb 87
Loading of ACET	11 Feb 87
Shipping of ACET to AMARC	12-16 Feb 87
Assembly of ACET at AMARC	17-19 Feb 87
Check-out of ACET	20 Feb 87
ACET Demonstration	23 Feb - 6 Mar 87
Disassembly of ACET	9-11 Mar 87
Loading of ACET	12 Mar 87
Shipping of ACET to WPAFB OH	13-18 Mar 87

Even a casual review of the summary schedule presented in Table 11 reveals that this was a high risk approach. For example, materials were purchased before the designs were finalized and approved, and installation of modifications began before the fabrication of the modifications were completed. This schedule required detailed planning with built-in allowances for changes, constant communications between government and contractor personnel, and a great deal of hard work and overtime to meet.

(3) Modifications

Of all the modifications incorporated in preparation for the AMARC demonstration, making provisions for variable lateral and longitudinal wheel base spacing for the nose and main gear loading ramps, as well as the load bearing area on the deck of the ACET, was the most critical to the conversion of the ACET from a Research & Development (R&D) vehicle to an operational evaluation transporter. The range of parameters required for the aircraft which can be accommodated are presented in Table 12. The aircraft considered in the development of these requirements were the F-16, A-6, A-7, T-38, F-100, F-8, E-2, F-101, and F-4. The weight range reflects the weights of these aircraft, as stored at AMARC.

TABLE 12

DESIGN REQUIREMENTS FOR LOADING RAMPS AND AREA

CHARACTERISTIC	RANGE
Lateral wheel spacing	116 - 230 inches
Longitudinal wheel spacing	213 - 286 inches
Main wheel width	7 - 12 inches
Nose wheel width	5 1/2 - 23 inches
Weight	23,000 - 40,000 pounds

The main landing gear ramps (Figure 95) were redesigned to meet these requirements. The new ramps were fabricated in four sections, with the load carrying member being AM-2 landing mat. The landing mat had the necessary strength capability and size to meet the requirements for both the main and nose wheel widths, as well as the maximum loading on the main and nose wheel tires. Each of the main landing gear ramps was redesigned from one continuous piece, to four interlocking sections. This was done to allow two people to move and position the ramps without the need for special handling equipment. Also, the angle of the main gear ramps was



Figure 95. New Loading Ramp and Trailing Wheel Assemblies

decreased from 11 degrees to approximately 7 degrees to reduce the loading on the winch motor and aircraft structural members while the aircraft is being pulled onto the deck of the ACET.

The nose gear ramp design was changed from one piece to three, interlocking sections, Figure 95, each easily handled by two people. As indicated above, the nose ramp is also fabricated from AM-2 landing mat. Also, the angle of the nose wheel ramp was increased to conform to the new nose wheel track on the deck of the ACET. This change does not have a significant impact on the winching loads, since the nose ramp primarily rotates the nose of the aircraft upward. The maximum winching loads occur when the main landing gear are rolling up their respective ramps.

A suitable load-bearing area was obtained on the aft deck of the ACET by removing the original main gear tracks and replacing them with 8-foot sections of landing mat (Figure 96). By placing four 8 foot sections of mat on either side of the nose wheel track, a bearing surface was obtained which handled the lateral main wheel spacing of all the aircraft that can be accommodated by the ACET without having to reposition any equipment on the deck of the transporter. Since the original nose track is also the main longitudinal structural member, it could not be removed. Therefore, a cap was designed and installed on the nose wheel track. This cap, fabricated from AM-2 landing mat, permitted the loading of aircraft with wider nose wheels. While the nose gear is at a higher elevation than the main gear, it does not appear that the approximately 1 1/2 degrees of nose-up pitch will cause any problems.

Since the original trailing stabilizer wheels were permanently attached to the main gear ramps, a new stabilizer wheel assembly had to be designed, fabricated, and installed on the vehicle, Figure 95. The new assembly is offset out-board to allow the main gear ramps to be placed in the proper location for loading the aircraft with the longest lateral wheel spacing, namely the Navy's E-2 aircraft. A pneumatic strut system is used to apply the required normal load at the wheel/ground interface to prevent sideslipping of the vehicle in a crosswind or a side slope.

For the AMARC demonstration, the ACET was required to have the capability of loading and off-loading aircraft on soft (CBR less than 3), uneven terrain. To meet this requirement, additional bearing surfaces were installed near the rear of the vehicle (Figure 97). To allow for the expected unevenness in terrain, pneumatic struts were incorporated into the system. Provisions were also included in this system which allowed the vertical load to be different on each side, thus providing the flexibility necessary for off-runway loading and off-loading.

Finally, in order to provide additional protection against FOD and to minimize the amount of dust created during off-runway operations, FOD suppression skirts were designed for the ACET (Figure 98). The design of these suppression skirts was based upon spray suppression skirts developed for ACV operations over water.



Figure 96. Installation of New Load-Bearing Panels



Figure 97. Low Bearing Strength Support Mechanism

F
11/18/84

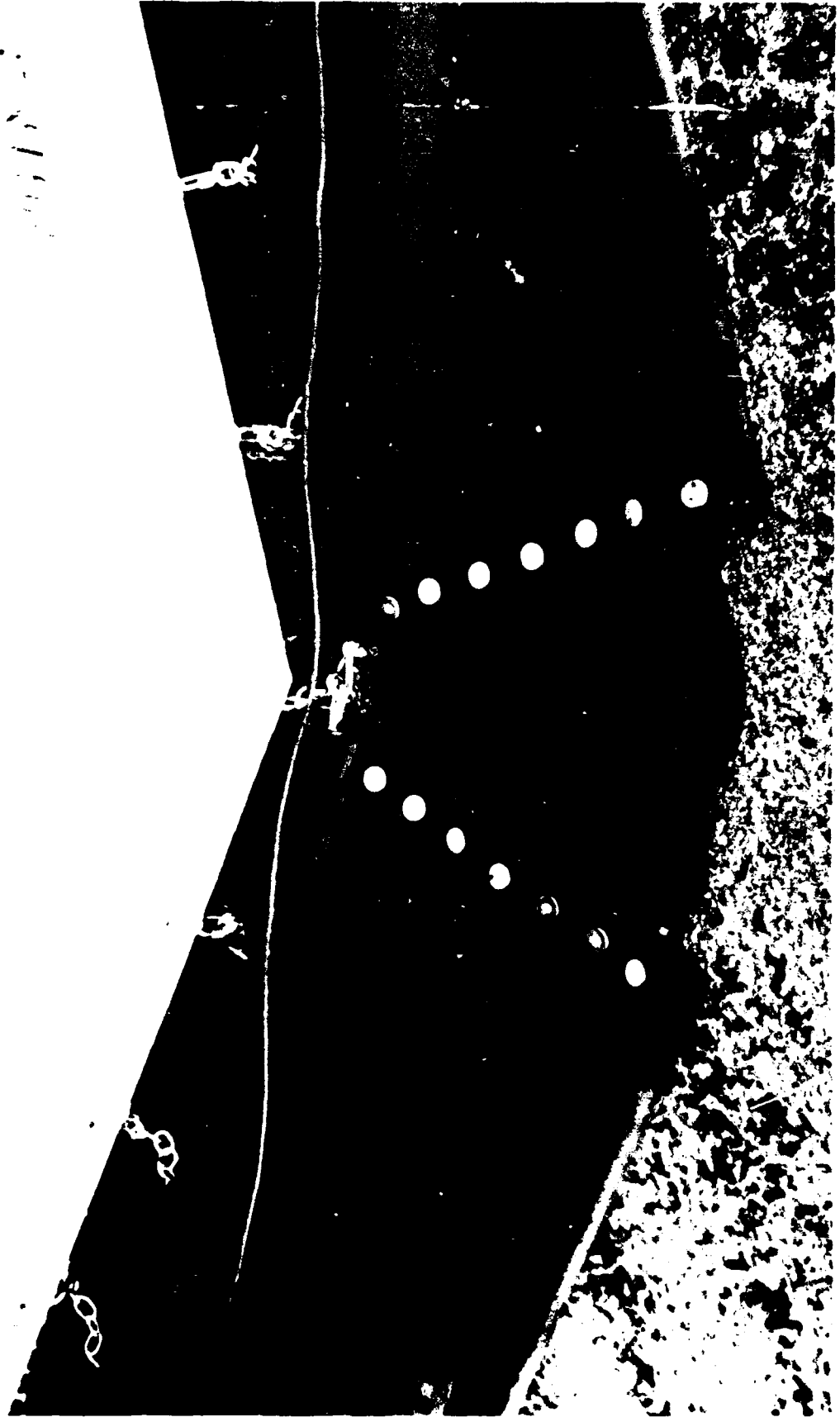


Figure 98. FOD Suppression Skirt

b. Demonstration

On 12 February 1987, the two trucks, carrying the ACET and related support equipment, departed the local area bound for Davis-Monthan AFB AZ. The plan called for the trucks to arrive at Davis-Monthan AFB on the morning of 17 February 1987. The ACET Advance Team departed on 12 February 1987 to ensure that all of the support required from AMARC was available and/or in place when the ACET arrived.

(1) Assembly and Check-out

The two trucks carrying the ACET and related support equipment arrived at 0900 on 17 February 1987. Both AMARC and the ACET Advance Team had made excellent preparations for the arrival of the ACET and the rest of the ACET Demonstration Team. A crane and operator, and a forklift and operator were made available to the ACET Team to assist in the off-loading and assembly of the ACET, for as long as required. Two mechanical technicians were assigned to our project to help with the assembly of the ACET. In addition, a liaison person was detailed to the ACET Demonstration Team. He handled all of the unanticipated support and/or tool requests. His services were invaluable during the assembly of the transporter.

The two trucks were off-loaded using the crane and the forklift (Figure 99). This operation was completed by 1300 on 17 February 1987. The three major components of the ACET were then placed on 55-gallon steel drums, see Figure 100. Assembly was started before close of business on 17 February 1987 (Figure 101). Three days later; Friday, 20 February 1987; the ACET, now fully assembled, was lowered off the drums via mobile crane (Figure 102). A total of 270 manhours were expended in the assembly of the transporter. Of the total, AMARC provided 140 manhours. This assembly time included a number of unscheduled repairs resulting from damage during shipping. Extremely high winds were encountered while the trucks were crossing Texas. As a result, both of the ASP-10 lower exhaust stubs had to be rebuilt (Figure 103) prior to installation. In addition, a significant number of nut plates had to be replaced because of damage during disassembly and stripping out during assembly. The number of plates damaged during assembly was held to a minimum when it was discovered that the build-up of fine sand in the nut plates was causing the problem during assembly. Corrective action was taken and the problem was resolved. Also, because of the extremely tight schedule the program was working against, the installation of the FOD suppression skirts (Figure 104), replacement of damaged fingers with fingers fabricated from a material supplied by Goodyear (Figure 105), and the correction of several deficiencies in the modification for the AMARC demonstration discovered during final check-out prior to shipping, had to be accomplished on-site.

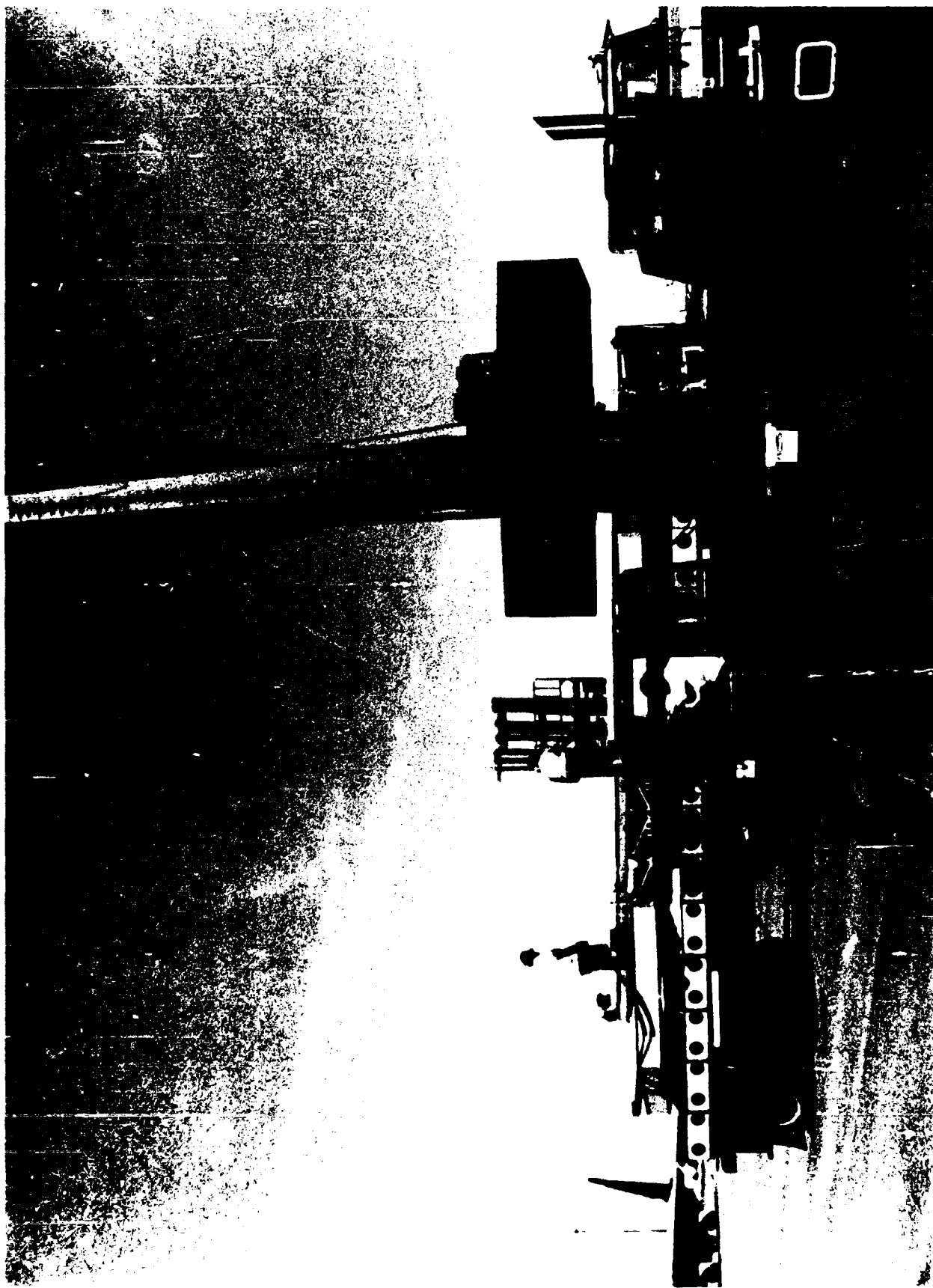


Figure 99. Off-Loading of the ACET

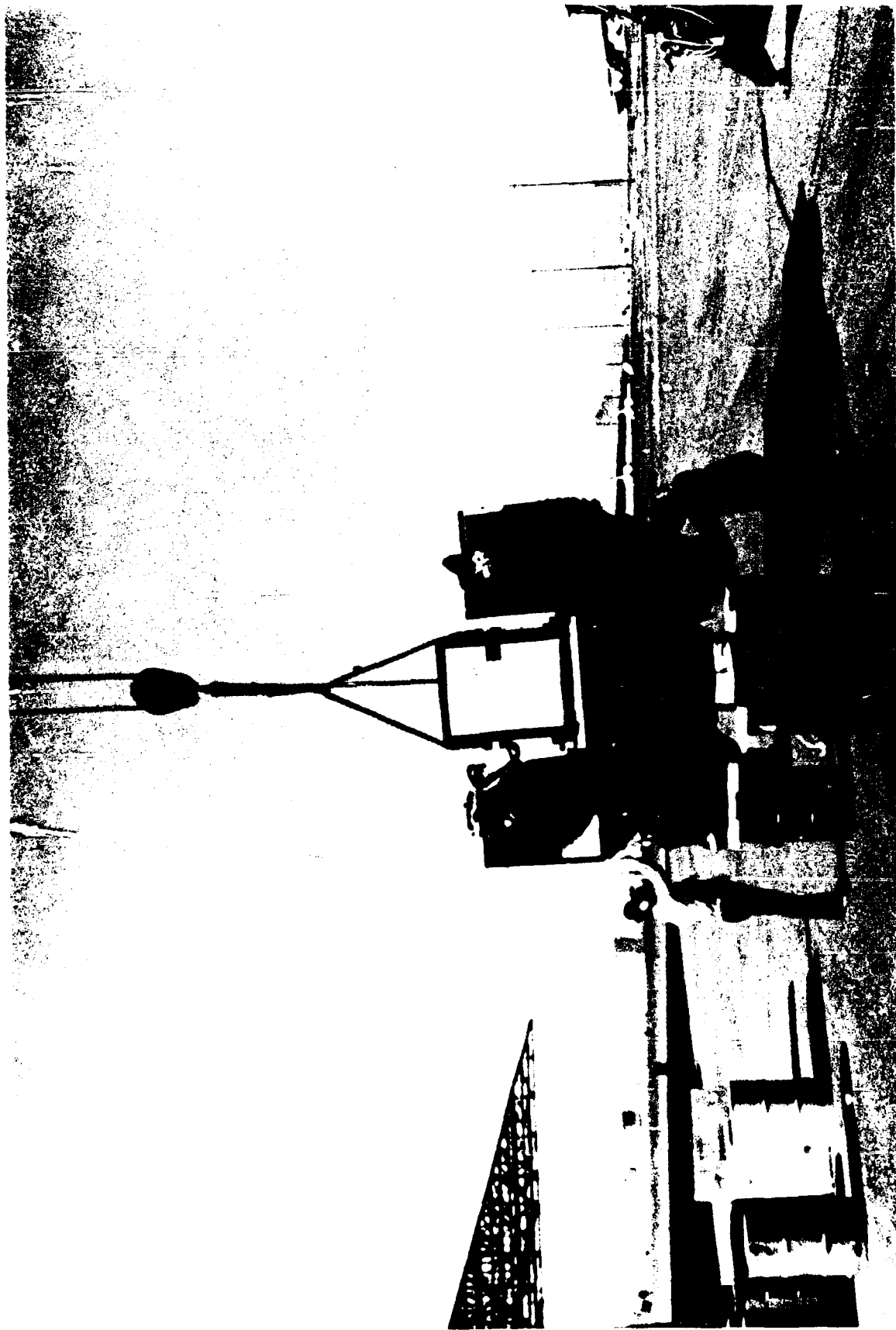


Figure 100. Forward Module Positioned on Maintenance Stands



Figure 101. Start of ACET Assembly



Figure 102. Assembled ACET Lowered to Ground



Figure 103. Repair of Lower ASP-10 Exhaust Stub



Figure 104. Installation of FOD Suppression Skirts



Figure 105. Preparing Goodyear Fingers for Installation

Except for several discrepancies discovered during the pre-test inspection, the check-out run went extremely well. The ACET functioned, as advertised, with both ASP-10's starting on the first attempt. The run lasted for 0.3 of an hour. This time was used to familiarize AMARC personnel with the towing characteristics of the transporter. The entire run was conducted on a hard surface, with the ACET unloaded. The ACET was parked under a sheltered area for the weekend, since rain was forecast. With the completion of the vehicle checkout, the first major benchmark of the AMARC demonstration was successfully achieved.

During a meeting on Friday, 20 February 1987, the decision was made to use a Navy F-4J as the first aircraft to be moved. The specific aircraft to be moved was located in Area 11, and was classified as a "Strike" aircraft. This means that the airframe had already been stricken from the inventory because of excessive corrosion. The empty weight of a Navy F-4J is slightly heavier than the USAF F-4E, 32,000 lbs for the Navy aircraft vs 30,500 lbs for the USAF F-4E.

(2) Demonstration

On Monday, 23 February 1987, the ACET was moved from the Reclamation Hangar to the location of the F-4J in Area 11. The distance between the two points was 0.9 miles. The surface conditions were dry, with a 10- to 30-mph wind. This test did not go smoothly. While the newly installed FOD suppression skirt did help control the dust to a certain degree, the cloud of dust resulting from operating on a dry, sandy surface caused significant visibility problems. A component failure occurred just as the ACET entered Area 11. When the ACET transitioned from a paved road to the unsurfaced storage area, it was necessary to tow the ACET over an area with a significant side slope. The lateral directional control capability of the modified trailing wheels was exceeded by the combination of the gravitational force resulting from the side slope and the aerodynamic force caused by the wind, and the transporter began to swing to the right. The pivot point was the tow vehicle hitch pin. During the resulting rotation, the left trailing wheel assembly was broken off at the weld line of the attachment plates (Figure 106). Excessive dust prohibited seeing the exact cause of the failure. With only one trailing wheel assembly serviceable and the high surface winds, the ACET could not be maneuvered with the precision required to park the transporter in front of an aircraft in preparation for loading. Therefore, a level area was selected and the ASP-10's were powered down. The total time of the run was 1.5 hours. A posttest inspection of the damage confirmed that the trailing wheel attachment bracket would have to be modified before the next operation could be attempted.

Before the end of the day, a rough design had been developed and a material had been selected. Steel plate, three-fourths of an inch thick, was selected because of the availability of the material. Having agreed on the preliminary design, the ACET Demonstration Team was divided into two units. One group worked on the final design and fabrication of the modification, while the other prepared the ACET for the modification. This approach was used to reduce the down time to an absolute minimum.

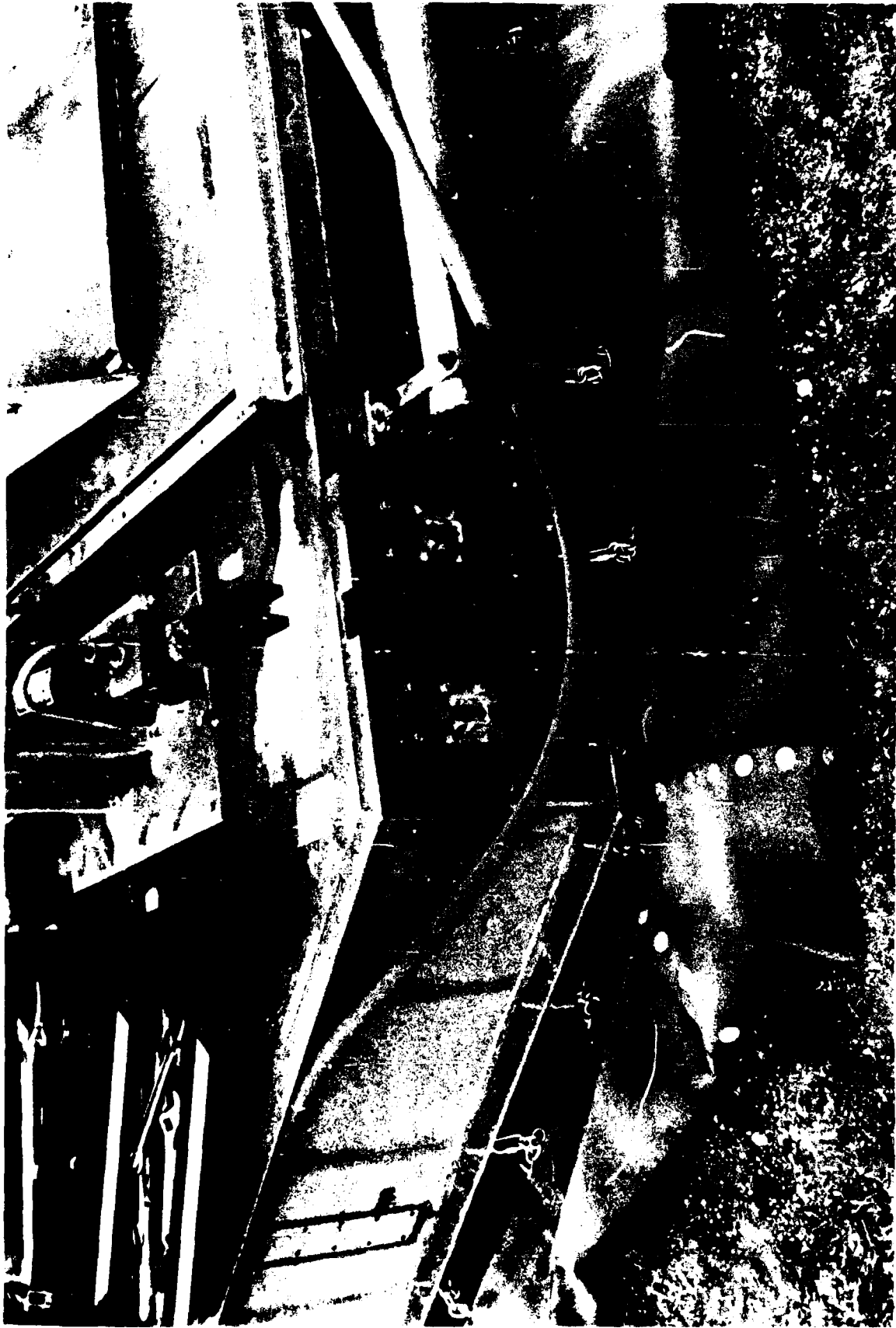


Figure 106. Failure of the Left Trailing Wheel Assembly

Fabrication of the attachment brackets began on 24 February 1987. Again, AMARC provided excellent support to the program with extremely qualified machinists and welders and the necessary equipment. AMARC also cleared our non-union personnel to work in their union shops. Excellent progress was made during the normal duty shift on 24 February 1987. However, the need to return the ACET to an operational status increased substantially with the start of a forecasted two days of rain. AMARC management, eager for us to meet this window of ideal test conditions, authorized 8 manhours of overtime to facilitate the fabrication of the new parts. Even with the overtime authorization, the new trailing wheel attachment brackets (Figure 107) were not installed until 1500 on 25 February 1987. During a subsequent attempt to position the ACET in front of the F-4J aircraft, there was a clearance problem between the new attachment brackets and the trailing wheel arms. The tolerance was enlarged and the trailing wheels were re-installed before close of business on 25 February 1987. The movement of the F-4J aircraft was then scheduled for 26 February 1987.

The movement of the F-4J, or any aircraft, was accomplished in three steps. The steps required to move the aircraft were:

- (a) Position the ACET in front of the F-4J aircraft to be moved.
- (b) Load the F-4J onto the ACET.
- (c) Tow the loaded ACET from Area 11 to the Reclamation Hangar.

Operations started at 0830 on 26 February 1987. By this time, a total of 1.25 inches of rain had fallen, with intermittent showers forecast for the entire day. The condition of the surface was exactly what AMARC had indicated was a major problem for them (Figure 108). The rain had soaked down into the soil, leaving the surface impassable for high-pressure aircraft tires. AMARC deferred the movement of two noncritical aircraft because of the surface conditions. All of the variables had finally fallen into place to provide an operational test of the capabilities of the ACET. The ACET met the challenge and proved that this technology could be employed by AMARC to overcome an operational restriction they must face during the rainy season.

The ACET was positioned in front of the F-4J (Figure 109) in 17 minutes. This included 5 minutes of operational checks prior to moving the ACET. The AMARC tow vehicle driver spotted the transporter in front of the aircraft on the first attempt. To accomplish this, the driver had to execute a series of precise turning and backing maneuvers. The ease with which he performed these maneuvers attests to his skill as a driver, and the maneuverability of the ACET.

After the transporter was spotted, the loading operation began. Landing mats were first laid down to provide a level surface for the nose and main wheel ramps. Next, the ramps were assembled (Figure 110) and



Figure 107. New Trailing Wheel Assembly Attachment Bracket



Figure 108. Condition of Tow Path in Area 11



Figure 109. ACET Spotted in Front of F-4J Aircraft

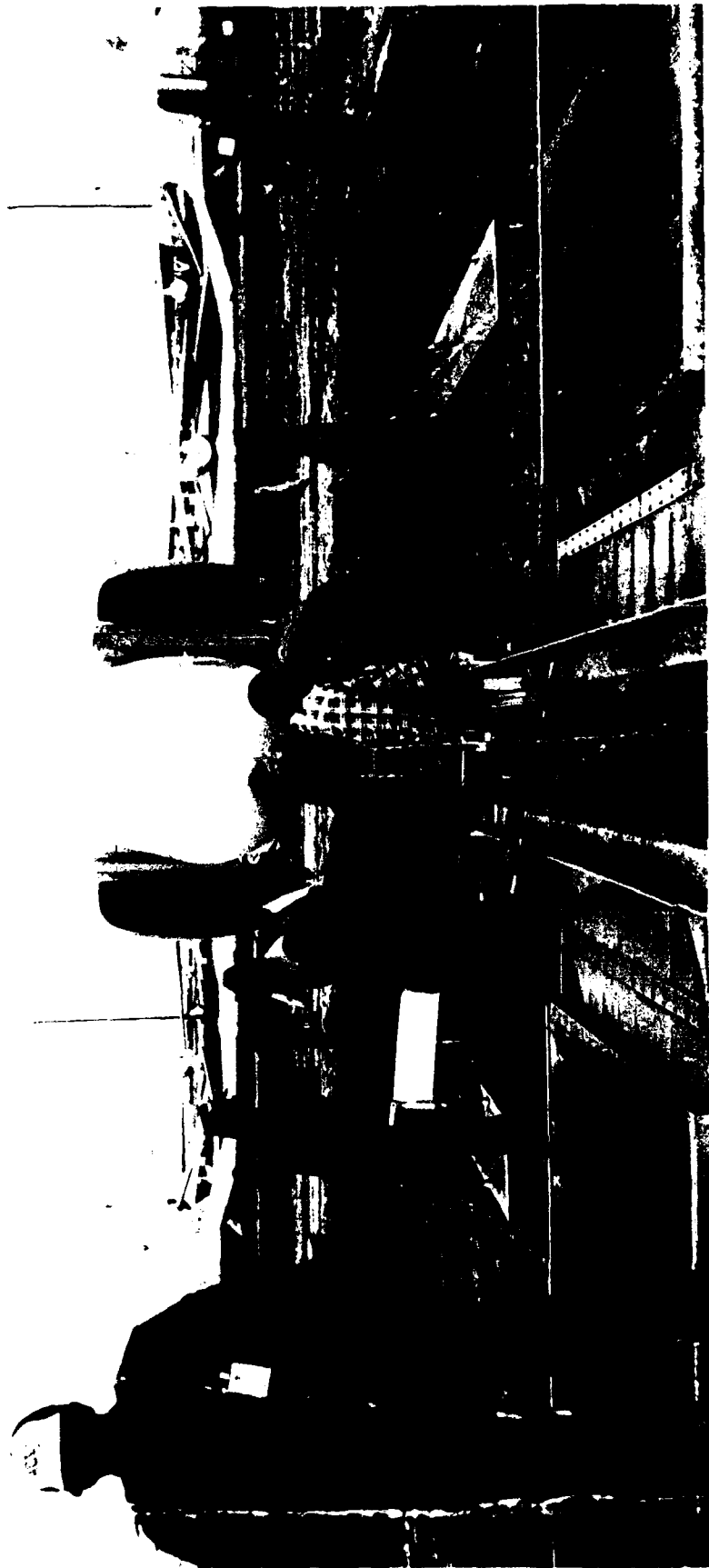


Figure 110. Field Assembly of Ramps

positioned for the F-4J wheel track (Figure 111). This part of the operation proved to be somewhat bothersome. Fine sand penetrated all of the pivot points and restricted the movement of these joints during assembly. Based upon this operational experience the ramps will have to be modified to allow free movement during assembly. While the transportation and handling of the ramp sections does require additional manpower, this approach provides the required capability of loading/off-loading a variety of aircraft with only minimal vehicle reconfiguration. Once the ramps were ready, AM-2 landing mat was laid between the ramps and the aircraft tires (Figure 112) to prevent the tires from sinking into the soft soil.

Preparations were now complete for the loading of the F-4J aircraft. The AMARC towing crew recommended attaching the winching bridle to the main gear via chains and winching from these points. The Navy Engineering and Safety representatives on site to observe the test did not agree. Their recommendation was to attach the bridle to the catapult hooks. The decision was made to winch the F-4J onto the vehicle using the catapult hooks (Figure 113) to minimize the possibility of damaging the aircraft. Using this location required a two-step procedure. The length of the bridle had to be reduced after the nose wheel was on the deck of the ACET. While changing the length of the bridle did consume some time, the loading operation went smoothly. However, this operation clearly demonstrated that a different method of attaching the winch cable to the aircraft must be developed to streamline the operation.

The final stage of the operation, the towing of the ACET with the F-4J as payload, went just as briefed. The trip from Area 11 to the Reclamation Hangar required 32 minutes of operating time, and covered 1.9 miles. The surfaces traversed included wet sand, with and without standing water; asphalt; and concrete. Everything concerning this operation was positive. The attitude of the ACET with the F-4J loaded at the forward position (Figure 114) was perfect. This ensured minimum drag and skirt wear. The MB-2 tow vehicle had sufficient drawbar capability to tow the vehicle without getting stuck (Figure 115). Also, the FOD suppression skirts were very effective in controlling wet sand (Figure 116) and water (Figure 117). Additional suppression skirts will reduce even further the amount of wet sand being kicked up. The shortness of the operating time reflects the increased confidence of the tow vehicle driver, improved understanding of the ACET among personnel involved in the operation, and higher tow speeds.

The demonstration of the ACET was cut short when, during the installation of instrumentation to record air cushion cell pressures and towing loads, and preparations for movement of a Navy E-2B aircraft, a loss of engine oil was discovered in the port (left) ASP-10. Further inspection of the engine revealed a hairline crack in the accessory gear box housing. This crack made the engine unserviceable until the housing was replaced. Replacement of the accessory gear box housing required that the ASP-10 be removed from the ACET and placed in a maintenance stand. During the initial planning for the demonstration the decision was made that a major engine failure would be an unrecoverable situation for such



Figure 111. Ramps Positioned for F-4 Series Aircraft



Figure 112. Preparations for Loading F-4J Aircraft



Figure 113. Winch Bridle Attachment Using Catapult Hooks

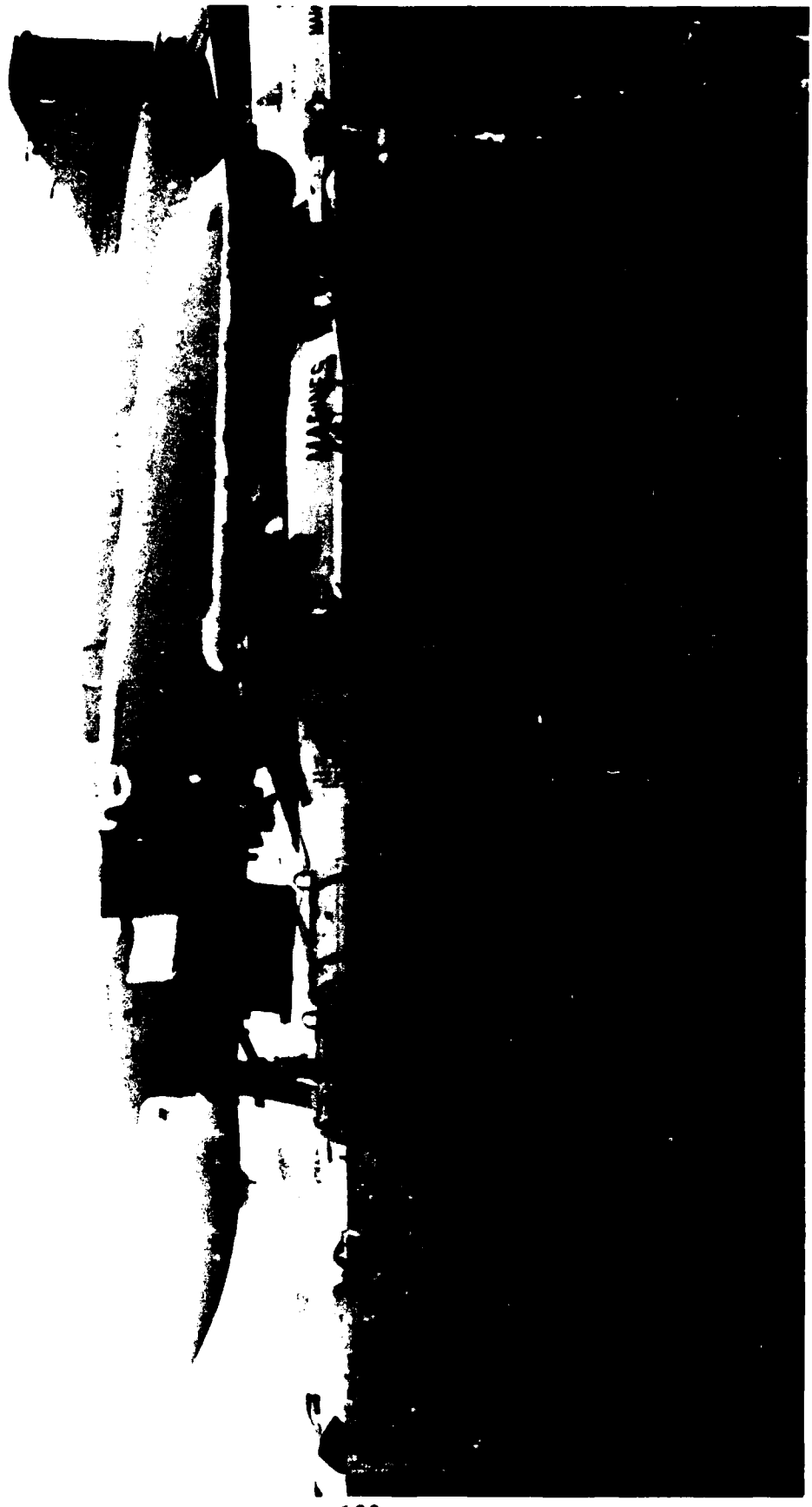


Figure 114. ACET Attitude with F-4J as Payload



Figure 115. MB-2 Getting Stuck in Area 11 (Scope of Problem)



Figure 116. ACET Being Towed Out of Area 11



Figure 117. ACET Being Towed Out Across Wet Ramp

a short demonstration (two weeks). Therefore, all of the spare ASP-10 parts, the spare engine, and maintenance stands were not shipped to Davis-Monthan AFB. The minimum estimated turn-around time for repairing the damaged engine was four working days, with overtime. This also assumed that all required spares could be obtained within one working day. The optimistic nature of this schedule and the return of dry weather because of a shift in the jet stream were the primary reasons that the ACET Demonstration Team recommended an early cessation of the demonstration. The Team's recommendation was subsequently approved by both FDL and AMARC management personnel.

(3) Assessment

During a status briefing on 2 March 1987, the Commander of AMARC and the Center Administrator expressed considerable enthusiasm in the ACET, and a strong desire to continue to explore the potential benefits the ACET concept offers in the support of the AMARC contingency requirement. This position was subsequently reaffirmed during a meeting between the FDL Commander, the Chief of the Vehicle Equipment Division, the AMARC Commander, and the Center Administrator. All parties agreed that, based on the results of the initial demonstration; the ACET, with a number of refinements, offered a viable alternate solution for the movement of contingency aircraft during rainy seasons. Everyone agreed a second demonstration was justified. This demonstration would provide fuel consumption and operations/maintenance cost estimates to AMARC supervisors and planners. Also, a second demonstration would yield valuable operational experience to evaluate what refinements, modifications, and/or design changes are required for an AMARC dedicated ACET design.

c. Findings

Both the ACET Demonstration Team and AMARC Operational and Engineering personnel have reviewed the performance of the transporter during the 17 February - 6 March 1987 demonstration. AMARC's review of the first ACET Demonstration at Davis-Monthan AFB, a Technical Observations Deficiency (TOD) Report, is included in the report as Appendix B. The ACET Test Team's Observations and Comments are presented in Appendix C. Generally, the two lists agreed on problem areas and/or deficiencies uncovered during the demonstration. A number of the recommendations, while worthy of consideration and certainly germane to an AMARC dedicated design for a transporter, were judged to be beyond the scope of the Second Demonstration and current Wright Research and Development Center (WRDC) In-House efforts. These areas were:

- (1) On-Board Propulsion System,
- (2) Mobility of a Non-Operational ACET,
- (3) Storage of Ready-Status ACET.

Any future work in these areas will require the identification of a funding source.

Post-demonstration inspection of both ASP-10's revealed damage to both fan assemblies. This damage was determined to be extensive and necessitated repair before the Second Demonstration. Both engine/fan assemblies were removed from the ACET and returned to MDL for a complete inspection and overhaul of all damaged components in preparation for the next Demonstration. The damage to the ASP-10's was restricted to the fan assemblies. The inspection of the combustion or hot sections of the ASP-10's did not reveal any damage.

Three different fingers were installed on the ACET for this demonstration (Figure 118). The difference in the fingers was the material used to fabricate the segmented fingers. Two of the materials were obtained from Bell Avon, Inc. The primary difference between these two materials was the weight of the material per square yard. The two weights were 41 ounces/square yard and 70 ounces/square yard, respectively. Both materials had the same tensile strengths: 525 pounds/inch in the direction of the nylon fabric (warp), and 475 pounds/inch transverse to the nylon fabric (fill). These materials have been qualified for ACV operations. After technical discussions concerning the ACET, Goodyear supplied a limited amount of material of comparable strength for evaluation at AMARC. Unfortunately, the limited operations at AMARC, 3.1 hours of operating time and 1.9 miles of towing operations, were insufficient to draw any conclusions. However, the Goodyear material did not show any more wear than either of the Bell Avon materials.

2. SECOND DEMONSTRATION AT AMARC

a. Goals

This Second Demonstration, although not part of the original planning, offered an excellent opportunity to obtain operational data on the ACET. Additional experience was needed by AMARC Management before an accurate assessment of the ACET could be accomplished. Of particular interest were fuel consumption rates, operational procedures, turnaround times, and operations/maintenance costs for multiple aircraft movements. Collecting data in all these areas would allow AMARC Operational and Engineering personnel to prepare a set of specifications for an ACET based upon AMARC's operational requirements.

The Second Demonstration was scheduled early August 1987. This, historically, was the occurrence of the next rainy season at Davis-Monthan AFB. Also, the Summer rainy season has, in the past, had the heaviest rainfalls. Four aircraft were identified to be moved during this demonstration. All of the aircraft were to be F-4 series aircraft, three USAF and one Navy example.

b. Preparations

Both the ACET Test Team and personnel at AMARC involved in the initial demonstration of the ACET evaluated the performance of the transporter. A number of deficiencies and modifications were reviewed and discussed (see Appendices B and C). A number of valid considerations had



Figure 118. Fingers Fabricated From Different Materials

to be shelved because of funding and schedule constraints. The following corrective actions were agreed upon as part of the post-demonstration evaluation of the ACET's performance during the initial demonstration:

(1) The loading ramps (Appendix B, Item 2) were reworked to facilitate the aligning and placement of these ramps during the preparations for loading.

(2) The trailing lateral stabilizer arms (Appendix B, Item 4) were redesigned. The new assemblies were fabricated and installed on the ACET prior to the start of the second demonstration.

(3) An improved nose wheel steering towbar (Appendix B, Item 5) was designed and fabricated. This new design included a self-tracking capability to steer the nose wheel along the center of the nose wheel ramp and track during the loading/offloading process. Also, the new towbar totally eliminated the requirement for a yoke cable (Appendix B, Item 6).

(4) The aircraft loading/off-loading procedures (Appendix B, Item 7) were reviewed and modified to resolve deficiencies and ground safety issues in this area.

(5) Additional FOD skirting (Appendix B, Item 8) was installed to provide added protection for critical components of the ACET and the aircraft being transported.

(6) Additional protection for the ASP-10's (Appendix B, Item 12) was fabricated to reduce the amount of fine debris ingested by the fans.

(7) The accessory gearbox housing on the port (left) ASP-10 had to be replaced. Based upon the post-demonstration inspection and review of video tapes of the runs at AMARC, the hot sections of both gas turbine engines were borescoped as part of a preventative maintenance program performed on the ASP-10's. Both engines passed this visual inspection without a major or grounding write-up. The fan assemblies were split from their respective engines and disassembled for inspection. Both fan assemblies had received extensive damage during the First Demonstration and required overhauling. After the rebuilding of the fan units, they were then dynamically balanced before being mated to their gas turbine engines.

(8) The loading/off-loading winch motor was overhauled and the winch cable replaced as part of the general maintenance program on the ACET.

(9) An airflow control valve was designed and fabricated for the transporter. The purpose of this valve was to eliminate the negative (nose down) pitch attitude of the ACET when it is operating with zero payload. Correction of this adverse attitude was necessary to reduce nose skirt wear and to improve the ground handling of the vehicle.

While the incorporation of all these modifications significantly improved the performance of the ACET in the AMARC operating environment, they did little to change the overall appearance of the transporter. Externally, the ACET looked almost the same as it was during the First Demonstration.

On 5 July 1987, an ACET Advance Team traveled to Davis-Monthan AFB to install the modifications and the overhauled ASP-10's in preparation for the Second Demonstration in August 1987. Everything went smoothly with only minor "on site" changes required. Prior to departing, the Advance Team powered up the ACET and determined that all subsystems were functioning correctly and the vehicle was now ready for the Second Demonstration.

c. Demonstration

On 9 August 1987, the ACET Test Team traveled to Davis-Monthan AFB for the start of the Second Demonstration of the ACET at AMARC. Included in this demonstration was the training of AMARC towing crews and flight line mechanics in all aspects of the ACET's operation.

The Second Demonstration was down-scoped by AMARC prior to the arrival of the Test Team. Only a single F-4J was to be used during the demonstration and training. AMARC had placed primary emphasis on the training of personnel since the capability of the ACET to transport an F-4 aircraft over a rain soaked surface had been clearly shown during the initial demonstration.

(1) Since it had not rained prior to the start of the training program, fire hoses were used to soak the ground around the ACET and the F-4 storage location. A tug driver, having no previous operating experience with the ACET, was able to position the transporter in front of the F-4 in approximately 40 minutes. This time was typical for a first time operator. With additional practice, the time required to spot the ACET decreases significantly. Exact time required remains a function of the individual's abilities. Backing the ACET up to aircraft over this artificially soaked wet soil provided the only opportunity to observe the performance of the modifications made to the fan inlet and the trailing wheels since the anticipated rainy season failed to materialize. FOD ingestion into the fan assembly was negligible, practically non-existent, as result of the inlet modifications. The trailing wheels also worked as intended. They tracked well with no tendency to plane on the wet soil, as was observed with the original configuration during the initial run.

(2) The nose wheel yoke, designed to replace the cables previously used in the loading and offloading of aircraft, worked but the nose wheel of the aircraft rubbed the side of the nose wheel ramp while the aircraft was being winched onto the platform. This problem was further compounded during the offloading process. The first attempt to offload the F-4 aircraft was made on the paved surface in front of the Reclamation Shelter. AMARC Operational personnel want to be able to push the aircraft off the ACET manually. The first attempt was not very

successful because of the nose wheel dragging against the track. Six men were required to roll the empty F-4 off the back of the platform. The nose wheel yoke was modified so that the aircraft could be steered up and down the ramps. The steering bar modification provided an improvement. However, it was concluded that the offloading technique developed during the Wright-Patterson tests was still the best solution. For the rest of the demonstration, an MB-4 tow vehicle was used to pull the aircraft off of the ACET with the winch being used to provide a breaking force. Coordination between the tow vehicle operator and the winch operator was accomplished by using two-way radio communicators installed in ear protectors with voice activated throat and boom microphones. Using this procedure, the time required to offload the aircraft was reduced to 15 minutes. The stop watch was started when the ASP-10's were shut down and was stopped when the nose wheel of the aircraft hit the pavement.

(3) Even though the anticipated rainfall never developed, all of the AMARC towing crew, approximately 16 people, were trained on all aspects of the ACET's operation. In addition, three flight line mechanics were trained in the operation of the ASP-10's. Thus the Second Demonstration ended with the AMARC personnel being well trained in the operation of the ACET.

3. RESULTS OF DEMONSTRATIONS

The performance of the ACET during the two demonstrations clearly highlighted the fact that the air cushion transporter technology offered a promising solution to the problem of moving contingency aircraft during the rainy seasons of this region. During the First Demonstration, a towing crew, composed of WRDC and AMARC personnel, was able to move a Navy F-4J aircraft during a period when AMARC deferred the movement of two other aircraft because of the soil conditions.

As discussed, the First Demonstration revealed a number of deficiencies in the design of various ACET subsystems. Wherever feasible, modifications were designed and incorporated prior to the Second Demonstration. A limited check-out of the modifications incorporated on the ACET was achieved. The results were promising. However, additional operational performance data on these modifications must be collected and evaluated if the ACET is to fully meet the requirements of AMARC. This database can only be obtained through the daily operation of the transporter in the field. To achieve this objective, the ACET must be retained at AMARC in an operational status to be used anytime the surface conditions at Davis-Monthan preclude the use of established towing procedures.

SECTION VII

CONCLUSIONS AND RECOMMENDATIONS

1. Conclusions

The ACET has proved to be a highly maneuverable ground transporter, capable of crossing snow, ice, rock, clay, and soil of various makeup with grass cover. The tow forces required to move the transporter were less than 10 percent of the total vehicle weight, even at the maximum payload of 60,000 Lbs. In all conditions tested during this evaluation, the tow forces for the ACET were considerably less than the rolling friction for tires. The difference between these forces increased as the testing progressed to the more austere surfaces.

The testing of small scale models does not provide accurate data which can be used to predict the performance of the full-scale ACET. The analytical techniques have not been developed to accomplish this task. The cost of developing accurate, dynamically scaled models at the 1/10 scale is prohibitive. Any compromises made during the development of the model have a significant impact on the test results obtained from this model. Also, larger scale models will reduce the influence of an unscaled atmosphere on the test results.

Heave oscillations can be controlled with skirt venting and passive venting. There is a question of whether this venting should be in the individual cells or at the convergent section of the plenum to achieve maximum control. However, the ACET can be operated in a stable manner throughout the entire operating envelope for the vehicle.

The decision to change from a "jupe" to a segmented finger skirt system was an excellent decision. The segment finger skirt has excellent offrunway performance over austere surfaces. This performance is a major factor in keeping the tow loads below 10 percent of the total weight. An adequate skirt material for extended overland operations still has not been found. This deficiency must be resolved if the maintenance costs of the ACET are to achieve an acceptable level.

While the ASP-10's were an excellent choice for demonstrating the feasibility of using air cushion technology to solve current ground mobility problems, these engines are unacceptable for an operational vehicle. An alternate engine/fan unit must be identified if a high degree of Reliability and Maintainability is to be demonstrated. This unit/units must have sufficient power to drive a Self-Propulsion System for the ACET.

The performance of the ACET during the two demonstrations at AMARC clearly established the feasibility of using the technology developed under the ACET Program to solve the problem of moving contingency aircraft during the rainy seasons experienced by this region.

The total capability of the ACET can only be achieved if the requirement for a tow vehicle is eliminated. The offrunway performance of

any tow vehicle within the current USAF inventory is considerably less than that of the ACET. Aside from increasing the offrunway capabilities of the ACET, a Self-Propulsion Modification will increase the maneuverability of the transporter in confined spaces by reducing the overall length of the vehicle. Finally, eliminating the tow vehicle will reduce the number of personnel required to operate an ACET. This will have a positive impact on operational costs and will reduce the cost of using this type of vehicle.

The ultimate goal of any Research and Development program is the transition of technology to a "USER." The ACET Technology Program afforded the opportunity to transition, not only, the technology, but also, a prototype vehicle to AMARC. Work still remains, if the vehicle is to achieve its full potential. However, the adaptability of the ACET during the AMARC demonstrations provides a solid foundation for accomplishing this goal.

2. Recommendations

The ACET is a prototype/demonstrator vehicle. As such, a number of compromises and simplifications were made to demonstrate the feasibility of the concept at the lowest possible cost. A number of refinements could be incorporated into the vehicle to enhance its operational capability. Clearly the ground mobility requirements of an organization such as AMARC are not the same as those for TAC. However, there are overlapping requirements that are basic to the vehicle regardless of the application. These requirements should be reviewed and prioritized so that programs can be initiated to provide the technology currently needed to solve a number of ground mobility problems.

If the ACET Technology is to be used to solve current and future USAF ground mobility problems, technical efforts must be initiated to investigate alternate skirt materials for protracted overland operations, evaluate various engine/fan combinations, including diesel engines and centrifugal flow fans, more suited to ACET operations, and continue testing of the ACET to further define the critical parameters required for the development of a Self-Propulsion Modification for the ACET.

The development of an Air Cushion Technology database within the USAF must continue if this technology is to be applied to ground mobility problems. Model testing should be continued in an effort to overcome problems encountered during this program and to reduce development costs of future programs.

SECTION VIII

REFERENCES

1. T.D. Earl, W.G. Cockayne, C.E. Satterlee, AATS Initial Design Program, Volume IV, AATS Preliminary Design, AFWAL-TR-81-3029, Bell Aerospace Textron, Buffalo, NY, April 1981.
2. T.D. Earl, I.W. DePay, G. Tothill, Air Cushion Equipment Transporter (ACET) Report Volume I, Design and Fabrication, AFWAL-TR-86-3088, Volume I, Bell Aerospace Canada Textron, Grand Bend, Ontario, Canada, January 1983.
3. R.W. Helm, T.D. Earl, G.C.C. Smith, Air Cushion Equipment Transporter (ACET) Report, Volume II, Testing, AFWAL-TR-86-3088, Volume II, Bell Aerospace Canada Textron, Grand Bend, Ontario, Canada, June 1986.
4. D.L. Fischer, 1st Lt USAF, Calibration of an Axial Fan at Various Power Settings for Use on a Quarter Scale XC-8A Air Cushion Model, AFWAL-TR-80-3094, November 1980.
5. ASME Research Committee on Fluid Meters, Fluid Meters Their Theory and Application, 5th Edition, ASME, 1959.
6. J.R. Amyot and H.S. Fowler, An Experiment on Active Control of Air Cushion Heave Dynamics, Seventeenth Canadian Symposium on Air Cushion Technology, Ottawa, Canada, October 1983.

APPENDIX A

FLOW CALCULATION PROGRAM

```

1 C*****
2 C*   PROGRAM FAN4 DETERMINES VOLUME FLOW OF FAN      *
3 C*   USING FAN CALIBRATION RIG DATA                *
4 C*****
5     PROGRAM FANCAL
6 $DEBUG
7     REAL MU,MDOT,MCFS,MF,MFCFS,MFCFM,K,MCFM
8     CHARACTER*9 FNAME
9     6 NCOUNT=0
10    IF (NCOUNT .EQ. 0 ) GOTO 5
11    GOTO 1
12    5 WRITE(*,'(A\)' ) ' OUTPUT FILE NAME? '
13    READ (*,'(A9)' ) FNAME
14    OPEN(2,FILE=FNAME,STATUS='NEW' )
15 C*****
16 C*   FNAME IS 9 CHARACTERS OR LESS                  *
17 C*****
18    1 J=1
19    WRITE(*,2) J
20    2 FORMAT(1X,'DATA POINT NO.      ',I3)
21    GOTO 21
22 C*****
23 C*   MU IS THE MASS FLOW RATE, INITIAL, LBF*SEC/FT**2      *
24 C*   MDOT IS THE MASS FLOW RATE, INITIAL, LBM/SEC          *
25 C*   CFS IS THE MASS FLOW RATE, INITIAL, CUBIC FT/SEC     *
26 C*   MCFM IS THE MASS FLOW RATE, INITIAL, CUBIC FT/SEC    *
27 C*   MF IS THE MASS FLOW RATE, INTERPOLATED, LBM/SEC      *
28 C*   MFCFS IS THE MASS FLOW RATE, INTERPOLATED, CUBIC FT/SEC *
29 C*   MFCFM IS THE MASS FLOW RATE, INTERPOLATED, CUBIC FT/SEC *
30 C*   K IS THE COUNTER                                     *
31 C*****
32    19 J=J+1
33    WRITE (*,2) J
34    21 WRITE (*,20)
35    20 FORMAT(1X,'INPUT DATA P1D,P2D,POD,PEXD,T2F,TOF,D,CD' )
36 C*****
37 C*   P1D IS THE UPSTREAM ORFICE PRESSURE, IN. OF WATER      *
38 C*   P2D IS THE DOWNSTREAM ORFICE PRESSURE, IN. OF WATER    *
39 C*   POD IS THE ATMOSPHERIC PRESSURE, MM OF HG              *
40 C*   PEXD IS THE FAN EXIT PRESSURE, IN. OF WATER           *
41 C*   T2F IS THE DOWNSTREAM TEMP., DEGREES F                 *
42 C*   TOF IS THE AMBIENT TEMP., DEGREES F                   *
43 C*   D IS THE ORFICE THROAT DIAM., IN.                     *
44 C*   CD IS THE COEFFICIENT OF DISCHARGE RATIO              *
45 C*****
46    KANSI=2
47    IF ( NCOUNT .EQ. 2 ) GOTO 30
48    22 WRITE(*,'(A\)' ) ' D? '
49    READ (*,'(F5.2)' ) D
50    IF ( KANSI .EQ. 2 ) GOTO 23
51    GOTO 35
52    23 WRITE(*,'(A\)' ) ' CD? '

```

```

53     READ (*,'(F5.2)') CD
54     IF (KANSI .EQ. 2 ) GOTO 24
55     GOTO 35
56 24  WRITE(*,'(A\)' ) '  POD? '
57     READ (*,'(F6.2)') POD
58     IF ( KANSI .EQ. 2 ) GOTO 30
59     GOTO 35
60 30  WRITE(*,'(A\)' ) '  P1D ? '
61     READ (*, '(F5.2)') P1D
62     IF (P1D .EQ. 0.0) GOTO 910
63     IF ( KANSI .EQ. 2 ) GOTO 25
64     GOTO 35
65 25  WRITE(*,'(A\)' ) '  P2D ? '
66     READ (*, '(F5.2)') P2D
67     IF ( KANSI .EQ. 2 ) GOTO 26
68     GOTO 35
69 26  WRITE(*,'(A\)' ) '  PEXD ? '
70     READ (*, '(F5.2)') PEXD
71     IF ( KANSI .EQ. 2 ) GOTO 27
72     GOTO 35
73 27  WRITE(*,'(A\)' ) '  T2F ? '
74     READ (*, '(F5.2)') T2F
75     IF ( KANSI .EQ. 2 ) GOTO 28
76     GOTO 35
77 28  WRITE(*,'(A\)' ) '  TOF ? '
78     READ (*, '(F5.2)') TOF
79 35  WRITE (*,'(A)' ) '  DO YOU WISH TO CHANGE ANY INPUTS ? '
80     WRITE (*,'(A)' ) '  YES OR NO ? ( 1=Y. 2=N ) '
81     READ (*,'(I1)' ) KANSI
82     IF ( KANSI .EQ. 2 ) GOTO 45
83     WRITE (*,'(A)' ) '  WHICH INPUT DO YOU WANT TO CHANGE ? '
84     WRITE (*,'(A)' ) '  D=1, CD=2, POD=3, P1D=4, '
85     WRITE (*,'(A)' ) '  P2D=5, PEXD=6, T2F=7 OR TOF=8 '
86     READ (*,'(I1)' ) ICHG
87     IF ( ICHG .EQ. 1 ) GOTO 22
88     IF ( ICHG .EQ. 2 ) GOTO 23
89     IF ( ICHG .EQ. 3 ) GOTO 24
90     IF ( ICHG .EQ. 4 ) GOTO 30
91     IF ( ICHG .EQ. 5 ) GOTO 25
92     IF ( ICHG .EQ. 6 ) GOTO 26
93     IF ( ICHG .EQ. 7 ) GOTO 27
94     IF ( ICHG .EQ. 8 ) GOTO 28
95 45  PO=PCD*2.78496
96  C*****
97  C*  CONVERSION OF ATM. PRESS. TO LBF/SQUARE FT      *
98  C*****
99     T2=T2F+459.69
100    TO=TOF+459.69
101  C*****
102  C*  CONVERSION OF TEMP TO DEGREES, RANKIN      *
103  C*****
104    P1=(P1D*5.204)+PO

```

```

105      P2=(P2D*5.204)+P0
106      PEX=(PEXD*5.204)+P0
107 C*****
108 C*      ( ). CONVERSION OF PRESS. TO LBF/SQUARE FT      *
109 C*      +, CONVERSION OF GAGE PRESS. TO ABSOLUTE PRESS., LBF/      *
110 C*      SQUAKE FT      *
111 C*****
112      ADEN=P0/(53.34*TO)
113      FDEN=P1/(53.34*TO)
114 C*****
115 C*      THE UNITS FOR THE GAS CONSTANT ARE (FT*LBF)/(LBM*DEGREES R) *
116 C*      ADEN IS THE AMBIENT AIR DENSITY, SLUGS/CUBIC FT      *
117 C*      FDEN IS THE FLOW DENSITY, SLUGS/CUBIC FT      *
118 C*****
119      DFT=D/12.0
120      AREA=3.14159*(DFT**2.0)/4.0
121 C*****
122 C*      AREA IS THE AREA OF THE ORIFICE THROAT, SQUARE FT      *
123 C*****
124      BETA=D/8.25
125 C*****
126 C*      THE INSIDE DIAMETER OF THE PIPE IS 8.25 IN.      *
127 C*      BETA IS THE RATIO OF THE ORIFICE THROAT DIA. TO THE INSIDE *
128 C*      DIA. OF THE PIPE, ASME FLUID METER, PAGE 52      *
129 C*****
130      BETA4=BETA**4
131      BETA16=BETA**16
132      BETA2=BETA**2
133      Y=1.0-((0.41+(0.35*BETA4))*(1.0-(P2/P1))*0.71429)
134 C*****
135 C*      Y IS THE EXPANSION FACTOR AND IS A RATIO, ASME FLUID METERS *
136 C*      P. 52. THE FORM OF THE EQUATION IS FOR THE STATIC PRESS.      *
137 C*      MEASURED AT THE INLET PRESS. TAP, P1, ASME FLUID METERS,      *
138 C*      P. 208.      *
139 C*      FOR 1D AND 1/2D TAPS THE FLOW COEFFICIENT IS OF THE FORM      *
140 C*      K = KO + B*LAMDA, WHERE      *
141 C*      LAMDA = 1000./(RD**0.5) = 1000./(BETA*RD)**0.5      *
142 C*      ASME FLUID METERS, P. 65      *
143 C*      B IS THE LIMITING VALUE OF K FOR ANY SPECIFIC VALUES OF D      *
144 C*      AND BETA WHEN RD BECOMES INFINITELY LARGE      *
145 C*****
146      A=0.00025/((8.25**2.0+BETA2)+0.0025*8.25)
147 C*****
148 C*      CTO=K      *
149 C*****
150      CTO1=(0.6014-0.01352*(8.25**(-0.25)))
151      CTO2=(0.3760+0.07257*(8.25**(-0.25)))*(A+BETA4+(1.5*BETA16))
152      CTO=CTO1+CTO2
153      B=(0.0002+0.0011/8.25)+(0.0038+0.0004/8.25)*(BETA2+(16.5+5.0*8.25)
154      1*BETA16)

```

```

155 C*****
156 C*   THE VALUE 8.25 IN A, CTO AND B CALCULATIONS IS THE PIPE DIAM.   *
157 C*****
158     FCI=CD/((1.0-BETA4)**0.5)
159 C*****
160 C*   FCI IS THE INITIAL VALUE FOR THE FLOW COEFFICIENT               *
161 C*   CD IS THE COEFFICIENT OF DISCHARGE AND IS A FUNCTION OF         *
162 C*   REYNOLDS NUMBER BASED ON PIPE DIAMETER RATIO OF ORIFICE        *
163 C*   DIAMETER TO PIPE DIAMETER AND PIPE, CRANE TECHNICAL PAPER      *
164 C*   NO. 410, PAGE A-20.                                             *
155 C*****
166     K=0.0
167     10 MDOT=FCI*Y*AREA*((2.*32.174*FDEN*(P1-P2))**0.5)
168 C*****
169 C*   MDOT IS IN LBM/SEC, IF                                           *
170 C*   AREA IS IN SQUARE FT,                                          *
171 C*   FDEN IS IN LBM/CUBIC FT AND                                     *
172 C*   P1 AND P2 ARE IN LBF/SQUARE FT, ABSOLUTE.                      *
173 C*****
174     K=K+1.0
175     MCFS=MDOT/FDEN
176 C*****
177 C*   MCFS IS THE FLOW RATE IN CUBIC FT/SEC                           *
178 C*****
179     MCFM=MCFS*60.0
180 C*****
181 C*   MCFM IS THE FLOW RATE, CUBIC FT/MIN                             *
182 C*   MCFM IS THE INITIAL ESTIMATE OF THE FLOW RATE                   *
183 C*   THE NEXT STEP INVOLVES INTERPOLATION TO GET THE FINAL VALUE     *
184 C*****
185     MU=(0.00000035/(492.0**0.75))*T2**0.75
186 C*****
187 C*   DRIEST INTERPOLATION OF SUTHERLANDS THEORY OF VISCOSITY         *
188 C*   SCHLICHTING, BOUNDARY LAYER THEORY, P. 313                     *
189 C*   TO=492.0, DEGREES, RANKIN                                       *
190 C*   MUO=0.00000035 (LBF*SEC)/SQUARE FT                             *
191 C*****
192     RD=(48.0*MDOT)/(3.14159*D*MU,
193 C*****
194 C*   RD IS REYNOLDS NUMBER BASED UPON ORFICE DIAMETER AND VISCOSITY *
195 C*****
196     LAMDA=1000.0/((BETA*RD)**.5)
197     FCN=CTO+(B*LAMDA)
198     MF=FCN*Y*AREA*((2.*32.174*FDEN*(P1-P2))**0.5)
199     MFCFS=MF/FDEN
200     MFCFM=MFCFS*60.0
201     IF(ABS(MFCFM-MCFM).LE.5.)GOTO 100
202     IF(K.GT. 150.) GOTO 910

```

```

203 C*****
204 C*   IF THE CALCULATED FLOW, BASED UPON TABULATED DATA, DOES NOT   *
205 C*   AGREE WITH FLOW CALCULATED USING THE REYNOLDS NUMBER (RD), THE  *
206 C*   FLOW COEFFICIENT MUST BE ADJUSTED UNTIL REASONABLE AGREEMENT   *
207 C*   IS REACHED REFERENCE "FLOW OF FLUIDS THROUGH VALVES, FITTINGS  *
208 C*   AND PIPE", CRANE TECHNICAL PAPER NO. 410, P. 3-24.           *
209 C*****
210     FCI2=(FCI+FCN)/2.0
211     FCI=FCI2
212     GOTO 10
213 100 CONTINUE
214     P1G=(P1-PO)/144.0
215     P2G=(P2-PO)/144.0
216     PEXG=(PEX-PO)/144.0
217 C*****
218 C*   CONVERSION OF ABSOLUTE PRESS. TO GAGE PRESS., LBF/SQUARE IN.   *
219 C*****
220     PA=PO/144.0
221 C*****
222 C*   CONVERSION OF AMBIENT PRESS. TO LBF/SQUARE IN.                 *
223 C*****
224     WRITE(*,1000)
225 1000 FORMAT(3X,'P1G',6X,'P2G',4X,'PEXG',5X,'PA',4X,
226 1'MFCFM',4X,'FCN',5X,'Y',8X,'RD',8X,'K',6X,'CD')
227     WRITE(*,2000)P1G,P2G,PEXG,PA,MFCFM,FCN,Y,RD,K,CD
228 2000 FORMAT(1X,F6.3,2X,F6.3,2X,F6.3,2X,F6.3,2X,F6.1,
229 12X,F6.4,2X,F6.4,2X,F10.1,2X,F3.0,2X,F6.3)
230     WRITE(*,3000)
231 3000 FORMAT(3X,'MF',6X,'FDEN')
232     WRITE(*,4000)MF,FDEN
233 4000 FORMAT(1X,F6.3,2X,F6.3)
234     IF ( NCOUNT .EQ. 2 ) GOTO 333
235     WRITE (*,'(A)') ' WRITE P1G AND MF TO DISK FILE FOR '
236     WRITE (*,'(A)') ' PLOTTING PURPOSES ? (1=Y, 2=N) '
237     READ (*,'(I1)') NANSI
238     IF (NANSI .EQ. 2) GOTO 19
239 333 WRITE (2,901) P1G,MF
240 901 FORMAT (1X,F8.3,1X,F8.3)
241     NCOUNT = 2
242     GOTO 19
243 910 WRITE (*,'(A)') ' DO YOU WISH TO SET UP ANOTHER FILE ? '
244     WRITE (*,'(A)') ' YES OR NO ? (1=Y,2=N) '
245     READ (*,'(I1)') JANSI
246     IF ( JANSI .EQ. 2 ) GOTO 900
247     GOTO 6
248 900 CONTINUE
249     END

```

APPENDIX B

AMARC TECHNICAL OBSERVATIONS DEFICIENCY REPORT

Air Cushion Equipment Transporter (ACET)
Technical Observation Deficiency Report

Of foremost importance to our operations at AMARC is the ability of an ACET to go into extremely muddy desert storage areas and return with the desired contingency aircraft in a timely manner to the flight line or ramp surface. This will involve a self-propelled ACET with an easily-manuevered set of loading ramps. AMARC personnel feel that a 2 hour maximum time limit for aircraft retrieval to be a reasonable constraint for timeliness. Therefore here are our requirements for improvement areas of the present ACET prototype:

1. On-board propulsion system, preferably a highly reliable diesel or Otto cycle engine driving a propeller. Current gas turbine engine/fan units are thought to be too susceptible to FOD damage and/or fan blade erosion. Also, replacement parts on the ST-6A engine are not readily available, thus decreasing maintainability. Our parking areas simply do not have wide enough corridors to facilitate the articulated tug/ACET combination when backing up to the desired aircraft. This requirement is very important and could not possibly be implemented for the remainder of the demonstration, but should be incorporated in an AMARC-dedicated ACET design.
2. Improved loading ramps were fabricated for this initial demonstration and were used loading an F-4 aircraft. They were extremely manpower-intensive in application. AMARC feels that these ramps must be made substantially easier to align and set in place. At times, there were 6 to 8 employees involved in maneuvering these 4-part loading ramps into correct position. This operation should be able to be easily performed by 2 workers.
3. Fuel consumption & operations/maintenance cost estimates must be quantified to at least a range of anticipated per hour operational expenses to give AMARC supervisors and planners a better grasp of the dollar scope of ACET operation.
4. Improved trailing lateral stabilizer arms must be fabricated which actually keep in constant contact with the ground at all times, despite unlevelness of the terrain. Also the arms must be able to withstand higher lateral loading forces without noticeable deformation. Perhaps a spring loaded arm of some sort could be designed to allow deflection and then return to normal positioning when unloaded. These trailing arms and brackets actually cost the AMARC demonstration 3 days (of 4 total) of downtime for maintenance. Plus the lateral stability demonstrated was at best - marginal. They simple did not perform well here.
5. Improved nose wheel steering towbar must be designed and fabricated to allow steering from in front of the aircraft when loading. AMARC cannot afford to take the safety risk involved with having one of our towing personnel directly under and in back of a 15T or heavier aircraft and its nose wheel. The consequences could be dire in case of winch or cable failure.

6. Some sort of universal safety yoke cable must be fabricated to preclude the possibility of an uncontrolled aircraft in the loading and offloading modes. The cable yoke which was used would not suffice to reliably restrain even lighter fighter type aircraft and, in fact, was responsible for a near-mishap in offloading an F-4 here. The cable clamps used are not the recommended method to make looped cable ends, as they are susceptible to slippage with any nut torquing differences. AMARC requests total deletion of cable clamps in the safety cable. The integrity of our rigging equipment must be without question - sound.
7. Offloading procedures must be reviewed and modified to facilitate ease, smoothness, and especially safety considerations.
8. Additional FOD skirting should be investigating to further abate dust/mud spray. Perhaps a double flap system could be tested.
9. Shielding for transporting aircraft must be fabricated (either attached to ACET or portable) to protect it from the mud spatter. Our contingency plans don't allow extra time for aircraft cleaning.
10. Provision for easy ACET deck, skirt, screen, and finger cleaning should be investigated, as an excessive amount of time and 'elbow grease' is involved in this work currently. This could be a secondary initiative after the operational shortcomings are addressed.
11. The mobility of a non-operational ACET must be addressed. Our crane and flatbed trailer loading scheme is only good for short distance at very slow speed and only on the hardened ramp surface. A dolly or large cart affair which would permit deflated ACET towing could be a solution here. Our crane operator does not feel comfortable carrying the ACET with an extended boom and (when he is physically closer) too much danger is involved if the unit starts swinging. The ACET overhangs a trailer grossly widthwise plus the crane could not venture out into muddy desert storage area to retrieve an inoperative ACET.
12. Lower engine exhaust stacks should be ducted with an upward deflector at the tip to limit the amount of exhaust gas impelling debris created.
13. Storage of Ready-Status ACET must be addressed since AMARC plans for this unit would only call for very infrequent use and, consequently, the majority of the time would be storage. Leaving the unit stored flush with the ground, as it is currently, would surely accelerate corrosion and deterioration due to insect, rodent, and bird nesting damage. AMARC feels elevated ACET storage would let the segmented fingers and skirts hang free, promote better drainage, and avoid the inherent earth-ground contact problems.

With these requirements listed here, we trust your FIEMB engineers will work to overcome these significant technical challenges. We stand ready to assist you in any way within our capabilities in meeting our requirements for this type of aircraft mobility.

APPENDIX C

FDL COMMENTS ON AMARC'S TECHNICAL OBSERVATIONS DEFICIENCY REPORT

FDL Comments
to
AMARC's Technical Observations Deficiency Report for the ACET
(Atch 1 to Col Grounds Ltr, 1 Apr 87)

Item 1: On-Board Propulsion System - This item addresses both a redesign of the lift system and making the transporter self-propelled. While these modifications are key factors for an AMARC dedicated design, the cost and time required to implement these configurations place them beyond the scope of the next demonstration and current in-house efforts. The replacement of the ASP-10's with an engine/fan combination currently available within the USAF/DOD inventory would insure ready access to spare parts and a significant reduction in operating costs. However, a lift system change would require a review of all potential candidates to determine which units meet the design requirements for the ACET, i.e.: pressure, air flow, weight, size, etc. Once a unit is selected, the necessary modifications to the ACET structure and control systems will have to be designed, fabricated, and checked out. The estimated cost for this effort is approximately \$75,000, and would require 9 months to complete. The estimated cost for developing a self-powering modification for the ACET is in excess of \$500,000, and would require 18 months of technical effort. While this is currently prohibitive, the Flight Dynamics Laboratory (FDL) is developing an All Terrain Crash Rescue Vehicle (ATCRV) for the Air Force Engineering Services Center (AFESC) at Tyndall AFB FL. This vehicle has an air cushion augmentation system for soft surface and amphibious operations. A supplemental propulsion system is also being developed for cushion-borne operations. This technology could be applied to a self-propelled, AMARC dedicated ACET design.

Item 2: Improved Loading Ramps - The observations of the on-site engineer for AMARC are somewhat misleading. Some difficulty was experienced with the placement and alignment of these ramps during the preparations for loading the F-4J aircraft. However, the sources of these problems were identified and corrective action is currently being taken to facilitate the use of these ramps. The reason that 6 to 8 people were involved in the positioning of the ramps was strictly because all of the personnel "on-site" were eager to assist in the ACET operation. The ramps were designed to be positioned by two people. The second demonstration will offer an excellent opportunity to evaluate the realistic manpower requirements for the ACET.

Item 3: Fuel Consumption and Operations Maintenance Costs - As indicated in Item 2, the operations conducted during the 17 Feb - 6 Mar 87 demonstration were not characteristic of a typical ACET operation. The second demonstration will provide the necessary data base to evaluate the costs of ACET operations.

Item 4: Improved Trailing Lateral Stabilizer Arms - The performance of the trailing lateral stabilizer arms was unacceptable. New trailing wheel assemblies have been designed and will be fabricated before the next demonstration. The performance of the arms is critical to the successful placement of the ACET in front of the aircraft to be towed.

Item 5: Improved Nose Wheel Steering Towbar - The towbar designed and fabricated for the demonstration is acceptable for a de-commissioned aircraft with a non-operative hydraulic system, but is totally unacceptable for positioning an aircraft with a serviceable hydraulic system. This item has been re-designed and will be ready for the next demonstration. The new towbar will eliminate the requirement for a bridle of any kind to load the aircraft, since the winch cable will attach directly to the new towbar.

Item 6: Universal Safety Yoke Cable - The towbar designed to satisfy Item 5 also satisfies this requirement, since it completely eliminates the problems which occurred during the off-loading of the F-4J at AMARC.

Item 7: Off-Loading Procedures - The procedures for this operation are currently being reviewed, and research is being conducted in this area to resolve any problems and facilitate the process of getting an aircraft off the ACET.

Item 8: Additional Foreign Object Damage (FOD) Skirting - Additional skirting is available and will be installed prior to starting the demonstration. Photographs and video tape of the 26 Feb 87 towing operation have been reviewed. The primary flow paths have been identified. The major cause of FOD during ACET operations is the air flow exiting the three air cushion cells. Operations during the dry season will always generate a substantial amount of dust. FOD skirting can control the path of the dust, but it will not eliminate the problem. The same is true of operations during the rainy seasons. Installation of additional skirting in strategic areas will greatly reduce the mud spray to critical areas of the ACET and the payload by controlling the flow exiting the cells. However, the problem, which is less critical on a wet surface, cannot be totally eliminated.

Item 9: Shielding for Transported Aircraft - Installation of the additional FOD skirting should eliminate the problem of mud spattering on the aircraft while it is being transported on the ACET. The effectiveness of this approach will be evaluated during the demonstration.

Item 10: ACET Cleaning - The amount of mud build-up on the ACET will be greatly reduced by the installation of the additional FOD skirting. However, the entire ACET was washed in approximately 15 minutes, using a fire hose, after the 26 Feb 87 operation. This appears to be an acceptable solution for cleaning the ACET.

Item 11: Mobility of a Non-Operational ACET - While this is a key issue for an AMARC dedicated ACET design, it is beyond the scope of this demonstration effort and will have to be addressed at a later date.

Item 12: Lower Engine Exhaust Stacks - Additional protection for the ASP-10's is being designed and fabricated to reduce the amount of fine debris ingested by the fans. The current configuration of the ASP-10 lower exhaust stacks directs the exhaust gases to the right or left, depending on the engine, away from the ACET and parallel to the ground plane. Impingement of these two exhaust plumes on the ground surface is minimal and any FOD generated is of a secondary nature. Also, the installation of an upward deflector raises the question of hot exhaust gas impingement on the ACET and aircraft structure. A potential alternative would be to replace the dual exhaust stacks with a single exhaust stack which directs the exhaust plume upward and outboard. This approach was considered during the design phase of the ACET. The cost, approximately \$50,000, was considered excessive for the potential benefits to be gained.

Item 13: Storage of Ready-Status ACET - While this is a key issue for an AMARC dedicated ACET design, it is beyond the scope of this demonstration effort, and will have to be addressed at a later date.